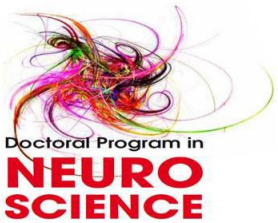

UNIVERSITA' DEGLI STUDI DI VERONA

DEPARTMENT OF NEUROSCIENCE, BIOMEDICINE AND MOVEMENT SCIENCES

GRADUATE SCHOOL OF LIFE AND HEALTH SCIENCES
DOCTORAL PROGRAM IN NEUROSCIENCE

CYCLE XXX 2014-2017

THE OSCILLATING LATERAL HYPOTHALAMUS AND THE OREXINERGIC SYSTEM

S.S.D. BIO/17

Coordinator: Prof. Leonardo CHELAZZI

Supervisor: Prof. Marina BENTIVOGLIO

Dott. Idris Ayodeji AZEEZ

The oscillating lateral hypothalamus and the orexinergic system –
Dott. Idris Ayodeji AZEEZ
PhD Thesis

Contents

I. Acknowledgements **6**

II. Thesis abstract **8**

III. List of abbreviations **10**

1. General introduction **12**

1.1 The orexins / hypocretins and the orexinergic system 12

1. 1.1.1 The intermingling with melanin-concentrating hormone neurons 20
2. 1.1.2 Wiring and modulation of orexinergic neurons: intra- and extra-hypothalamic inputs 21
3. 1.1.3 Diurnal changes in the orexinergic system 28
4. 1.1.4 The orexinergic system and circadian regulation 31
5. 1.1.5 Plastic changes in the synaptic wiring of orexinergic cell bodies 35

1.2 Orexin and the control of sleep and wake 39

6. 1.2.1 The role of orexin in vigilance states 39
7. 1.2.2 Deficient orexinergic signalling in narcolepsy 41

1.3 Orexins in aging and aging-related neurodegenerative disorders 44

8. 1.3.1 Orexins in the normal aging brain 44
9. 1.3.2 Orexins in Alzheimer’s disease and Parkinson's disease 46

1.4 Extracellular matrix in the brain 49

10. 1.4.1 Components of the brain extracellular matrix 52
11. 1.4.2 Involvement of the extracellular matrix in neuroinflammation and neurodegeneration 58

1.5 Specific objectives of the experimental studies 60

2. Study of the synaptic wiring of orexinergic neuron soma in the periods of sleep or wake predominance in adult mice 61

2.1 Introduction 61

2.2 Materials and methods 62

12. 2.2.1 Animals and experimental design 62
13. 2.2.2 Electroencephalography recording 63
14. 2.2.3 Tissue processing and immunofluorescence 63
15. 2.2.4 Microscopy and quantitative analyses 64

2.3 Statistical analyses 65
2.4 Results 66
16. 2.4.1 Sleep and wake states 66
17. 2.4.2 Excitatory and inhibitory presynaptic elements 66
18. 2.4.3 Postsynaptic markers 70
2.5 Discussion 74
2.6 Tables 79
2B. *Addendum*: preliminary data on astrocytes in the lateral hypothalamus during day and night 80
2B.1 Purpose 80
2B.2 Materials and methods 80
19. 2B.2.1 Animals 80
20. 2B.2.2 Tissue processing and immunofluorescence 80
21. 2B.2.3 Microscopy and data analysis 81
2B.3 Results 82
2B.4 Comments 87
3. Synaptic wiring of orexinergic neuronal cell bodies during day and night: from adult to aged mice and study of a murine model of Alzheimer's disease 89
3.1 Introduction 89
3.2 Materials and methods 91
22. 3.2.1 Experimental design and animals 91
23. 3.2.2 Tissue processing and immunofluorescence 92
24. 3.2.3 Microscopy and quantitative analyses 93
3.3 Statistical analyses 95
3.4 Results 95
25. 3.4.1 Triple immunofluorescence of orexinergic neurons and glutamatergic or GABAergic presynaptic terminals 95
26. 3.4.2 Quantitative analyses of the input to orexinergic cell bodies 97
3.5 Discussion 106
3.6 Tables 110
4. Extracellular matrix in the lateral hypothalamus and other brain regions: diurnal organization in basal conditions and in experimental sleeping sickness 112
4.1 Introduction 112

4.2 Materials and methods 114
27. 4.2.1 Animals and infection 114
28. 4.2.2 Brain tissue processing and immunofluorescence 115
29. 4.2.3 Microscopy and quantitative analyses 115
30. 4.2.4 Western blot 116
4.3 Statistical analyses 116
4.4 Results 116
31. 4.4.1 Diurnal organization of the extracellular matrix in the lateral hypothalamus and other regions in basal conditions 116
32. 4.4.2 Western blot analysis 121
33. 4.4.3 Diurnal organization of the extracellular matrix in the lateral hypothalamus of *Trypanosoma brucei brucei*-infected animals 122
4.5 Discussion 124
5. Summary and conclusions 126
6. References 128

I. Acknowledgements

All glory and adorations are due to the God Almighty for seeing through the course of the Doctoral program and making the completion of this Thesis a reality.

I highly appreciate my parents for their unrelenting support over the years. I pray they live long to enjoy the fruits of their labor. I am also grateful to my other family members who have been supportive all along.

A very special gratitude to my supervisor, Prof. Marina Bentivoglio, whom for a certain, I cannot thank well enough, other than ‘’to pray that God bless her with long life, good health, eternal joy and peace in all’’. She has been very supportive all through the period of this Doctoral program. She has trained me with every resources at her disposal in the last six years, hence turning me to a ‘budding neuroscientist and a fine researcher’. *Molto grazie!*

My sincere gratitude goes to my mentor, the Dean, Faculty of Veterinary Medicine, University of Ibadan, Prof. James Olopade, who has been instrumental to this success story from the very onset. I can only wish him more of God’s blessings in all his endeavors. Many thanks to Dr (Mrs) Funmi Olopade and members of the Neuroscience unit, Department of Veterinary Anatomy, University of Ibadan.

To the members of ‘Bentivoglio unit’- Prof. Gigliola Grassi-Zucconi, Drs. Anna Andrioli, Tiziana Cotrufo and Chiara Tesoriero, I value you so much especially for your ‘listening ears’, encouragement and willingness to help at all times. Also, I highly appreciate the help of Drs. Claudia Laperchia, Federico Del Gallo and Grygoriy Tsenov. Thanks are due Dr. Erika Lorenzetto for her technical assistance at the confocal microscopy. To our MSc students, Lejdi Jaupaj and Filippo Corghi, all the best as you round off your program.

My stays in Naples (in 2015 and 2016) were fruitful owing to the tutorship of Dr. Luigia Cristino on the analyses of synaptic wiring of orexinergic neurons, and the technical assistance of Dr. Roberta Imperatore. You are both highly appreciated.

Big thanks to Dr. Raffaella Mariotti for the opportunity to use her unit for Western blot procedures whenever I so wish and Dr. Ilaria Scambi for her tireless effort and technical assistance from time to time.

All members of staff of the Department of Neuroscience, Biomedicine and Movement Sciences, Section of Anatomy and Histology, are well appreciated for their kindness and enabling working environment, from the Director- Prof. Andrea Sbabarti, to the secretarial staff- Mrs Nadia Lovato, Sarah Caloi and Emanuela Grandis, and many more others.

I so much appreciate the Dean, Faculty of Veterinary Medicine, University of Jos, Prof. Lami Lombin, the Head- Prof. Hambolu Olajide and the academic staff, Department of Veterinary Anatomy for their invaluable support.

Gratitude to Prof. Tomas Hokfelt of the Karolinska Institute, Stockholm, Sweden and Prof. Alexej Verkhratsky of the University of Manchester, England for their precious time and efforts in painstakingly reviewing this Doctoral Thesis.

Thank you, Adeola for being my best friend.

Grazie mille a tutti!

II. Thesis abstract

Neurons which release the orexins (OX)/hypocretins peptides and are located in the lateral hypothalamus (LH) are key regulators of energy metabolism, arousal and sleep-wake stability, motivated behaviors. This thesis presents three data sets focused on the synaptic wiring of OX-A cell bodies in relation to state-dependent behavior in mice.

The **first study** (Chapter 2; Laperchia et al. 2017) tested the hypothesis of synaptic plasticity phenomena of OX soma innervation in basal conditions. Adult mice were sacrificed during day or night periods in which sleep or wake predominance, respectively, were assessed by electroencephalography in matched mice. Excitatory and inhibitory terminals on OX somata were evaluated with multiple immunofluorescence. The total number of these terminals did not vary between day and night, but glutamatergic terminals prevailed at night and GABAergic ones at daytime. The findings thus revealed a striking daily fluctuation in the axosomatic wiring of OX neurons, with a switch from prevalent excitatory innervation during wake to prevalent inhibitory innervation during sleep.

An ***addendum*** to Chapter 2 presents methodological approaches to the analysis of astrocytes surrounding OX neurons, at day and night time points in antiphase as above, and preliminary observations.

The **second study** (Chapter 3) tested the hypotheses that the above diurnal fluctuation could be altered during aging and in the pathology that characterizes Alzheimer's disease (AD). The same paradigm and approaches of the first study were applied to 3 month-old and 20 month-old TASTPM mice, which provide a model of AD and in which main pathological features were investigated, and to matched wild-type (WT) mice. The day/night fluctuation in the inhibitory/excitatory wiring of OX somata was replicated in young WT and TASTPM mice, but was lost in aged WT mice and TASTPM mice. In addition, an overall decrease of presynaptic terminals on OX cell bodies was found in aged WT and TASTPM mice *vs* young ones, and in TASTPM mice *vs* WT ones (all sampled during daytime). In 15 month-old TASTPM mice stereological OX cell counts revealed significant loss (34% decrease), and densitometric evaluation showed a significant enhancement OX immunosignal intensity, suggesting a potential compensatory increase of peptide synthesis.

The **third study** (Chapter 4) tested the hypothesis that extracellular matrix (ECM) components, reported to be among the players regulating neural plasticity, could be involved in the daily reorganization of OX cell body wiring. The study was conducted in healthy mice and in a murine model of the parasitic encephalitis African trypanosomiasis or sleeping sickness. The ECM was labelled by *Wisteria*

floribunda agglutinin (WFA) immunofluorescence. Marked day/night variations were observed in confocal microscopy, with a diffuse ECM distribution at daytime, and a more compact organization and condensation around OX cell bodies at night. Furthermore, WFA expression in the LH, evaluated with Western blotting, was significantly enhanced at night compared to day. This diurnal variation of ECM organization was not found in other brain areas (suprachiasmatic nucleus, neocortex, hippocampus), and was lost in the LH after African trypanosome infection. These findings indicate regional day/night fluctuation of the ECM in the LH, and its disruption in a chronic neuroinflammatory pathology which leads to sleep-wake dysregulation.

Keywords: orexin, lateral hypothalamus, synaptic plasticity, circadian timing, aging, Alzheimer's disease, extracellular matrix, African trypanosomiasis

III. List of abbreviations

ACTH	adrenocorticotropic hormone
AD	Alzheimer's disease
AMPA	α-amino-3-hydroxy-5-methylsoxazole-4-propionate
ANOVA	analysis of variance
APP	amyloid precursor protein
ATP	adenosine triphosphate
Aβ	amyloid-beta
BF	basal forebrain
BNST	bed nucleus of the stria terminalis
CNS	central nervous system
CRF	corticotropin releasing factor
CSF	cerebrospinal fluid
CSPGs	chondroitin sulfate proteoglycan
CX3CR1-GFP$^{-/-}$	chemokine (C-X3-C motif) receptor 1-green fluorescent protein
dpi	days post-infection
ECM	extracellular matrix
EDS	excessive daytime sleepiness
EEG	electroencephalogram
EMG	electromyogram
GABA	γ-aminobutyric acid
Geph	gephyrin
HA	hyaluronic acid/ hyaluronan
HFD	high-fat diet
HIF-1α	hypoxia-inducible factor 1 alpha
HLA	human leucocyte antigen
HPA	hypothalamic-pituitary-adrenal axis
Icv	intracerebroventricular
IgGs	immunoglobulins
ISF	interstitial fluid
LH	lateral hypothalamus
MANOVA	multivariate analysis of variance
MCH	melanin concentrating hormone
MnPO	median preoptic nucleus
MS	multiple sclerosis
NDS	normal donkey serum
NMDA	N-methyl-D-aspartate receptors
NPY	neuropeptide-Y
NREM	non-rapid eye movement (sleep)
OX	orexin A and B or orexin-A
OXR	orexin receptor
PD	Parkinson's disease

PNNs	perineuronal nets
PBS	0.01M phosphate-buffered saline, pH 7.4
PS	paradoxical sleep
PSD95	postsynaptic density 95
PV	Parvalbumin
PVH	Paraventricular nucleus of the hypothalamus
PVT	paraventricular nucleus of the thalamus
P2XRs	purinergic receptors
REM	rapid eye movement (sleep)
SST	somatostatin
SWS	slow wave sleep
Syn	synaptophysin
TASTPM	TAS10 *thy1-APP695swe x* TPM *thy1 PS1.M146*- transgenic mice
Tbb	*Trypanosoma brucei brucei*
Tg	transgenic
TMN	tuberomammillary nucleus
TN-R	tenascin-R
TRF	thyrotropin releasing factor
VGAT	vesicular GABA transporter
VGluT2	vesicular Glutamate transporter 2
VLPO	ventrolateral preoptic nucleus
VTA	ventral tegmental area
WFA	*Wisteria floribunda* agglutinin
WT	wild-type
ZT	*Zeitgeber time*

1. General introduction

The experimental work presented in this thesis is focused on the synaptic wiring of orexinergic neuronal cell bodies, which are located in the lateral hypothalamus (LH), with particular reference to their diurnal plasticity in basal conditions. The study has been performed in the healthy brain, in adult and aged mice, and in a murine model of Alzheimer's disease (AD). On the basis of the findings that will be here presented, the phenotype of the extracellular matrix (ECM) surrounding orexinergic neurons in the LH was also investigated during day and night, and compared with the ECM in other brain areas. Current knowledge on these topics is highlighted in the first chapter of this thesis.

1.1 The orexins / hypocretins and the orexinergic system

Orexin (OX)-A and B, also known as hypocretin 1 and 2, are a unique pair of alternatively spliced neuropeptides derived from a single common precursor encoded by the *prepro-orexin* gene. OX peptides in the brain are synthesized by neurons located exclusively in the hypothalamus (lateral hypothalamic area and perifornical area). They were first reported in two independent publications in 1998. One group designated the peptides as 'hypocretins' because of their hypothalamic location and similarity with the gut peptide secretin (de Lecea et al. 1998). The other group named the peptides 'orexins' (from the Greek *orexis*: appetite), because they were found to stimulate food intake (Sakurai et al. 1998). In particular, the intracerebroventricular (icv) injection of orexins during the light period induced feeding behavior in rats and mice (Sakurai et al. 1998).

Orexinergic neurons are projection cells, variable in size (the cell body diameter ranges from 15 to 40 μm) and shape (spherical, fusiform or multipolar), and have been assumed to number around 3,000-4,000 in the rat brain, and approximately 30,000–70,000 in the human brain (Thannickal et al. 2000; Sakurai 2007; Brownell and Conti 2010; Callander et al. 2013). The OX peptides are highly conserved, with identical OX-A sequences and just two amino acid substitutions in OX-B in humans and mice. Nonhuman vertebrates, including the zebrafish (which contains 16-60 OX neurons in the LH of larvae and adults, respectively) (Elbaz et al. 2013), produce OX, although OX-like peptides seems to lack in invertebrates (Sakurai et al. 1998; Scammell and Winrow 2011). The OX peptides are unique in that they do not have significant structural similarities to known families of regulatory peptides, hence other neuropeptides, such as neuropeptide Y (NPY), secretin, and similar peptides have not been shown to bind to OX receptors (OXRs) (Holmqvist et al. 2001).

OX-A consists of 33 amino acids with two disulfide bridges, while OX-B is a linear peptide of 28 amino acids with two alpha helices (Lee et al. 1999). The OX-A peptide has C terminus amidation and N terminus cyclisation with a pyroglutamyl

residue. Before synaptic release, the peptides undergo packaging into dense core vesicles (de Lecea et al. 1998).

OX-A and B are largely colocalized in the same neurons, and OX-A is more stable and biologically active than OX-B, possibly due to post-translational modifications (de Lecea et al. 1998; Sakurai et al. 1998; Nixon and Smale 2007). Henceforth, the acronym OX will be here used to refer to both OX-A and OX-B or to OX-A only, unless specified otherwise.

A wealth of evidence, including phenotyping and ultrastructural data, indicates that orexinergic neurons are excitatory and utilize glutamate as neurotransmitter. Orexinergic cell bodies show glutamate immunoreactivity (Abrahamson et al. 2001), orexinergic axon terminals establish mainly asymmetric synapses (de Lecea et al. 1998; Peyron et al. 1998; Diano et al. 2003; Torrealba et al. 2003) and glutamate is stored at the presynaptic terminal in small, clear, synaptic vesicles different from the vesicles which contain the peptide (Torrealba et al. 2003).

Orexinergic neurons also produce the peptide dynorphin, and other neuropeptides co-derived from prepro-dynorphin (Chou et al. 2001). In the rat LH, dynorphin was found to be expressed only in OX neurons, with 96% of them containing dynorphin at both the mRNA and peptide levels. In the LH of mice, a similar degree of expression was observed as in rats (Chou et al. 2001). Mice with targeted deletion of the *prepro-orexin* gene still had neurons highly expressing *prodynorphin* mRNA, whereas OX/ataxin-3 mice, in which OX neurons degenerate selectively in early adulthood (Hara et al. 2001), lack both *prepro-orexin* and *prodynorphin* mRNAs in the LH (Chou et al. 2001). Little is known about the conditions that facilitates the release of these co-neurotransmitters (Liu et al. 2002; Crocker et al. 2005). Recent data indicate, however, that dynorphin can be involved in the regulation of OX neuron activity during vigilance states (Ferrari et al. 2018) (see 1.1.2).

Another neuropeptide, neurotensin, which is involved in neuroendocrine and feeding behavior regulation and in reward mechanisms, is co-expressed in OX neurons (Furutani et al. 2013). In addition, neurotensin-immunoreactive fibers contact OX neurons and could be implicated in maintaining their activity (Furutani et al. 2013).

Furthermore, orexinergic neurons secrete neuronal activity-regulated pentraxin (NARP, also called NP2 or NPTX2) (Reti et al. 2002), a protein involved in the clustering of α-amino-3-hydroxy-5-methylsoxazole-4-propionate (AMPA) glutamate receptors, which is involved in circadian synaptic changes (see 1.1.3 and 1.1.4) of OX neurons (Appelbaum et al. 2010).

The actions of OX are mediated by orexin-1 receptor (OX1R) and orexin-2 receptor (OX2R) via two G-protein coupled receptors that have 7-transmembrane domains

and some similarity to other neuropeptide receptors (Fig. 1.1) (Sakurai and Mieda 2011; Inutsuka and Yamanaka 2013). OX1R is thought to couple to Gq, and OX2R can signal through Gq or Gi/Go, but coupling mechanisms seem to differ in different cell types and have not been thoroughly examined in neurons (Scammell and Winrow 2011).

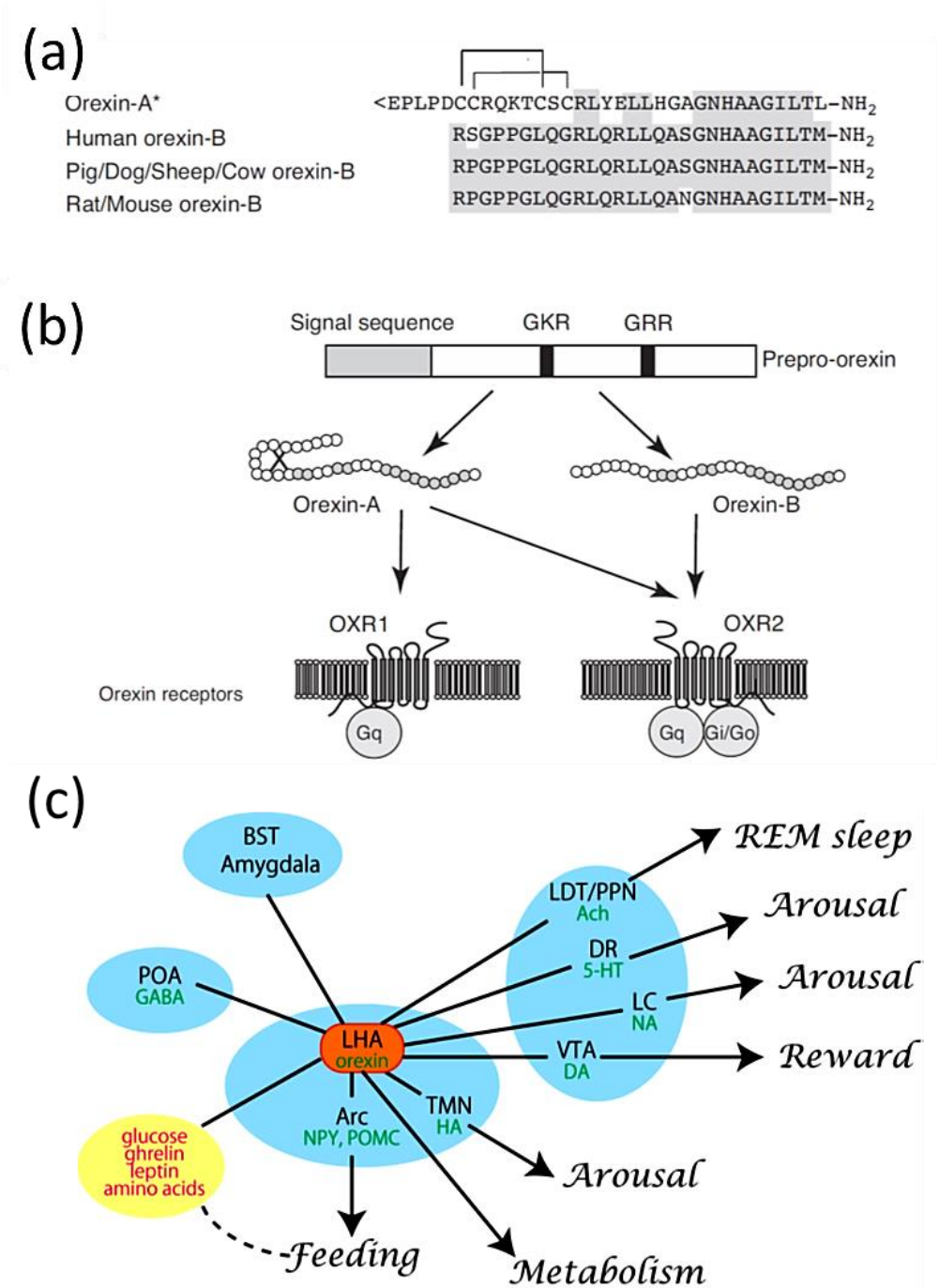

Fig. 1.1: a: Sequence of orexin (OX)-A (the same sequence has been identified in different mammals) and OX-B in different species, with indication of the topology of the two intrachain disulfide bonds of OX-A. Shadows indicate amino acid identity. **b**: OX-A and OX-B are derived from a common precursor peptide, prepro-orexin. OX receptor

(R)-1 is coupled to the Gq subclass of heterotrimeric G proteins, whereas OXR-2 is coupled to Gi/o and/or Gq. **c**. Diagram illustrating the integrative physiological roles of OX neurons. They regulate the hypothalamic nuclei involved in feeding behavior. They regulate sleep and wake, promoting wakefulness, through connectivity with neurons of the preoptic area, and brain stem. Abbreviations are in the generalist list; other abbreviations: LHA, lateral hypothalamic area; POMC, proopiomelanocortin. Sources: Sakurai and Mieda 2011; Inutsuka et al. 2013.

OX1R and OX2R are highly conserved across mammals, with 94% identity in the amino acid sequences between humans and rats. OX1R has greater affinity (~100-fold higher) for OX-A over OX-B, whereas OX2R, which shares 64% amino acid homology with OXR-1, accepts both ligands with similar affinities (Sakurai et al. 1998). *OX1R* and *OX2R* mRNAs have a different complementary distribution, which suggests that these receptors have distinct physiological roles through different neuronal pathways (Marcus et al. 2001). Of note, the only identified OXR in zebrafish corresponds structurally to the mammalian OX2R (Elbaz et al. 2017a).

The efferent projections of OX neurons match the expression pattern of OXRs throughout the brain. The dorsomedial nucleus of the hypothalamus (DMN), paraventricular nucleus of the hypothalamus (PVH), and locus coeruleus (LC) highly express *OX1R* mRNA, whereas *OX2R* mRNA is prominent in the neocortex, septal nuclei, hippocampus, and some other hypothalamic nuclei, including the histaminergic tuberomammillary nucleus (TMN), express only *OX2R* mRNA (Marcus et al. 2001; Yamanaka et al. 2010) (see also 1.2.1).

From the LH, the orexinergic neurons project extensively to other brain structures (sparing the cerebellum), and to the spinal cord (Peyron et al. 1998) (Fig. 1.2), constituting the central orexinergic system (Nuñez et al. 2009). The term ‘’orexinergic system’’ usually refers to the OX peptides and their receptors as well as to OX neurons and their projections to different parts of the central nervous system (CNS).

Orexinergic neurons not only give origin to long-range projections (Fig. 1.2), but also contribute to local networks in their target areas, where they modulate functional activities. OX can act presynaptically to induce release of γ-aminobutyric acid (GABA) or glutamate, thus generating effects on downstream neurons (Scammell and Winrow 2011).

Research on OX has focused on the CNS, where these peptides have been discovered, but their occurrence in the periphery has also been reported. For example, small amounts of OX may be produced, and OXRs expressed, elsewhere, such as in the testes (Jöhren et al. 2001) and in the adrenal gland (Randeva et al. 2001). OX-producing neurons have also been described in the submucosal and myenteric plexuses of the stomach and small intestine (Kirchgessner and Liu 1999),

although this is controversial as these neurons may contain an OX-like peptide that could cross-react with anti-OX antisera (Baumann et al. 2008; Scammel and Winrow 2011).

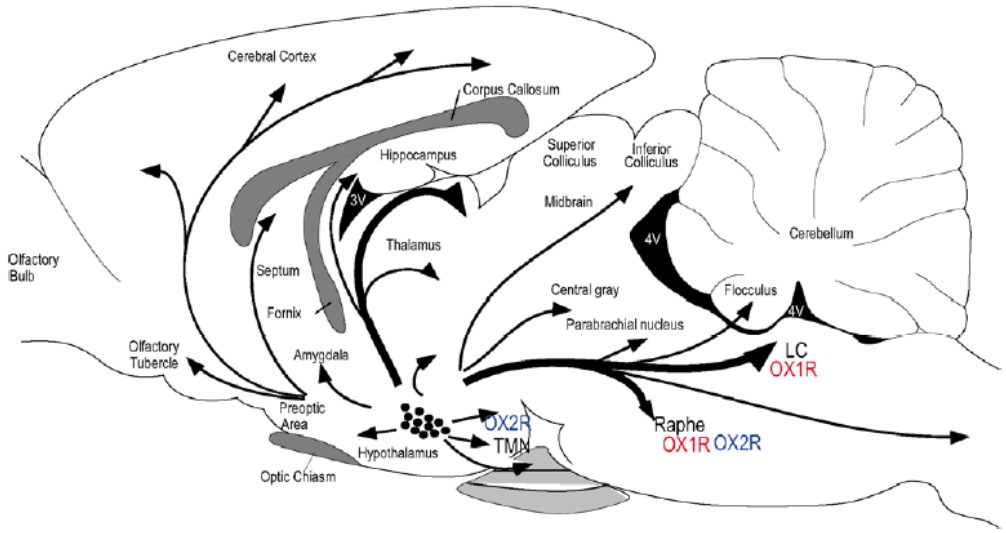

Fig. 1.2: The orexinergic system: OX cell bodies (black dots) reside in the lateral hypothalamus area and project widely to the neuraxis. The thickness of arrows represents the relative abundance of projections. Abbreviations are in the general list. Reproduced from Tsujino and Sakurai 2009.

Hypothalamic neurons containing the OX peptides (Fig. 1.3) have been implicated in multiple functions (Fig. 1.1), especially related to the control of a variety of homeostatic functions including energy expenditure (Date et al. 1999; Sakurai 2014). The broad range of functions influenced by the orexinergic system has led to the description of these neurons as ‘’physiological integrators’’ (Fig. 1.1C) (de Lecea et al. 1998; Inutsuka and Yamanaka 2013).

As mentioned above, these peptides were recognized as regulators of feeding behavior since their identification. Subsequent studies showed that OX plays a crucial role in sleep and wake regulation (see 1.2.1) and, as it will be dealt with below (see 1.2), OX deficiency produces symptoms of the sleep disorder narcolepsy (Peyron et al. 2000; Scammell et al. 2012; Tsunematsu and Yamanaka 2012) (see 1.2.2). OX2R has been thought to have a major role in maintaining wakefulness, and OX1R is likely to be involved in a broad range of other functions, including emotion, reward and autonomic regulation (review in Sakurai 2014).

Fasting induces upregulation of *prepro-orexin* mRNA levels (Sakurai et al. 1998) and transgenic (Tg) mice lacking the OX neurons fail to rouse in response to lack of food, supporting the appetite-regulating role of the OX peptides (Yamanaka et al. 2003a). In addition, chemogenetic activation of OX neurons simultaneously

increases locomotor activity and food intake (Inutsuka et al. 2014) and blockade of OXRs reduces food intake (Haynes et al. 2000) and binge eating behavior (Piccoli et al. 2012). However, other studies indicate that following icv administration OX-A stimulate only modestly food intake compared to other orexigenic peptides like NPY and galanin, and the effects of OX-B on food intake were found to be inconsistent (Edwards et al. 1999; Taheri et al. 1999, 2000).

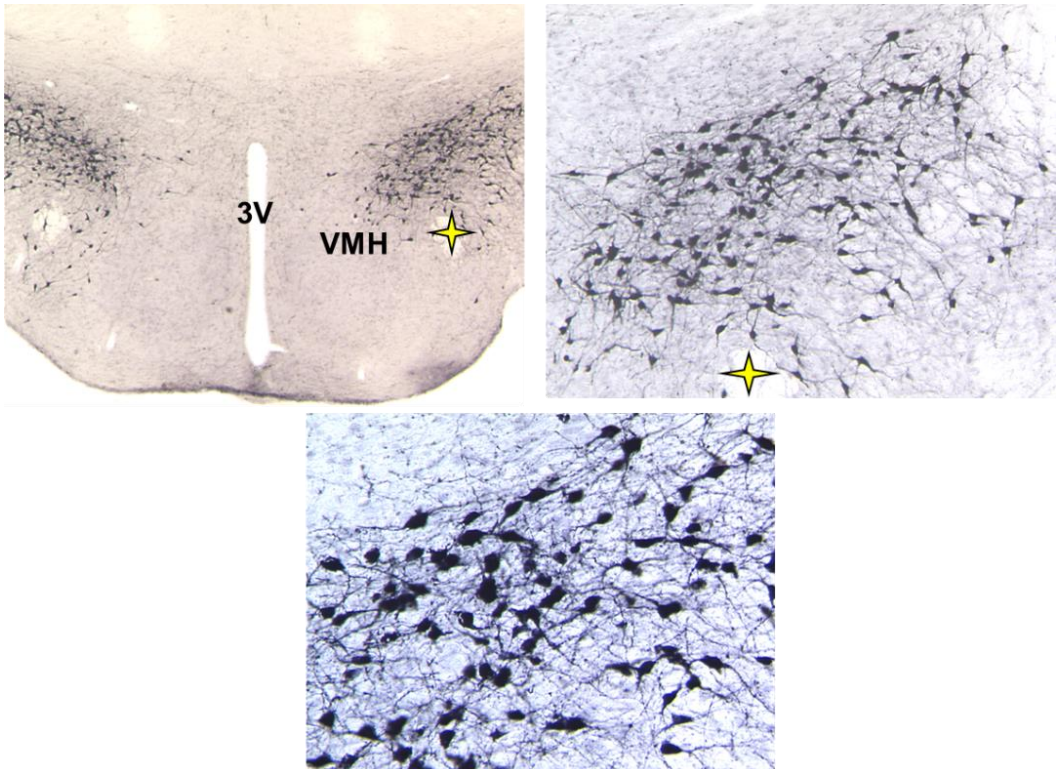

Fig. 1.3: Selective location of orexin-A-containing neurons (at different magnifications) in the lateral hypothalamus of 3 month-old mouse (nickel-intensified immunohistochemistry). From archival lab material. 3V, third ventricle; ✦ denotes the fornix.

While OX antagonists may block the physiological roles of these peptides, the coreleased neurotransmitters may still be able to exert their physiological roles (Scammell and Winrow 2011). For instance, Tg mice lacking OX neurons (OX neuron ablated mice) have stronger tendencies toward obesity when compared with Tg mice lacking the OX encoding genes (*prepro-orexin* knockout mice) (Hara et al. 2001).

In OX/ataxin-3 mice, in addition to sleep/wake cycle abnormalities, the disruption in energy homeostasis leads to late-onset obesity, even if they eat less than their wild-type (WT) littermates, pointing to a key role of OX in energy homeostasis (Hara et al. 2001). In WT mice despite an orexigenic effect of acute OX treatment,

chronic icv OX infusion does not lead to weight gain (Yamanaka et al. 1999). Moreover, recent findings have revealed that OX neuron activity decreases after eating onset and their silencing leads to eating facilitation (González et al. 2016), which is in line with the obesity observed in OX-deficient mice (Hara et al. 2001). OX plays a role in the maintenance of wakefulness during food searching and in reward-related food consumption (Cason et al. 2010), which highlights the importance of OX in the control of different aspects of food intake (Blasiak et al. 2017).

In addition, OX regulates autonomic functions and neuroendocrine axes, including the hypothalamic-pituitary-adrenal axis (HPA), as well as plasticity mechanisms related to reward (Jászberényi et al. 2000; Kuru et al. 2000). Documented results clearly indicate a role for orexinergic neurons in reward processing, arousal, drug-related effects and addictive behaviors. Orexinergic neurons are directly activated by corticotropin releasing hormone (CRH) and stress (Winsky-Sommerer et al. 2004) and are involved in stress-induced overconsumption of food (Piccoli et al. 2012), and reinstatement of alcohol- and drug-seeking behavior (Kastman et al. 2016; Schmeichel et al. 2016). The functional link between the HPA axis and OX neurons is reciprocal, since OX induce c-*fos* mRNA (which reveals neuronal activity; see 1.1.3) in the PVH, and an increase in plasma levels of adrenocorticotropic hormone (ACTH) and corticosterone in rats (Kuru et al. 2000). These pathways may be involved in stress-induced over-activation of OX neurons, leading to reward-based binge eating behavior (Blasiak et al. 2017).

The stimulation of the LH was found to potentiate the effect of an ineffective dose of morphine and induced morphine sensitization (Razavi et al. 2014). In the rat, chemical stimulation of the LH by unilateral administration of a cholinergic agonist resulted in a change in conditioned place preference suggesting the involvement of OX in drug-seeking behavior (Taslimi et al. 2011). The administration of OX in the ventral tegmental area (VTA) also induced conditioned place preference in a dose-dependent manner in rats (Taslimi et al. 2012; Riahi et al. 2013; Haghparast et al. 2017). In the same area, the VTA, OX administration increases the number of N-methyl-D-aspartate (NMDA) receptors in the cell membrane, rendering the neurons more responsive to the excitatory effects of glutamate for several hours (Borgland et al. 2006, 2008; Scammell and Winrow 2011).

The orexinergic system also plays a role in cognitive processes. A mechanism for this could be represented by the control of neurotransmission in the hippocampus by direct and indirect modulation of various pathways (Stanley and Fadel 2012). In particular, OX-mediated modulation of GABA and glutamate release in the hippocampus could be a potential contributor to cognitive performances (Stanley and Fadel 2012).

In vitro and *in vivo* studies have shown that OX is neuroprotective and has anti-apoptotic properties, reducing neuronal damage caused by ischemia or oxidative insult in hypothalamic, hippocampal, and cortical tissues (Yuan et al. 2011; Butterick et al. 2012; Sokołowska et al. 2012; Nixon et al. 2015). While the mechanism is not fully defined, OX appears to increase resistance to oxidative stress by upregulation of hypoxia-inducible factor 1 alpha (HIF-1α) (Sikder and Kodadek 2007; Yuan et al. 2011; Butterick et al. 2013; Feng et al. 2014). HIF-1α is a transcription factor that alters mitochondrial activity by increasing ATP production through oxidative phosphorylation, and affects the expression of transferrin, a protein important in the regulation of iron metabolism in the brain (Semenza 2001; Weinreb et al. 2013).

In addition, recent evidence suggests an anti-cancer role for OX (Graybill and Weissig 2017). In an experimental model of glioblastoma multiforme, an aggressive brain cancer, findings confirmed the presence of both OXRs. Interestingly, treatment of these cells with OX-A, and not OX-B, resulted in a dose-dependent significant decrease in the rate of cell viability (Biegańska et al. 2012).

Orexinergic neurons link forebrain structures involved in the processing of emotion and motivation and the brain stem regions which regulate wakefulness and reward (review in Sakurai 2014). As such, cues associated with reward and arousal have been demonstrated to stimulate OX neurons (Sakurai et al. 1998; Harris et al. 2005). High OX level in the cerebrospinal fluid (CSF) has been associated with increased purposeful behaviour. For instance, it has been shown that yard play produces a substantial increase in CSF OX levels in dogs, although no significant increase beyond baseline was found following comparable treadmill locomotion (Wu et al. 2011; Boddum et al. 2016).

In particular, orexinergic neurons link forebrain structures implicated in the processing of emotion and motivation, such as the amygdala, bed nucleus of the stria terminalis (BNST) and nucleus accumbens, with brain stem regions that regulate wakefulness (Sakurai 2014). The activation of orexinergic neurons by the limbic system maintains wakefulness during emotional arousal. In humans, increased levels of OX, measured in the amygdala, have been found during social interactions and in connection with social-induced positive emotions (Blouin et al. 2013). Experimental studies have associated the involvement of the orexinergic system in emotion and emotional memory with the abundant input received by the orexinergic neurons from the limbic system (Hara et al. 2005; Harris et al. 2005; Flores et al. 2014; Wu et al. 2014).

Orexinergic neurons also innervate brain regions related to nociception, especially the LC. The central administration of OX reduces nociceptive responses in mouse models of thermal, inflammatory and visceral pain and a role for OX in the direct

link between nociception and analgesia has been identified (Bingham et al. 2001; Yamamoto et al. 2002; Inutsuka et al. 2016).

The connectivity of the orexinergic system with multiple neuronal systems implies that OX neurons provide links for different brain functions. It has been envisaged that a multiparametric perspective, such as genetics, receptor subtype-selective pharmacology, optogenetics and chemogenetics, would be needed to further unravel the integrative physiological roles of the orexinergic system (Mieda 2017).

1.1.1 The intermingling with melanin-concentrating hormone neurons

OX neurons are intermingled in the LH with neurons expressing the peptide melanin-concentrating hormone (MCH) (Bittencourt 2011) (Fig.1.4). There are about 12,000 MCH-expressing neurons in the rat (Modirrousta et al. 2005). Altogether, the OX and MCH neurons account for a low proportion (less than 1%) of LH neurons (Broberger et al. 1998; Sakurai 2007; Hassani et al. 2009). This highlights the heterogeneity of the LH, which is very rich in neuronal subsets containing different peptides (Gerashchenko and Shiromani 2004).

MCH neurons have been implicated in some of the same homeostatic functions as OX neurons, such as energy balance and sleep regulation (Pissios et al. 2006; Peyron et al. 2009; Kessler et al. 2011). Although they anatomically overlap in distribution in the LH (Fig.1.4), functionally, OX and MCH neurons play opposite roles, in particular in the regulation of sleep/wake states (see 1.2.1).

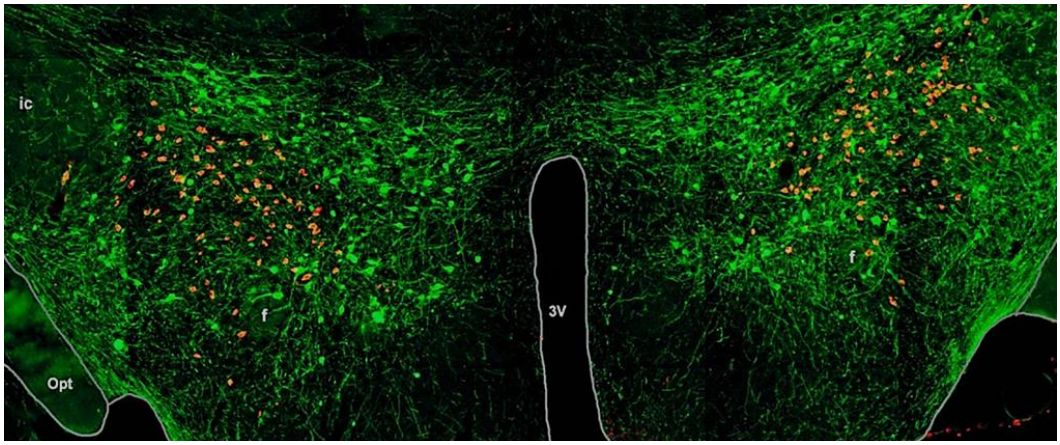

Fig. 1.4: Confocal microscopy image of the neuronal populations containing orexin-A (orange) or melanin-concentrating hormone (green) in the tuberal hypothalamus on a coronal section of a mouse brain. ic, internal capsule; f, fornix; opt, optic tract; 3V, third ventricle. Reproduced from Peyron and Kilduff 2017.

Icv injections of MCH increase food intake in satiated rats (Guesdon et al. 2009), MCH knockout mice are hyperactive and lean (Shimada et al. 1998), and fasting increases levels of *MCH* mRNA (Bertile et al. 2003). The optogenetic activation of MCH neurons in mice induces sleep, but not food consumption (Konadhode et al. 2013). However, MCH signalling can promote motivational behaviors leading to overconsumption of highly-palatable, calorically-dense food (Georgescu et al. 2005) and is involved in stress-induced binge eating (Pankevich et al. 2010), cocaine (Chung et al. 2009) as well as alcohol consumption (Duncan et al. 2005; Karlsson et al. 2016).

The involvement of MCH in food intake in animals has prompted the investigation of potential therapeutic effects of MCH receptor (MCHR) antagonists as anti-obesity agents in humans, although no compound has hitherto proceeded to Phase II (Macneil 2013; Blasiak et al. 2017). In addition, treatment of hippocampal neurons with corticosterone *in vitro* increases MCH expression (Kim and Han 2016). This implies that MCH neurons constitute another substrate through which stressors can affect feeding behavior (Hervieu 2003). Similarly to the orexigenic systems, the relationship between MCH signalling and stress is reciprocal. Blockade of MCHR1 has strong anxiolytic and antidepressant effects (Borowsky et al. 2002; Smith et al. 2006) and MCHR1 knockout mice exhibit reduced depressive-like behavior (Roy et al. 2007).

In the genetic rat model of depression provided by the Flinders Sensitive Line, the total number of OX neurons was found to be higher (16% increase) compared to controls, with no changes in the number of MCH neurons. The increased OX levels have been associated with an induction of depressive state, indicating that OX negatively modulates emotion (Mikrouli et al. 2011).

From the perspective of specific experimental manipulations, the estrogen receptor α agonist was found to decrease the number of MCH-expressing neurons following castration of male mice (Muschamp et al. 2007), indicating a hormonal regulation of this peptide.

1.1.2 Wiring and modulation of orexinergic neurons: intra- and extra-hypothalamic inputs

The LH is the most extensively interconnected area of the hypothalamus (Burt et al. 2011). As briefly dealt with below, OX neurons receive abundant input from structures the limbic system, which could be important for increasing arousal during emotional stimuli and are also regulated by various peripheral metabolic cues, including ghrelin, leptin and glucose, indicating that OX neurons provide a link between energy homeostasis and vigilance states (Sakurai et al. 2005; Yoshida et al. 2006; Sakurai 2007).

Multiple neuronal systems interact with OX neurons (Sakurai 2007). Anterograde tract tracing analyses in rats, based on injections of biotinylated dextran, confirmed that many brain regions innervate the OX neurons directly, with the heaviest afferents coming from the lateral septum, preoptic area, BNST, and posterior hypothalamus (Yoshida et al. 2006). Interestingly, it was also demonstrated that hypothalamic regions preferentially innervate OX neurons in the medial and perifornical fields, while most projections from the brain stem target the lateral field (Yoshida et al. 2006). This indicates that subpopulations of OX neurons may have different physiological functions (Inutsuka and Yamanaka 2013).

In the Tg mouse line with human *prepro-orexin* promoter, retrograde tract tracing with tetanus toxin has identified several areas and neurons in connection with OX neurons, including the basal forebrain (BF) cholinergic neurons, GABAergic neurons of the ventrolateral preoptic nucleus (VLPO), and serotonergic neurons in the median raphe and paramedian raphe (Sakurai et al. 2005). Retrograde tract tracing confirmed that regions involved in emotions, including the amygdala, nucleus accumbens and BNST, innervate OX neurons (Sakurai et al. 2005). The interactions between the limbic system with inputs from corticotropin releasing factor (CRF) neurons, and the orexinergic system have been proposed to maintain wakefulness during stressful events (Winsky-Sommerer 2004).

Of special interest and relevance for the modulation of OX neurons is the synaptic wiring of their somata. It has been stated that unraveling the integration onto these neurons of synaptic inputs from various brain areas would be important to understand the cellular mechanism underlying the essential functions mediated by LH (Burt et al. 2011).

The integrative features of neurons in the CNS strongly depend on the number, density and distribution of the synaptic afferents and efferents (Megías et al. 2001). While the majority of the synaptic inputs in the CNS are received by the dendrites, the synaptology of the cell somata is critical for the generation of the action potential and therefore the control of the neuron firing (Spruston 2008). Neuronal cell bodies in the CNS are either dominated by inhibitory inputs (especially the cell bodies of projection neurons), or have an approximate ratio of excitatory to inhibitory inputs of 1:1 (e.g. inputs onto the perikarya of interneurons) (Shepherd 2004; Douglas et al. 2004; Pinto et al. 2004). Of note, ultrastructural and electrophysiological studies in mice have reported that OX perikarya receive numerous putative excitatory inputs that greatly outnumber inhibitory inputs (Horvath and Gao 2005).

In particular, glutamatergic axons have been reported to account for the majority of excitatory inputs on OX soma, although the source of these excitatory synapses remains to be determined. They likely derive from local glutamatergic neurons, but they may also originate from other hypothalamic and from extra-hypothalamic

regions (Li et al. 2002; Horvath and Gao 2005). Some of the excitatory inputs onto OX somata originate from CRH-producing hypothalamic neurons, suggesting a possible pathway for stress-induced activation of the OX system, given the role of CRH neurons in the response to stress (Winsky-Sommerer 2004).

The observed prevalence of excitatory over inhibitory synapses on the soma of orexinergic neurons was found to be in contrast to perikaryal arrangements of inhibitory boutons in other hypothalamic areas, such as the arcuate nucleus, where inhibitory boutons dominate neuronal perikarya (Horvath and Gao 2005).

In their study of the synaptic wiring of OX cell bodies, Horvath and Gao (2005), did not address, however, the time points of their sampling of the animals. In view of the diurnal changes in the activity of orexinergic neurons (see 1.1.3) the issue of the balance between excitatory and inhibitory inputs onto OX somata has been re-examined in the work of this thesis during day and night, taking into account the behavioral states of the animals (see Laperchia et al. 2017, Chapter 2).

Recordings from transgenic mice expressing green fluorescent protein (GFP) in OX neurons demonstrate that agonists of ionotropic glutamate receptors activate them, while glutamate antagonists inhibit their activity. These results indicate that OX neurons are tonically activated by glutamate (review in Inutsuka and Yamanaka 2013).

In addition, the local network in the LH plays an important role in OX neuron activity regulation. First, regulation of OX neurons is effected within the local orexinergic network itself. Immuno-electron microscopy analyses have shown that OX neurons are directly innervated by OX neurons (Yamanaka et al. 2010). Results from patch-clamp recordings in slice have revealed that OX neurons are directly and indirectly activated by OX via OX2R (Fig. 1.5). Furthermore, OX activates indirectly OX neurons by increasing in them spontaneous excitatory post-synaptic currents (sEPSCs). OX2R is the primary mediator also of this indirect activation (Yamanaka et al. 2010). Although OX-B application elicited in OX neurons of OX1R−/− mice an activation comparable to that elicited in WT OX neurons, OX neurons in OX2R−/− mice failed to respond to OX-B (Yamanaka et al. 2010). These results suggest that OX neurons form a positive feedback circuit between them, which could be responsible for the maintenance of their high level of activity (Yamanaka et al. 2010).

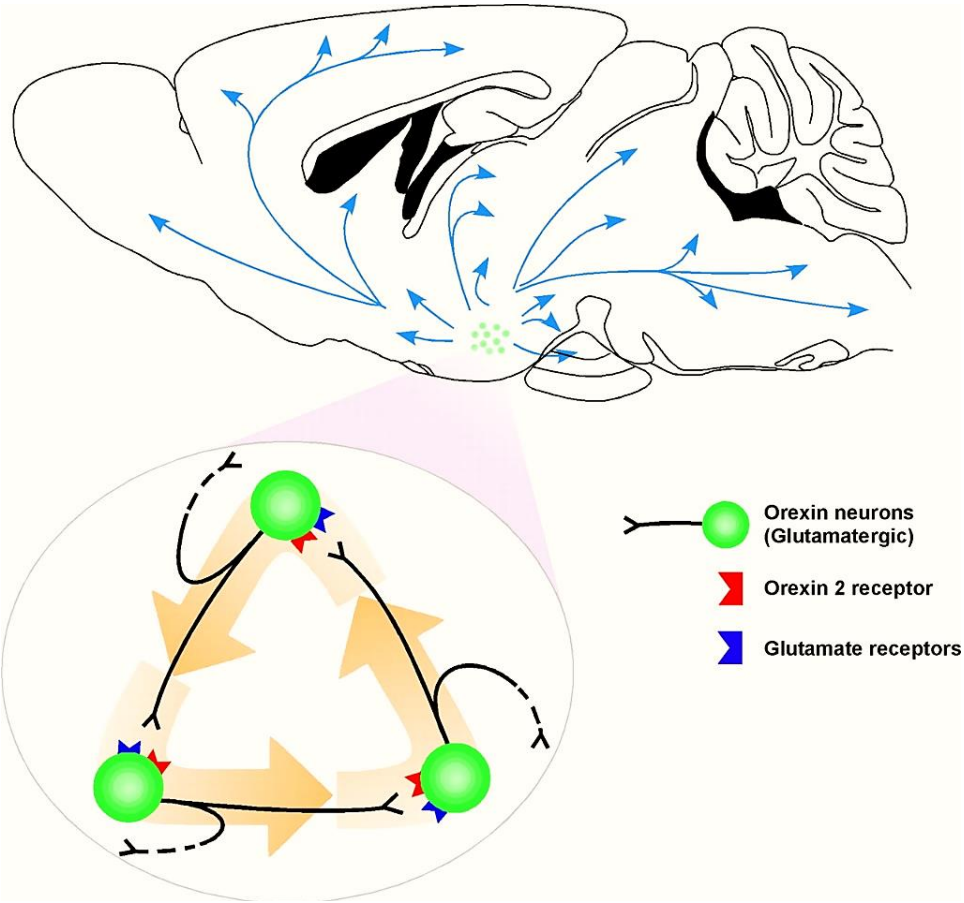

Fig. 1.5: Schematic summary of the mechanism underlying orexin (OX)-induced activation of OX neurons which give origin to widely distributed projections. OX neurons directly innervate other OX neurons activating them through OX2R. This could form a positive feedback circuit, to preserve the activity of OX neurons and thus maintain arousal. Glutamate receptors include AMPA, NMDA, and metabotropic glutamate receptors. Reproduced from Yamanaka et al. 2010.

GABA receptors ($GABA_AR$ and $GABA_BR$) have a role in the homeostatic regulation of neuronal excitability, thus enhancing the stabilization of neural networks (Turrigiano 1999). *In vitro* studies have shown that OX neurons are hyperpolarized and inhibited by both $GABA_AR$ and $GABA_BR$ agonists, whereas MCH neurons are inhibited by $GABA_AR$ agonists (Eggermann et al. 2003; Van Den Pol et al. 2004; Xie et al. 2006).

A recent report has confirmed that OX neurons are inhibited by local GABAergic inputs (Ferrari et al. 2018). The local GABAergic neurons send projections onto OX neurons during sleep, but their firing is depressed during wakefulness by cholinergic disinhibition or by dynorphins released from OX neurons (Ferrari et al. 2018) (see also 1.1).

Studies in epifluorescence and confocal microscopy have revealed somatostatin (SST)-immunopositive varicosities and fibers in the vicinity of OX neurons, and these frequently appeared to contact their perikarya and proximal dendrites (Toossi et al. 2016). GABAergic synapses upon OX somata by SST-immunopositive neurons could further provide an inhibitory influence through SST release upon or in close proximity to OX perikarya or proximal dendrites and also by co-release and action of GABA upon GABAergic synapses on their somata or dendrites (Toossi et al. 2016).

Glycine, a primary inhibitory neurotransmitter in the CNS aside GABA, is widely distributed throughout the brain stem and spinal cord. Functional glycine receptors (GlyR) and glycinergic synapses onto OX neurons identified by electrophysiology and immuno-electron microscopy were found to directly inhibit OX neurons *in vitro*. OX neurons were found to be potently hyperpolarized by glycine in a concentration-dependent manner (Hondo et al. 2011). The expression of GlyR at glycinergic synapses on OX neurons provides a basis for a functional and molecular role of glycine in the physiological regulation of OX neurons (Hondo et al. 2011). However, the origin of glycinergic fibers innervating OX neurons in the LH remains unknown, so that the neuronal pathways that mediate glycine-induced inhibition of OX neurons need to be identified (Hondo et al. 2011; Karnani et al. 2011).

MCH-containing axon terminals establish asymmetric contacts (Bittencourt et al. 1992), and contribute to the synaptic inputs onto OX neurons (Guan et al. 2002; Burt et al. 2011) (Guan et al. 2002; Burt et al. 2011). It has also been postulated that the inhibitory GABA boutons onto OX soma are those that also contain NPY (Horvath et al. 1997) and may originate from the arcuate nucleus (Broberger et al. 1998; Elias et al. 1998; Horvath et al. 1999; Horvath and Gao 2005).

Some populations of LH neurons besides OX- or MCH-expressing neurons (Fig. 1.6), such as CRF, NPY, thyrotropin-releasing hormone, neurotensin, and GABAergic neurons (see 1.2), express neurotransmitters with known electrophysiological actions on OX neurons. The actions of these LH neuronal populations may be important for fine tuning the firing activity of OX neurons to maintain optimal levels of prolonged output to sustain wakefulness and stimulate consummatory behaviors (review in Burt et al. 2011).

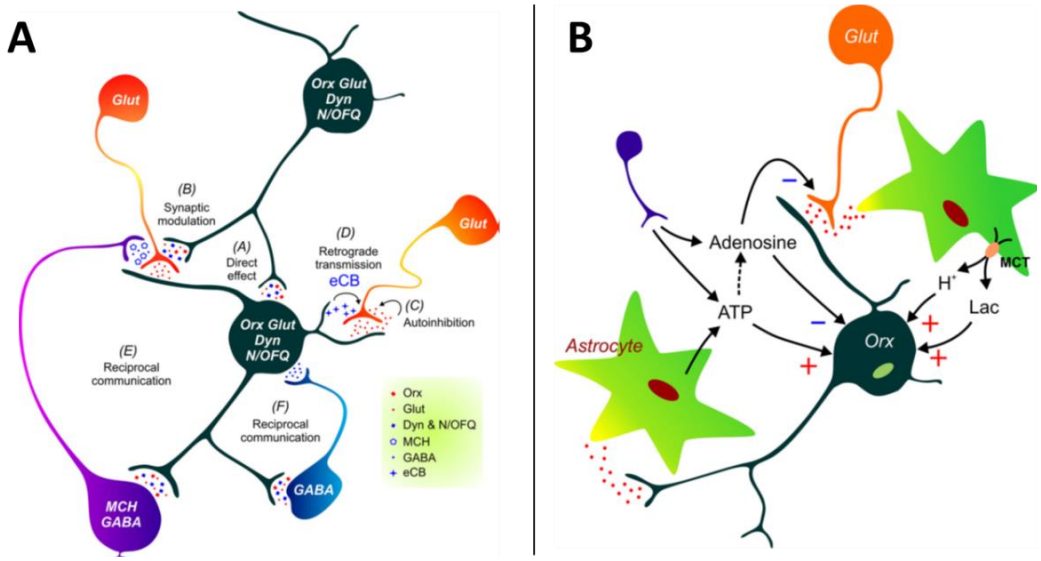

Fig. 1.6: **A**. Regulation of orexin (Orx)-containing neurons by local neurotransmitters. The activity of orexinergic neurons is controlled directly or indirectly by positive and negative feedback mechanisms mediated by neurotransmitters and neuromodulators released by neurons in the lateral hypothalamus. Glutamate (Glut), dynorphin (Dyn), nociceptin/orphanin FQ (N/OFQ), endocannabinoids (eCB), MCH-containing and GABAergic neurons are depicted. **B**. Schematic illustration of the regulation of orexinergic neurons by astrocytes. Glutamatergic transmission can be stimulated in orexinergic neurons via the monocarboxylate transporters (MCTs)- MCT-mediated astrocyte-neuron lactate shuttle. Reproduced from Burt et al. 2011.

Furthermore, leptin receptor-expressing GABAergic neurons have been identified among OX neurons in different species and leptin has been shown to affect the synaptic organization of other hypothalamic peptidergic systems (Horvath et al. 1999; Håkansson et al. 1999; Pinto et al. 2004).

Monoamine neurotransmitters such as dopamine, noradrenaline, and serotonin (5-HT) hyperpolarize and inhibit OX neurons via D1/D2-, alpha 2-adrenergic and 5-HT1A receptors (Yamanaka et al. 2003b; Bubser et al. 2005; Messina et al. 2018). Other factors that reportedly influence the activity of OX neurons include environmental factors such as physiological fluctuations in acid and carbon dioxide levels. It should be noted that factors related to feeding (such as glucose, ghrelin, and leptin) inhibit the activity of OX neurons. The large variety of neurotransmitters and factors that regulate the activity of OX neurons demonstrates the role of these neurons in diverse processes, including functions regulated by circadian rhythms, such as energy balance and vigilance level (review in Inutsuka and Yamanaka 2013).

The local network within the LH and perifornical area consists, as elsewhere in the brain, of neurons and glia, and "gliotransmission" also shapes the output of the LH

neurons, including orexinergic ones (Fig. 1.7). Modulation and negative feedback regulation of excitatory glutamatergic inputs and the release of astrocyte-derived factors, such as lactate and adenosine triphosphate (ATP), can affect the excitability of OX neurons. OX neurons utilize lactate derived from astrocytes as energy substrate (Parsons and Hirasawa 2010). Glutamatergic transmission has been proposed to stimulate OX neurons via the astrocyte-neuron lactate shuttle mediated through the monocarboxylate transporters (review in Burt et al. 2011).

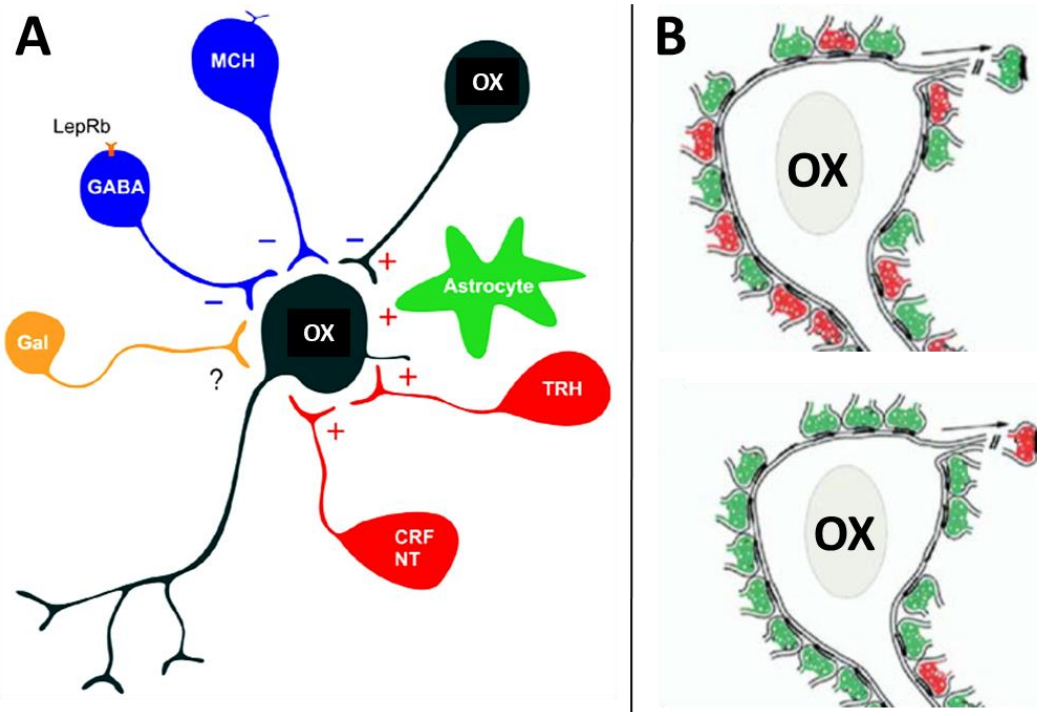

Fig. 1.7: **A**. Local network within the LH. A number of neuronal populations have been identified within the LH/PFA in addition to OX-neurons, including those MCH, TRH, CRF, neurotensin (NT), galanin (Gal) and leptin receptor (LepRb)-expressing GABAergic neurons. Most of these neurotransmitters have been demonstrated to modulate the excitability of OX neurons. These neurons, along with astrocytes, constitute a local network that can fine-tune the activity levels of this brain area through complex interactions. **B**. Schematic illustration of the fasting-induced plasticity of the organization of input to orexinergic neurons: inhibitory is in green and excitatory input in red. The regulatory signals for such synaptic changes are not yet well defined. Adapted from; Horvath and Gao 2005; Burt et al. 2011.

The activation of astrocytes or neurons can induce the release of extracellular ATP, which can also act as a transmitter molecule (Fig. 1.7) (Guthrie et al. 1999; Druzin et al. 2002; Burt et al. 2011). Extracellular ATP directly depolarizes OX neurons via ionotropic purinergic receptors (P2XRs) expressed on the plasma membrane, while having little effect on synaptic inputs, whereas hydrolyzed adenosine from ATP released from neurons can have direct and indirect synaptic effects leading to the inhibition of OX neurons (Wollmann et al. 2005). OX neurons coexpress the P2X(2)R subunit, and, conversely, 80% of the P2X(2)R-immunoreactive neurons in the LH are also OX-immunoreactive in the rat (Florenzano et al. 2006).

1.1.3 Diurnal changes in the orexinergic system

Given the role of the LH in physiological functions critical for survival which undergo substantial changes during 24 h (e.g. food intake and metabolism, sleep and wake states), it may not be surprising that diurnal (day/night) and circadian (*circa diem*) changes have been reported in the LH. Gene profiling in mice has shown some similarities and some differences in gene expression undergoing diurnal changes in the LH compared to other hypothalamic regions (Gerstner et al. 2006).

It is worth recalling, in this respect, that functional, cellular, molecular fluctuations in the hypothalamus during 24 h can be related in different studies to daytime (the light period) and night-time (the period of darkness), the animal's rest and activity and/or state-dependent behavior (sleep and wake).

State-dependent behavior, in which all behavioral performances are inscribed, consists of three states: wake, rapid eye movement (REM) sleep (also called paradoxical sleep), non-REM sleep (also referred to as slow wave sleep, SWS), defined by neurophysiological parameters and, in particular by electroencephalogram (EEG) recording. REM sleep is preceded by non-REM sleep in an obligatory sequence of cycles (non-REM sleep followed by REM sleep) repeated during the animal's sleep period. The wake period corresponds to the activity phase of the animal, and the sleep period to the rest phase. In nocturnal animals, such as laboratory rodents, the activity period, characterized by wake predominance, corresponds to the period of darkness, and the rest period, characterized by sleep predominance, to the light period.

The Fos protein (encoded by immediate early gene c-*fos*) is a marker of neuronal activity, induced by different stimuli (Herdegen and Leah 1998). However, Fos is also expressed in basal conditions in different cell groups of the brain and undergoes in some of these groups a spontaneous oscillation in basal conditions during 24 h (Grassi-Zucconi et al. 1993, 1994).

In the LH, Fos is expressed in basal conditions in hypothalamic neurons including OX, MCH, non-OX and non-MCH neurons (Verret et al. 2003; Modirrousta et al. 2005). In undisturbed rats maintained under a 12 h light/dark cycle, more Fos-immunoreactive nuclei in OX neurons during the night than during daytime has been reported (Estabrooke et al. 2001). This was also documented when rats were maintained under constant darkness, indicating an endogenous oscillation (Estabrooke et al. 2001). In addition, with EEG recording a positive correlation between Fos expression and the amount of wakefulness and a negative correlation with the amount of sleep (non-REM and REM sleep) in the 2 h preceding the animal sacrifice were found in OX neurons (Estabrooke et al. 2001).

The firing of OX neurons has been reported to peak during the active phase in mice and rats (Lee et al. 2005; Mileykovskiy et al. 2005; McGregor et al. 2017). Conversely, MCH release and unit neuronal activity peak prior to and during the inactive phase (Hassani et al. 2009).

The discharge of OX neurons across the sleep/wake cycle can be determined by unit activity and EEG recordings. In rats maintained under a 12 h light/dark cycle, single unit recordings of OX neurons showed a relatively high discharge rate during active waking with a positive correlation of discharge rate with EEG amplitude. Very low discharge rate of OX neurons occurred instead during SWS and REM sleep. This further emphasizes the role of OX in the maintenance of wakefulness (Lee et al. 2005). In contrast, MCH neurons do not fire during waking, but fire sparsely during non-REM sleep and maximally during REM sleep (Hassani et al. 2009; Toossi et al. 2016), which further shows the sleep-promoting role of MCH neurons.

The OX function in stimulating arousal and increasing energy expenditure, as well as the MCH function in decreasing arousal and energy expenditure correlate well with Fos expression in OX and MCH neurons as it has been shown that they respond differently to sleep deprivation (SD) and sleep recovery (SR) (Modirrousta et al. 2005). In these paradigms, the number of Fos-immunopositive OX neurons significantly decreased following SR as compared to SD, while the number of -Fos-immunopositive MCH neurons significantly increased during SR as compared to SD (Modirrousta et al. 2005). Such findings further illustrate the opposite influence of these two neuronal systems.

Experimental studies have suggested the influence of light on OX neurons (Boddum et al. 2016). In the grass rats, a diurnal species, a light pulse has been found to stimulate immediate-early gene induction in OX neurons, whereas dim light housing conditions lowers OX immunoreactivity in the brain (Adidharma et al. 2012; Deats et al. 2014). In contrast, in the mouse, which is nocturnal, 6 h daily exposure to dark pulses (arousal cues for nocturnal species) for 10-16 days activates OX neurons (Marston et al. 2008). Despite the above-mentioned findings indicating that

OX neurons are primarily active during the dark phase in mice, it was demonstrated that exposure to constant light activates mouse OX neurons during positively reinforced tasks (Marston et al. 2008). This is consistent with the lack of the arousing effect of light in humans suffering from narcolepsy (see 1.2.1), although this was suggested to be an indirect effect since no direct pathway from the retina to OX neurons has been found (Hajek et al. 1989; McGregor et al. 2011).

In rats, a diurnal variation in *prepro-orexin* mRNA in the hypothalamus and significant diurnal variation in OX-A immunoreactivity were observed in the preoptic/anterior hypothalamus and the pons, but not in other brain areas, including the LH and the posterior hypothalamic regions. This may correlate with changes in the synthesis of the OX-B peptide, and it would be interesting to determine whether there is diurnal variation in OX-B immunoreactivity as well (Taheri et al. 2000).

It has been generally assumed that the number of OX or MCH neurons, as well as that of cholinergic or histaminergic neurons, detectable by immunocytochemistry remain constant across different behavioral states. A recent study indicates instead a physiological diurnal variation in the number of OX neurons (McGregor et al. 2017). A significantly greater number (24% increase) of OX-immunopositive neurons, without a variation in soma size, was found in undisturbed mice sacrificed during the dark phase compared to the light phase. The finding indicates that OX expression does not reach the threshold for immunocytochemical detection in all OX neurons during the phase of the animal's rest, further corroborating a diurnal oscillation of the peptide expression. In contrast, there was no significant difference in the number of MCH-immunoreactive neurons between the animals in either phase, but a 15% increase in the soma size of MCH cells was found during the light phase compared to the dark phase (McGregor et al. 2017). A diurnal fluctuation in number similar to that of OX neurons (34% increase, with no soma size variation) was found in the same study in histaminergic neurons of the TMN visualized by immunopositivity to histidine decarboxylase (the histamine synthesizing enzyme), while the number of cholinergic neurons (evaluated by choline acetyltransferase immunohistochemistry) in the nucleus of the horizontal diagonal band did not show diurnal variations (McGregor et al. 2017). Given that both OX neurons and TMN histaminergic neurons promote wakefulness, the data indicate that the level of molecule synthesis parallels neuronal activity.

A marked diurnal fluctuation was found in the percentage of Fos-expressing OX neurons following peripheral glycine administration (Hondo et al. 2011). The administration of glycine was found to decrease the activity of OX neurons as examined by Fos immunoreactivity. The number of Fos-positive OX neurons in glycine-treated mice was significantly lower during both the light and dark periods than in saline-treated mice at the same time points (Hondo et al. 2011). There was no reduction in number of OX neurons after glycine administration, suggesting that

glycine does not exert harmful effects on OX neurons, and the finding points instead to diurnal variations in their activation in response to glycine (Hondo et al. 2011).

OX (OX-A) levels can be reliably detected in the cerebrospinal fluid (CSF). Reports from animal studies indicate that the OX release in the CSF presents a circadian pattern (McGregor et al. 2011). Concerning clinical correlates of diurnal changes in OX levels in the CSF, dampening of this diurnal variation has been reported in depressed subjects (Salomon et al. 2003). Along a similar line, reduced levels of OX in the CSF have been reported in people who have attempted suicide, which could suggest that a poorly functioning OX system could play a role in mood disorders (Brundin et al. 2009).

Seasonal changes in OX signalling have also been reported besides daily fluctuations, indicating that the orexinergic system is subjected to a more long term modulation of baseline signalling besides a diurnal modulation, as is the case for other neurotransmitter systems such as the serotoninergic system (Sarrias et al. 1989; Praschak-Rieder et al. 2008).

In humans, the study of OX levels in the CSF by radioimmunoassay revealed that it varies with season, principally correlating with day length period. The monthly average of CSF OX values was found to vary between months with a peak in the summer and a minimum at winter (Boddum et al. 2016).

1.1.4 The orexinergic system and circadian regulation

All the above-mentioned data point to a circadian regulation of the expression, activity and release of OX, as it has been repeatedly stated (e.g. Estabrooke et al. 2001; Deboer et al. 2004; Marston et al. 2008).

Circadian rhythmic changes are generated in mammals by a master clock which resides in the suprachiasmatic nucleus (SCN), lying on the optic chiasm in the anterior hypothalamus. This circadian pacemaker receives direct input from the retina though the retinohypothalamic tract, which originates from melanopsin-containing retinal ganglion cells, and entrains endogenous biological rhythms, synchronizing them to the light/dark cycle. The firing of SCN neurons varies across 24 h, regulated by a molecular clock and communicates. In rats, the diurnal variation in *prepro-orexin* mRNA in the hypothalamus and significant diurnal variation in OX-A immunoreactivity were observed in the preoptic/anterior hypothalamus and the pons, but not in other brain areas, including the LH and the posterior hypothalamic regions. This finding may result in changes in the synthesis of the OX-B peptide. However, it would be interesting to determine whether there is diurnal variation in OX-B immunoreactivity (Taheri et al. 2000), as well as temporal signals to the rest of the brain and body through neural pathways and humoral factors (van Esseveldt et al. 2000; Antle and Silver 2005; Morin and Allen 2006).

A fundamental property of circadian oscillators is that they require an external signal to adjust their rhythm to the external 24 h light/dark cycle (Duffy et al. 2011; Najjar and Zeitzer 2017). The external time cues capable of entraining organisms are referred to as *Zeitgeber* (ZT; the German term for "time giver"). Besides light, other cues may act as ZT, and the most commonly studied nonphotic entraining cues are represented by environmental cues such as temperature, food intake, social cues, exercise, and a powerful synchronizing agent is provided by melatonin, the hormone secreted by the pineal gland. The light/dark cycle has anyhow a powerful entraining effect on the human circadian system (review in Pillai and Leverenz 2017).

Almost all SCN neurons express GABA as a primary neurotransmitter (Buijs and Kalsbeek 2001; Saper et al. 2005). Based on differential expression of neuropeptides along with differences in the afferent and efferent connections, the SCN has been subdivided in two main compartments (Antle and Silver 2005). The dorsomedial compartment, or shell, comprises small arginine vasopressin (AVP) and neurotensin-containing neurons, relatively poor in dendritic arbors. The ventrolateral region of the nucleus, or core, is formed by relatively large neurons with extensive dendritic arbors, which express vasoactive intestinal polypeptide (VIP), besides other peptides and the calcium binding protein calbindin (Moore 1992; Romijn et al. 1999; Moore et al. 2002). SCN output originates from neurons of the shell subregion.

SCN efferents mostly target a nearby region, the subparaventricular zone along the wall of the third ventricle, and from there the information processed in the SCN reaches hypothalamic effectors of body temperature, food intake, sleep/wake regulation (Saper 2013). Information processed by the SCN is therefore transmitted mostly through polysynaptic pathways.

As for the relationships of OX neurons with the circadian timing system, the extensive OX projections target also structures of the neural circadian system (McGranaghan and Piggins 2001; Bäckberg et al. 2002). Initial studies of the termination of OX fibers indicated that they are densely aggregated in the region surrounding the SCN (the peri-SCN region) rather than entering the nucleus itself (Peyron et al. 1998). More recent analyses indicate that OX neurons form putative synaptic contacts onto SCN neurons, and both OXR transcripts have been found in the SCN (Belle et al. 2014). In rodents, the exogenous application of OX was found to suppress the electrical activity of the cells of the SCN (Klisch et al. 2009). This in turn suggests that OX released in the vicinity of SCN neurons during states of arousal can influence the excitability of the master circadian pacemaker (Brown et al. 2008; Klisch et al. 2009; Belle et al. 2014; Belle and Piggins 2017).

Tagging SCN neurons in mice with enhanced green fluorescent protein (EGFP) that reports the activity of the Per1 promotor has provided data on the responsivity of SCN neurons to OX. In these mice, many SCN neurons express the Per1-driven construct (Per1-EGFP+ve), but in some neurons this construct is not detected (EGFP−ve) (Kuhlman et al. 2000; Belle et al. 2009). Such heterogeneity also

extends to the neurophysiological response of SCN neurons during the day, but not at night. Experimental data have revealed that the intrinsic excitability state of Per1-EGFP+ve and EGFP−ve neurons during the day determines how the SCN cells respond to OX (Belle and Piggins 2017).

It has been reported that OX mediate the presynaptic release of GABA in the SCN and that this is critical for the OX modulatory suppression of SCN neuron activity during the day (Belle et al. 2014). OX- GABA- $GABA_AR$-mediated action also operates to suppress activity in SCN EGFP−ve neurons, eliciting distinct and diverse electrical behaviors in these SCN cell populations. The vast majority of moderately hyperpolarized action potential-discharging EGFP−ve (~94%) and Per1-EGFP+ve (~71%) cells were found to be hyperpolarized and silenced by OX (Belle and Piggins 2017). This demonstrates that the magnitude of OX actions on the SCN depends primarily on the intrinsic membrane potential of SCN neurons (Belle and Piggins 2017).

Furthermore, OX signalling has been implicated in the integration of non-photic communication in the SCN. The activities of structures involved in non-photic circadian entrainment are modulated by OX neurons (Pekala et al. 2011; Palus et al. 2015) as well as by neurons of the dorsal raphe nucleus (Kohlmeier et al. 2013). The phase of the SCN clock can be reset by non-photic/arousal-promoting stimuli (Mistlberger and Antle 2011; Hughes and Piggins 2012) during the day. This is associated with suppression of SCN cell activity and clock gene expression (Maywood et al. 2002; Hamada et al. 2004).

In the adult brain, NPY has been documented to inhibit SCN electrical activity, suppress Per1 expression, and phase-advance the SCN clock during the day (review in Belle and Piggins 2017). The suppressive action of OX on SCN electrical activity during the day accentuates the actions of NPY to potently inhibit the SCN cell activity and phase-shifts the SCN clock (Belle et al. 2014). These effects of OX may be important in relieving SCN inhibition of behavioral activity without affecting overall circadian rhythmicity (van Oosterhout et al. 2012; Belle and Piggins 2017).

The relationship of the orexinergic network with the local GABAergic circuits in the modulation of spiking activity in cells is raising increasing attention. For instance, OX action through GABAergic interneurons suppresses the electrical activity of MCH neurons. This provides a switching mechanism which isolates properly the conflicting signals of sleep/wake. Such local ‘switch control’ has been documented experimentally to operate in the SCN circuit as well, presumably acting to avoid conflicts between circadian and arousal signals in animals. However, investigation of how a ‘switch control’ is achieved by the SCN *in vivo* to govern behavior remains to be studied (Belle et al. 2014; Apergis-Schoute et al. 2015; Belle and Piggins 2017).

Mediators of the HPA axis are key regulators of response to stress, and influence the circadian timing system and brain centers regulating the control of food intake

(Fig. 1.8) (Dallman et al. 1995; Balsalobre et al. 2000; Segall et al. 2009; Nader et al. 2010). Disturbances in the circadian rhythmicity of the HPA axis functioning could be caused by chronic exposure to stress, artificial light exposures and reduction in sleep hours, among others (Stevens and Zhu 2015; Koch et al. 2016). Also, the disruption in food intake-related processes could be caused by psychological stress. As mentioned previously, food intake is under the regulation of OX and other related neuropeptides (Fig. 1.8) (Kyrou et al. 2006; Antunes et al. 2010; Blasiak et al. 2017).

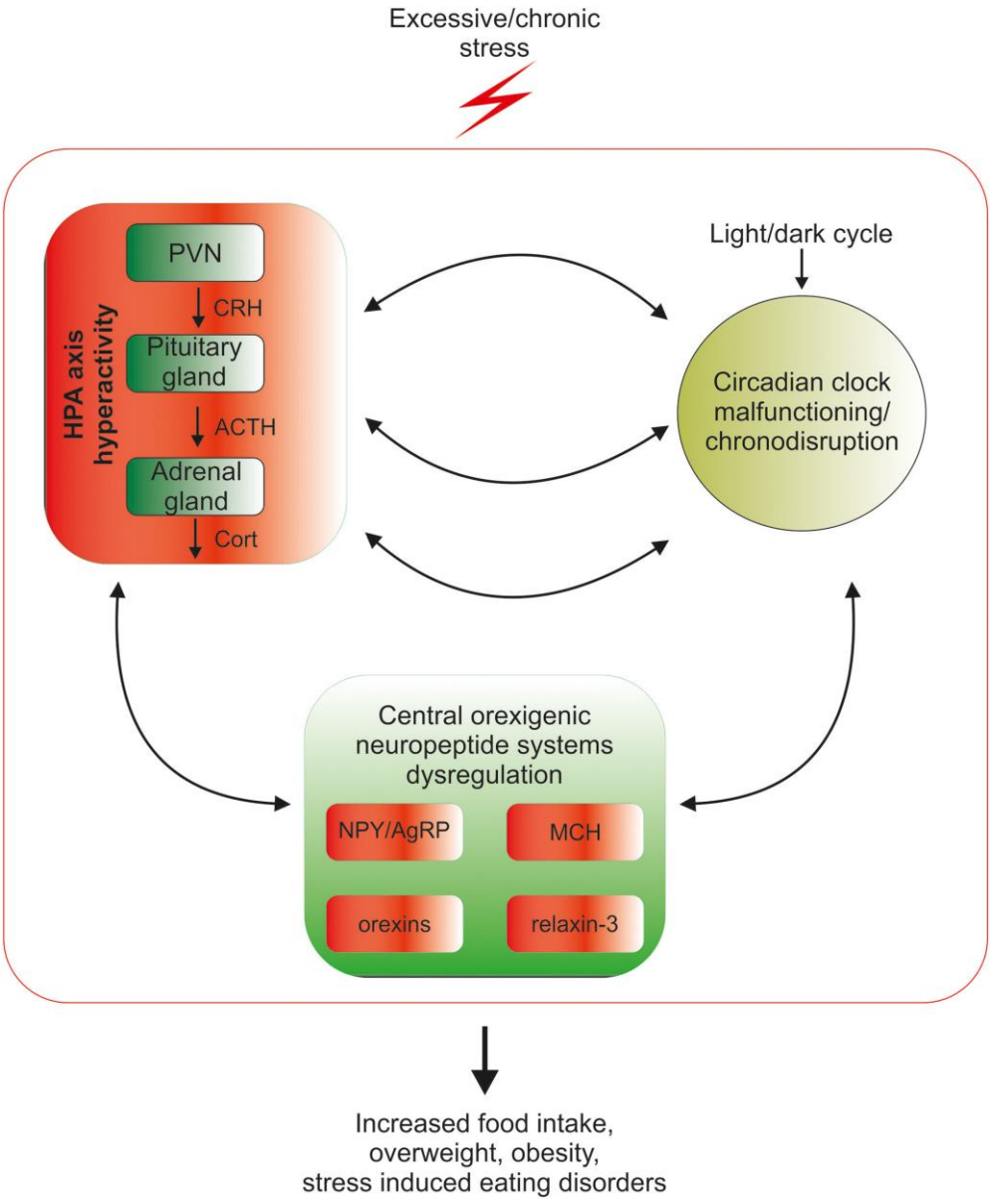

Fig. 1.8: Mutual relationship between the biological circadian clock, stress and orexigenic peptide systems. Circadian clock structures in the brain are under the direct influence of the stress HPA axis mediators: CRH, ACTH and glucocorticoids; therefore,

excessive exposure to stress disrupts the circadian rhythmicity of the organism. Through excessive release of HPA mediators, chronic stress deregulates the synthesis and action of orexigenic brain peptides, which can lead to overconsumption of food, weight gain, obesity and stress-related eating disorders. The control of orexigenic peptide synthesis during prolonged stress exposure is dysregulated at several levels, since excessive stress disrupts circadian rhythmicity, which directly controls both neuropeptide release and HPA axis function. The cycle of excessive stress influences on food intake-promoting peptide system activity and circadian clock structures is closed by the sensitivity of both HPA axis and clock structures to orexigenic peptide system mediators. Reproduced from Blasiak et al. 2017.

Altogether the orexinergic system integrates circadian and metabolic influences in shaping nutritional states and arousal (Selbach and Haas 2006). The orexinergic and circadian timing systems are interconnected. As a result, OX levels in the brain are dependent on the SCN circadian patterns (Yoshida et al. 2001; Deboer et al. 2004; Zhang et al. 2004) and OX neuron activation (Marston et al. 2008). OX fibers and OXRs are present in the SCN (Belle et al. 2014). The activities of SCN neurons are influenced by OX, which can cause phase shifts in cultured SCN neurons and advances in phase in organotypic brain slices (Klisch et al. 2009). The circadian clock control of OX and MCH synthesis makes it necessary to monitor daily rhythms in experimental schemes where disturbances of reward and behaviors are to be examined (Blasiak et al. 2017).

Concerning MCH, there are also reports that the action of MCH on the stress axis is circadian time-dependent. In the rat, *MCH* mRNA expression also fluctuates in a circadian manner, with a low level during the light/inactive phase and a peak after the onset of the dark/active period (Bluet-Pajot et al. 1995). Innervation of MCH neurons by SCN efferents (Abrahamson et al. 2001) allows the influence of the circadian master clock on MCH neurons. The potential feedback of MCH on circadian structures still needs to be verified, but the presence of MCH-receptors on SCN neurons, and reciprocal connections with neurons influencing circadian clock function, notably OX neurons, support a reciprocal interaction of circadian and OX-MCH systems (Guan et al., 2002; Chee et al. 2013; Blasiak et al. 2017).

Following icv MCH injections in the early light/inactive phase, activation of the HPA axis by activation of CRH neurons and stimulation of ACTH release were observed (Jezová et al. 1992). Increased plasma corticosterone levels and anxiety-like behavior were also observed after icv MCH injection during the light phase (Smith et al. 2006). In mice, MCHR1 antagonists reversed the effect of chronic and acute stress (Smith et al. 2009; Lee et al. 2011).

1.1.5 Plastic changes in the synaptic wiring of orexinergic cell bodies

Neuronal activity is regulated in a homeostatic manner so that increases in activity are compensated for by decreases in excitability and decreases in activity by increases in excitability (Turrigiano 1999). These changes are mediated in part by

changes in GABA-Rs, as well as by reciprocal changes in receptors to the excitatory neurotransmitter glutamate (Turrigiano et al. 1998; Kilman et al. 2002; Marty et al. 2004).

A key attribute of the hypothalamic circuits is their remarkable ability to undergo "synaptic rewiring" to maintain the body's homeostatic functions, and in particular OX functions (Alpár and Harkany 2013). Plastic changes of OX neurons, and in particular the presynaptic wiring of their cell bodies, provide a striking example of these adaptive properties.

Following food deprivation, the number of the excitatory input onto OX soma was found to increase, and it was proposed that this could result from multiple humoral and neuronal signals (Horvath and Gao 2005). Interestingly, re-feeding after fasting partially reversed fasting-induced changes in OX synaptology, while leptin administration concomitant to food withdrawal prevented fasting-induced plasticity (Horvath and Gao 2005). This is similar to a finding documented in propiomelanocortin neurons of the arcuate nucleus (Pinto et al. 2004). In *ob/ob* mice (which are leptin deficient and provide a genetic model of obesity), there is an imbalance in the excitatory and inhibitory synaptic density in neurons of the arcuate nucleus, which is rapidly normalized by systemic administration of leptin (Pinto et al. 2004).

The wiring and fasting-induced synaptic remodeling of the OX neurons correlate well with their involvement in the control of arousal and alertness, and it has been suggested that synaptic changes in this circuitry could also underlie functional alterations, such as insomnia, and metabolic disturbances, including obesity (Horvath and Gao 2005).

Experimental evidence on the involvement of the orexinergic network in homeostatic hypothalamic mechanisms was also obtained in nonhuman primates. Fasting for 24 h in monkeys was found to reduce by 50% the level of circulating leptin levels and to increase Fos expression in neurons of the LH, arcuate nuclei and median preoptic area (MnPO) (Diano et al. 2003). A threefold increase of Fos expression was found in OX neurons of the fasted monkeys with respect to controls. In the arcuate nucleus, the Fos-expressing neurons targeted by orexinergic axons contained neuropeptide Y. The presence of leptin receptors on OX neurons and their activation during a metabolic challenge, together with innervation of their targets, indicates that the orexinergic system integrates environmental cues in the regulation of diverse brain activity in nonhuman primates (Diano et al. 2003).

An excitatory-to-inhibitory switch of synapses on OX cell bodies has been reported in obese mice, both in the genetic model represented by *ob/ob* mice and in mice subjected to high-fat diet (HFD), a model of diet-induced obesity (Cristino et al. 2013). In this study, in which many parameters related to retrograde

endocannabinoid signaling were examined, the synaptic changes were found to be reversed by leptin administration, indicating that this synaptic wiring changes were driven by leptin (Cristino et al. 2013).

Experimental exposure to HFD is known to induce various forms of functional and structural plasticity within the reward circuitry (Sharma et al. 2013). A recent report in rats has pointed out plastic changes in OX neurons following exposure to HFD (Linehan et al. 2018). A short-term exposure to a HFD increased the level of glutamate, thereby priming excitatory synapses to OX neurons to undergo activity-dependent long-term depression. However, this priming was transient as it disappeared following a prolonged exposure to HFD. The observed changes may alter OX network properties and could also underlie their physiological role in reward-based feeding (Linehan et al. 2018).

Dynamic remodelling of OX neuron wiring has also been described in response to changing physiological needs such as sleep. Ultrastructural analysis of OX soma in mice following chronic prolonged wakefulness (SD induced by modafinil treatment) showed an increased number of synapses on OX soma, which also resulted in an increase in synaptic strength (Rao et al. 2007). This suggests that prolonged wakefulness could lead to the reorganization of excitatory synapses on OX neurons. As such, experience-dependent plasticity in OX neurons may underlie prolonged wakefulness induced by physiological and environmental factors (Rao et al. 2007, 2008).

In vertebrates, the rhythmic expression of various synaptic and trafficking genes has been postulated to affect behavior by remodelling synapses across day and night (Panda et al. 2002). In the zebrafish, a diurnal vertebrate, live imaging studies have demonstrated a diurnal rhythm in the number of synapses on the axons of OX neurons. Two-photon imaging of synaptophysin (Syn) (a marker of presynaptic terminals) on OX neurons showed dynamic synaptic modifications during day and night. The number of synapses on OX axons were under circadian rhythmicity, which was proposed to be solely regulated by circadian clock (Appelbaum et al. 2010).

Under a condition of SD in the zebrafish, circadian regulation of synapses was dominant, with decreases in synapse number from baseline circadian time (CT14) to the end of SD period (CT20) as observed in non-sleep-deprived controls. However, homeostatic effects were modest (17%), and only observed after 6 h of SD. The findings provide *in vivo* evidence, in a model organism like the zebrafish, of the regulation of OX synaptic plasticity (Appelbaum et al. 2010).

Furthermore, a recent study in zebrafish larvae has reported that the rhythmic structural plasticity of inhibitory synaptic contacts on OX neuron dendrites is modulated by consolidated wake and sleep, and therefore independent from the

circadian clock (Elbaz et al. 2017b). During development, the number of inhibitory synapses on the dendrites of OX neurons increases. Live imaging of inhibitory synapses on OX neuron dendrites showed that the synapse number increases during the night under light/dark conditions and there were no changes under constant light or dark conditions. During the night, SD reduced the synapse number and the number also increased during the post-deprivation daytime sleep (Elbaz et al. 2017b). However, it would be important to understand whether these synapses are physiologically active or silent (Appelbaum et al. 2010; Elbaz et al. 2017b).

In mice, following 6 h of SD, enhancement of $GABA_AR$ immunostaining and increase in the sensitivity to a $GABA_AR$ agonist and amplitude of inhibitory post-synaptic currents (IPSCs) were found in OX neurons (Matsuki et al. 2015). Following 4 h SD, the data differed from results in rats, in which *in vivo* and *ex vivo* studies showed an increase in the amplitude of miniature EPSCs (mEPSCs) in OX neurons (Rao et al. 2007).

In mice, it has been reported that the difference in discharge profiles of the OX and MCH neurons is in line with the different homeostatic responses of these neurons to SD. SD during the day has been found to result in increased $GABA_AR$ and $GABA_BR$ labeling on OX neurons, at variance with MCH neurons (Toossi et al. 2016). Hence, the different changes in both $GABA_AR$ and $GABA_BR$ after SD indicate a homeostatic downscaling after prolonged activity of OX neurons, as reflected by studies based on Fos induction and recording, and upscaling after inactivity of MCH neurons (Toossi et al. 2016). Following SD, OX neurons show changes in $GABA_ARs$ similar to those reported in cholinergic BF neurons (Modirrousta et al. 2007).

The above findings indicate that the organization of inputs to OX somata is not hard wired, but rather changes dynamically in the face of a fluctuating environment or physiological demands, as stated by Horvath and Gao (2005). The above data in the zebrafish indicate that neuronal circuits involved in OX neuron wiring are plastic over the course of the day (Appelbaum et al. 2010). Thus, an intriguing question is whether under physiological conditions (i.e. in the absence of any experimental manipulation) there could be a state-dependent reorganization of synaptic inputs onto OX neuron somata, since, as mentioned above, the study by Horvath and Gao (2005) did not address the time points of their sampling, and the studies in the zebrafish did not address the diurnal organization of excitatory inputs to OX neurons. This issue has been examined by work for the present thesis (see Laperchia et al. 2017; Chapter 2).

Further studies are needed to determine the molecular mechanisms behind dynamic changes in the OX soma wiring. These processes could also provide new insights in disturbances associated with physiological aging and in neurodegenerative diseases, such as AD. Presented in this thesis are data related to the diurnal

organization of the synaptic inputs onto OX neuron somata in aged mice and in a murine model of AD.

1.2 Orexin and the control of sleep and wake

1.2.1 The role of orexin in vigilance states

All the data presented above converge on the evidence that OX neurons and their extensive connectivity provide a link between energy homeostasis and vigilance states.

As mentioned above (see 1.1), *OX1R* and *OX2R* mRNAs show a wide distribution, with partly overlapping but complementary patterns, in the brain (Lu et al. 2000; Marcus et al. 2001; Mieda et al. 2011). This is consistent with the extensive orexinergic projections, which are especially dense in monoaminergic and cholinergic nuclei of the brain stem and hypothalamus which play key roles in the modulation of sleep/wake states (Peyron et al. 1998; Nambu et al. 1999). These nuclei express OX1R and OX2R in a differential manner (Marcus et al. 2001; Mieda et al. 2011). As stated previously (see 1.1), histaminergic neurons in the TMN exclusively express OX2R, while noradrenergic neurons in the LC exclusively express OX1R. In the DR, serotonergic neurons express OX1R and/or OX2R. Mesopontine cholinergic neurons of the laterodorsal (LDT) and pedunculopontine (PPT) nuclei express *OX1R* but not *OX2R* mRNA. Intriguingly, many GABAergic neurons expressing OXRs are intermingled with these monoaminergic and cholinergic neurons (Mieda et al. 2011, 2017).

In agreement with the above findings, electrophysiological recording in brain slice preparations or isolated cells have shown that neurons of the above cell groups are activated by OX *in vitro*. LC noradrenergic cells, VTA dopaminergic cells, DR serotonergic cells and TMN histaminergic cells have all been shown to be activated by OX. It is important to note that, as also stated below, many of these monoaminergic neurons are implicated in increasing arousal and promoting wakefulness (review in Sakurai 2007).

The wake-active serotonergic neurons send inhibitory projections to OX neurons (Li et al. 2002; Muraki et al. 2004; Sakurai et al. 2005). The LC noradrenergic neurons have inhibitory effects on OX neurons (Li et al. 2002; Yamanaka et al. 2006). Histamine seems instead to exert little effect on OX neurons (Yamanaka et al. 2003). Interestingly, in rats, a change in the action of noradrenaline on OX neurons - from excitation to inhibition - following a 2 h period of total SD has been reported (Grivel et al. 2005). It has been proposed that this mechanism could contribute to the growing sleepiness that accompanies SD (Yamanaka et al. 2006).

The activity of monoaminergic neurons in the TMN, LC and DR is known to be synchronized and strongly associated with sleep and wake states: the neurons fire tonically during wakefulness, less during non-REM sleep, and not at all during REM sleep. Such findings indicate that OX-mediated arousal results from the

activation of these wake-active monoaminergic neurons. Specifically, OX neuron activation during wakefulness exerts an excitatory effect on the wake-active neurons, thereby sustaining their activity (Sakurai et al. 2007).

OX exerts an excitatory effect also on cholinergic neurons. Cholinergic neuronal populations of LDT and PPT are involved in the maintenance of wakefulness (Shouse and Siegel 1992; Alam et al. 1999; Eggermann et al. 2001). Other populations of LDT/PPT neurons are implicated in the regulation of REM sleep and muscle atonia during REM sleep. In cats, direct injection of OX into LDT results in an increased wake time and a decreased REM sleep time. However, it has lso been shown that OX inhibits PPT cholinergic neurons by activating GABAergic interneurons. This indicates that OX neurons affect the activities of cholinergic neurons directly and indirectly to regulate arousal and REM sleep (review in Sakurai 2007).

Besides the crosstalk with the neural circuits implicated in the promotion of wakefulness, OX neurons also receive projections from nuclei involved in sleep regulation. It has been reported that OX promotes both wakefulness and energy expenditure by interconnecting with the sleep-promoting VLPO (Mavanji et al. 2015). Neurons of the preoptic area (POA), including the VLPO and MnPO GABAergic/galaninergic neurons, are active during sleep. They are considered to be a sleep center (Saper et al. 2010). They densely innervate OX neurons (Sakurai et al. 2005; Yoshida et al. 2006). The optogenetic stimulation of POA fibers inhibits OX neuronal activity (Saito et al. 2013), while the chemogenetic activation of POA indeed increases sleep (Saito et al. 2013; Zhang et al. 2015). Importantly, VLPO/MnPO neurons and monoaminergic neurons reciprocally inhibit each other (Xu et al. 2015; Mieda 2017). Both the $GABA_AR$ agonist muscimol and the $GABA_BR$ agonist baclofen strongly inhibit OX neurons (Li et al. 2002; Yamanaka et al. 2003; Xie et al. 2006).

OX neurons are also innervated by BF cholinergic neurons (Li et al. 2002; Sakurai et al. 2005; Xie et al. 2006). Carbachol, an agonist at muscarinic receptors, activates a subset of OX neurons (Yamanaka et al. 2003; Sakurai et al. 2005). Thus, OX neurons are inhibited by sleep-promoting neurons and activated by wake-promoting BF neurons. These negative feedback mechanisms may also be important for the fine adjustment of OX neuronal activity to stabilize wakefulness (Tabuchi et al. 2013; Mieda 2017).

On the basis of all the above data on the relationships with the distributed neuronal system of sleep and wake regulation, the orexinergic network plays a critical role especially in the transition between vigilance states (de Lecea and Huerta 2014) and in the maintenance of wakefulness and its stability.

1.2.2 Deficient orexinergic signalling in narcolepsy

The role of OX neurons in sleep-wake state transitions has been demonstrated by the wealth of findings indicating that deficient OX network signalling causes the lifelong sleep disorder narcolepsy (Fig. 1.9), in humans and animals (Kilduff and Peyron 2000; Peyron et al. 2000; Sutcliffe and de Lecea 2002; Crocker et al. 2005; Thannickal et al. 2009).

Narcolepsy, which affects about 1 in 2000 people, is one of the most common causes of chronic sleepiness in humans (Mignot 1998). The onset of this sleep disorder is usually peripubertal, between the ages of 10 and 20, with persistent daytime sleepiness and often a fragmented sleep at night. The diagnosis is not straightforward, with an average time from the onset of symptoms to diagnosis from 5 to 15 years (Roth et al. 2013; Thorpy and Krieger 2014; Scammell 2015). A hallmark of narcolepsy is also represented by disordered regulation of REM sleep. The normal sequence of non-REM-REM sleep (see 1.1.3) is disrupted in the so-called sleep-onset REM periods, which are very frequent in narcolepsy, and in which REM sleep is preceded by wakefulness. Furthermore, in narcolepsy REM episodes can occur at any period of day, with intrusion also into wakefulness. The most dramatic of the REM sleep–like states is cataplexy, which is a sudden episode of partial/complete paralysis of voluntary muscles, usually triggered by strong emotions (Scammell 2015).

Soon after the discovery of OX, two animal studies implicated OX signalling in narcolepsy: (*i*) functionally null spontaneous mutations in the *OX2R* gene were found to be responsible for familial canine narcolepsy (Lin et al. 1999), and (*ii*) targeted deletion of OX in mice (orexin−/− mice) were shown to exhibit a phenotype of sleep/wake alterations similar to human narcolepsy (Chemelli et al. 1999).

The *prepro-orexin*- and OX2R knock-out mice and the OX2R-mutated dogs showed marked narcoleptic symptoms, whereas the OX1R knock-out mice exhibited mild or minute sleep/wake abnormality (Willie et al. 2003). Invariably, this indicates OX2R has a critically involved in the control of sleep/wakefulness (Yamanaka et al. 2010).

Post-mortem studies of the brain of narcoleptics reported that OX peptides are undetectable in the cortex and pons, in which OX innervation is normally found (Fig. 1.2), and 80–100% reduction in the number of OX containing detectable *prepro-orexin* mRNA and OX immunoreactivity in the LH (Peyron et al. 2000; Thannickal et al. 2000, 2003).

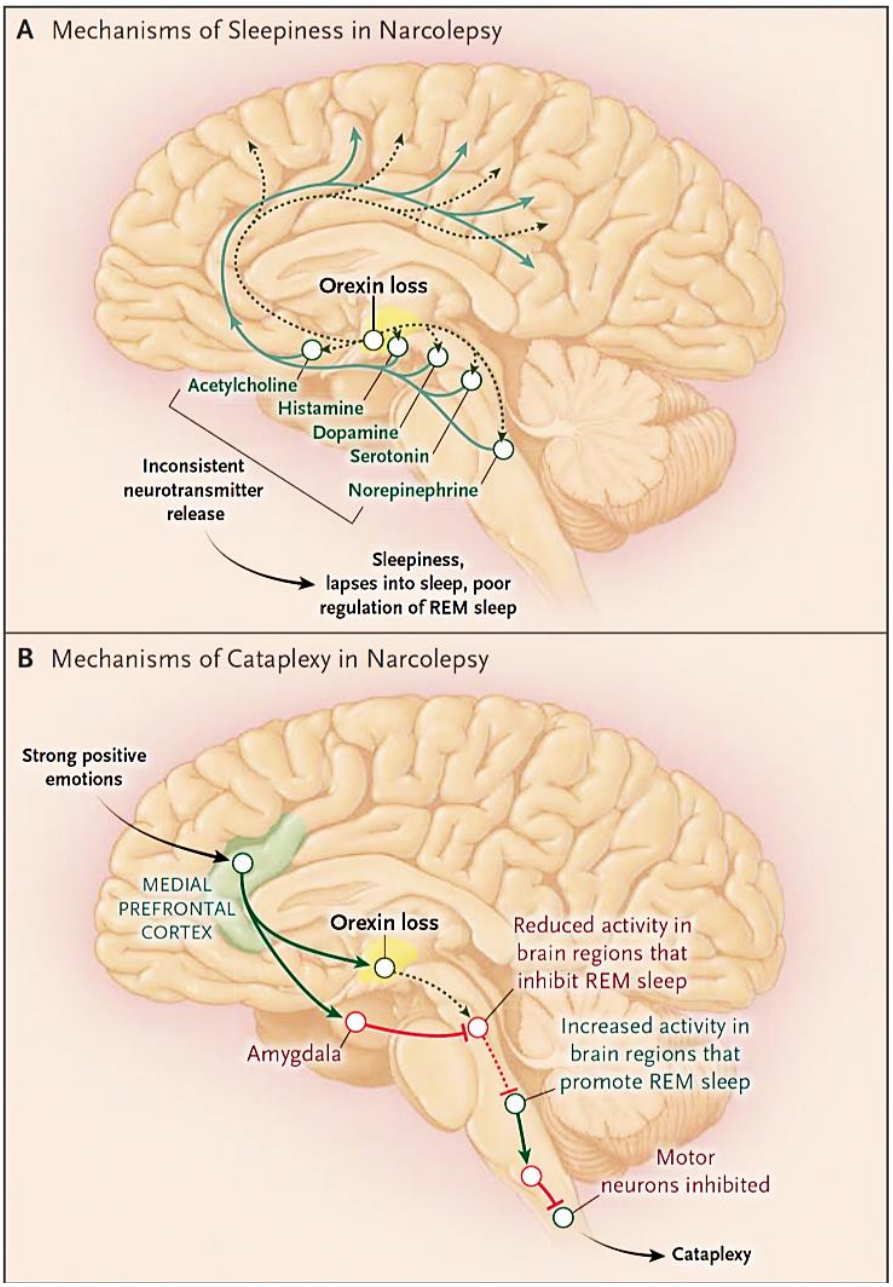

Fig. 1.9: Neurobiologic mechanisms of narcolepsy. **A**. Orexinergic (OX) neurons maintain wakefulness by stimulating a variety of wakefulness-promoting neurons in the cortex, basal forebrain and brain stem. With loss of OX neurons in individuals with narcolepsy, neurons in these target regions may fire less consistently, leading to sleepiness and lapses into sleep. **B**. These neurons also excite brain stem regions that suppress rapid-eye-movement (REM) sleep. Strong positive emotions are thought to activate neurons in the medial prefrontal cortex that excite OX neurons and the amygdala. OX neurons loss lead to imbalance in this pathway, inhibiting brain regions that suppress REM sleep, thus permitting the activation of descending pathways that strongly inhibit motor neurons; the result is partial or complete cataplexy. Pathways

shown in green are excitatory; red are inhibitory. Open circles indicate neuron soma, and dotted lines indicate reduced activity. Reproduced from Scammell 2015.

Two types of narcolepsy have been defined: type 1, narcolepsy with cataplexy, with severe loss of OX neurons; type 2, narcolepsy without cataplexy, which includes most of the symptoms in type 1 but not cataplectic episodes. The discovery that narcolepsy type 1 is caused by an almost complete loss of OX neurons has boosted research on both the neurobiology of this sleep disorder and on the orexinergic system (Trotti et al. 2013; Baumann et al. 2014; Goldbart et al. 2014; Scammell 2015).

In patients affected by narcolepsy with cataplexy, the OX level in the CSF is very low or undetectable. Therefore, a low CSF level of OX is now one of the diagnostic criteria for narcolepsy type I (Nishino et al. 2000; Mignot 2002; Tsujino and Sakurai 2009). In individuals suffering from narcolepsy without cataplexy, the frequency of cases in whom OX concentration in the CSF is low or undetectable is instead much lower (Fronczek et al. 2009; Thannickal et al. 2009).

Since OX neurons contain co-transmitters such as glutamate, dynorphin, and neurotensin (see 1.1), the loss of these co-expressed molecules may also contribute to the symptoms of human narcolepsy (review in Mieda 2017). Of note, MCH neurons are spared in the brain of narcoleptics (Peyron et al. 2000; Thannickal et al. 2000; Thannickal et al. 2009).

Recent reports have indicated that, compared to controls, narcolepsy patients have 94% more histaminergic neurons in the TMN (review in Shan et al. 2015). This increase was found to be higher in narcolepsy patients with >90% OX neuron loss than in patients with ≤75% OX neuron loss. Similarly, the number of histaminergic TMN neurons was increased (53%) in OX ligand knockout mice compared to WT mice, whereas orexin/ataxin-3 transgenic mice showed an intermediate (28%) increase (Valko et al. 2013). This may raise interesting hypotheses on compensatory mechanisms. The finding of an increase of histaminergic neurons in the TMN of the narcoleptic brain, is, however, currently debated (Shan et al. 2015).

The process that destroys OX neurons in narcolepsy remains unknown, although immune-mediated mechanisms are still under discussion and genetic factors are clearly important (Liblau et al. 2015). More than 98% of people with type 1 narcolepsy carry the susceptibility gene HLA-DQB1*06:02, a finding that makes this the strongest known association between the disease and human leukocyte antigen (HLA). This gene is predicted to enhance the risk of narcolepsy by a factor of about 200 (Rogers et al. 1997; Tafti et al. 2014). Recent reports have hypothesized that an autoimmune driven process could be implicated in the loss OX neurons in narcoleptic patients (Kornum et al. 2011; Mahlios et al. 2013), but no

conclusive evidence has been hitherto obtained, and mutations of *prepro-orexin*- or OXR genes are very rare in human narcolepsy.

Regardless of the cause of neuronal loss, the OX signalling deficiency in narcolepsy with cataplexy shows that this neuropeptidergic system has an important role in the regulation of sleep and wakefulness, especially in the maintenance of long, consolidated awake periods (Crocker et al. 2005; Sakurai 2007).

1.3 Orexins in aging and aging-related neurodegenerative disorders

1.3.1 Orexins in the normal aging brain

A number of physiological parameters primarily based on hypothalamic regulation change during normal aging. These include changes in the pattern of sleep and in the consolidation of vigilance states, metabolism, food intake, endocrine and autonomic regulations. As dealt with above, orexinergic signalling is implicated in many of these functions. A number of studies in animals and in humans have reported a decline in the number of OX neurons and OX signalling during aging, involving these neurons and their functional impairment in the process of senescence.

In mice, no age-related changes in the *prepro-orexin* and *prodynorphin* mRNA levels in the LH have been found in an initial study (Terao et al. 2002). However, there was a significant reduction in the *OX1R* mRNA levels in the hippocampus, while *OX2R* mRNA level was significantly reduced in several brain areas besides the hippocampus (thalamus, pons and medulla), with a dampened decrease in the hypothalamus, neocortex and BF of aged animals compared to controls. The findings indicate that alterations in the expression of *OXR* mRNAs could be implicated in age-related functional impairments (Terao et al. 2002).

In rats, a significant reduction (28%) has been reported in the number of neurons expressing the *prepro-orexin* gene in aged animals compared to the adults, and it has been suggested that this could contribute to aging-related dysfunctions (Porkka-Heiskanen et al. 2004). Similarly, a marked reduction in OX neuron immunosignal intensity and *OX* mRNA level was found in the LH of the aged animals compared to adults (Porkka-Heiskanen et al. 2004). Following 6 h of SD, OX neuron immunosignal intensity was found to be significantly upregulated in the adult rats compared to aged ones (Porkka-Heiskanen et al. 2004).

Furthermore, a significant reduction (40%) of OX neurons across all sectors of the LH has been documented in aged rats compared to adults (Kessler et al. 2011). Similarly, in aged rats a reduction (<30%) in the number of the MCH neurons in the medial field of the LH has been reported (Kessler et al. 2011). However, the loss of hypothalamic neurons was not global during aging, as the pan neuronal marker (NeuN) immunoreactivity revealed no significant difference in the total cell number between the adult and aged rats. The pathological mechanisms behind the

age-related reduction in the number of defined neuronal subsets remain unclear (Kessler et al. 2011).

The BF neurons, especially the cholinergic neurons, are innervated by the diverse neuronal groups within the LH, and OX neurons contribute a substantial proportion of the LH input to the BF neurons (Fadel et al. 2005)[i]. In rats, a significant reduction (30%) has been reported in OX inputs onto the cholinergic neurons in aged animals compared to adults in which dense OX fibers are present (Stanley and Fadel 2012). In addition, there are alterations in the OX innervation of the BF nuclei in the aged guinea pigs (Zhang et al. 2005). There was a significant decrease in the immunosignal intensities of OX fibers in the nuclei of the diagonal band of Broca and the magocellular preoptic nucleus of aged animals, although no difference was observed in the medial septal nucleus (Zhang et al. 2005). Although it has been hypothesized that the observed changes could result from a decrease in OX peptides and/or the loss of the targeted cholinergic neurons, the exact mechanisms behind aging-related degeneration of OX fibres remain to be determined. The observed alterations could impair OX drive in the modulation of the functional outputs of BF neurons, in turn leading to a dysfunctional cholinergic transmission during aging (Zhang et al. 2005; Stanley and Fadel 2012).

In healthy humans, the plasma concentration of OX-A was found to be significantly higher in aged individuals than in younger ones (Matsumura et al. 2002). The mechanisms behind such increase remain unclear, and could hypothetically be related to a decrease in plasma concentration of leptin in aged individuals (Matsumura et al. 2002).

A *post-mortem* study of human brains has reported a decrease in the total number and density of OX neurons across all sectors of the hypothalamus in aged individuals compared to adults (Hunt et al. 2015a). In particular, a 23% and 10% decrease in the OX neuron immunopositivity was found in the brain of aged individuals compared to infants and adults, respectively. In the dorsomedial hypothalamus and perifornical area, a significant reduction in the density of OX neurons was observed in aged individuals and adults compared to children and infants (Hunt et al. 2015a).

In aged macaque monkeys, besides sleep impairment and locomotor disturbances, the density of OX-B fibers innervating the LC was significantly reduced compared to adult animals (Downs et al. 2007). However, there were no age-related changes in the neuronal number and levels of OX-B concentration in the serum. The reduction in OX axonal density innervating the LC in the aged nonhuman primate could partly explain the impairment of sleep consolidation in elderly people, although it would be necessary to ascertain if there are alterations in OX-A and OXR levels in humans as well (Downs et al. 2007).

Similarly, aging-related degenerative changes have been documented in OX fibers innervating the brain stem in cats (Zhang et al. 2002). Swollen 'spot like' structures/varicosities indicative of degenerated OX fibers were seen in close proximity to perikarya of neurons in the LC, dorsal raphe and tegmental nuclei of the aged animals only. The degeneration of OX fibers could implicate a disruption in OX system neurotransmission during the aging process (Zhang et al. 2002).

1.3.2 Orexins in Alzheimer's disease and Parkinson's disease

Several reports in the last years have indicated that OX may play a role in some aspects of neurodegenerative disease pathogenesis. Loss of OX neurons and sleep disturbances are known comorbidities of several neurodegenerative diseases, including AD and Parkinson's disease (PD) (Thannickal et al. 2000; Fronczek et al. 2007; Nixon and Smale 2007; Nixon et al. 2015).

AD, the most common cause of dementia, is a chronic, aging-related, progressive neurodegenerative disease characterized by two pathological hallmarks: extracellular amyloid β (Aβ) deposition (plaques) and intracellular neurofibrillary tangles (Serrano-Pozo et al. 2011). The central posit of the ''amyloid hypothesis'', still under discussion, is that amyloid deposition is the causative factor for the initiation of the neurodegeneration cascade, which includes inflammation, gliosis, neuronal damage, neuronal and synaptic loss (DeMattos et al. 2012). OXR2 polymorphism has been proposed as a potential risk factor for the development of AD, but it should be noted that no increased risk of AD has been reported in narcoleptic patients (Scammell et al. 2012; Gallone et al. 2014; Nixon et al. 2015).

Sleep disturbances and alterations of circadian rhythms have been repeatedly reported in AD. These include daytime sleepiness and napping, nocturnal awakenings, REM sleep alterations, cyclic agitation, dysregulation of appetite (Slats et al. 2013). In AD patients, the severity of dementia correlates with sleep impairment and it has been proposed that sleep alterations represent a main reason for institutionalization (Pollak and Perlick 1991).

Neurons of the circadian timing and sleep-wake-regulatory systems are among the neuronal populations targeted by AD (Fronczek et al. 2009). Degeneration of the SCN, with loss of vasopressin and vasoactive intestinal peptide-expressing neurons (see 1.1.4), has been described (Zhou et al. 1995; Farajnia et al. 2012; Pillai and Leverenz 2017). Loss of melatonin diurnal rhythm and decreased melatonin levels in the serum and CSF have also been documented in AD patients (Liu et al. 1999; Zhou et al. 2003).

In the *post-mortem* study of brains of AD sufferers, OX neuron number was found to be decreased by 40% compared to healthy individuals (Fronczek et al. 2012). Despite such quantitative decrease, there were no overt changes in OX cell

morphology, distribution and immunostaining intensity of OX-immunoreactive neurons between the AD brains and healthy controls (Fronczek et al. 2012).

The ventricular CSF levels of OX have been found to be reduced by 14% in AD subjects compared to controls (Fronczek et al. 2012). No correlation was found between AD-associated decrease in OX number and CSF OX levels with age and gender (Fronczek et al. 2012). A correlation had, however, been reported between impairment in the sleep/wake structure and lumbar CSF levels of OX (Friedman et al. 2007). Further studies are required to ascertain the exact correlations between OX neuron numbers and OX CSF levels in AD (Fronczek et al. 2012).

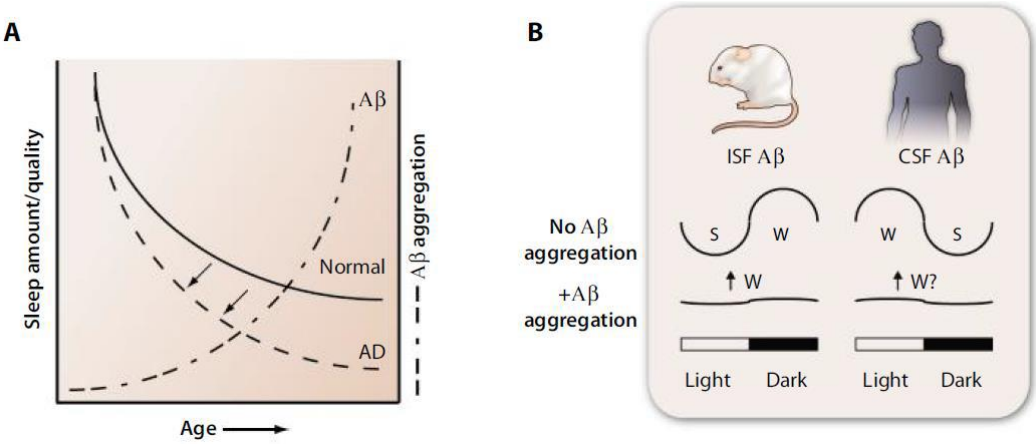

Fig. 1.10: Correlation of amyloid-ß (Aß) with the sleep-wake cycle, as indicated by the findings by Kang et al. 2009 and Roh et al. 2012. **A**: While sleep quality and amount decline with age, Aß aggregation increases in Alzheimer disease (AD) and is associated with sleep decrease. **B**: The levels of Aß in the interstitial fluid (ISF) of mice (which are nocturnal animals) and in the cerebrospinal fluid (CSF) of humans show a diurnal oscillation, increasing during wakefulness (W) and decreasing during sleep (S). The findings obtained in mice indicate that this diurnal oscillation is lost following Aß aggregation. Reproduced from Gerstner et al. 2012.

In a Tg mouse model of AD, the monitoring of the interstitial fluid (ISF) levels of Aβ in the hippocampus has revealed diurnal fluctuations with a 75% increase during the dark period compared to the light period. The ISF levels correlated positively with wakefulness (Fig. 1.10), but there was a negative correlation with the time spent asleep (Kang et al. 2009). Similar findings were recorded in the CSF of healthy adult humans. Also, in humans with the preselinin gene mutations, the diurnal rhythm of CSF Aβ level was observed to be attenuated (Roh et al. 2012). Following SD, the Tg mice spent more time asleep, but ISF levels still fluctuated. The icv infusion of OX significantly increased the ISF levels of Aβ in the light period. However, infusion of OXRs antagonist abolished the diurnal fluctuations

(Kang et al. 2009). The restoration of the diurnal rhythms following OX antagonist removal has suggested that OXRs are needed to maintain ISF Aβ diurnal fluctuations (Kang et al. 2009). Similarly, in a double mutant mouse model of AD, there was a diurnal fluctuation of ISF Aβ levels prior to plaque deposition in the hippocampus and striatum, which was lost in the middle-aged Tg mice which had loads of Aβ plaques (Fig. 1.10) (Roh et al. 2012). The accumulation of Aβ correlated with impairment of sleep in mice with prevention of Aβ plaque formation normalizing the sleep/wake structures (Kang et al. 2009; Roh et al. 2012).

The circadian rhythmicity of CSF OX levels sampling at different time points during 24 h in AD patients and aged controls showed that the orexinergic system is significantly affected, with a decrease of mean OX CSF levels and increase of the OX circadian rhythm amplitude in AD compared to elderly controls. Nevertheless, lack of data on polysomnographic recordings does not allow a correlation between orexinergic system dysregulation and sleep–wake rhythm in AD (review in Liguori 2016). Further evaluation of the circadian activity of AD patients (related to CSF OX levels changes and synaptic wiring of OX neurons) during the course of AD progression is needed (Liguori 2016).

PD is the second most prevalent aging-related neurodegenerative disease after AD, affecting 1–2% of the aging population. Symptoms include tremor, muscular rigidity, akinesia, impairment of postural reflexes; sleep disorder is part of non-motor symptoms of PD, which can precede the motor ones (McGeer et al. 2003; Takahashi et al. 2015). The disease is pathologically characterized by progressive loss of dopaminergic neurons in the substantia nigra pars compacta and appearance of Lewy bodies (intraneuronal inclusions containing abnormal aggregates of misfolded α-synuclein protein). Different brain regions and types of neurons can also be involved (review in Antony et al. 2013).

It has been reported that the incidence of prior narcolepsy diagnosis is five times higher than expected in PD patients, suggesting that narcolepsy or narcolepsy treatments might influence the development of PD (Christine et al. 2012). Owing to the implication of this non-motor dysfunction, the involvement of the OX system in PD has raised considerable interest (Thannickal et al. 2007).

Loss of OX neurons (about 50%) has been reported in *post-mortem* studies of PD victims (Fronczek et al. 2007). Also, the ventricular CSF levels of OX was found to be significantly reduced (25%), and this correlated positively with the number of OX neurons (Fronczek et al. 2007). Low levels of OX level in ventricular CSF have also been documented in late-stage PD patients (Drouot et al. 2003). A 40% reduction in OX levels was recorded in the prefrontal cortex of PD victims compared to healthy individuals (Fronczek et al. 2007). The correlation of OX CSF levels with OX cell number indicates that a dysfunction of the OX system is a factor in the pathogenesis of non-motor dysfunctions in PD.

MCH neurons were also found to be affected in PD (Thannickal et al. 2007): 12% of MCH neurons were found to be lost in stage I and 74% loss was recorded in stage V indicating the loss of MCH neurons correlates with the severity of PD (Thannickal et al. 2007). A similar reduction was recorded for OX neurons, with 12% and 74% loss in stages I and V, respectively (Thannickal et al. 2007). However, there was an increase in MCH cell size which was not observed in OX neurons. A previous report had also reported an increase in the size of MCH neurons in PD (Cabello et al. 2002).

It has been reported that drugs aimed at treating PD could selectively damage OX neurons (Katsuki and Michinaga 2012). However, OX has recently been shown to protect against 1-methyl-4-phenylpyridinium (MPP+)-induced toxicity, which causes dopaminergic neuron death, through induction of HIF-1α (see 1.1) in a dopamine-producing neuronal cell line (Feng et al. 2014).

Altogether these findings suggest that OX might protect against the development of neurodegenerative disease, and that OX loss in AD and PD could exacerbate disease progression by increasing susceptibility to oxidative damage (Nixon et al. 2015).

Although Huntington's disease (HD) is not an aging-related neurodegenerative disease, it is worth mentioning in the present context that OX loss has been documented also in HD. This is a fatal hereditary neurodegenerative disorder characterized by motor abnormalities, psychiatric symptoms and cognitive deficits (Aziz et al. 2008). It is caused by a CAG repeat expansion in the *huntingtin* gene encoding a polyglutamine tract expansion in the huntingtin protein. Neuropathology includes cortical atrophy and loss of striatal medium spiny neurons (Ross et al. 2014; Lim et al. 2017). The age of symptom onset is highly variable, with a mean age around 45 years (Ross et al. 2014).

Pathological studies in the brain of HD victims have shown a reduction in the number of OX neurons, with cell body atrophy, ranging from 10% (Petersén et al. 2005) to 38% (Gabery et al. 2010) loss, with a normal level of OX-A in the CSF (Aziz et al. 2008). A 38% loss of OX neurons was documented in a transgenic model of HD, the R6/2 mice (Petersén et al. 2002; Peterseén et al. 2005).

1.4 Extracellular matrix in the brain

As mentioned at the beginning of this introductory chapter (see 1) and stated below in the study objectives (see 1.5), the findings herewith obtained on diurnal changes in the synaptic wiring of OX cell bodies brought to focus interest also on the ECM, since dynamic adaptation of the ECM can change forms of synaptic plasticity and organization in the adult brain (Frischknecht and Happel 2016).

The ECM constitutes the essential physical scaffolding for cells, and acts as a biomechanical and biochemical support required for tissue rearrangement, differentiation and homeostasis (Frantz et al. 2010).

Neurobiology pioneers, Camillo Golgi and Santiago Ramón y Cajal discovered that neurons are surrounded by a mesh-like structure (Celio et al. 1998). In particular, the so-called "perineuronal nets" (PNNs) were first described as reticular structures by Golgi in the late 1800s (Spreafico et al. 1999).

Before 1970, it was generally accepted that brain tissue is predominantly made of closely apposed neurons and glia, with a very minute amount of ECM. The emergence of several new techniques in the last decades has been of great help in the revision of this view, as it is known that the ECM molecules fill up significant amounts of the extracellular space (Tani and Ametani 1971; Yamaguchi 2000). Thus, initially, the ECM has been seen as a key component for guaranteeing the structural stability of neuronal tissue. Subsequent studies have recognized that the ECM undergoes significant changes during brain maturation (Frischknecht and Happel 2016).

The extracellular space accounts for about 10-20% of the total volume of the mature brain (Nicholson and Sykova 1998). The highly organized ECM which fills the extracellular space is made of molecules already present in the embryo, with important roles in CNS development. These molecules are key players in the adult CNS, where they are present in almost every structure of the brain and spinal cord. The brain ECM is synthesized by neurons and glia (Dityatev et al. 2010a). It has been documented that the ECM is highly heterogeneous in the brain and throughout different developmental stages, including in the LH (Ruoslahti 1996; Köppe et al. 1997; Horii-Hayashi et al. 2015, 2017).

When compared to the systemic ECM, the ECM of the adult brain is unusual in at least two respects. First, the brain exhibits limited ultrastructural well-defined stromal space, unlike other organs and, second, common ECM components of systemic organs (e.g. fibronectin and collagen) are virtually absent from the adult brain ECM where different types of proteoglycans are abundantly expressed and localized to intercellular spaces (Bonneh-Barkay and Wiley 2009).

In the late developmental phases, the ECM in the brain is composed of proteoglycans and glycoproteins like neurocan and tenascin-C, while these components are downregulated in the adult brain. The adult brain ECM is chiefly made of the glycoprotein tenascin-R (TN-R), chondroitin sulfate proteoglycans (CSPGs) such as brevican and aggrecan, with the unbranched polysaccharide hyaluronic acid (HA) as structural backbone (Frischknecht and Happel 2016). A large variety of other components of the ECM include reelins, laminins,

thrombospondins, heparin-sulfate proteoglycans, guidance molecules and transcription factors (Frischknecht and Happel 2016).

The maturation of the ECM closely matches the end of the so-called developmental "critical periods" in the respective brain regions. The key study that elucidated the ECM as the regulatory switch between juvenile and adult plasticity came from the injection of the ECM-cleaving enzyme chondroitinase ABC into the visual cortex of adult rats combined with monocular deprivation. Local weakening of the ECM "re-juvenated" the visual cortex and restored the critical period of ocular dominance plasticity (Frischknecht and Happel 2016). In the follow-up study, visual acuity was restored in adult animals with long-term monocular deprivation by the same manipulation (Pizzorusso 2002).

These and other studies led to the hypothesis that the brain ECM converts juvenile into adult plasticity by structural tenacity by limiting the reorganization of synaptic components (Gundelfinger et al. 2010). The adult brain has thus established an effective way to structurally stabilize neuronal networks shaped during experience-dependent learning, which is fundamental for an effective long-term memory storage and recall (Frischknecht and Happel 2016).

The ECM serves many functions including the regulation of synaptogenesis and synaptic plasticity, compartmentalization of the neuronal surface, neuroprotection, regulation of ion homeostasis and neuron-glia interactions (Frischknecht and Happel 2016). Data from experimental studies indicate that ECM molecules function as synaptic and perisynaptic scaffolds by directing the clustering of neurotransmitter receptors in the postsynaptic compartment and thereby present barriers to reduce the diffusion of membrane proteins away from synapses (Dityatev et al. 2010b). The ECM is thus recognized as a migration and diffusion barrier that allows the trapping and presentation of growth factors to their receptors at the cell surface (Dityatev et al. 2010b).

The ECM also contributes to the migration and differentiation of stem cells in the brain neurogenic niches and organizes the polarized localization of ion channels and transporters at contacts between astrocytic endfeet and blood vessels (review in Dityatev et al. 2010a).

At the synapses in the CNS, which are composed of distinct components, the ECM is present in the synaptic cleft and also extends extra-synaptically along the presynaptic terminal, postsynaptic cell, and perisynaptic process of astrocyte and processes of neighboring microglial cells which periodically make contact with the synaptic structure (Fig. 1.11). The concept of such 'multi-partite synaptic assembly' evolved over recent years, when it became clear that complex multidirectional relations exist between all the distinct components of synapses in the CNS (Verkhratsky and Nedergaard 2014). Advances in the understanding of the ECM

led also to progression from the tripartite view of synaptic signaling (Araque et al. 1999) to the tetrapartite view (Dityatev and Rusakov 2011; Verkhratsky and Nedergaard 2014).

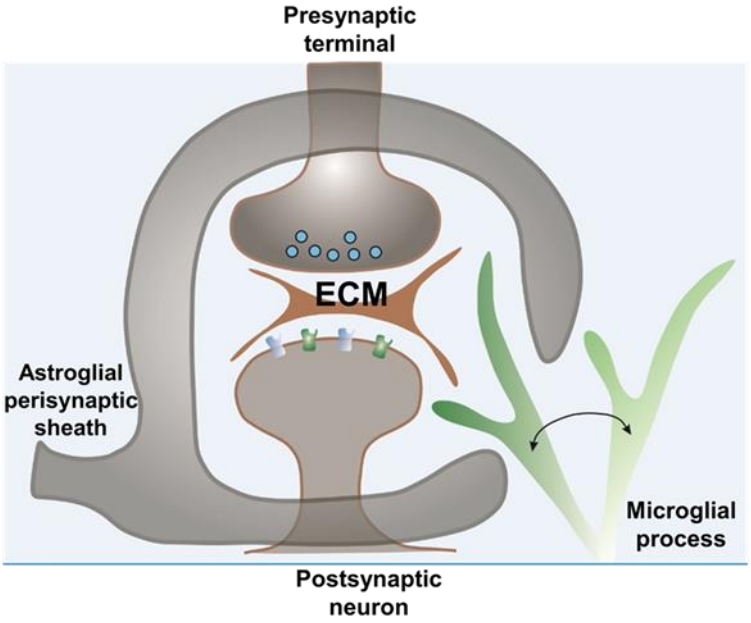

Fig. 1.11: The majority of synapses in the CNS are composed of several components: the presynaptic terminal; the postsynaptic neuron; the perisynaptic process of the astrocyte; the process of a neighbouring microglia cell that periodically contacts the synaptic structure; and the ECM present in the synaptic cleft and also extending extra-synaptically. Adapted from Verkhratsky and Nedergaard, 2014.

The molecular compositions and densities of ECM vary across the different regions of the CNS (Gundelfinger et al. 2010). While the organization of ECM/PNNs is well characterized in some brain regions, and especially in the cerebral cortex, there is dearth of information on the structural organization of the ECM of the hypothalamic circuitry. Certain hypothalamic neurons retain plasticity throughout adulthood (Horii-Hayashi et al. 2017). Analysis of the CGSP-components of the anterior-posterior hypothalamic regions have documented the presence of PNNs, as well as non-PNNs formed and loose ECM (Horii-Hayashi et al. 2017). The functional correlations of the structural variability of the hypothalamic ECM is not yet understood (Horii-Hayashi et al. 2017).

1.4.1 Components of the brain extracellular matrix

The functional attributes of the adult CNS ECM depend on its molecular composition. The ECM is located in three principal compartments: the basement membrane, the neural interstitial matrix and the PNNs.

The basement membrane is a sheet-like layer that serves as a boundary between CNS parenchymal tissue and endothelial cells and is predominantly made of collagen, fibronectin and proteoglycans such as perlecan (Lau et al. 2013). The fibrous protein most abundant within the interstitial ECM is collagen type IV. This molecule is essential for regulating cell adhesion and directing tissue development through its role in chemotaxis and cell migration, while also providing strength to the ECM (Rozario and DeSimone 2010). Perlecan is an essential component of the vascular ECM, interacts with various components of the ECM and has also a role in the endothelial barrier functioning (Farach-Carson et al. 2014). Fibronectin directs the reorganization of the interstitial ECM (Frantz et al. 2010).

In the CNS, the most prominent accumulation of ECM molecules is found in the PNNs. They are made of HA, CSPGs belonging to the family 'lecticans', link proteins and TNR (Kwok et al. 2011). PNNs are a meshwork of ECM, highly elaborate and specialized ECM structure loosely wrapped around synapses and somata of a small proportion of neurons (Frischknecht and Happel 2016). They are especially rich in aggrecan and CSPGs and are found primarily around the fast-spiking, GABAergic interneurons containing the calcium-binding protein parvalbumin (PV) in several brain regions (Dityatev et al. 2007). Recent evidence indicates that PNNs can be found around select group of neurons within the CNS, including glutamatergic neurons (Horii-Hayashi et al. 2015, 2017). PNNs have been found in the vicinity of glial processes that abut onto CNS synapses (Matthews et al. 2002; Brückner et al. 2004). These specialized structures create barriers to the diffusion of neurotransmitters and other signaling molecules (Frischknecht et al. 2009), and limit plasticity of synapses and axonal processes (García-Alías and Fawcett 2012).

During development and in adulthood, the molecules of PNNs are involved in synaptic regulating, including GABAergic and glutamatergic neurotransmission, through their effects on dendritic spines and other components of the synaptic structure (Faissner et al. 2010; Song and Dityatev 2017).

The activities of neurons could facilitate and promote the formation of PNNs (Dityatev et al. 2007; Sorg et al. 2016) , which protect neurons from oxidative stress (Morawski et al. 2015), and are also involved in the modulation of the excitability of GABAergic interneurons (Sorg et al. 2016). They are able to alter the balance of the excitatory/inhibitory inputs to interneurons. The PNNs could regulate the plasticity playing a role in the development of synaptic contacts, as scaffolds for inhibitors of synapse formation and by limiting the motility of receptor on synaptic contacts (Fig. 1.12) (Sorg et al. 2016).

The PNNs were observed to be largely normal in mice deficient in the key ECM proteins such as versican, brevican and neurocan (Dours-Zimmermann et al. 2009). However, the key ECM/PNNs marker *Wisteria florunda agglutinin* (WFA) (Härtig et al. 1994) was not reactive to the primary neurons cultured from the neocortex in

the aggrecan-deficient mice, illustrating they were abnormal (Giamanco et al. 2010). This indicates a crucial role of aggrecan as a PNN component (Giamanco et al. 2010).

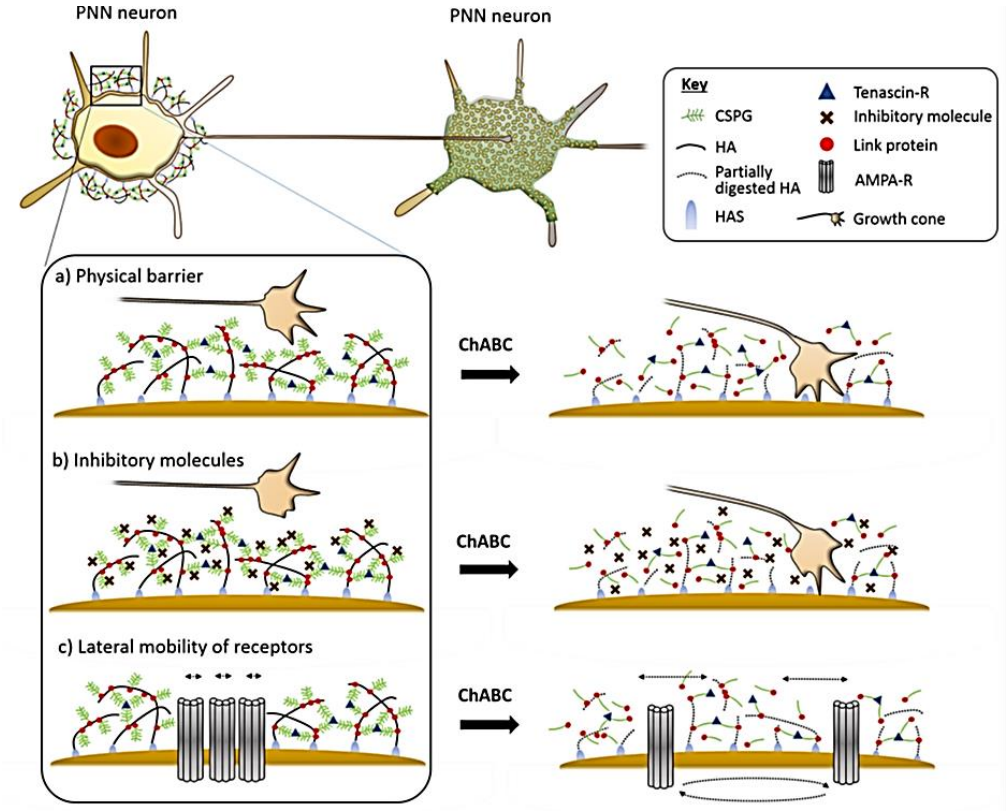

Fig. 1.12: Limitation of plasticity by perineuronal nets (PNNs) via three mechanisms and reinstatement of plasticity by treatment with chondroitinase ABC (Ch-ABC). Plasticity involving PNN-surrounded neurons is limited via: (a) physical barrier by PNNs to incoming synaptic inputs; (b) binding of molecules via specific sites on CSPGs of PNNs (molecules, such as semaphorin 3A, inhibit new synaptic inputs); and (c) prevention of lateral diffusion of AMPA receptors, limiting the ability to exchange desensitized receptors in the synapse for new receptors from extrasynaptic sites. The treatment with Ch-ABC disrupts PNNs, thereby reinstates juvenile-like states of plasticity. HA, Hyaluronic acid; HAS, hyaluronic acid synthase. Reproduced from Sorg et al. 2016.

HA, a unique glycosaminoglycan, is extruded extracellularly. It is the backbone of ECM in PNNs and in the perisynaptic extracellular space outside the PNNs. Also present in the CNS are hyaluronan synthases, the synthesizing enzymes of HA (HASs; HAS1 and HAS3). The different isoenzymes (HASs) possess different biochemical properties. HAS3 is the most active HAS and produces HA polymers with shorter chains (~2×105 Da), whereas HAS1 and HAS2 synthesize HA

polymers with high MW chains (~2×106 Da) (Itano et al. 1999; Itano and Kimata 2002). Recent findings indicate that HAS1 is predominantly located in the membrane of the axon and may function in the maintenance of PNNs, although it is not the most abundant HAS in the brain (Li et al. 2017).

HA binds and coordinates the CSPGs cross-linked glycoproteins for the formation of the ECM meshwork (Frischknecht and Happel 2016). Perisynaptic HA-based ECM may create barriers for diffusion of synaptic molecules and contributes to the compartmentalization of the synaptic machinery (Wlodarczyk et al. 2011).

The combinations of numerous molecules create diverse biochemical properties on the PNNs. The HA-link proteins HAPLN 1, 3, and 4 bind to both the HA backbone and the CSPGs for stabilization of the PNNs in the CNS (Kwok et al. 2011). However, the loose interstitial ECM does not possess the HAPLN. (Galtrey et al. 2008).

CSPGs (>15 isoforms are identified in the CNS) consist of a protein core (Corvetti 2005) and can be categorized based on the distinct properties of their core proteins, sulfation patterns, location, size and modular composition (Schaefer and Schaefer 2010). Modular CPSGs have multiple protein domains and are the major constituents of the healthy CNS ECM. They are further subdivided into HA-binding and non-HA binding (mainly basement membrane CSPGs) (Rauch 2004). The major proteoglycans belong to the lectican family members and are represented by aggrecan, neurocan, brevican and versican. They function in promoting or inhibiting neuritic growth (Bandtlow and Zimmermann 2000).

Studies have highlighted the essential roles of the sulfation patterns of CSPGs in PNNs formation. Tg mice with reduced chondroitin 6-sulfate (C6S) show poor regeneration after a lesion in the CNS (Lin et al. 2011), while Tg mice overexpressing chondroitin 6-O-sulfotransferase 1 (C6ST-1) retain a juvenile-like CS sulfation and show impaired PNN formation (Miyata et al. 2012). In addition, overexpression of C6ST-1 prevents the maturation of electrophysiological properties of PV-expressing interneurons and reduces the inhibitory effects of these cells because of impaired PNN formation. As a result, Tg mice overexpressing C6ST-1 retain a juvenile level of ocular dominance plasticity even in adulthood (Miyata et al. 2012). Interestingly, overexpression of C6ST-1 selectively decreases aggrecan in the aged brain without affecting other PNN components (Miyata et al. 2012; Miyata and Kitagawa 2016).

Heparan chondroitin sulfate proteoglycans (HSPGs) and CSPGs are prominent ECM constituents of the subependymal zone. An important role for CSPGs in the neurogenic niche has been suggested by the observation that collective removal of glycosaminoglycan chains from CSPGs by chondroitinase ABC leads to severe disturbances in the proliferation and neurogenic differentiation of stem cells

(Bradbury et al. 2002)[ii]. As a result of their extensive exposure on the protein backbone and their acidic nature, glycosaminoglycans have been suggested to accumulate and present growth factors to respective receptors on stem cell surfaces. Stem cell biology is essentially dependent on these soluble and highly diffusible molecules (Dityatev et al. 2010a).

The composition of CSPGs in PNNs has been distinguished from that of the loose ECM with the use of extraction procedures (Deepa et al. 2006). The composition and appearance of PNNs varies across different regions of the CNS (Vitellaro-Zuccarello et al. 2007). For instance, in some brain regions, PNNs appear as distinct structures separate from the loose ECM, whereas in the ventral spinal cord they are denser with higher intensity labeling of PNNs and the surrounding neuropil (Vitellaro-Zuccarello et al. 2007). Also, PNNs and the cell types surrounded by PNNs can be heterogeneous even within a single region (Sorg et al. 2016).

The is dearth of information on the quantitative analysis of the distribution patterns and cell specificity of PNNs, which could perhaps shed light on their functional roles. In mice and rats, a recent study on PNN associated neurons in different brain areas shows their distribution and expression differs within the different brain areas (Lensjø et al. 2017). The most abundant expression was found in cortex (medial entorhinal and visual), while low level expression was observed in the dorsal hippocampus with intense expression in the CA2 subfield. Species differences in expression were found in the hippocampus (Lensjø et al. 2017). PNNs enwrapped PV neurons in the visual cortex, whereas they were found to enwrap mainly excitatory CamKII- expressing neurons in the hippocampal CA2 field. In the medial entorhinal cortex, in addition to PV cells, reelin-expressing cells colocalized with PNNs. Interestingly, following the enzymatic removal of PNNs, there was a considerable effect on the number of PSD-95 or gephyrin puncta (see Chapter 2) (Lensjø et al. 2017).

Tenascins are a family of large ECM glycoproteins with four known members in the vertebrates: tenascin-W, tenascin-C (TN-C), tenascin-X and TN-R. The discovery of TN-R was a multistep process. It was originally described as low molecular weight J1 glycoprotein using an antibody recognizing both TN-C (the high molecular weight J1 glycoprotein) and TN-R (Kruse et al. 1985). TN-R was also discovered independently in the chicken and named ‘restrictin’, since its expression is restricted to the nervous system (Rathjen et al. 1991). TN-R is highly homologous between species: when compared with rat TN-R, the homology of the protein coding region of the human TN-R is 93% and 87% for amino acid and nucleotide sequences, respectively, and when compared with chicken TN-R, it is 75% for both sequences. Functional regions of the molecule are the first 23 amino acids, a cysteine-rich N-terminal region corresponding to a typical signal peptide, 4.5 epidermal growth factor-like domains, 8 or 9 fibronectin type III repeats, and a

carboxyl-terminal region globular domain resembling the β and γ chains of fibrinogen (Carnemolla et al. 1996).

TN-R accumulates in large polymers at nodes of Ranvier and participates in the macromolecular organization of PNNs by assemblage of protein complexes of ECM proteins, glycosaminoglycans and proteoglycans (Kwok et al. 2011). The lecticans, including aggrecan, versican, neurocan and, brevican (with highest affinity) binds to TN-R. Interactions with lecticans can result in collaborative or inhibitory action depending on the developmental context. Lecticans share the same binding site on TN-R, namely, the fibronectin type repeats domains 3–5 (Lundell et al. 2004; Anlar and Gunel-Ozcan 2012).

Some neuronal cells and type-2 astrocytes produce *TN-R* mRNA *in vitro*, while *in vivo* mRNA expression suggests synthesis by certain subpopulations of neurons, release into the ECM and probably receptor-mediated binding by PV neurons in cortical and deep gray matter (Wintergerst et al. 2001). During the embryonic period, TN-R is observed in many species and postnatally the expression decreases in oligodendrocytes but not in mature neurons in rodents where it is observed in particular cortical regions and layers and in the PNNs of the gray matter in the spinal cord (Galtrey et al. 2008).

TN-R interacts with cell surface as well as ECM molecules homo- or heterophilically. TN-R has multiple, sometimes opposite roles. Its versatility includes adhesive or anti-adhesive, growth-promoting or inhibiting effects, depending on the type of targeted cells, receptors and signaling pathways, their location in the CNS, the composition of the surrounding ECM, and the time of interactions. It affects cell migration, differentiation and adhesion (Anlar and Gunel-Ozcan 2012).

TN-R deficiency results *in vitro* in reduced oligodendrocyte differentiation and delayed myelin basic protein expression: this is corrected by addition of TN-R (Czopka et al. 2009). The autocrine role of TN-R on oligodendrocyte differentiation had earlier been documented (Pesheva et al. 1997). On the other hand, TN-R overexpression results in reduced migration in embryonic stem cells which travel shorter distances and differentiate more. TN-R also induces the generation of GABAergic neurons (Hargus et al. 2008). Although ECM molecules such as laminin, fibronectin, TN-C are involved in certain human diseases, TN-R has not been implicated in human diseases except oligodendrogliomas and gangliogliomas (El Ayachi et al. 2011).

Mice deficient for TN-R display less developed PNNs, WFA staining that does not extend well to the dendritic shaft and a decrease in axonal conduction velocities in the CNS (Weber et al. 1999). In an experimental model of ischemic stroke in rats, in addition to neuronal loss, peri-infarct regions showed loss of PNNs WFA

labelling and, to a lesser degree, loss of CSPG core protein staining (Hobohm et al. 2005).

1.4.2 Involvement of the extracellular matrix in neuroinflammation and neurodegeneration

As mentioned above, PNNs have been studied for their contributions to synaptogenesis, neuroprotection, and experience-dependent synaptic plasticity, including critical period plasticity (Soleman et al. 2013). However, little attention has been given to the ECM organization within the neuropil (interstitial ECM) during neuroinflammation. The ECM is, however, increasingly implicated in neurodegenerative conditions (Bonneh-Barkay and Wiley 2009).

TN-R expression is affected by various molecules, is inhibited by tumor necrosis factor-α produced by activated microglia after peripheral nerve injury (Angelov et al. 1998) and upregulated by platelet derived growth factor, thyroid hormone and TN-R itself (Pesheva and Probstmeier 2000). Following spinal cord injuries, TN-R is upregulated around the lesions sites (Gaudet and Popovich 2014). Certain effects of TN-R on plasticity and repair are mediated by cytokines. By activating microglia, TN-R indirectly promotes the local secretion of cytokines and growth factors including, transforming growth factor-β and nerve growth factor (Liao et al. 2005).

During excitotoxicity (in the kainic acid toxicity model), many of the associated neurodegenerative changes are linked to ECM alterations. ECM changes have been documented to include reduction in laminins and phosphocan, and increases in neurocan and brevican. However, it seems that degeneration of the ECM does not directly cause neurodegeneration but rather makes neurons susceptible to activation-associated cell death (Kaminska et al. 1997).

In multiple sclerosis (MS), a demyelinating disease with neuroinflammatory stigmata, accumulation of laminins in active MS lesions, associated with the basement membrane of endothelial cells, has been reported (Van Horssen et al. 2007). This laminin accumulation was not seen in inactive MS lesions. Also, high molecular weight HA synthesized by astrocytes in chronic lesions were evident (Van Horssen et al. 2007). There was matrix metalloproteinase (MMP)-19 upregulation associated with microglia (Van Horssen et al. 2006). A striking loss of TN-R and TN-C was also documented in acute MS lesions, in contrast to the TN-R and TN-C accumulation in chronic MS lesions (Gutowski et al. 1999).

In chronic demyelinated MS lesions, accumulation of a high-molecular-weight HA synthesized by astrocytes has been reported (Back et al. 2005). This was thought to inhibit remyelination as oligodendrocyte progenitor cells do not mature into myelin-forming cells in demyelinating lesions where high-molecular-weight HA is present (Back et al. 2005).

Aberrant changes in ECM components have been documented to be associated with the pathological hallmarks of AD (Morawski et al. 2014) (see 1.3.2), and the remodelling could mediate cell proliferation, differentiation and apoptosis (Dityatev et al. 2010b; Soleman et al. 2013). The functional consequences of such remodelling may be dependent on the local specific organization of the ECM as established in animal models. During AD pathology, any or all of the key ECM components might be affected, though the reports on changes in ECM components in AD are contradictory (Lepelletier et al. 2015).

Proteoglycans such as the specific HSPG, perlecan have been shown to be present in both Aβ plaques and NFTs. They are thought to contribute to disease pathogenesis by accelerating the formation of Aβ through preventing proteolytic degradation. It has also been previously reported that high molecular fibronectin forms appear more frequently and at higher amounts in plasma in AD patients than in age-matched controls (Lemańska-Perek et al. 2009), and the levels of plasma fibronectin are higher in AD patients than in healthy controls and individuals with mild cognitive impairment (Muenchhoff et al. 2015). In contrast, unchanged plasma fibronectin concentrations have also been described in AD (Rattan et al. 1988).

Collagen IV, perlecan and fibronectin expression has been reported to be increased in subclinical AD and AD patients in the frontal and temporal cortex, whereas no further increase was detected between subclinical AD and AD, supporting the hypothesis that significant ECM changes occur during the early stages of AD (Lepelletier et al. 2015).

Although changes in ECM and PNNs are reported in the initial stages of AD, the relationship between the changes in ECM components and the hyperphosphorylation of tau is unclear. A recent report indicates that the overexpression of tau may break the balance of ECM components and structure of the PNNs by regulating HASs expression and HAS1 axonal localization. This has been suggested to promote AD progression by regulating neuronal plasticity (Li et al. 2017).

Furthermore, a *post mortem* report in AD has indicated a loss of two-thirds of the PNNs labelled by WFA, with the PNNs intact in healthy control subjects (Baig et al. 2005). There was a granular disintegration of PNNs around some PV neurons in the cerebral cortex, though the density of PV neurons did not differ (Baig et al. 2005). In another report, the cortical neurons associated with PNNs were largely spared from neurofibrillary changes in AD even in severely damaged regions (Brückner et al. 1999).

Concerning neuroinflammatory paradigms, it is worth reporting that in a mouse model of American trypanosomiasis or Chagas disease, caused by the intracellular parasite *Trypanosoma cruzi*, immunohistochemical assays have shown an increase

in the level of expression of the ECM components fibronectin and laminins in the cerebellum of acute and chronic infected animals compared to uninfected controls (Silva et al. 1999).

1.5 Specific objectives of the experimental studies

The laboratory in which this thesis was performed has long been engaged in diencephalic mechanisms of regulation of state-dependent behavior (sleep and wake) in the adult and aged healthy brain (e.g. Palomba et al. 2008; Colavito et al. 2015), and in rodent models of diseases in which the alternation of sleep and wake and/or the sleep structure are altered (Etet et al. 2012; Laperchia et al. 2016; Tesoriero et al. 2016).

In this framework, the present investigations focused on the study of the synaptic wiring of orexinergic neurons and the surrounding ECM in normal conditions in the periods of sleep or wake predominance in mice, in a murine model of AD and in a murine model of sleeping sickness.

The main specific aims of the thesis are as follows:

1) Study of the synaptic wiring of OX cell bodies in the periods of sleep or wake predominance in adult mice

2) Study of the synaptic wiring of OX cell bodies in the periods of sleep or wake predominance in aged mice, as well as in the AD model provided by adult and aged double-mutant TASTPM mice

3) Study of the ECM of the LH of adult mice in the periods of sleep or wake predominance in basal conditions, and in a murine model of sleeping sickness

2. Study of the synaptic wiring of orexinergic neuron soma in the periods of sleep or wake predominance in adult mice

This study has been published in the article indicated below, from which the text and figures are reproduced. The candidate's contribution to the findings has been substantial, as he has processed the tissue and performed the quantitative analyses for the entire part related to the visualization of presynaptic neurotransmitter transporter and related postsynaptic scaffold protein at excitatory and inhibitory synapses.

Brain Struct Funct
DOI 10.1007/s00429-017-1466-3

SHORT COMMUNICATION

The excitatory/inhibitory input to orexin/hypocretin neuron soma undergoes day/night reorganization

Claudia Laperchia[1,2] · Roberta Imperatore[3,4] · Idris A. Azeez[1] · Federico Del Gallo[1] · Giuseppe Bertini[1] · Gigliola Grassi-Zucconi[1] · Luigia Cristino[3] · Marina Bentivoglio[1]

Received: 19 July 2016 / Accepted: 20 June 2017

2.1 Introduction

Orexin (OX)/hypocretin-producing neurons represent a relatively small neuronal population which resides in the perifornical and lateral hypothalamus (LH). These cells give origin to a widely distributed innervation of the neuraxis, with an extensive connectivity with other hypothalamic and extrahypothalamic circuits (Peyron et al. 1998; Burt et al. 2011). The activity of OX neurons and related networks represents a key element in the regulation of wakefulness stability and arousal, energy homeostasis, as well as motivated behaviors including feeding, reward seeking, and responses to anxiety and stress (Kukkonen 2013; de Lecea and Huerta 2014; Mahler et al. 2014; Sakurai 2014).

The local extracellular concentration of OX in the LH (Yoshida et al. 2001) and the level of OX-A in the cerebrospinal fluid of rats and primates (Fujiki et al. 2001; Zeitzer et al. 2003; Zhang et al. 2004) oscillate during 24 h, with higher values during the animal's activity period than during the rest period. Studies based on cFos immunoreactivity, a marker of neuronal activation, indicate that in basal conditions in rats (Estabrooke et al. 2001; Modirrousta et al. 2005) and mice

(Marston et al. 2008; Palomba et al. 2015a), the activity of OX neurons increases at night (the activity/wake period) and decreases at daytime (the rest/sleep period) in rodents, which are nocturnal.

Electrophysiological recordings in rats have shown that OX neurons discharge during wake and are silent during sleep (Lee 2005; Mileykovskiy et al. 2005). Altogether, these findings point to a daily change in the activity of orexinergic cells.

Different paradigms have pointed out synaptic plasticity phenomena in OX neurons in response to challenges. In particular, reorganization of excitatory/inhibitory inputs onto OX perikarya after food restriction and in obesity (Horvath and Gao 2005; Cristino et al. 2013) and increased excitatory innervation after prolonged wakefulness (Rao et al. 2007a) have been reported in mice. In larvae of zebrafish, a diurnal vertebrate, it has been evaluated that the number of inhibitory synapses on OX dendrites peaks during the night (Elbaz et al. 2017b). However, it has not been hitherto investigated whether the excitatory/inhibitory balance in the innervation of OX cell bodies undergoes daily changes in basal conditions. Here, in mice not subjected to any manipulation, we tested the hypothesis that the excitatory/inhibitory wiring of OX cell bodies is remodeled during the periods of wake and sleep predominance.

To this purpose, we used established methodological approaches based on multiple immunofluorescent labeling of presynaptic terminals and postsynaptic scaffolding proteins (Henny and Jones 2008; Ippolito and Eroglu 2010; Cristino et al. 2013; Inan et al. 2013). We first identified and quantified with epifluorescence neurochemical excitatory (glutamatergic) and inhibitory (GABAergic) appositions on OX-A cell bodies. Using presynaptic vesicular transporters combined with synapse scaffold proteins as postsynaptic markers, we then verified and quantified with confocal laser-scanning microscopy that the contacts of these varicosities with OX-A cell bodies formed synapses.

2.2 Materials and methods

2.2.1 Animals and experimental design

Adult (3–6 months old) male C57BL/6J mice were maintained under a 12/12-h dark/light or light/dark cycle (lights on time corresponding to Zeitgeber time, ZT, 0), under veterinarian control and controlled environmental (temperature and humidity) conditions, with free access to food and water. Mice were destined for analyses with epifluorescence and confocal microscopy (n = 28), or electroencephalography (EEG) recording (n = 8). The animals destined for microscopic analyses were left undisturbed, avoiding any potential stressful condition and tissue damage and/or inflammatory reaction due to electrode implant for EEG recording. They were randomly divided in two groups sacrificed during a 2-h period during the day (ZT 3–4, n = 14), or night (ZT 15–16, n = 14). For sacrifice, the mice were deeply anesthetized with tribromoethanol (20 mg/kg, ip)

and transcardially perfused with 0.01-M phosphate-buffered saline, pH 7.2 (PBS), followed by 4% paraformaldehyde in PBS. The brains were removed, postfixed for 2 h, and cryoprotected in 30% sucrose in PBS at 4°C. These experiments were performed twice, using first five mice per day or night group destined for epifluorescence, and then replicated using nine mice per group (three for epifluorescence and six for confocal microscopy). Additional mice, matched with the first experimental session, were destined for EEG recording to assess sleep and wake states in the 2 h period used for the sampling for microscopic analyses, and during two consecutive days.

All procedures received approval by the Animal Care and Use Committee of the University of Verona (CIRSAL) and authorization by the Italian Ministry of Health, in strict adherence to the European Communities Council (86/609/EEC) directives and the ARRIVE guidelines, in accordance with the National Institute of Health Guide for the Care and Use of Laboratory Animals (NIH Publications No. 80-23), minimizing the number of animals used and avoiding their suffering.

2.2.2 Electroencephalography recording

For EEG and electromyography (EMG) monitoring, mice were chronically implanted with electrodes under isoflurane anesthesia. Four epidural electrodes were used for EEG recordings. One was placed over the left frontal zone (AP: +1.7, L: -1.5, DV: +0.0 mm from bregma), two over the right and left parietal zones (AP: -2.5, L: ±2.0, DV: +0.0 mm from bregma), respectively, and one over the cerebellum (AP: -5.8, L: 0.0, DV: +0.0 mm from bregma). All electrodes were soldered to a connector secured to the skull with dental cement. In addition, a pair of wires acting as electrodes was sutured to the nuchal muscle for the acquisition of EMG signals. After surgery, the animals were allowed at least 10 days of recovery; EEG and EMG signals were then recorded in undisturbed conditions for 48 h (starting from ZT 0). Post-acquisition determination of vigilance states at ZT3–4 and ZT 15–16 was done by visual inspection in consecutive 10-s epochs according to standard criteria (Baracchi and Opp 2008) (Fig. 2.1). Briefly, wakefulness was attributed on the basis of low-amplitude, mixed-frequency (theta and delta) EEG accompanied by EMG activation. Slow-wave sleep (SWS) was identified by increased absolute EEG amplitude, integrated values for the delta frequency band greater than those for theta, and a reduction of the EMG signal. Paradoxical sleep (PS) was characterized by low-amplitude EEG, with integrated values for the delta frequency band lower than those for the theta frequency band and muscle atonia.

2.2.3 Tissue processing and immunofluorescence

Varicosities apposed to OX perikarya were analyzed with triple immunofluorescence using epifluorescence and confocal microscopy. The primary antibodies listed in Table 1.1 were used to visualize OX-immunopositive cells, together with the presynaptic marker synaptophysin (Syn) combined with either the

vesicular glutamate transporter (VGluT)2 as marker of glutamatergic elements, or the vesicular GABA transporter (VGAT) as marker of GABAergic elements. Notably, among glutamatergic vesicular transporters, VGluT2 is predominant in brain regions regulating energy balance and behavioral/homeostatic integration, including the LH (Liguz-Lecznar and Skangiel-Kramska 2007). For the analyses of varicosities and postsynaptic scaffold proteins with confocal microscopy, the postsynaptic density (PSD) protein 95 was used for excitatory synapses and gephyrin (Geph) for inhibitory synapses (Table 1).

The brains destined for epifluorescence were embedded in OCT matrix, cut on a cryostat into 10-mm-thick coronal sections, and mounted on slides in three adjacent series. Every 12th section through the anteroposterior extent of the LH was stained with cresyl violet for cytoarchitectonic reference, and sections from the two adjacent series were processed for triple immunostaining to visualize OX/ VGluT2/Syn or OX/VGAT/Syn. The brains of the mice destined for confocal microscopy were serially cut with a freezing microtome into coronal sections at a 30-mm thickness. Four series of adjacent sections through the anteroposterior extent of the LH were processed free floating for triple immunofluorescence to visualize OX/VGAT/Syn, and OX/VGluT2/Syn, or OX/VGluT2/PSD95 and OX/VGAT/Geph. For the immunofluorescence procedure, all sections were pre-incubated in a solution of 0.3% Triton X-100 in 0.1-M phosphate buffer, pH 7.4, for 1 h, and then incubated overnight in a mixture of primary antibodies and diluted in the pre-incubation solution (Table 1). After rinsing in PBS, sections were incubated for 2 h in a mixture of secondary antibodies: Alexa Fluor 350-conjugated donkey anti-goat IgGs or Alexa Fluor 594-conjugated donkey anti-goat IgGs; Alexa Fluor 594-conjugated donkey anti-rabbit IgGs or Alexa Fluor 647-conjugated donkey anti-rabbit IgGs; and Alexa Fluor 647 donkey anti-mouse IgGs (all from InVitrogen, Carlsbad, CA, USA). The sections were then incubated for 2 h with Alexa Fluor488-conjugated goat anti-guinea pig IgGs (InVitrogen). After rinsing in PBS, the sections processed free-floating were mounted on slides. All sections were coverslipped with Aquatex mounting medium (Merck, Darmstadt, Germany).

To further control antibody specificity, additional sections were processed omitting each of the primary or secondary antibodies. No signal of the omitted reagent was detected in these control sections.

2.2.4 Microscopy and quantitative analyses

In epifluorescence microscopy, the method used by Cristino et al. (2013) was followed to determine the colocalization of Syn+/VGluT2+ and Syn+/VGAT+ in varicosities apposed to OX perikarya. In brief, triple immunostained sections were observed with a DMI6000 (Leica, Manheim, Germany) microscope equipped with x–y–z motorized stage, a digital camera Leica DFC 340FX, and the Leica Metamorph imaging software (Leica Meta-Morph AF, Manheim, Germany).

Multichannel images were acquired and analyzed using the Leica Application Suite (LAS) AF 2.2.0 software. OX- cell bodies with the full extent of the nucleus were randomly sampled through the perifornical area, where these cells are densely distributed, using the fornix as landmark. Sixty cells per vesicular transporter (VGlut2 or VGAT) and per animal were analyzed, and four images per cell in serial Z planes (1.6 mm step size) were acquired. Images were deconvolved using the Metamorph imaging deconvolution software by application of ten iterations. Varicosities were examined in single optical slices and considered as appositions to cell bodies when overlap among the elements was evident upon full rotation of the images. Counts of appositions were performed with a semi-automated method using the Metamorph Imaging Investigator software.

To verify whether appositions of varicosities represented axosomatic contacts, the analysis was repeated with the confocal microscope Leica SP5 (Leica, Mannheim, Germany) using a 63X oil-immersion objective (numerical aperture 1.4). Serial Z planes (0.5 µm) images were captured with the LAS software, and collapsed into a single maximum projection image to which colors were assigned. Twenty cells per antibody combination and per animal were analyzed. The cell body profile of OX neurons was drawn at each single plane on the basis of the OX signal channel. For each plane, a contact was identified as the clusters of pixels (green: VGluT2+ or VGAT+; red: Syn+) adjacent to an OX soma profile in which at least one pixel (x = 98.47; y = 98.47 nm; z = 503.54 nm) showed merging (yellow) in all the orthogonal views of imaged stacks. Clusters of pixels visible in adjacent z levels were not counted twice.

To verify whether the contacts represented synapses, the same method of acquisition and analysis was applied to sections processed for pre- and postsynaptic markers. A synapse was identified as a continuum between presynaptic ($VGluT2^+$ or $VGAT^+$) and postsynaptic ($PSD95^+$ or $Geph^+$) elements in $OX\text{-}A^+$ cell profiles, with no evident separation among the three elements.

For the representative 3D image in three dimensions, synaptic boutons on OX-A neurons were reconstructed from images stacks with the Imaris software 7.4 (Bitplane, Zurich, Switzerland) on merged images, in which only the OX-A signal and the $VGluT2^+/Syn^+$ or $VGAT^+/Syn^+$ colocalization were visualized. Levels, contrast, and brightness were adjusted with the Imaris software to optimize the images.

2.3 Statistical analyses

For the analysis of neurophysiological recordings, a two way (days x time points) repeated analysis of variance (ANOVA) followed by post hoc testing with Bonferroni's correction was performed to compare the average proportions of time spent in the different vigilance states during the sampled 2 h periods. Multivariate ANOVA (MANOVA) was used to determine the statistical interaction between the

number of excitatory and inhibitory synapses in the day/night groups (IBM SPSS software; Chicago, IL, USA). The significance threshold was set at $p<0.05$.

2.4 Results

2.4.1 Sleep and wake states

The neurophysiological recordings showed a definite prevalence of sleep states during the sampled day period and of wakefulness during the sampled night period (Fig. 2.1b, c). In particular, the average proportion of time spent in the different vigilance states at ZT 3–4 and ZT 15–16 was significantly different (wakefulness: F1,7 = 46.071, p B 0.001; SWS: F1,7 = 42.071, p < 0.001; PS: F1,7 = 41.222, p < 0.001; Fig. 2.1c). Mice slept (summing up SWS and PS) significantly more during day than during night in both the analyzed days. On day 1, mice slept about two times more during the analysed daytime period (ZT 3–4: 64.90 ± 4.55% of total time, mean ± standard error of the mean) than at night in antiphase (ZT 13–15: 32.55 ± 7.11% of total time, p < 0.001, Fig. 1c). The finding was replicated by the analysis of day 2 when the total sleep time was about three times higher in the analyzed daytime period (ZT 3–4: 70.14 ± 4.11%) than in the analyzed night period (ZT 13–15: 24.81 ± 6.95%, p = 0.001). Wakefulness significantly prevailed during the analyzed night periods (day 1: ZT 13–15: 67.45 ± 7.11% of total time; day 2: 75.19 ± 6.95%) and its relative proportion was lower in the analyzed daytime periods (ZT 3–4: day 1: 35.10 ± 4.55% of total time; day 2: 29.86 ± 4.11%) (Fig. 2.1c).

The findings were very consistent across animals (Fig. 2.1c). Of note, the percentage of time spent in each vigilance state was similar in the analyzed periods of the 2 days of recording (day 1 and day 2; Fig. 2.1c) with no significant difference between the 2 days (wakefulness: F1,7 = 0.042, p = 0.844; SWS: F1,7 = 0.063, p = 0.809; PS: F1,7 = 0.003, p = 0.959).

2.4.2 Excitatory and inhibitory presynaptic elements

Triple immunofluorescence resulted in the effective visualization of OX- cell bodies together with Syn+ immunosignal and VGluT2$^+$ or VGAT+ immunosignal in varicosities during both the sampled day and night periods (Fig. 2.2). At the observation, the intensity of immunofluorescence of OX- somata appeared higher at night than at day. The main diameter of OX- cell bodies sampled for the analysis ranged from 25.6 ± 3.73 to 28 ± 2.83 lm, in agreement with the previous observations (Peyron et al. 1998).

In both epifluorescence and confocal microscopy, Syn$^+$/VGAT$^+$ (Fig. 2.2a, b) and Syn$^+$/VGluT2$^+$ (Fig. 2.2g, h) varicosities appeared to contact OX- cell bodies in sections from both the sampled periods, and were also seen around immunonegative somata intermingled with the OX- ones (Fig. 2.2a, c, e, f). Confocal images were further viewed using 3D rotation with magnification to confirm that the presynaptic elements were in contact with the OX-A$^+$ cell profile through three spatial axes. By

this examination, the $Syn^{+}/VGluT2^{+}$ or $Syn^{+}/VGAT^{+}$ varicosities appeared to be in contact with OX- cell bodies, since no space was observed between the two with rotation through three axes (Fig. 2.2, small images).

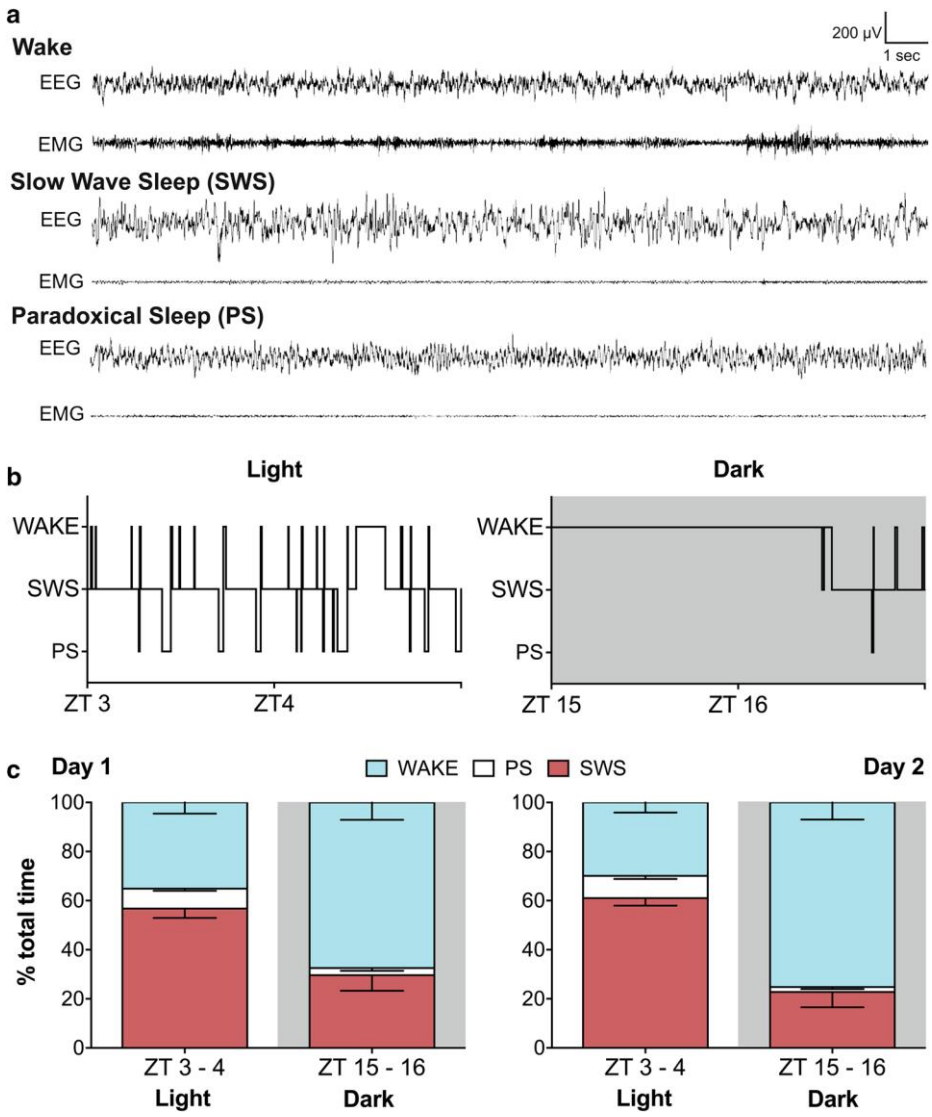

Fig. 2.1: Sleep–wake states analyses. **a.** Representative 20-s epochs of electroencephalography (EEG) and electromyography (EMG) signals during each vigilance state. **b.** Representative hypnograms during the light period (ZT 3–4, on the *left*) and the dark period (ZT 15–16, on the *right*); *PS* paradoxical sleep, *SWS* slow-wave sleep. **c.** Percentages (mean ± SEM) of the total time (120 min) spent in each vigilance state. Note that the percentages are consistent in the first (day 1) and second (day 2) days of recording used for the analyses

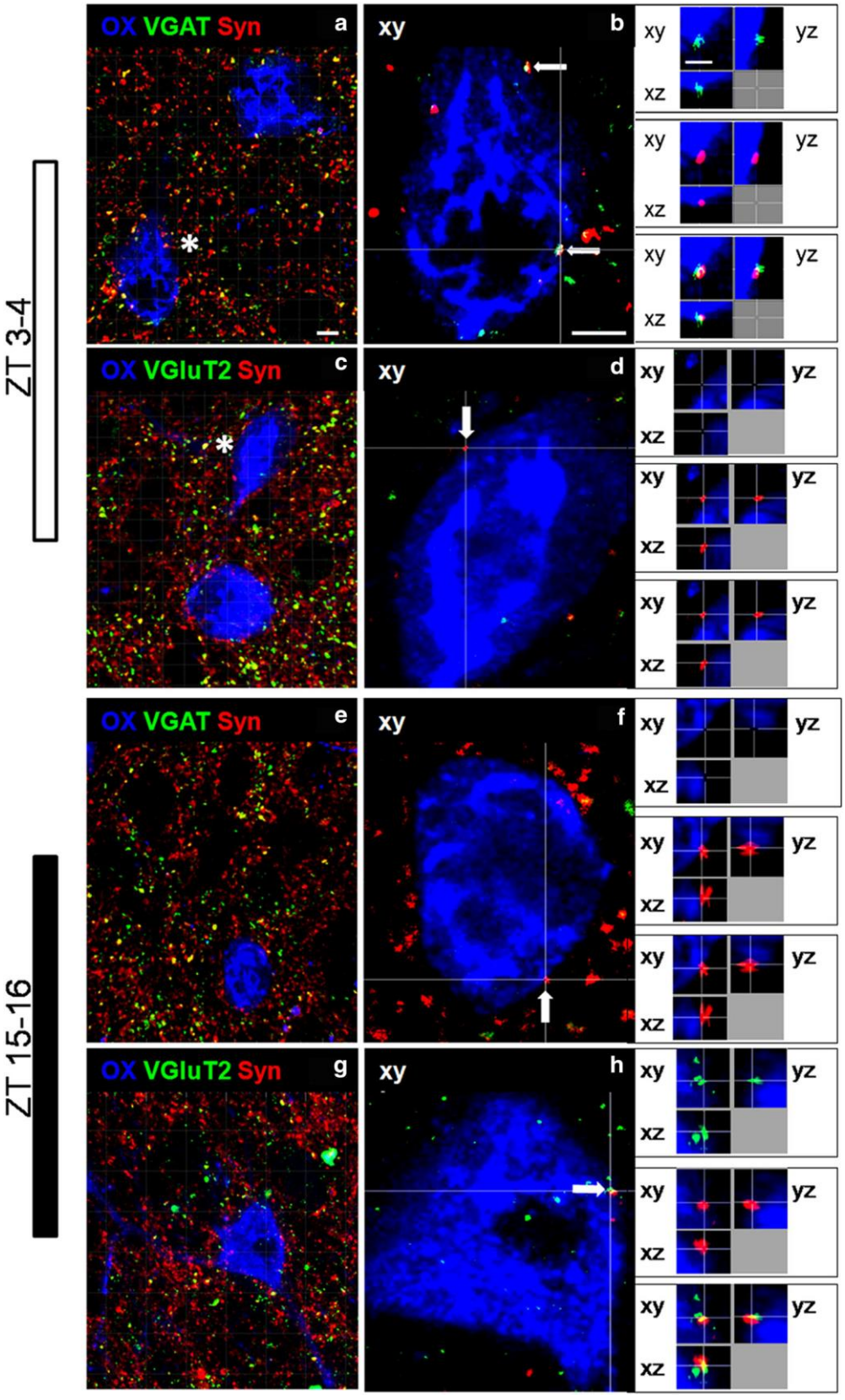
ZT 3-4
ZT 15-16
OX VGAT Syn
a
xy
b
xy
yz
xz
OX VGluT2 Syn
c
d
e
f
g
h

Fig. 2.2: Inhibitory or excitatory varicosities apposing orexinergic cell bodies in the sampled light and dark periods. a, c, e, g Confocal microscopy images (maximum intensity projections) of triple immunostained sections showing Syn+ (red) varicosities together with VGAT+ or VGluT2+ (green) varicosities (the merging is in yellow) in relation to orexinergic neurons (blue). The asterisks indicate the OX cells shown at higher magnification in the matched images. Varicosities surrounding non-orexinergic (OX-immunonegative) neurons are also evident. b, d, f, h Contacts (arrows) between inhibitory (VGAT+/Syn+) or excitatory (VGLUT2+/Syn+) varicosities with OX soma visualized in a single optical section (xy). The intersection between the white lines identifies the contacts shown in orthogonal projections, at higher magnification, in the lateral insets. Inhibitory or excitatory varicosities are defined as the apposition between the presynaptic elements (VGAT+/ Syn+; VGluT2+/Syn+) in three dimensions, i.e., in all the combination of the axes (xy; yz; xz) as double immunostaining and in merged image. Scale bars 5 µm

At the quantitative analysis of pairs of 10-µm-thick sections in epifluorescence, the mean total number of presynaptic appositions per OX- soma during day (18.74 ± 2.81) and night (19.86 ± 3.01) was not significantly different (Fig. 2.3a). Differences were, however, found between the mean number of glutamatergic or GABAergic varicosities per OX- soma during day and night (Fig. 2.3a). In particular, a prevalence of glutamatergic (Syn+/ VGluT2^{+}) varicosities was found in the animals sampled at night (mean number of appositions per OX- cell body: 13.83 ± 2.81) vs those sampled at day (4.62 ± 1.84). A prevalence of the mean number of GABAergic (Syn^{+}/ VGAT^{+}) varicosities per OX- soma was instead documented in the animals sampled during day (14.11 ± 1.94) vs night (6.03 ± 1.39). This resulted in a ratio of VGluT2/ VGAT varicosities per OX- soma of ~3:1 in the mice sacrificed during the night, and a ratio of ~1:3 in those sacrificed during the day. In terms of relative proportion of Syn+ varicosities per OX- soma, the data indicated that VGluT2^{+} elements accounted for 24.20 ± 7.00% and VGAT+ elements for 75.82 ± 7.00% at daytime, whereas VGluT2+ elements accounted for 70 ± 5.62% and VGAT+ elements for 30 ± 5.62% at night. The results were very consistent across animals of each group (Fig. 2.3b). The statistical analysis showed that the above differences were highly significant: MANOVA showed a significant multivariate main effect for the time of sacrifice (Wilk's $\lambda = 0.065$; $F(2,13) = 93.97$; $p<0.001$, partial $\eta^2 = 0.935$; power to detect the effect: $\alpha = 0.05$). Given the test significance, the univariate effects were also examined: the mean number of Syn+/VGluT2+ Varicosities per OX- cell body was significantly higher at night ($F(1,14) = 76.54$), and that of Syn^{+}/VGAT^{+} varicosities at daytime ($F(1,14) = 91.38$) (Fig. 2.3a).

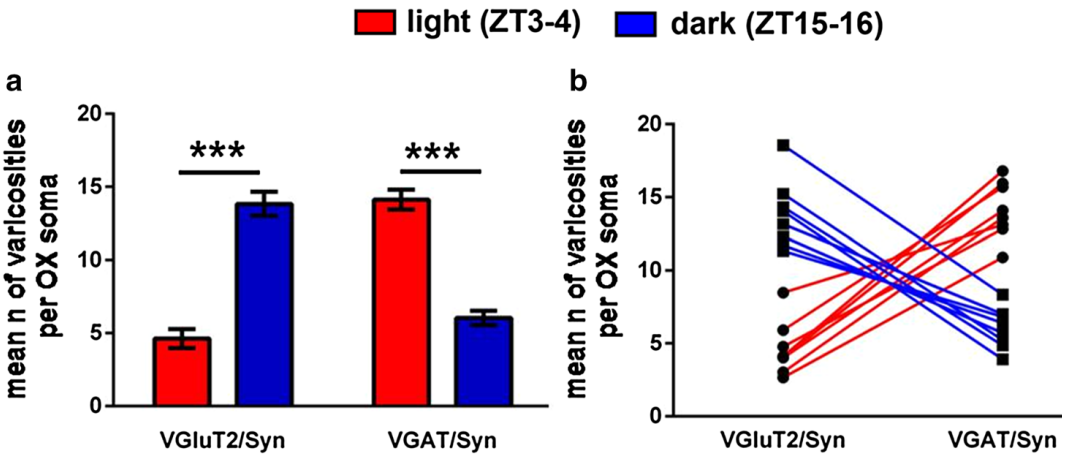

Fig. 2.3: Quantitative analyses of excitatory and inhibitory varicosities apposing orexinergic cell bodies in the sampled light and dark periods. a Mean number (±SEM) of excitatory (VGluT2+/Syn+) or inhibitory (VGAT+/Syn+) varicosities apposed to OX-A+ cell bodies (n = 60 cells per mouse; n = 8 mice per group). ***p<0.001, multivariate analysis of variance (MANOVA), F = 2,13. b Scatter plots of the mean number of excitatory and inhibitory varicosities per OX-A soma in each of the animals. Note that the individual data sets are very consistent across animals.

Quantitative analysis of confocal microscopy images confirmed that the mean number of VGluT2+/Syn+ varicosities per OX- soma was higher during night (9.833 ± 0.519) than during day (3.867 ± 0.519). Conversely, the mean number of VGAT+/Syn+ varicosities per OX- soma was higher during day (9.833 ± 0.422) than during night (4.033 ± 0.422) and, therefore, a ratio VGluT2/VGAT of ~4:1 during night and ~1:4 during day was found in the mean number of appositions per OX- cell body in confocal microscopy, matching the results obtained with epifluorescence.

In the statistical analysis of this confocal microscopy data set, one-way MANOVA confirmed a significant multivariate main effect for the time of sacrifice (Wilks' λ = 0.004, F(2,3) = 62.602, p = 0.004, partial η^2 = 0.977; power to detect the effect was 0.999). Significant univariate main effects for the time of sacrifice were obtained for both VGAT (F(1,4) = 94.613, p = 0.001, partial η^2 = 0.959) and VGluT2 (F(1,4) = 66.064, p = 0.001, partial η^2 = 0.943).

2.4.3 Postsynaptic markers

To further assess in detail whether the Syn+ varicosities formed GABAergic or glutamatergic synapses, sections triple immunostained for vesicular transporters, and the postsynaptic scaffold proteins Geph and PSD95, respectively, were analyzed in confocal microscopy (Fig. 2.4). In series triple stained for OX, VGAT, and Geph, staining for Geph appeared punctate and could be detected opposite to

the VGAT+ varicosities and associated with the surface of OX- cell bodies (Fig. 2.4b, f). In series triple stained for OX, VGluT2, and PSD95, VGlut2+ varicosities appeared to abut PSD95+ puncta associated with OX- cell bodies (Fig. 2.4d, h). Confocal images were further viewed using 3D rotation with magnification, and confirmed that the pre- and postsynaptic elements were in contact through three spatial axes during both the day and night sampled periods (Fig. 2.4, small images).

Quantitative analysis (Fig. 2.5a) showed a significant prevalence at night of the mean number of excitatory VGluT2+ varicosities in contact with PSD95 per OX- soma (17 ± 0.349) with respect to daytime (4.9 ± 0.348). The mean number of VGAT+ in contact with Geph per OX- soma was instead significantly lower during night (5.1 ± 0.945) and higher at daytime (14.933 ± 0.945).

The findings were consistent across animals (Fig. 2.5d), showing a ratio VGluT2 + PSD95/VGAT + Geph of ~3:1 at night and of ~1:3 at daytime.

One-way MANOVA revealed a significant multivariate main effect for the time of sacrifice (Wilks' k = 0.023, $F(2,3) = 346.150$, $p<0.001$, partial $\eta^2 = 0.996$). Significant univariate main effects for the time of sacrifice were obtained for VGAT ($F(1,4) = 54.187$, $p<0.001$, partial $\eta^2 = 0.931$), and for VGluT2 ($F(1,4) = 601.685$, $p<0.001$, partial $\eta^2 = 0.993$).

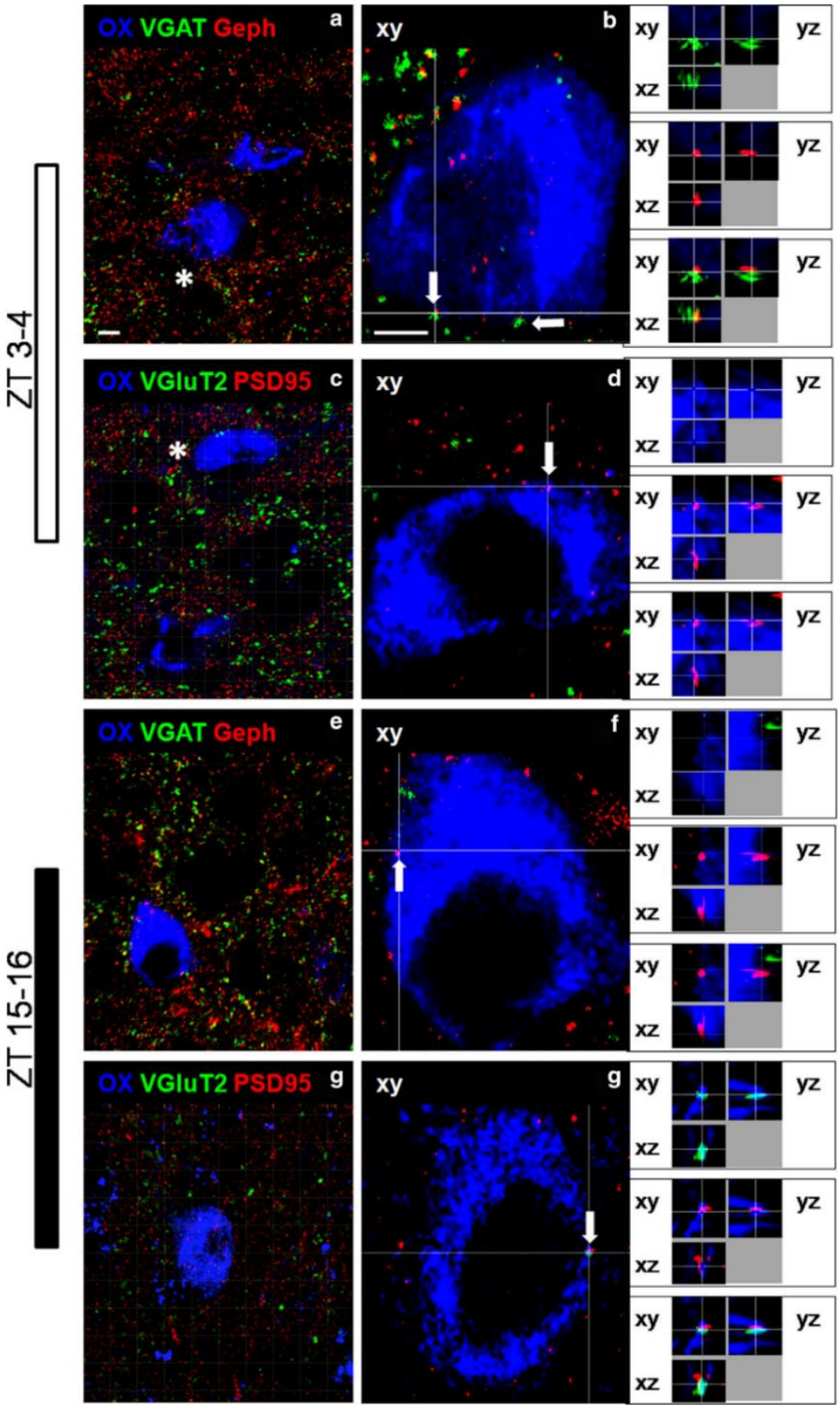
ZT 3-4
ZT 15-16
OX VGAT Geph
OX VGluT2 PSD95
a
b
c
d
e
f
g
xy
xz
yz

Fig. 2.4: Inhibitory or excitatory synaptic contacts in orexinergic cell bodies in the sampled light and dark periods. a, c, e, g Confocal images (maximum intensity projections) of triple immunostained sections showing VGAT+ or VGluT2+ (green) varicosities, the postsynaptic scaffold proteins gephyrin (Geph) or PSD95 (red; the merging is in yellow) and orexinergic neurons (blue), shown at higher magnification in each matched image (indicated in a and b by asterisks). b, d, f, h Contacts visualized at high magnification in a single optical section (xy) show that VGAT+ Varicosities abut a Geph+ punctum (arrows in b and f); VGluT2+ varicosities abut a PSD95+ punctum (arrows in d and h); the postsynaptic puncta are located on the surface of the OX-A+ cell bodies. The intersection between the white lines identifies the contacts analyzed along their orthogonal projections, shown at higher magnification in the lateral insets. Inhibitory or excitatory synaptic contacts are defined as a continuum between presynaptic and postsynaptic elements in three dimensions, i.e., along all the combination of the axes (xy; yz; xz) as double immunostaining and in merged image. Scale bars 5 µm

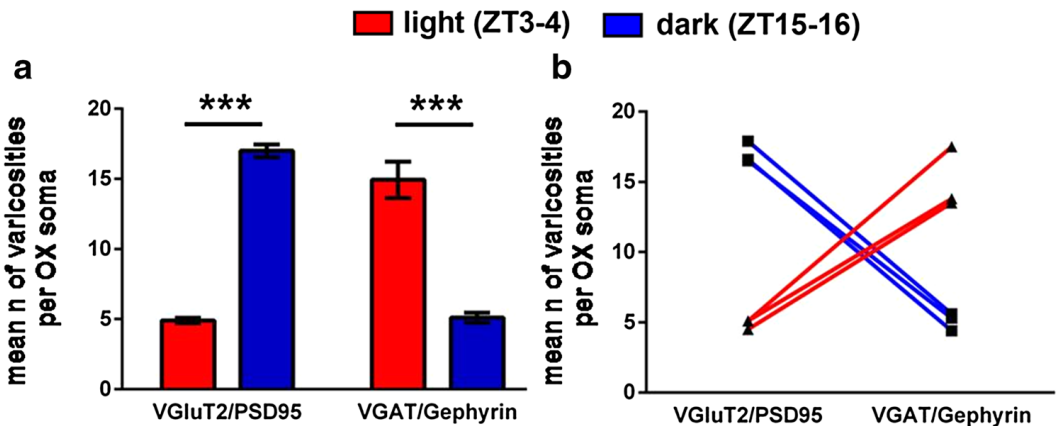

Fig. 2.5: Quantitative analyses of excitatory and inhibitory synaptic contacts in orexinergic cell bodies in the sampled light and dark periods. a Mean number (±SEM) of excitatory (VGluT2+/PSD95+) or inhibitory (VGAT+/Gephyrin+) synapses per OX-A+ cell body (n = 20 cells per mouse; n = 3 mice per group). ***p<0.001, MANOVA, F = 2,3. b Scatter plots of the mean number of excitatory and inhibitory contacts per OX-A+ soma in each of the animals, showing that the results are consistent

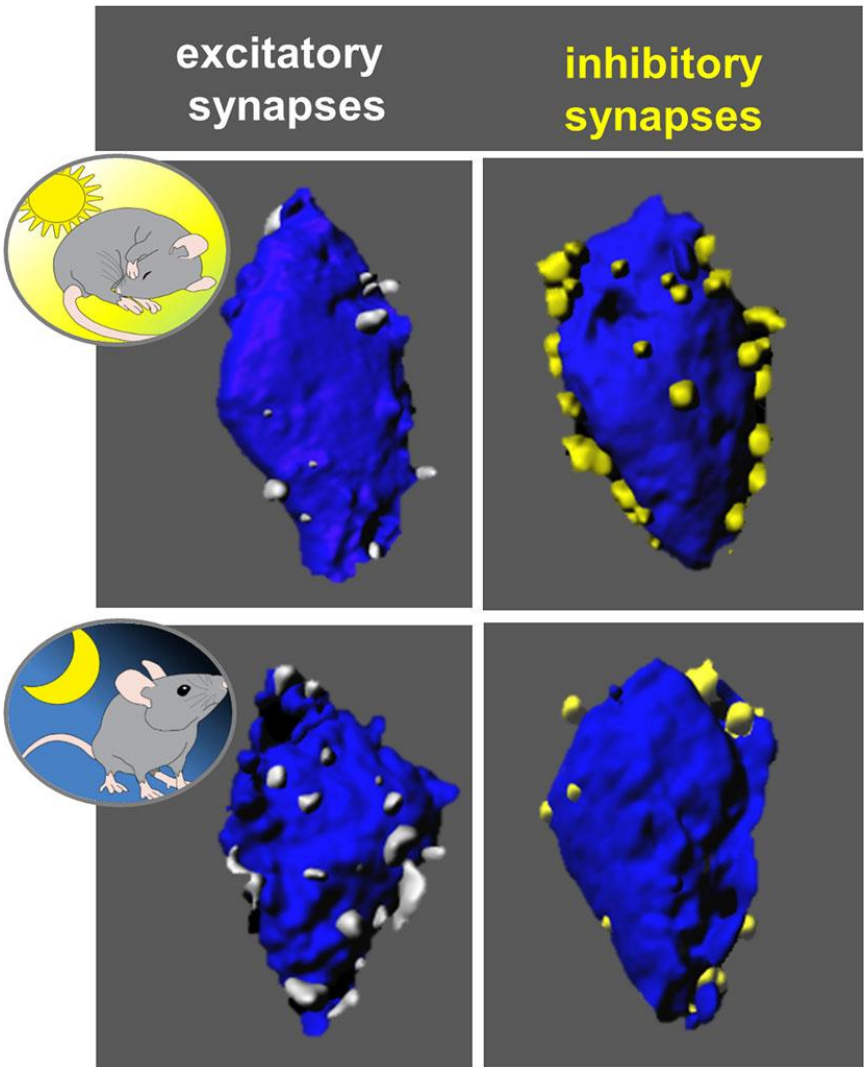

Fig. 2.6: Summary of the day/night switch of excitatory and inhibitory synaptic contacts with orexinergic cell bodies. Examples of orexinergic cell bodies (shown in 3D reconstructions) summarize the day/ night variation of the excitatory/inhibitory input observed in the present study

2.5 Discussion

The present findings provide novel evidence of a switch in the innervation of orexinergic cell bodies, in basal conditions, from a prevalence of excitatory inputs at night, during a period we demonstrated to correspond to wakefulness predominance, to a prevalence of inhibitory inputs in the antiphase, during a period we demonstrated to correspond to sleep predominance (Fig. 2.6). As expected in

nocturnal animals, the analysis of vigilance states in the matched mice (a strategy here adopted to avoid any possible perturbation caused by EEG recording in the mice used for microscopic analyses) indicated that in the 2 h periods of sampling, the animals were predominantly asleep during the day and predominantly awake during the night. The data obtained with EEG recordings were remarkably consistent across animals as well as in the 2 analyzed days. The percentages of time spent in each vigilance state were similar to those previously reported in mice (Tobler et al. 1997). The multiple presynaptic labeling strategy adopted here with epifluorescence has been previously validated at the ultrastructural level with the visualization of asymmetric and symmetric synaptic boutons on OX cell bodies (Horvath and Gao 2005; Cristino et al. 2013). In the present study, the findings were consistent in the epifluorescence and confocal microscopy analyses, and were replicated and validated by the use of presynaptic and postsynaptic markers in confocal microscopy, showing that they formed synaptic contacts. Day/night plasticity of the orexinergic network has been described in the larval zebrafish, related to rhythmic changes in synapse density (Appelbaum et al. 2010) rather than, as in our study in mice, to neurotransmitter phenotype.

In addition, recent findings based on live imaging of single synapses in zebrafish larvae have reported an increase in the number of inhibitory synapses in the dendrites of orexinergic neurons during the night, corresponding to sleep as assessed on the basis of behavioural parameters in this diurnal model organism (Elbaz et al. 2017b). Such findings support the present data, obtained in cell bodies, on the increase of inhibitory axosomatic synapses in orexinergic neurons during a period corresponding to sleep in mice. Moreover, taking also into account excitatory synapses, we here reveal a daily reorganization of the overall excitatory/inhibitory balance in the innervation of orexinergic cell bodies in mice.

Different sets of previous data in mice have pointed out a remarkable synaptic plasticity in the wiring of OX cell bodies in different paradigms: food deprivation (Horvath and Gao 2005), genetic and diet-dependent murine models of obesity (Cristino et al. 2013), and prolonged wakefulness (Rao et al. 2007a). Altogether, these data have indicated dynamic changes of the wiring of OX neurons to face internal and external challenges (Horvath and Gao 2005).

The present findings show that a dynamic daily fluctuation of the excitatory/inhibitory innervation of OX somata is part of the repertoire of adaptive properties of these neurons in basal, unperturbed conditions. Of note, the previous ultrastructural and multiple immunolabeling analyses have identified a high number of asymmetric, excitatory synapses on the soma of orexinergic neurons (Horvath and Gao 2005), at variance with other neuronal cell types in which excitatory synapses prevail on dendrites, and it has been proposed that the prevalent excitatory innervation of orexinergic perikarya could facilitate the responses of these neurons

to environmental demands (Gao and Hermes 2015). Chronic administration of modafinil for 7 days, inducing elevated locomotor activity taken as behavioral measure of prolonged wakefulness, led to an increased number of asymmetric synaptic contacts on orexinergic cell bodies and increased strength at glutamatergic synapses (Gao and Hermes 2015). Our data, which are extended to the analysis of postsynaptic scaffold proteins in basal conditions, show that a reorganization of excitatory synapses occurs daily in a dynamic balance with inhibitory ones. The neuronal cell body is the critical subcellular domain for action potential generation and the control of neuronal spiking (Spruston 2008). Our data are, therefore, in line with the previous finding that the firing of OX neurons is highest in rats during active wake and virtually ceases during sleep (Lee 2005). The silence of OX neurons during sleep could be caused by inhibitory input from GABAergic sleep-active neurons in the basal forebrain and/or preoptic area and tuberal posterior hypothalamus (Lee 2005; Saito et al. 2013). The perifornical area, on which the present analyses have been focused, is innervated mainly by hypothalamic sources, with the heaviest input from the ventrolateral and preoptic nuclei (Yoshida et al. 2006), in which GABAergic sleep-active neurons are located. Taken together with these previous data sets, the present findings suggest that the sleep-promoting synaptic network oscillates to silence OX neurons during sleep. Shifts in the presynaptic wiring of OX neurons could also account for the day/night changes reported for the OX effect on the suprachiasmatic nucleus, in which predominantly GABA-mediated presynaptic OX actions during the day switch to direct postsynaptic actions during the night (Belle et al. 2014).

The day/night switch of the synaptic wiring of OX somata here observed could gradually occur during 24 h and could be under circadian regulation or due to homeostatic mechanisms to be verified in future studies with experiments under constant light or dark conditions and with sleep deprivation. By means of the latter manipulations in zebrafish larvae, the rhythmic plasticity of inhibitory synapses in the dendrites of orexinergic neurons was found to be independent of the circadian clock and homeostatically regulated by vigilance states (Elbaz et al. 2017b). Concerning the postsynaptic plasticity of orexinergic neurons, sleep deprivation experiments in mice have shown that the immunostaining of GABA receptors on orexinergic cell bodies increases as a function of enforced wakefulness during the day, thus stimulating homeostatic downscaling of OX neuron activity (Toossi et al. 2016).

This type of homeostatic adaptation also occurs in a reciprocal manner in melanin-concentrating hormone neurons, a sleep-active peptidergic cell population intermingled with OX neurons, in which GABA receptor immunoreactivity decreases with increasing wakefulness (Toossi et al. 2016). Such data on GABA receptors further strengthen the present findings on the plasticity of the postsynaptic component of orexinergic cell bodies, and suggest that daily changes in cell body

innervation could be a property of different populations of sleep/wake-regulatory neurons in the LH. On the other hand, the oscillation of OX- release in the cerebrospinal fluid is under the circadian control of the suprachiasmatic nucleus and sleep homeostatic mechanisms (Deboer et al. 2004; Zhang et al. 2004).

The present data open many other questions. Inputs to orexinergic neurons originate from a variety of sources in the forebrain and brainstem, and from an abundant local network within the hypothalamus, including orexinergic synapses (Sakurai et al. 2005; Yoshida et al. 2006; Yamanaka et al. 2010; Burt et al. 2011), contingents of cholinergic terminals (Henny and Jones 2006), glycinergic inhibitory terminals (Hondo et al. 2011), and serotonergic terminals which inhibit directly and indirectly orexinergic neurons (Chowdhury and Yamanaka 2016), as well as somatostatin varicosities which can release GABA (Toossi et al. 2012), thus showing complex, multiple interactions in the afferent regulation of OX cell activity. VGAT is the transporter for both GABA and glycine (Wojcik et al. 2006), and the present investigation remains to be extended to other neurotransmitter-identified terminals, although very few non GABAergic or glutamatergic varicosities apposed to orexinergic cell bodies were here observed.

Different mechanisms could account for the remarkable, spontaneous daily changes in the excitatory/inhibitory wiring of OX- somata here identified. These mechanisms could involve presynaptic determinants (Ettorre et al. 2012), as well as cytoskeletal proteins, as reported for myosin phosphorylation under rhythmic Rho1 activity in the daily expansion and retraction of axon terminals in Drosophila clock neurons (Petsakou et al. 2015). Synaptic proteins, such as Syn itself, could also be implicated, given the role of Syn in the regulation of activity-dependent synapse formation and competition (Tarsa and Goda 2002).

Furthermore, synaptic plasticity could involve extracellular matrix (Dityatev et al. 2010a; Dityatev and Rusakov 2011) and phenomena of neurotransmitter switching (Spitzer 2015). Perisynaptic glia could also be involved in synaptic wiring changes, considering the key role of astrocytes ensheathing presynaptic terminals (Heller and Rusakov 2015; Papouin et al. 2017), and the local role of astrocyte derived lactate as critical energy substrate of OX firing activity (Parsons and Hirasawa 2010). Of note, dynamic microglial cell processes are new players in the synaptic microenvironment (Miyamoto et al. 2013; Xavier et al. 2014), and microglial cells isolated from the murine cerebral cortex are endowed with an intrinsic molecular clock which can modulate synaptic strength (Hayashi et al. 2013).

Opening such intriguing questions, our findings add day/night changes of innervation to the key role of orexinergic signaling in the timing of behavioral states, supporting the view of OX neurons as ‘‘a hub’’ (Sakurai 2014) which links internal and external drives.

Acknowledgements

The study was supported by FUR (Fondo Unico per la Ricerca) and the European Commission project DESIRE (HEALTH-F2-602531-2013). Thanks are due Javier De Felipe and Alberto Munoz Cespedes for their suggestions for 3D reconstructions.

2.6 Tables

Table 1: Antibodies used in this study.

Antigen	Host	Immunogen	Supplier	Catalog#	Dilution	References
Orexin	Goat	Purified goat polyclonal antibody raised against a peptide mapping at the C-terminus of Orexin-A of human origin	Santa Cruz	sc-8070	1:100	Blanco-Centurion et al. (2013)
VGluT2	Guinea pig	Purified recombinant protein of rat VGluT2 (aa510-582)	Synaptic Systems	135 404	1:100	Perederiy et al. (2013)
VGAT	Guinea pig	Strep-Tag fusion protein of rat VGAT (aa2-115)	Synaptic Systems	131 004	1:100	Fekete et al. (2015)
Gephyrin	Mouse	Purified rat gephyrin	Synaptic Systems	147 011	1:50	Schneider Gasser et al. (2006)
PSD95	Rabbit	Synthetic peptides corresponding to residues surrounding Gln53 of human PSD95	Cell Signaling	3450T	1:100	Saunders et al. (2015)
Synaptophysin 1	Rabbit	Synthetic peptide GPQGAPTSFSNQM (aa 301 - 313 in human synaptophysin 1) coupled to key-hole limpet hemocyanin via an added N-terminal cysteine residue.	Synaptic Systems	101 002	1:200	Wimmer et al. (2006)
Synaptophysin	Mouse	Purified mouse monoclonal IgG1k	Millipore	MAB5258	1:500	Gokhale et al. (2012)

2B. *Addendum*: preliminary data on astrocytes in the lateral hypothalamus during day and night

2B.1 Purpose

The purpose for implementing the published findings (Laperchia et al. 2017) with this additional material is to present preliminary data on astrocytes in the same conditions of such previous study (basal conditions at two time points in antiphase during day and night).

The interest in astrocytes in the LH is motivated not only by the wealth of data on the partnership of astrocytes in synaptic transmission (Fig. 1.11), and especially in excitatory glutamatergic transmission (Verkhratsky and Butt 2007), but also by findings indicating "time-keeping" properties of astrocytes. In particular, clock gene expression has been reported in astrocytes, which maintain *in vitro* a circadian oscillation (Prolo 2005), and release ATP *in vitro* with a circadian rhythmicity (Womac et al. 2009), which depends on clock gene expression (Marpegan et al. 2011). Astrocytes are components of the local network of regulation of OX neuron activity (Burt et al. 2011) (Fig. 1.6B), and their role in supplying energy to OX neurons (Parsons and Hirasawa 2011) is critical also for the wake-promoting activity of these cells (Clasadonte et al. 2017) which is mediated by connexin-43 gap junctional coupling (Clasadonte et al. 2017).

On this basis, the study on the diurnal fluctuation of the excitatory/inhibitory balance in the synaptic wiring of OX cell bodies is currently being extended to astrocytes surrounding OX neurons. Data on the methodological approach set up for these analyses and preliminary observations are here presented.

2B.2 Materials and methods

2B.2.1 Animals

Male CX3CR1-GFP mice of 3 months of age were used. In these mice microglial cells are tagged with green fluorescent protein (GFP) by tagging of the chemokine fractalkine receptor CX3CR expressed by microglia (Mizutani et al. 2012). The use of these animals was motivated by the objective to analyze also microglia in the same paradigm, which is ongoing in a separate study.

The mice were maintained under the same conditions as described in section 2.2.1. Four mice were used for this pilot study based on confocal microscopy, and were sacrificed during a 2 h period during the day (ZT 3–4, n = 2) and at night (ZT 15–16, n = 2), with ZT 0 corresponding to the lights-on time. Animal perfusion was carried out using the same protocol described in section 2.2.1. The experimental procedures were pursued under the same ethical approval stated in section 2.2.1.

2B.2.2 Tissue processing and immunofluorescence

A freezing sliding microtome was used for sectioning, and 30 µm-thick coronal sections were collected in adjacent series through the anteroposterior extent of the

LH. The sections were processed free-floating for triple immunofluorescence with primary antibodies: goat anti-orexin-A (Santa Cruz; 1:100) to visualize OX-immunopositive cells, together with mouse anti- synaptophysin (Syn) (Millipore; 1:500) as presynaptic marker and rabbit anti-glial fibrillary acid protein (GFAP) Merck; 1:500) to visualize astrocytes (information on these antibodies is provided in Table 3.2 of Chapter 3). The immunofluorescence procedures described in section 2.2.3 were followed. Sections were incubated in the following secondary antibodies: Alexa Fluor 405-conjugated donkey anti-goat IgG; Alexa Fluor 568-conjugated donkey anti-rabbit IgGs and Alexa Fluor 647 donkey anti-mouse IgGs (all from InVitrogen, Carlsbad, CA, USA). The sections were then mounted on gelatinized slides and coverslipped with 0.1% paraphenylenediamine in a glycerol-based medium (90% glycerol and 10% PBS). Additional sections were processed omitting either the primary or secondary antibody to control for antibody specificity. No signal of the omitted reagent was detected in these sections.

2B.2.3 Microscopy and data analysis

The confocal microscope Leica SP5 (Leica, Mannheim, Germany) was used for tissue section analysis using a 63X oil-immersion objective with a constant zoom factor 1.0 (numerical aperture 1.3). Serial Z planes (0.50 µm) images were captured with the LAS software, and collapsed into a single maximum projection image to which colors were assigned. Acquired images were minimally and equally modified with the Imaris software for contrast and brightness. The filter channel visualizing GFP (i.e., microglia) was suppressed for the present observations.

The 3D reconstructions of astrocytes together with Syn+ presynaptic elements were done according to previous approaches (Verbich et al. 2012; Fogarty et al. 2013). For the 3D reconstruction images of astrocytes, the Imaris software 7.4 (Bitplane, Zurich, Switzerland) tools for filaments was used in identifying astrocytic ramifications, while the software tools for surface was used for reconstructing the soma of astrocytes from merged images, using first image stacks of astrocytes only, and then in combination with the OX soma and Syn signals. Pre-installed MATLAB software on the Imaris tool was used to detect axosomatic contact on OX neuron membrane colocalized with astrocytic processes. The Imaris software was also used in adjusting minimally the levels, contrast, and brightness for the optimization of images.

The analyses of the colocalization of presynaptic appositions to OX somata and the astrocytic processes were done as described by Fogarty et al. (2013) and Belmer et al. (2017), using the Imaris imaging software for surface rendering/ reconstruction. Briefly, the smoothing, surface rendering and surface creation tools were applied to the reconstruction of the astrocytic cell bodies and their processes. A matching morphology of the astrocytes acquired at the confocal microscope was created using the slice view tool. The line tool was used in measuring the minimum and maximum

diameter of their processes which were then subsequently reconstructed from the filament tool. In the course of the reconstruction procedure, the raw image acquired was compared with the reconstructed image to ensure that the structures present were preserved and no structure was introduced that was not present in the raw image.

The presynaptic appositions on OX soma and astrocytic processes were filtered based on OX neuron and astrocytic surfaces. Presynaptic (Syn^+) fluorescence signals unrelated to the OX soma or astrocytic processes were masked and filtered out, to visualize only presynaptic contacts associated with both the OX soma and astrocytic processes. Following the mathematical calculations of smallest diameter of Syn^+ terminals (using the line tool as above), the spot diameter of the Syn terminal was calculated using the spot layering tool. The spot detection tool was individually applied to axosomatic terminals on OX and astrocyte processes, respectively. The pre-installed MATLAB plugin was used in the detection and selection of Syn^+ terminals of a diameter of 0.3 µm as in previous protocols (Fogarty et al. 2013; Belmer et al. 2017). Spot colocalization tool was used for the localization of 'Syn+ on OX soma' or 'Syn+ on astrocyte processes' pairs within a distance of a 0.6 µm to identify the appositions of presynaptic terminals colocalized on OX soma and the astrocytic processes, respectively.

2B.3 Results

Confocal images of single optical slices of OX neurons in serial Z planes (0.5 µm step size) allowed the effective visualization of OX neurons when collapsed into the maximum intensity projections (Fig. 2B.1). The main diameter of OX soma was within the same range described by Laperchia et al. (2017). The presynaptic Syn^+ elements on OX soma and in the LH neuropil were visible during both the day and night sampled periods (Fig. 2B.1). Syn^+ elements surrounded, as expected, both OX-immunopositive and OX-immunonegative neurons (Fig. 2B.1). A fluctuation of Syn immunofluorescence was seen in the LH neuropil, with higher intensity at night than at daytime. This was adjusted for optimal visualization of the maximum intensity projection images of Syn at both time points, as shown in Fig. 2B.1.

Three-dimensional reconstruction of GFAP immunofluorescence resulted in the visualization of the highly ramified astrocytic processes (Fig. 2B.2). These showed a bushy phenotype, with dense filling of the neuropil, especially at the night time point (Fig. 2B.2B). When the 3D GPAP immunosignal was viewed together with OX and Syn immunofluorescence in merged images, astrocytic processes were seen to extend over OX cell bodies at both the day and night time points (Fig. 2B.3). The merging also showed overlap of astrocytic processes with Syn^+ elements apposed to OX cell bodies (Fig. 2B.3).

Analyses with 3D surface reconstruction of GFAP together with 3D spot detection of Syn showed appositions of Syn^+ presynaptic elements to OX somata (Fig. 2B.4).

The merge also revealed the colocalization of Syn^+ presynaptic terminals in contact with OX somata and the distal portion of astrocytic processes extending on OX somata and proximal dendrites (Fig. 2B.4).

All the adopted visualization approaches (Figs 2B.2, 2B.3, 2B.4) showed that the processes of astrocytes surrounding OX neurons were much more extended at night than at day. This finding is now being confirmed with additional data. It will also be determined whether the arrangement of astrocyte processes at night and day resulted in a different spatial covering of the OX neuron membrane, and in quantitative differences in the merge of astrocyte distal endings with axosomatic contacts.

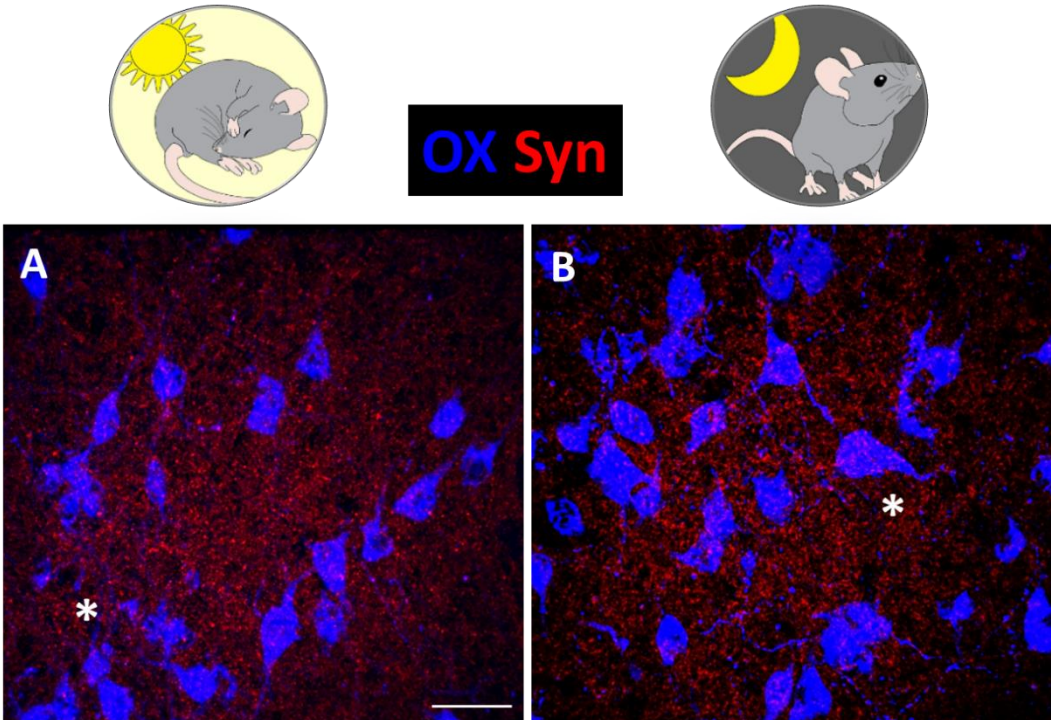

Fig. 2B.1: Maximum intensity projections confocal microscopy images of orexinergic (OX-A) neurons and presynaptic (Syn-immunopositive) terminals in apposition to OX soma in the sampled light and dark periods. Presynaptic elements surrounding OX-immunonegative neurons are also evident in the neuropil. The same field is presented also in the following figures and the asterisks indicate the spatial reference (in A and B, respectively) for Figs. 2B.2 and 2B.3. Scale bar = 30 µm.

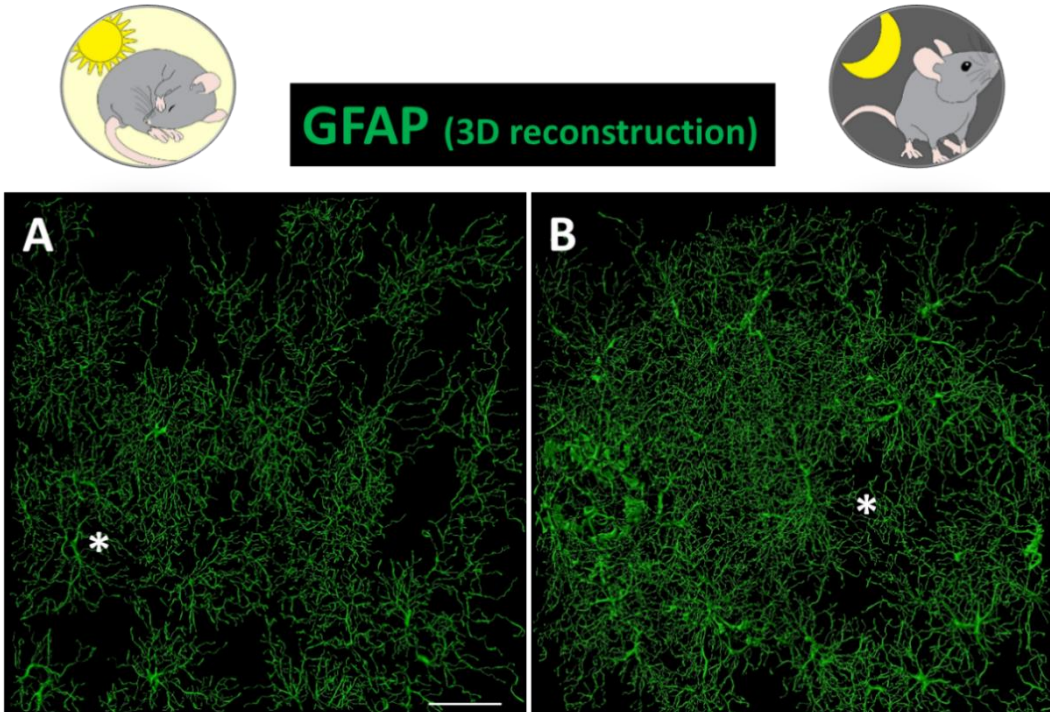

Fig. 2B.2: 3D reconstruction confocal microscopy images of astrocytes in the same field shown in Fig. 2B.1 and shown at higher magnification in Fig. 2B.3 (asterisks are for spatial reference). Maximum intensity projections images showing the different organization of astrocyte ramifications**.** Scale bar = 30 µm.

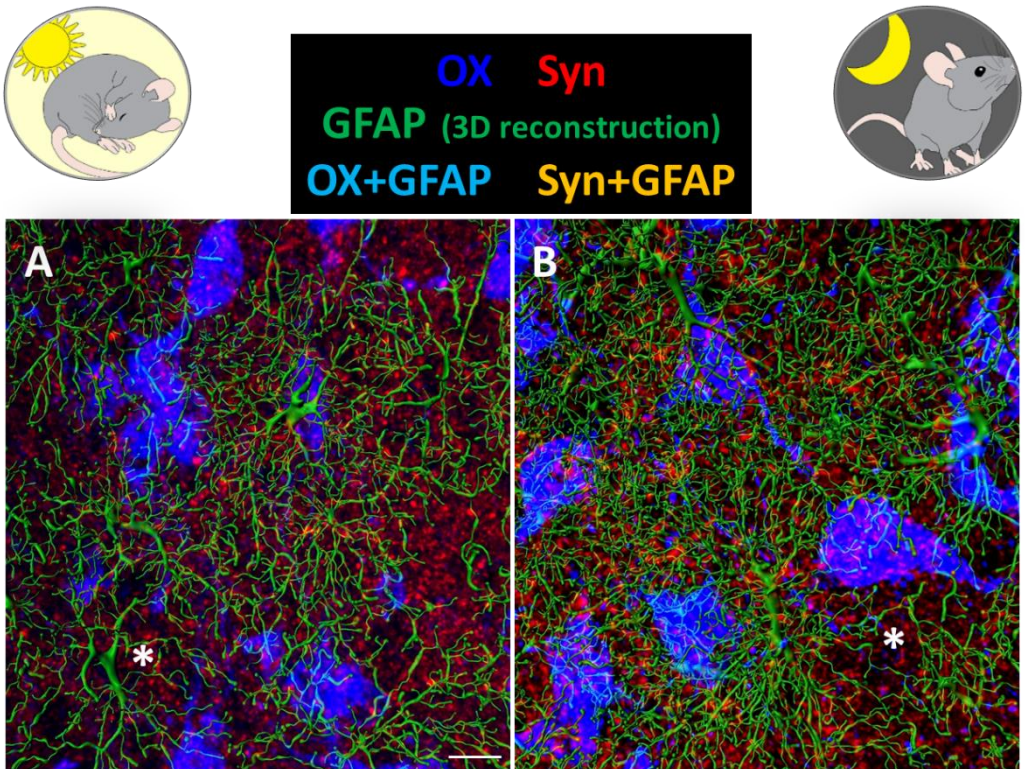

Fig. 2B.3: Higher magnification of the field marked by asterisks in Fig. 2B.2 showing astrocytes and presynaptic (Syn-immunopositive) elements and orexinergic neurons in the sampled light and dark periods. Note that processes of astrocytes extend onto OX somata and overlap spots of presynaptic elements. Scale bar = 15 µm.

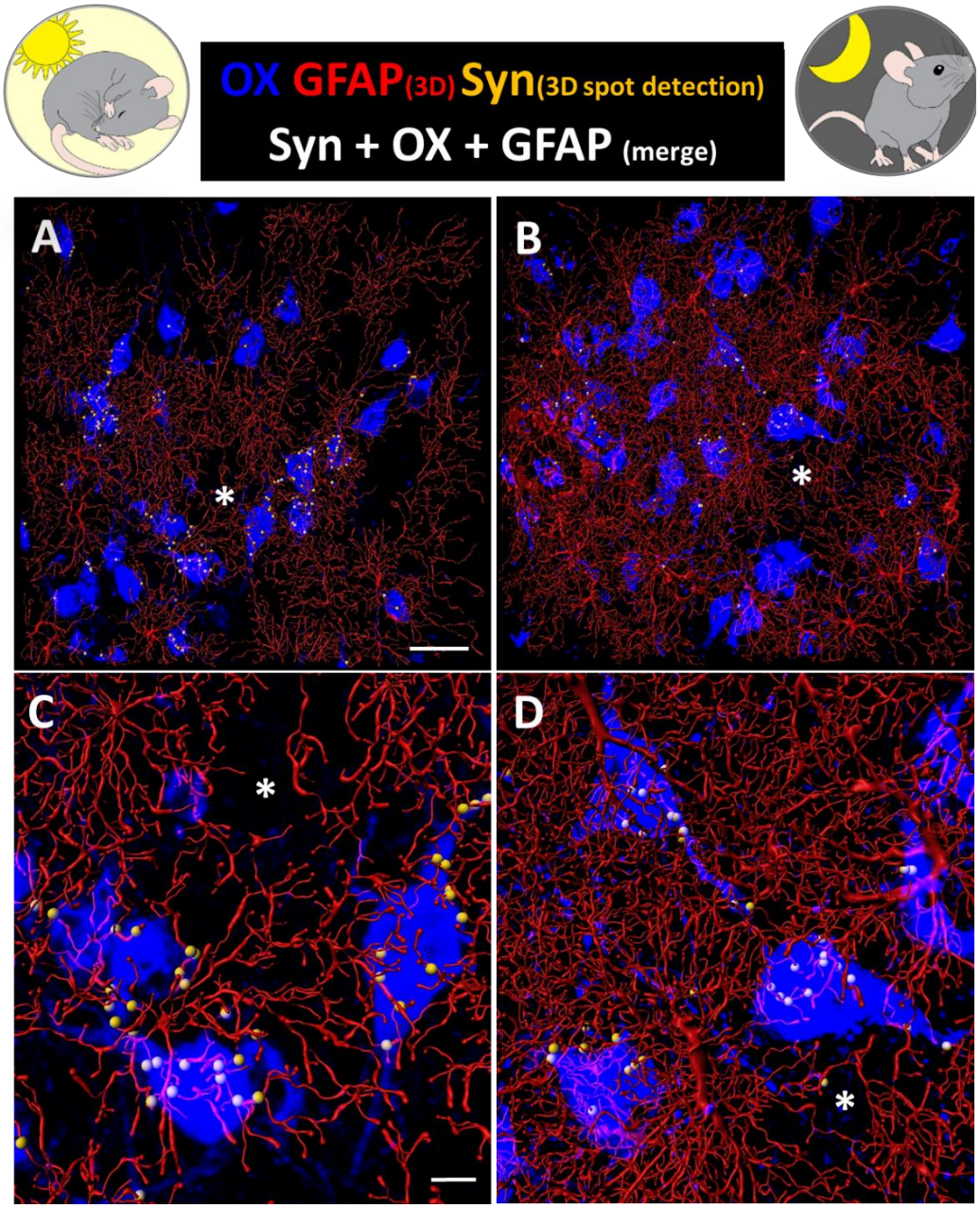

Fig. 2B.4: Merged images showing the overlap of axosomatic (Syn-immunopositive) terminals on orexinergic neurons with astrocytic processes in the sampled light and dark periods. **A, B**: maximum intensity projections confocal microscopy images of triple immunolabelling. **C, D**: following 3D reconstruction, higher power images of A, B (asterisks are for spatial landmarks) clearly show distal astrocytic processes onto the OX soma colocalized with axosomatic terminals. The Syn^{+} fluorescence signals within the neuropil not related to the OX soma/processes and astrocytic processes were masked and filtered out. Scale bars = 30 µm in A, 10 µm C.

2B.4 Comments

These preliminary observations suggest that diurnal changes occur in the spatial arrangement of astrocytes which surround OX neurons in the LH, in terms of the extent, orientation, and, possibly, degree of ramification of astrocytic processes.

It is known that astrocytic processes can undergo rapid morphological changes even in physiological conditions by the remodelling of their soma and processes (Theodosis et al. 2008). Such modifications have been documented in the SCN (see 1.1.4) according to circadian rhythmicity (Theodosis et al. 2008). It has also been reported that in the rat SCN GFAP immunoreactivity increases during the period of darkness and decreases during the light period with a circadian variation (Becquet et al. 2008). In mice, however, there are conflicting reports, since no circadian variation of GFAP immunoreactivity was found in the SCN in one study (Moriya et al. 2000), while in another study GFAP immunoreactivity was found to be highest in the middle of the light phase and lowest at the beginning of the dark phase (Santos et al. 2005). Furthermore, this oscillation was found to be maintained in total darkness conditions, indicating an endogenous rhythm (Santos et al. 2005).

Modifications of the astrocytic processes in other brain areas including the neocortex, hippocampus, cerebellum and brain stem, have been described in different conditions (review in Theodosis et al. 2008), but it is unclear whether plastic changes in astrocyte structure affect neuronal activity (Theodosis et al. 2008).

It has been proposed that glutamate release at synaptic sites could stimulate the protrusions or retractions of perisynaptic astrocyte processes (Lavialle et al. 2011). Other neurotransmitters could also be involved in the dynamics of astrocyte processes, which express receptors for most of CNS transmitters (Verkhratsky and Butt 2007). There are also suggestions that the diurnal remodelling of synapses by astrocytes could be related to their release of tumor necrosis factor-α (Lee and Haydon 2011), owing to the implication of this cytokine in sleep-wake modulation (Krueger 2008).

Astrocytes are a major source of extracellular adenosine, as such, there are suggestions regarding their involvement in sleep modulation (Schmitt and Wimmer 2015). Following SD, the level of adenosine derived from astrocytes was observed to increase in the hippocampus and cortex (Schmitt et al. 2012). However, following chronic SD, there was reduction in the elevated levels of adenosine observed in hippocampus during acute SD, suggestive of a positive feedback in preserving normal hippocampal functions (Clasadonte et al. 2014).

The most peripheral astrocytic processes, though quite small and thin for microscopic resolutions and rarely examined in electrophysiological studies, constitute about 80% of its cell membrane (Lavialle et al. 2011). It is important to recall in this context that the cytoskeletal protein GFAP may not actually reveal the full extent of perisynaptic glia, which instead express ezrin, a membrane-cytoskeleton linker (reviews in Derouiche et al. 2002; Theodosis et al. 2008;

Bernardinelli et al. 2014). In the brain, ezrin is exclusively expressed by astrocytes (Derouiche and Frotscher 2001) and ependymal cells (Berryman et al. 1993).

Although the present preliminary findings need to be confirmed, the adopted approaches for 3D reconstruction analyses of multiple immunofluorescence seem promising for the revelation of the relationships between GFAP-immunoreactive distal astrocytic processes and the inputs to OX neurons. Further ongoing analyses will clarify eventual time-related changes of this organization.

3. Synaptic wiring of orexinergic neuronal cell bodies during day and night: from adult to aged mice and study of a murine model of Alzheimer's disease

3.1 Introduction

The previous data (Chapter 2; Laperchia et al. 2017) provided evidence, in adult mice, of a fluctuation of the input to orexinergic neurons from a prevalent excitatory innervation at night, during a period of predominant wakefulness, to a prevalent inhibitory innervation at daytime, during a period of sleep predominance. The finding opens questions on the potential variations of this process during aging and in synaptopathies such as AD. The present study was aimed at the investigation of these issues to test the hypotheses that the diurnal fluctuation in the excitatory/inhibitory balance of the innervation of OX cell bodies could be modified by aging and by the pathological process underlying AD.

As discussed in Chapter 1, physiological functions controlled by the hypothalamus, including circadian rhythms, vary with age (see 1.2.1; see also Bonaconsa et al. 2013). Impairment of orexinergic signalling has been associated with aging-related dysfunctions (see 1.2.1; see also Foley et al. 2004; Corrada et al. 2010; Zink et al. 2014).

Of note, an aging-related reduction in the number of orexinergic neurons has been reported in the human and rodent brain (see 1.2.1). It has also been reported that the release of OX and OXR activation in the CNS decline with advancing age (see 1.2.1). No data is available, however, on the synaptic wiring of OX neurons during aging.

Concerning AD, as dealt with in Chapter 1 (see 1.2.3), not only disruption of circadian rhythmicity, but also sleep fragmentation have been reported in up to 40% of AD patients with mild to moderate dementia, and dysregulation of orexinergic signalling has been implicated in this functional disruption (reviews in Videnovic and Zee 2015; Liguori et al. 2016). Pathophysiological mechanisms that underlie alterations of circadian rhythmicity in AD have been described, with neuronal cell loss in the SCN and loss of pineal gland function considered as main contributors (Stopa et al. 1999; Wu et al. 2003), correlating positively with AD progression (Stopa et al. 1999; Liu et al. 2000; Videnovic and Zee 2015) (see 1.3.1; see also Bonaconsa et al. 2013).

Seminal studies have shown in the last years that the sleep-wake cycle can influence Aβ pathology which, in turn, can disrupt the sleep-wake cycle in a bidirectional relationship (Ju et al. 2014) (see 1.3.2). Of special interest are findings pointing to a regulatory role of OX on Aβ plaque deposition in amyloid precursor protein (APP) Tg mice during the sleep-wake cycle (Kang et al. 2009) (see 1.3.2).

Loss of about 40% OX neurons in *post-mortem* analyses of AD brains, and 14% reduction in CSF OX levels in AD patients compared to healthy control individuals have been reported (Fronczek et al. 2012) (see 1.3.2). However, the synaptic wiring of OX neurons has not been hitherto investigated in the brain of AD victims or in murine models of this disease.

The present study utilized as AD model double mutant mice carrying the TAS10 *thy1-APP695swe x* TPM *thy1 PS1.M146* mutations (TASTPM mice). In these mice, the deposition of Aß is progressive and age-related and is accompanied by astrocytosis and phosphotau accumulation, providing a useful model of AD (Howlett and Richardson 2009b).

The manuscript concerning the data presented in this chapter is in preparation. This manuscript will include the neurophysiological study of TASTPM mice of the age groups here used for the analysis of the diurnal fluctuation of OX soma innervation. Such neurophysiological part of the study has appeared in abstract form (Colavito et al. 2014) and is here shown in a figure (Fig. 3.1), presented as a premise to the present investigation. The study, performed in TASTPM mice and matched WT mice of 5 months and 21 months of age (n= 3 or 4 per group and per genotype; Colavito et al. 2014), showed that TASTPM mice do not exhibit the classical rhythmicity associated to phase and documented in WT mice (Fig. 3.1). In particular, 5 month-old TASTPM mice tended to present a lower amount of sleep (Fig. 3.1A) and a higher amount of wakefulness (Fig. 3.1B) compared to WT mice during light phase. The aged TASTPM mice tended to present a higher amount of sleep (Fig. 3.1A) and a lower amount of wake during the dark phase (Fig. 3.1B). Both WT and TASTPM 21 month-old mice showed an increase in the number of transitions between vigilance stages, independent of genotype (Colavito et al. 2014).
Another set of data, obtained previously in our lab, which will be included in the manuscript in preparation and has appeared in abstract form (SINS Congress 2015), concerns the number of OX neurons evaluated by stereological cell counts in young (3 month-old) and aged (18 month-old) TASTPM mice and matched WT mice. This investigation showed an aging-related reduction of OX neurons in the 18 month-old WT mice, which was significantly exacerbated in the 18 month-old Tg mice (SINS Congress 2015). In the work for the present thesis, OX cell counts have been performed in 15 month-old TASTPM mice and matched WT mice together with the evaluation of immunosignal intensity, as presented below. The reason for the analysis of OX immunosignal, which is indicative of the peptide expression, stems from experimental data indicating that partial loss of OX neurons in rats could be compensated by increased OX release (Gerashchenko et al. 2003).

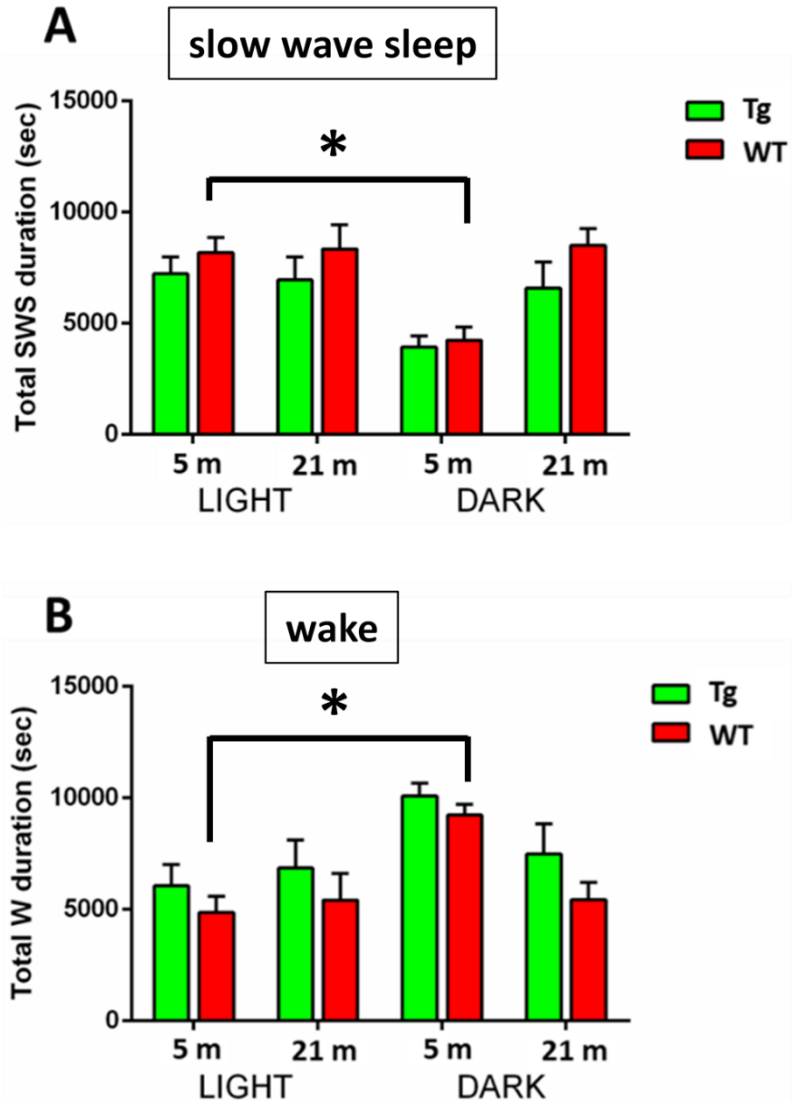

Fig. 3.1: Data from electroencephalographic recordings in adult and aged transgenic (Tg) TASTPM mice and matched wild-type (WT) mice (n= 3 or 4 per group). Note that compared to 5 month (m)-old WT mice, aged (21 m-old) WT mice and Tg mice of both age groups did not exhibit the classical rhythmicity associated to light or dark phase. Repeated measures ANOVA for sleep duration exhibited a phase-age interaction [$F(1,20)=8.08$, $p<0.05$] and a phase-genotype interaction [$F(2,20)=3.73$, $p<0.05$], and for wakefulness duration an age-phase interaction [$F(1,20)=8.41$, $p<0.05$] and a genotype-phase interaction [$F(2,20)=4.46$, $p<0.05$]. From Colavito et al. 2014.

3.2 Materials and methods

3.2.1 Experimental design and animals

The present study included different experimental groups (Table 3.1) for: ***i)*** observation of OX neurons and neurotransmitter transporter-characterized presynaptic terminals during day and night in adult C57BL/6J mice; ***ii)*** quantitative analyses of the diurnal fluctuation of the excitatory and inhibitory innervation of

orexinergic cell bodies in aged mice and in the AD model provided by TASTPM mice; ***iii)*** investigation of OX neurons in TASTPM mice; ***iv)*** neuropathological study of TASTPM mice.

The study of the diurnal organization of OX neuron input was pursued in TASTPM mice and WT mice of two age groups (Table 3.1): 3 month-old animals, an age which corresponds to early plaque formation in TASTPM mice (Howlett et al. 2004) and 20 month-old animals, which corresponds in TASTPM mice to an advanced stage of the pathological process (Howlett et al. 2008; Howlett and Richardson 2009a).

Male mice were used. WT and TASTPM mice of all age groups (Table 3.1) were maintained under a 12 h/12 h dark/light or light/dark cycle, under veterinarian control and controlled environmental (temperature and humidity) conditions, with free access to food and water. The animals were left undisturbed, avoiding any potential stressful condition. The experimental groups destined to the study of the diurnal fluctuation of OX neuron innervation (Table 3.1) were randomly divided in two groups sacrificed during a 2 h period during the day (ZT 3–4), or night (ZT 15–16), i.e. at the same time points adopted in our previous study (Chapter 2; Laperchia et al. 2017). The other experimental groups (destined for OX neuron analyses and for the neuropathological study of TASTPM mice; Table 3.1) were sacrificed during daytime. For sacrifice, the mice were deeply anesthetized with tribromoethanol (20 mg/kg, ip) and transcardially perfused with 0.01M phosphate-buffered saline, pH 7.2 (PBS), followed by 4% paraformaldehyde in PBS. The brains were removed, postfixed for 2 h, and cryoprotected in 30% sucrose in PBS at 4°C.

All procedures received approval by the Animal Care and Use Committee of the University of Verona (CIRSAL) and authorization by the Italian Ministry of Health, in strict adherence to the European Communities Council (86/609/EEC) directives and the ARRIVE guidelines, in accordance with the National Institute of Health Guide for the Care and Use of Laboratory Animals (NIH Publications No. 80-23), minimizing the number of animals used and avoiding their suffering.

3.2.2 Tissue processing and immunofluorescence

In three mice of the day or night groups, destined for the observation in confocal microscopy (Table 3.1), sections through the diencephalon were cut at a 30 µm thickness with a freezing microtome. Every second section through the LH was collected and processed free-floating for triple immunofluorescence to visualize OX-immunopositive cells, the presynaptic marker synaptophysin (Syn) and the vesicular glutamate transporter (VGluT)2 as marker of glutamatergic elements, or the vesicular GABA transporter (VGAT) as marker of GABAergic elements.

The brains of the above mice destined to the quantitative analyses of the daily organization of the synaptic input to OX cell bodies (Table 3.1) were embedded in OCT matrix, cut on a cryostat into 10 µm-thick coronal sections, and mounted on slides in three adjacent series. Every 12th section through the anteroposterior extent of the LH was stained with cresyl violet for cytoarchitectonic reference, and the adjacent series of sections were processed for triple immunolabelling to visualize OX/VGluT2/Syn or OX/VGAT/Syn.

For the multiple immunofluorescence procedure, the sections were processed free-floating (30 µm-thick sections) or on slide (10 µm-thick sections). They were preincubated in a solution of 0.3% Triton X-100 in 0.1M phosphate buffer, pH 7.4, for 1 h, and then incubated overnight in a mixture of primary antibodies (Table 3.2) diluted in the preincubation solution. After rinsing in PBS, the sections were incubated for 2 h in a mixture of secondary antibodies: Alexa Fluor 350-conjugated donkey anti-goat IgGs or Alexa Fluor 594-conjugated donkey anti-goat IgGs; Alexa Fluor 594-conjugated donkey anti-rabbit IgGs or Alexa Fluor 647-conjugated donkey anti-rabbit IgGs (all from InVitrogen, Carlsbad, CA, USA). The sections were then incubated for 2 h with Alexa Fluor488-conjugated goat anti-guinea pig IgGs (InVitrogen). After rinsing in PBS, the sections processed free-floating were mounted on slides. All sections were coverslipped with Aquatex mounting medium (Merck, Darmstadt, Germany).

To control antibody specificity, additional sections were processed as controls by omitting either the primary or secondary antibodies. No signal of the omitted reagent was detected in these control sections.

3.2.3 Microscopy and quantitative analyses

The 30 µm-thick sections processed for triple immunofluorescence were observed with the confocal microscope Leica SP5 (Leica, Manheim, Germany). Quantitative analyses of presynaptic terminals were performed in 10 µm-thick sections using epifluorescence: counts of Syn-immunopositive presynaptic terminals in contact with OX soma, and analyses of the diurnal fluctuation of their excitatory or inhibitory phenotype (Table 3.1). The other material (Table 3.1) was analyzed in bright-field light microscopy. Quantitative analyses were performed blindly of the experimental group assignment, and in all animals of each group.

The method used by Cristino et al. (2013), further validated by Laperchia et al. (2017), was followed to determine the mean number of presynaptic (Syn^+) terminals apposed to OX cell bodies, and the colocalization of $Syn^+/VGluT2^+$ and $Syn^+/VGAT^+$ in these terminals. Briefly, triple immunostained sections were observed with a DMI6000 (Leica, Manheim, Germany) microscope equipped with an x–y–z motorized stage, a digital camera Leica DFC 340FX, and the Leica Metamorph imaging software (Leica Meta-Morph AF, Manheim, Germany). Multichannel images were acquired and analyzed using the Leica Application Suite

(LAS) AF 2.2.0 software. OX cell bodies were randomly sampled from 3 to 5 sections through the perifornical area, where these cells are densely distributed, using the fornix as landmark.

For the analysis of the number of presynaptic terminals per OX soma (based on Syn and OX immunostaining), animals sacrificed at the day time point were used. The study of excitatory and inhibitory terminals (VGlut2 or VGAT, each colocalized with Syn) was pursued in pairs of sections, and in animals sacrificed at two time points in antiphase (Table 3.1; Laperchia et al. 2017). Sixty OX cells, sampled through the full extent of the nucleus, were used in each animal for these analyses (Syn immunolabeling on OX soma, or vesicular transporter + Syn immunolabeling on OX soma). Four images per cell in serial Z planes (1.6 mm step size) were acquired. Images were deconvolved using the Metamorph imaging deconvolution software by application of ten iterations. Terminals were examined in single optical slices and considered as appositions to cell bodies when overlap among the elements was evident upon full rotation of the images. Counts of appositions were performed with a semi-automated method using the Metamorph Imaging Investigator software.

Furthermore, as shown in Table 3.1, 15 month-old WT and matched Tg mice were used for counts of OX cells and densitometric analyses of OX immunosignal intensity. Unbiased stereological counts of OX-immunoreactive neurons were done with an Olympus BX63 microscope connected to a digital camera and equipped with the Neurolucida microstereo-investigator software with an optical fractionator work flow (MBF Bioscience, Williston, VT USA). The densitometric analysis of immunosignal intensity of OX-immunoreactive cells was performed using the same Olimpus microscope and the Image Pro Plus 7.0 software (Media Cybernetics, Silver Spring, MD, USA). OX neurons were sampled throughout the rostrocaudal extent of the LH, in sections regularly spaced (at 125 µm intervals), as done in previous studies (King et al. 2002; Nair-Roberts et al. 2008; Palomba et al. 2015a).

3.2.4 Amyloid-β deposition and glia immunophenotyping

Tg mice and matched WT mice of different age groups were used for this part of the study (Table 3.1). Brain sections were processed for the visualization of Aβ plaques, microglia and astrocytes. Information on the antibodies used for the immunohistochemistry procedures is presented in Table 3.2. Briefly, sections were first reacted in 0.3% H_2O_2 (MallincKrodt Baker Inc., Deventer, The Netherlands) in PBS for 20 min for inactivation of the endogenous peroxidase activity, and then washed 3 x 5 min. Sections were then preincubated in a blocking solution containing 0.3% Triton X-100 and 3% normal goat serum (NGS) in PBS, for 1 hr at room temperature. The incubation in the primary antibodies (Table 3.2) diluted in preincubation solution was performed overnight at 4◦C. The following day, sections were rinsed 3 x 5 min and incubated for 2 h in the appropriate secondary

antibodies: biotinylated goat anti-rabbit and goat anti-rat secondary antibodies (Vector Labs, Burlingame, CA, USA), respectively, diluted 1:200 in 1% NGS. The sections were then reacted in avidin-biotin-peroxidase solution (ABC kit, Vectastain, Vector Labs) for 30 min, followed by 3 x 5 min rinses in PBS. Visualization of the reaction products was achieved with a chromogenic solution of 3,3'-diaminobenzidine. The stained sections were dehydrated in graded alcohols, cleared in xylene, mounted on gelatinized glass slides and allowed to air dry overnight. They were then coverslipped with the water free-mounting medium Entellan.

3.3 Statistical analyses

The data were statistically evaluated by two-way analysis of variance (ANOVA) followed by Bonferroni *post-hoc* testing to compare the mean number of synaptic varicosities apposed to OX soma at each time point using Graph pad Prism 5 System (San Diego, CA). Multivariate ANOVA (MANOVA) was used to determine the statistical interaction between the number of excitatory and inhibitory inputs in the day/night groups (IBM SPSS software; Chicago, IL, USA). The Student's *t*-test was used to analyze the data generated from OX cell counts and densitometric evaluation. In all statistical analyses, significance threshold was set at $p<0.05$.

3.4 Results

3.4.1 Triple immunofluorescence of orexinergic neurons and glutamatergic or GABAergic presynaptic terminals

In adult mice sampled at day or night, triple immunofluorescence resulted in the effective visualization, in confocal microscopy, of OX-immunopositive cell bodies together with Syn immunosignal and VGluT2 or VGAT immunosignal (Fig. 3.2). At the observation, the intensity of immunofluorescence of OX^+ somata appeared higher at night than at day. To achieve uniformity in the observation, a threshold for OX signal saturation was used in both conditions (Fig. 3.2).

Syn^+, $VGluT2^+$ and $VGAT^+$ elements were seen throughout the neuropil in both the day and night groups (Fig. 3.2). In the merged images, triple immunolabeling allowed the visualization of $Syn^+VGluT2^+$ (Fig. 3.2c,i) and Syn^+VGAT^+ (Fig. 3.2f,l) presynaptic terminals in contact with the membrane of OX^+ cell bodies, with a dense perisomatic distribution. A dense distribution was also observed around OX-immunonegative somata intermingled with OX-immunopositive ones. Furthermore, it could be observed that very few presynaptic (Syn^+) elements in apposition to OX-immunopositive cell bodies did not show VGlut2 or VGAT immunolabelling.

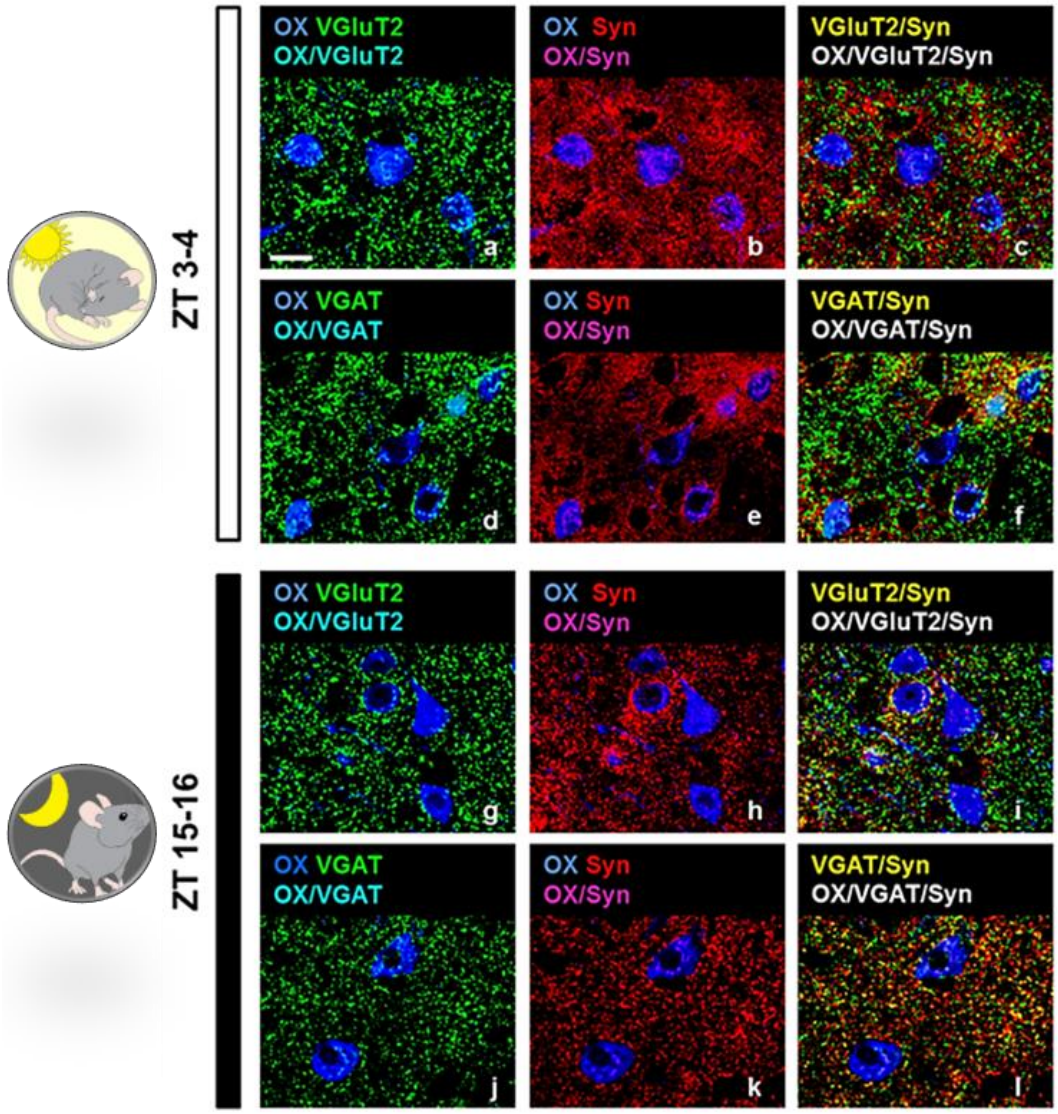

Fig. 3.2: Confocal microscopy images of triple immunofluorescence at daytime (*Zeitgeber* time, ZT, 3-4) and night (ZT 15-16). Neurons containing orexin-A (OX) are in blue. Excitatory (vesicular glutamate transporter, VGluT2 -immunopositive) or inhibitory (vesicular GABA transporter, VGAT -immunopositive) elements are in green (left column). Synaptophysin (Syn) immunopositivity is in red (middle column). Merged images (right column) show $Syn^{+}/VGlut2^{+}$ or $Syn^{+}/VGAT^{+}$ terminals in apposition to OX neuron membrane, or surrounding OX-immunonegative cell bodies. Scale bar: 20 μm. (Images collected in collaboration with Dr. Claudia Laperchia).

3.4.2 Quantitative analyses of the input to orexinergic cell bodies

The evaluation of the mean number of presynaptic terminals in apposition to OX somata (Fig. 3.3) showed highly significant age- and genotype-dependent variations. Concerning age, about 38% loss was documented in the aged (20 month-old) WT mice *vs* young (3 month-old) ones, and this reduction was more marked (about 48%) when evaluated between young and aged Tg mice. In the comparison between genotypes, very striking was the reduction of the input in the Tg mice of both age groups with respect to the matched WT groups, with a decrease to about half (about 48%) in the young Tg mice with respect to the young WT ones. Such reduction was about 57% in the aged Tg mice *vs* the aged WT ones (Fig. 3.3).

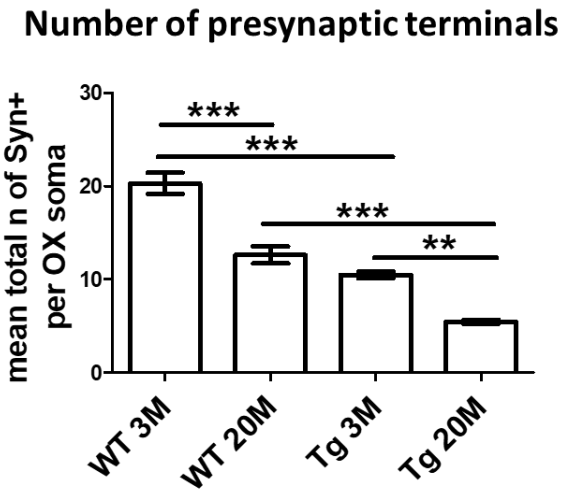

% reduction	
WT 3 m *vs* 20 m	37.88
WT 3 m *vs* Tg 3 m	48.37
Tg 3 m *vs* Tg 20 m	48.10
WT 20 m *vs* Tg 20 m	56.81

Fig. 3.3: Quantitative evaluation of presynaptic terminals (synaptophysin-immunopositive, Syn^{+}) in apposition to cell bodies containing orexin-A (OX) from transgenic (Tg) TASTPM mice of two age groups (3 months and 20 months) and matched wild-type (WT) mice. The animals were sampled during the light period. **p<0.01, ***p<0.001, one way ANOVA with Bonferroni post hoc test.

In all experimental groups, the mean total number of presynaptic (Syn+) terminals per OX soma during day and night was not significantly different (Figs. 3.4, 3.5) (3 month-old WT mice: 20.30 ± 1.13 at daytime, 18.50 ± 0.79 at night; 20 month-old WT mice: 12.60 ± 0.91 at daytime, 12.90 ± 0.49 at night; 3 month-old Tg mice: 10.50 ± 0.36 at daytime; 20 month-old Tg mice: 5.45 ± 0.22 at daytime, 5.51 ± 0.10 at night). This indicated that at both ages and in both genotypes the overall input to OX somata remained quantitatively stable, not showing diurnal fluctuations.

As mentioned above, pairs of 10-µm-thick sections were used for the evaluation of neurotransmitter transporter-characterized input to OX cell bodies. A prevalence of glutamatergic ($Syn^+/VGluT2^+$) terminals was found in the young WT mice sampled at night (mean number of appositions per OX cell body: 12.80 ± 0.79) *vs* those sampled at day (4.90 ± 0.55) (Fig. 3.4a). A prevalence of GABAergic ($Syn^+/VGAT^+$) terminals per OX soma was documented in the young animals sampled during daytime (mean: 14.20 ± 0.83) *vs* night (5.66 ± 0.44) (Fig. 3.4a). This resulted in a ratio of VGluT2/VGAT terminals of about 3:1 in the young mice sampled at night, and about 1:3 in those sampled at daytime.

In terms of relative proportion of Syn^+ varicosities per OX soma, in young WT mice the data indicated that $VGluT2^+$ elements accounted for 25.50 ± 2.94% and $VGAT^+$ elements for 74.50 ± 2.94% at daytime, whereas $VGluT2^+$ elements accounted for 69.00 ± 5.04% and $VGAT^+$ elements for 31.00 ± 5.04% at night. The results were very consistent across the young WT mice (Fig. 3.4b). The statistical analysis showed that the above differences were highly significant: MANOVA showed a significant multivariate main effect for the time of sacrifice (Wilk's $\lambda = 0.027$; $F(2,3) = 53.526$; $p=0.005$, partial $\eta 2 = 0.973$; power to detect the effect: $\alpha = 0.05$).

The prevalence of glutamatergic ($Syn^+/ VGluT2^+$) terminals found at night in the young animals was drastically dampened in the aged WT mice at night (mean number of excitatory appositions per OX cell body: 4.55 ± 0.34) *vs* day (2.74 ± 0.09), (Fig. 3.4c). In the evaluation of GABAergic ($Syn^+/VGAT^+$) terminals in the aged WT animals, similar numbers were found at the two time points (9.46 ± 0.64 day; 8.02 ± 0.80 night) (Fig. 3.4c). The findings were consistent across the aged WT mice (Fig. 3.4d). The statistical analysis showed that these differences were not significant (MANOVA: main effect for the time of sacrifice was not significant; Wilk's $\lambda = 0.065$; $F(2,3) = 7.339$; $p=0.070$, partial $\eta 2 = 0.830$; power to detect the effect: $\alpha = 0.05$).

Thus, in the evaluation of excitatory and inhibitory terminals in aged WT mice the findings resulted in a ratio of VGluT2/VGAT terminals per OX soma of 1.0:1.7 at night, and 1.0:3.4 at daytime. In terms of relative proportion of Syn^+ terminals per OX soma, the data indicated that $VGluT2^+$ elements accounted for 22.50 ± 2.28%

and VGAT+ elements for 77.50 ± 2.28% at daytime, whereas VGluT2^{+} elements accounted for 36.44 ± 6.56% and VGAT^{+} elements for 63.56 ± 6.56% at night. Therefore, in aged WT mice inhibitory (VGAT^{+}) terminals were relatively more prevalent over excitatory (VGluT2^{+}) terminals at both day and night, without a significant diurnal fluctuation.

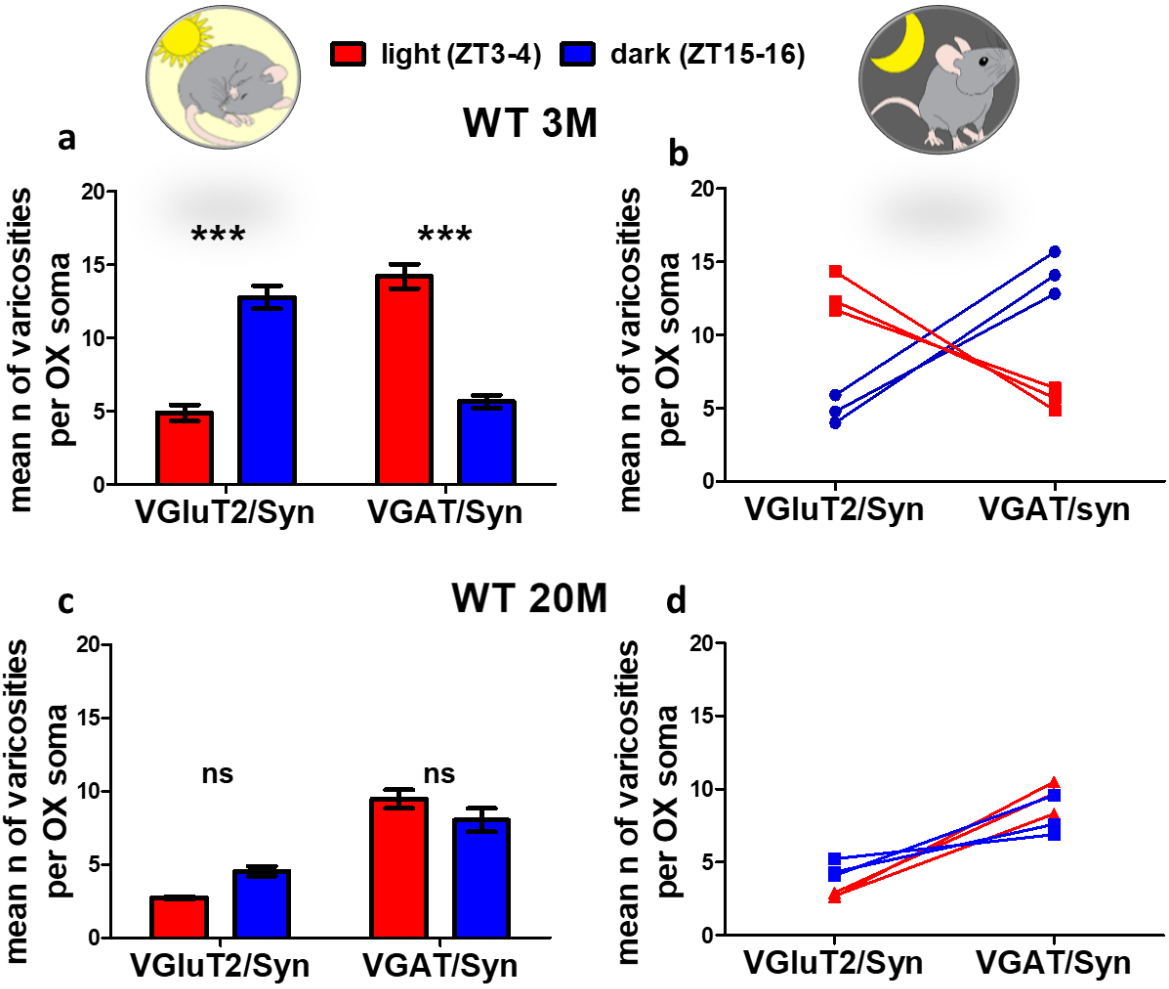

Fig. 3.4: Quantitative analyses of excitatory and inhibitory varicosities in contact with cell bodies containing orexin-A (OX) in the sampled light and dark periods in young adult (3 months, M, of age; **a,b**) and aged (20 M; **c,d**) wild-type (WT mice. **a,c**: Mean number (±SEM) of excitatory (VGluT2+/Syn+) or inhibitory (VGAT+/Syn+) terminals (n = 60 cells per mouse; n = 3 mice per group). ***p<0.001, ns, not significant; multivariate analysis of variance (MANOVA), F = 2,3. **b,d** Scatter plots of the mean number of excitatory and inhibitory varicosities per OX soma in each of the animals. Note that the individual data sets are very consistent across animals.

The same analyses showed interesting findings also in TASTPM mice. In the young Tg mice, a prevalence of glutamatergic ($Syn^+/VGluT2^+$) terminals was found in the animals sampled at night (mean number of appositions per OX cell body: 5.52 ± 0.31) *vs* those sampled at day (3.04 ± 0.25) (Fig. 3.5a). A prevalence of GABAergic ($Syn^+/VGAT^+$) terminals per OX soma was documented in the mice sampled during day (6.07 ± 0.45) *vs* night (2.96 ± 0.28) (Fig. 3.5a). The statistical analysis showed that the above differences were significant (MANOVA: significant multivariate main effect for the time of sacrifice (Wilk's $\lambda = 0.122$; $F(2,3) = 10.800$; $p=0.043$, partial $\eta 2 = 0.878$; power to detect the effect: $\alpha = 0.05$). Thus, the diurnal fluctuation documented in young WT mice was replicated in the matched Tg mice.

The ratio between excitatory and inhibitory terminals was, however, different in young Tg mice with respect to young WT ones, due to the overall decrease of the number of terminals in Tg mice. The ratio of VGluT2/ VGAT terminals per OX soma was about 2:1 in young Tg mice sacrificed at night, and about 1:2 in those sacrificed during the day. In terms of relative proportion of Syn^+ terminals per OX soma, the data indicated that in young Tg mice $VGluT2^+$ elements accounted for 34.16 ± 5.89% and $VGAT^+$ elements for 65.84 ± 5.89% at daytime, whereas $VGluT2^+$ elements accounted for 66.23 ± 0.76% and $VGAT^+$ elements for 33.77 ± 0.76% at night. The results were very consistent across the animals (Fig. 3.5b).

In the aged Tg mice (Fig. 3.5c), the mean number of glutamatergic ($Syn^+/ VGluT2^+$) terminals in the animals sampled at night (2.48 ± 0.25) was very similar to that documented at daytime (2.59 ± 0.25). Also the mean number of GABAergic ($Syn^+/ VGAT^+$) terminals was similar at night (2.29 ± 0.28) and day (2.40 ± 0.13). The statistical analysis confirmed that these differences were not significant (MANOVA: multivariate main effect for the time of sacrifice was not significant (Wilk's $\lambda = 0.170$; $F(2,3) = 0.429$; $p=0.686$, partial $\eta 2 = 0.222$; power to detect the effect: $\alpha = 0.05$).

Therefore, in the aged Tg mice, the ratio of VGluT2/ VGAT terminals was equal (about 1:1) at both the sampled time points. The relative proportion of excitatory and inhibitory terminals was also about equal at day and night: $VGluT2^+$ elements accounted for 51.74 ± 1.89% of Syn^+ terminals and $VGAT^+$ elements for 48.26 ± 1.89% at daytime, while $VGluT2^+$ elements accounted for 52.07 ± 1.60% and $VGAT^+$ elements for 47.93 ± 1.60% at night. The results were very consistent across animals also in the aged Tg group (Fig. 3.5d).

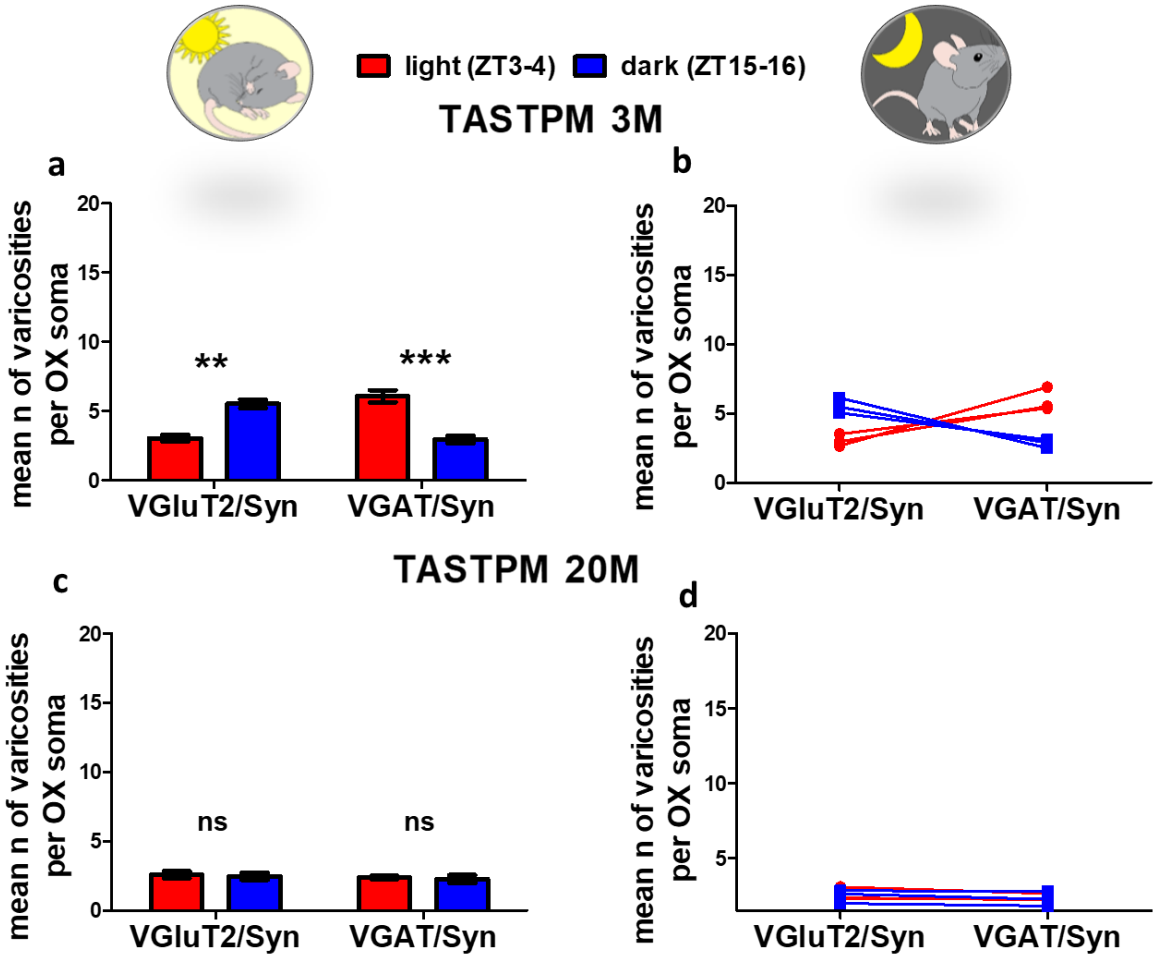

Fig. 3.5: Quantitative analyses, as in Fig. 3.4, in transgenic TASTPM mice of two age groups (n = 60 cells per mouse; n = 3 mice per group). ***p<0.001, ns, not significant; multivariate analysis of variance (MANOVA), F = 2,3. **b,d** Scatter plots of the mean number of excitatory and inhibitory terminals per OX-A soma in each of the animals. Note that the individual data sets are very consistent across the transgenic animals.

3.4.3 Orexinergic cell counts and immunosignal intensity

The observation of OX neuron immunoreactivity in 15 month-old Tg mice (sampled during daytime) showed marked alterations with respect to matched WT mice. OX neurons appeared sparser in Tg mice than in WT ones at low power observation (Fig. 3.6A,B). A marked reduction of immunostained dendritic arborizations (Fig. 3.6C,D) and shrinkage of some OX neurons, though with intense immunoreactivity of cell bodies (Figs. 3.6D, 3.7B) were seen in the Tg mice.

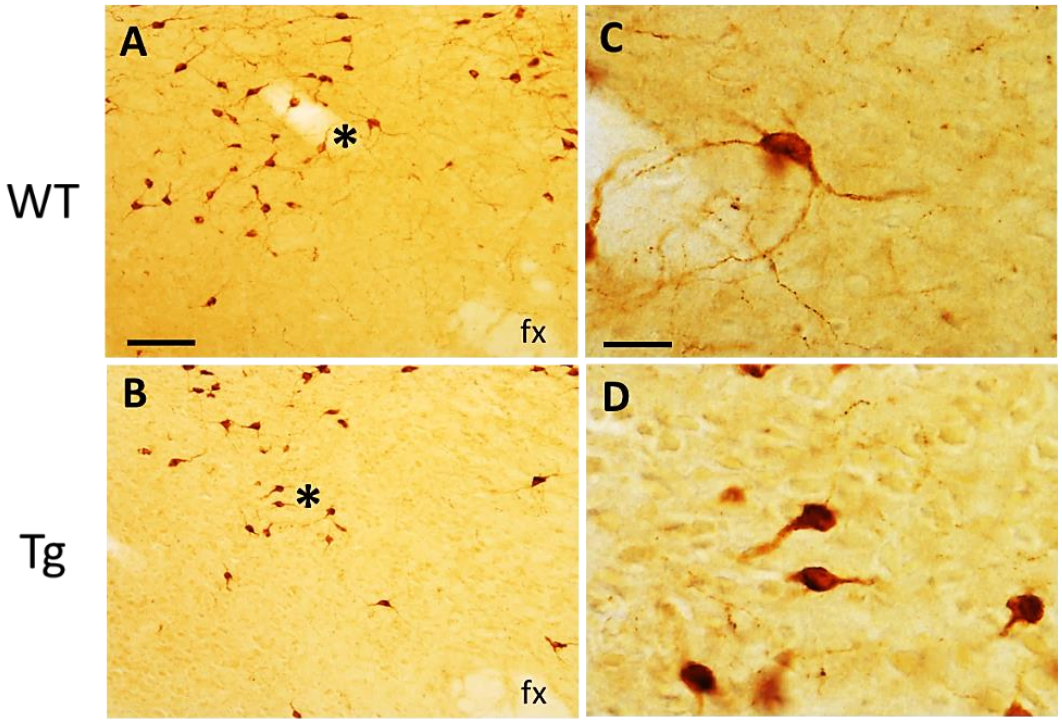

Fig. 3.6: Immunoreactivity of neurons containing orexin-A in a wild-type (WT) mouse (**A,C**) matched with a transgenic (Tg) TASTPM mouse (**B,D**) of 15 months of age (sampled in the light phase); fx indicates fornix. Note in the Tg mouse the decreased density of immunoreactive neurons, the shrinkage of intensely immunostained cell bodies, the swelling of proximal dendrites with a limited extent of dendritic immunoreactivity. Scale bars: 50 μm in A (and B), 20 μm in C (and D).

The stereological cell counts indicated a significant loss (34%) of OX-immunoreactive neurons in Tg mice *vs* matched WT ones (Fig. 3.7C). The evaluation of OX neuron immunosignal intensity by densitometric analysis confirmed that the immunostaining was significantly enhanced in the Tg mice with respect to the WT ones (Fig. 3.7D).

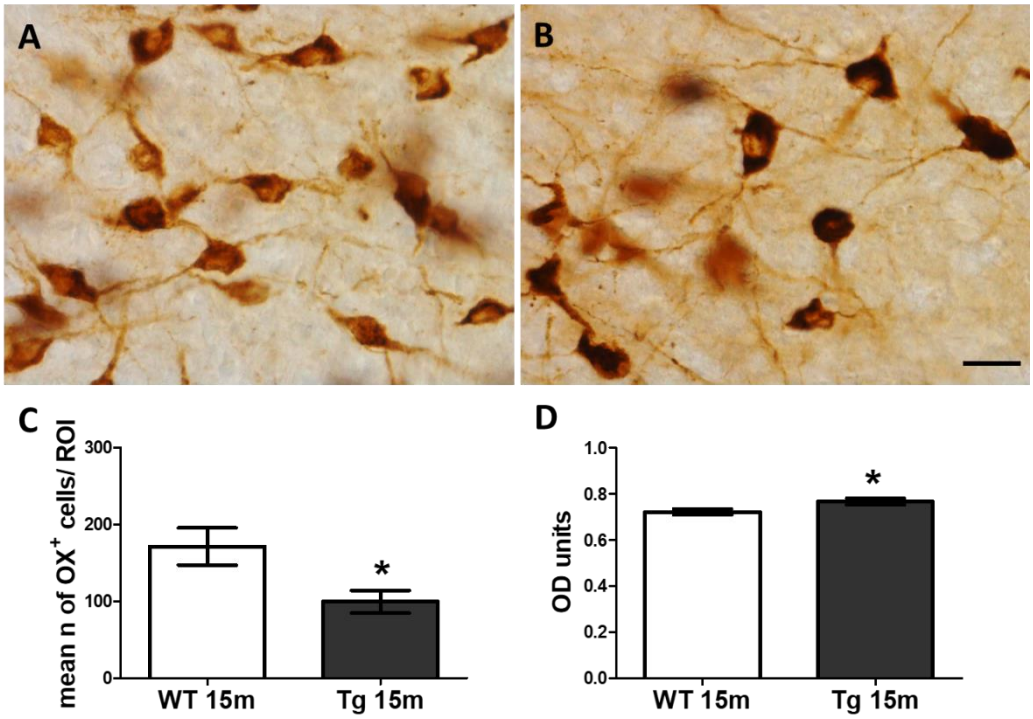

Fig. 3.7: **A,B**: Immunoreactivity of neurons containing orexin-A (OX) in a wild-type (WT) mouse (**A**) matched with a transgenic (Tg) TASTPM mouse (**B**) of 15 months of age (sampled during the light phase). Note in **B** the features shown also in Fig. 3.6B,D, and in particular the intense immunostaining. Scale bar: 20 μm. **C,D**: quantitative analyses. The bar graphs in **C** illustrate the results of stereological counts of orexinergic (OX^+) neurons in 15 month (m)-old WT and Tg mice. Note the significant reduction in the number of orexinergic neurons in the Tg mice (ROI, region of interest). The bar graphs in D illustrate the results of the densitometric analysis (OD, optical units). Note the significant increase of immunosignal intensity in the Tg mice. *$p<0.05$, Student's *t*-test.

3.4.4 Neuropathological features of TASTPM mice

Deposition of Aβ and immunophenotyping of microglia and astrocytes were investigated in TASTPM mice of different age groups (Table 3.1). Aβ aggregates were found in many brain regions of the 15 month-old TASTPM mice (Fig. 3.8B-

D). A progression of Aβ plaque load was found in the frontal and parietal cortices and hippocampal CA1 with increasing age. Aβ plaque deposits were 20-100 μm in diameter, mostly round-shaped and well demarcated, with marked intense immunostaining and a central core in the thalamus, while in the neocortex and hippocampus the Aβ deposits were weakly demarcated and irregularly shaped (Fig. 3.8B-D). Aβ plaques were relatively sparse in the hypothalamus, with a low intensity diffuse plaque phenotype.

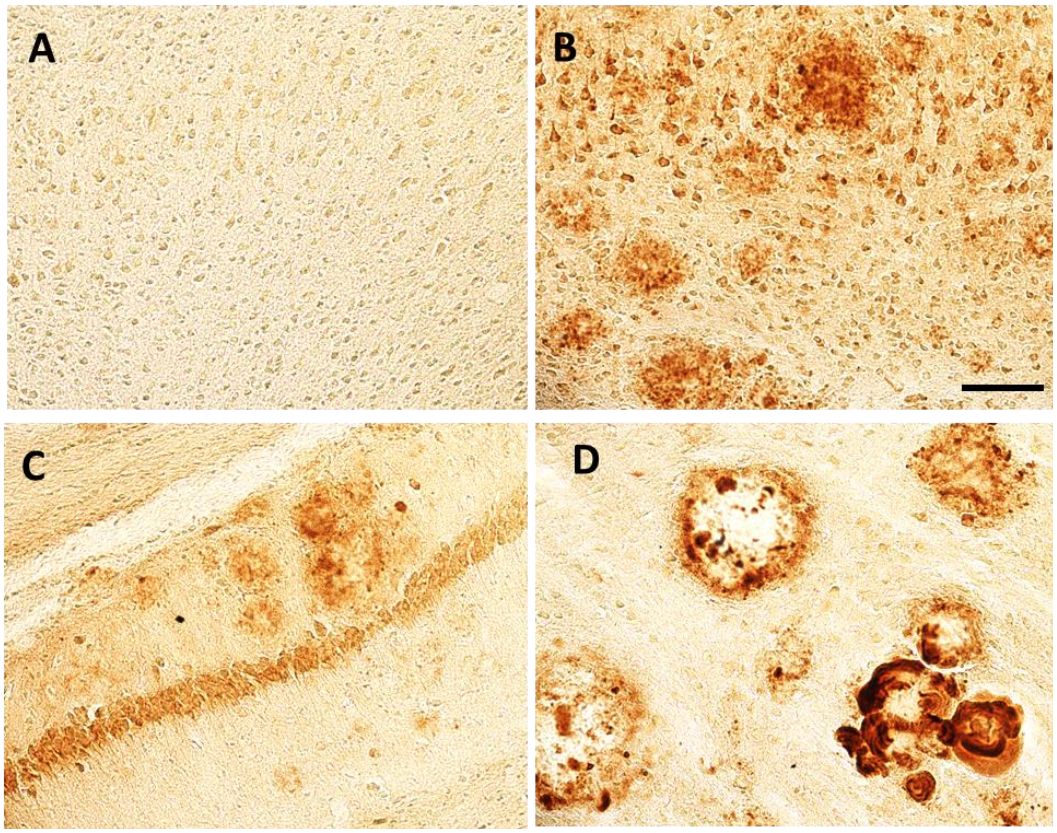

Fig. 3.8: Amyloid β plaque (visualized by amyloid precursor protein immunoreactivity) deposition in the neocortex (**B**), hippocampus (**C**) and thalamus (**D**) of 15 month-old TASTPM mice. No plaque deposits were seen in the cortex of an age-matched wild-type mouse (**A**). Scale bar: 50 μm.

GFAP immunoreactivity showed changes also in the astrocyte phenotype in the brain of Tg mice (Fig. 3.9B-D). Astrocytes were especially prominent around Aβ plaques (Fig. 3.9B,C). There was a generalized hypertrophy of the astrocytes (Fig. 3.9B-D), with increased reactivity which correlated with the amyloid plaque load. As shown in Fig. 3.9B, the diffuse Aβ deposits in the hippocampus were surrounded by astrocytes and astrocytes not associated to plaques were also present. The core of neuritic plaques in the thalamus was bordered and surrounded by astrocytes, which were also present in the damaged tissue halo (Fig. 3.9C). The astroglia

profiles in the hypothalamus appeared relative different, with shrinkage of cell bodies and prominent stout processes (Fig. 3.9D).

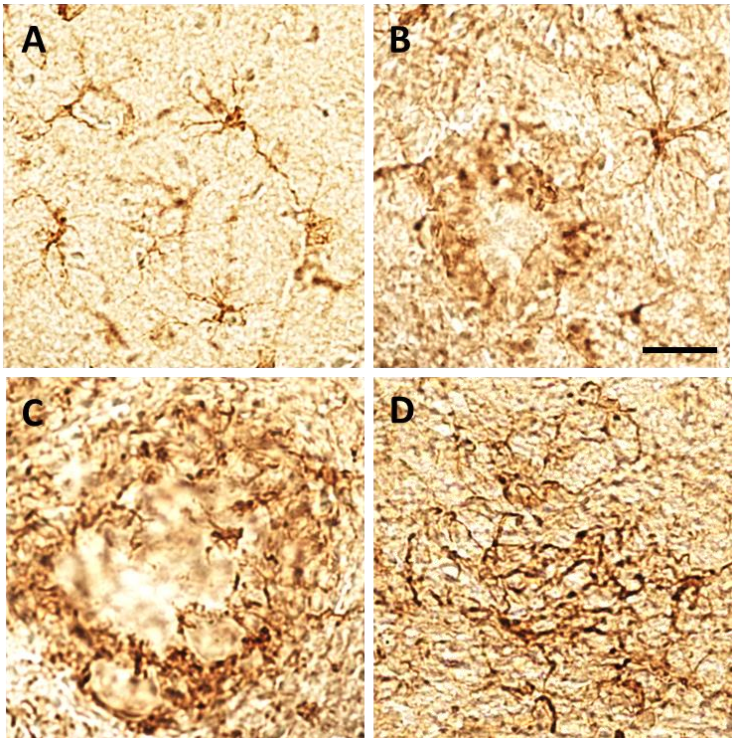

Fig. 3.9: Glial fibrillary acidic protein (GFAP) immunoreactivity in different brain regions of wild-type (A) and transgenic (Tg) TASTPM (B-D) mice of 15 months. Astrocyte immunolabeling shows marked cell hypertrophy in the hippocampus (B), thalamus (C) and hypothalamus (D) of Tg mice. Scale bar: 50 μm.

Ramified microglial cells, stained by CD11b immunoreactivity, were observed in the WT mice (Fig. 3.10A), but appeared hypertrophic, intensely immunostained and clustered especially around plaque deposits, delineating them in the age-matched Tg mice (Fig. 3.10B-D). All these features were very prominent in the thalamus of Tg mice, where tissue damage by Aβ plaques was especially marked, with hypertrophic bushy and amoeboid microglial cells scavenging the damaged tissue halo (Fig. 3.10C). Microglia with hypertrophic cell bodies and thick stout processes were prominent also in the hypothalamus of the Tg mice (Fig. 3.10D).

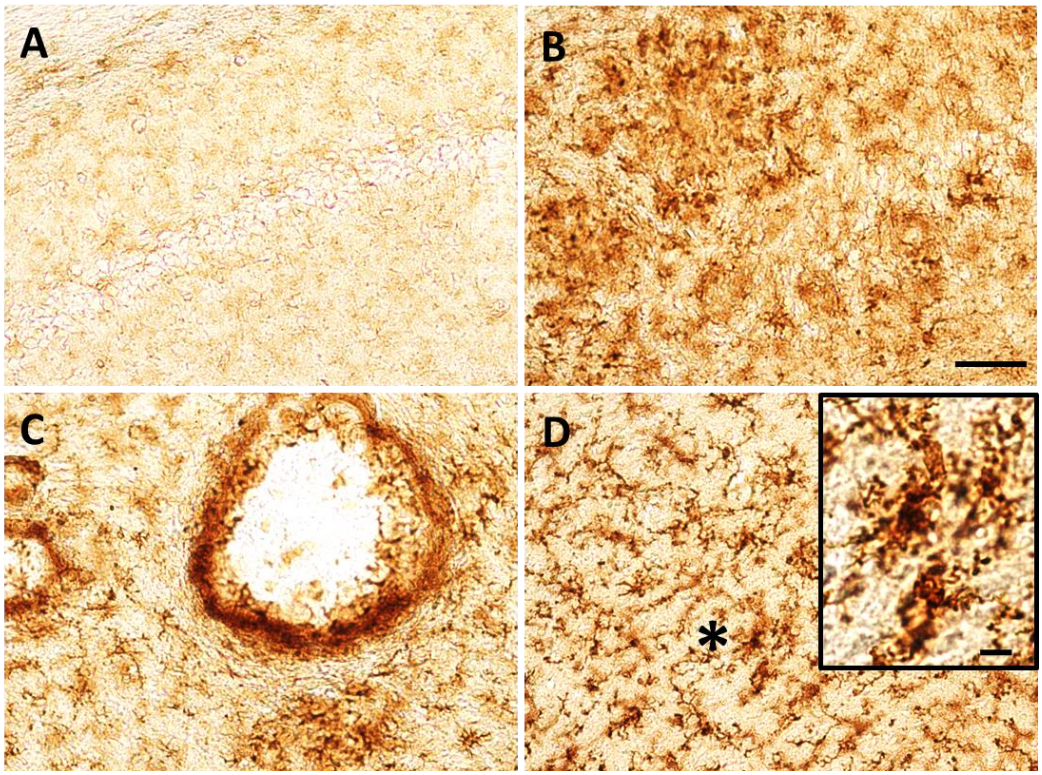

Fig. 3.10: Microglia immunophenotyping (CD11b immunoreactivity) in different brain regions of wild-type (WT) and transgenic (Tg) TASTPM mice of 15 months of age. Ramified microglial cells were observed in WT mice (hippocampus in **A)**. Note the bushy aspect of microglial cells and their clustering (indicative of activation) in Tg mice in the hippocampus (**B**), thalamus (**C**) and hypothalamus (**D**). The inset in D shows at higher magnification the area indicated by the asterisk. Note in B-D the hypertrophy and increased immunostaining intensity of microglial cells. Note also the marked clustering around plaque deposits, especially in the thalamus (C), in the Tg mice. Scale bar: 50 μm.

3.5 Discussion

The main findings of the present study revealed alterations of the wiring of OX cell bodies during aging as well as murine AD.

The data on the balance between excitatory and inhibitory terminals in contact with OX cell bodies at day and night showed in the young WT mice a switch from a prevalent excitatory innervation during the period of predominant activity and wake of the animals to a prevalent inhibitory innervation during the period of predominant rest and sleep, consistently with our previous study (Chapter 2; Laperchia et al. 2017). Interestingly, the present investigation showed that such diurnal fluctuation was lost in the aged WT animals. The statistical power might have been influenced by the limited sample size. However, the present analyses also

showed that in the aged WT mice the input to OX cell bodies was predominantly inhibitory at both time points.

The same analyses in the AD murine model provided by TASTPM mice showed that the diurnal fluctuation was maintained in the young Tg animals and lost in the aged ones, in which the trend towards a prevalent inhibitory innervation, documented in the aged WT mice, was also lost, configurating a similar organization during both day and night.

The use of multiple presynaptic labeling strategy in epifluorescence for the visualization of excitatory and inhibitory synaptic boutons on OX somata here adopted has been previously validated at the ultrastructural level (Horvath and Gao 2005; Cristino et al. 2013), and with the use of presynaptic markers combined with postsynaptic scaffold proteins (Laperchia et al. 2017).

Previous reports of alterations in the orexinergic system during aging in rats and other species have documented a decrease in the OX innervation of target regions (Downs et al. 2007), as well as in the expression of OX or OXRs in rodents (Terao et al. 2002; Porkka-Heiskanen et al. 2004), and alterations in the pattern of OX release across the diurnal cycle (Desarnaud et al. 2004) (see 1.3.1). Of note, the physiological aging process affects the number of OX-immunoreactive neurons, with an overall decrease of about 25% from infancy to older age in humans (Hunt et al. 2015b), and aging-related decreases in rodents (Porkka-Heiskanen et al. 2004; Sawai et al. 2010; Kessler et al. 2011) (see 1.3.1).

The present study adds to such previous findings a decline in the density of the innervation of OX cell bodies, with a 38% reduction in the number of presynaptic terminals in the aged WT mice compared to the young ones. Though the density of the innervation of OX neuron dendrites remains to be investigated, such finding suggests that the afferent control of OX neurons varies considerably with aging. Aging-related changes in OX neuron regulation are also strengthened by the present observation of a prevalent inhibitory input to OX cell bodies during both day and night. The absence in the aged WT mice of the fluctuation documented in young WT mice could be involved in weakened sleep-wake stability and changes in energy homeostasis during aging (see 1.3.1).

Concerning the AD model provided by TASTPM mice, our data point out sleep-wake alterations (Colavito et al. 2014; Fig. 3.1). Normal sleep/wake cycle has been described in the double mutant (APPswe/PS1dE9) mouse model of AD, with a normal diurnal fluctuation of interstitial fluid (ISF) Aβ prior to Aβ plaque formation. However, increase in amyloid plaque deposition has been reported to represent a factor in sleep-wake cycle deterioration and diurnal fluctuation of ISF Aβ alterations (Roh et al. 2012) (see 1.3.1).

The present findings point out a marked decrease of OX axosomatic innervation in TASTPM mice. Synaptic loss is a key feature of neocortical and hippocampal pathology in AD (Davies et al. 1987; Scheff and Price 2003). Loss of the presynaptic terminal marker Syn has been reported in many APP Tg mouse lines (Games et al. 1995; Hsia et al. 1999; Richardson et al. 2003; Rutten et al. 2005). In single mutant PDAPP mice, synaptotoxicity has been reported prior to plaque formation (Mucke et al. 2000). The present results are, however, the first documenting synaptic loss at hypothalamic levels in murine AD pathology, and the data here obtained in TASTPM mice point to a vulnerability of the orexinergic synaptic network since the early phases of the AD pathological process.

The present cell counts revealed a significant loss (34%) of OX neurons in TASTPM mice. Such loss could indicate, as in the data related to physiological aging, cell death and/or decrease of peptide production below the threshold for immunohistochemical visualization. The upregulation of immunosignal intensity of OX neurons in the Tg mice could, on the other hand, indicate a compensatory production of the peptide by OX neurons in response to immunostained neuron loss. Compensatory release of OX has also been hypothesized for the maintenance of OX-A level in the CSF after partial destruction of OX neurons in rats (Gerashchenko et al. 2003).

Concerning the neuropathological features of TASTPM mice, the present data have shown an age-related increase of Aβ plaque load in the sampled neocortical regions and hippocampal CA1 field which is in agreement with previous data on a progression of Aβ deposition throughout the animal's life, accompanied by reactive astrocytosis and phosphotau accumulation (Howlett et al. 2008). Aβ plaque formation in TASTPM mice follows a temporal series of events, with plaque load correlating positively with neuroinflammation (Howlett et al. 2004). Their genetic promoters (APPxPS1 genes) drive the formation of Aβ plaques, first beginning in the cortex and hippocampus, before spreading to other regions of the brain. Besides the extracellular deposits represented by Aβ plaques, we here observed intraneuronal deposits especially in the neocortex and in the pyramidal cell layer of the hippocampus. In line with the present observations is the previous report of a close association of activated astrocytes with amyloid plaque deposits (Matsuoka et al. 2001), which, in our material, was especially evident in the thalamus. In TASTPM mice, astrocytes have been reported to infiltrate the cell layers of the dentate gyrus (Howlett et al. 2008), similarly to the present observation of astrocytic infiltrates in the hippocampal CA1 field.

A marked clustering of microglia was here observed around Aβ plaque deposits, especially in the thalamus, consistently with previous reports in which microglia appeared closely apposed to plaque deposits in AD (Mandrekar-Colucci and Landreth 2010), and concentrated around plaque deposits in murine models

(Balducci and Forloni 2011). A previous study in aged (20 month-old) TASTPM mice has reported a highly enhanced expression of the microglial protein Iba-1 in contrast with relatively mild enhancement in CD11b immunolabelling (Howlett et al. 2008). It has been suggested that microglial cells in the vicinity of Aβ plaques are undergoing degenerative processes (Howlett et al. 2008).

Overall these results provide for the first time evidence of physiological aging-related changes and AD pathology-related alterations in diurnal, state-dependent organization of the input that regulates the orexinergic network.

3.6 Tables

Table 3.1 Experimental design and material

Genotype	Age/ Number	Purpose/s of the study
WT	5 m *n*=3 day; 3 night	Observation of triple immunofluorescent labeling in confocal microscopy (30 µm-thick sections)
Quantitative analyses: day/night sampling (10 µm-thick sections)		
WT	3 m *n*=3 day; 3 night	- Counts of Syn+ terminals on OX somata compared to young TASTPM mice - Diurnal fluctuation of excitatory and inhibitory terminals on OX somata compared to young TASTPM mice
WT	20 m *n*=3 day; 3 night	- Counts of Syn+ terminals on OX somata in aging and comparison with aged TASTPM - Diurnal fluctuation of excitatory and inhibitory terminals on OX somata in aging and comparison with aged TASTPM
TASTPM	3 m *n*=3 day; 3 night	- Counts of Syn+ terminals on OX somata in young AD mice - Diurnal fluctuation of excitatory and inhibitory terminals in young AD mice
TASTPM	20 m *n*=3 day; 3 night	- Counts of Syn+ terminals on OX somata in aged AD mice - Diurnal fluctuation of excitatory and inhibitory terminals on OX somata in aged AD mice
Quantitative analyses: OX neurons		
TASTPM WT	*n*=4; 15 m (daytime) "	- OX cell counts and analysis of immunosignal intensity in murine AD (30 µm-thick sections) - Matched controls
Neuropathological analyses		
TASTPM WT	*n*=4; 15 m "	- Aβ deposition and immunophenotyping of astrocytes - Matched controls
TASTPM WT	*n*=4 per age group; 9 m, 14 m, 15 m "	- Microglia immunophenotyping - Matched controls

Abbreviations Table 3.1: Aβ, β-amyloid; AD, Alzheimer's disease; m, months; OX, orexin-Syn, synaptophysin; WT, wild-type; OD, optical density

Table 3.2 Antibodies used in this study

Antigen	Host	Immunogen	Supplier	Catalog #	Dilution	References
Orexin-A	Goat	Purified goat polyclonal antibody raised against peptide at the C-terminus of Orexin-A of human origin	Santa Cruz	sc-8070	1:100	Blanco-Centurion et al. (2013)
VGluT2	Guinea pig	Purified recombinant protein of rat VGluT2 (aa510-582)	Synaptic Systems	135 404	1:100	Perederiy et al. (2013)
VGAT	Guinea pig	Strep-Tag fusion protein of rat VGAT (aa2-115)	Synaptic Systems	131 004	1:100	Fekete et al. (2015)
Synaptophysin 1	Rabbit	Synthetic peptide GPQGAPTSFSNQM (aa 301 - 313 in human synaptophysin 1 coupled to key-hole limpet hemocyanin via an added N-terminal cysteine residue	Synaptic Systems	101 002	1:200	Wimmer et al. (2006)
β-APP	Rabbit	22 amino acid synthetic peptide derived from the C-terminus of the human β-APP	Invitrogen Corps	51-2700	1:1000	Stone et al. (2000)
CD11b	Rat	Thioglycollate-elicited peritoneal macrophages (TPM)	Serotec	MCA711	1:500	Sato et al. (2012)
GFAP	Rabbit	Purified bovine GFAP	Merck	AB5804	1:500	Perriard et al. (2015)

4. Extracellular matrix in the lateral hypothalamus and other brain regions: diurnal organization in basal conditions and in experimental sleeping sickness

4.1 Introduction

Knowledge acquired on the ECM in the CNS (see 1.4) has highlighted that brain plasticity is not only dependent on neurons and glial cells, but also on what surrounds them (Sorg et al. 2016). Diverse molecules, secreted by neurons and non-neuronal cells, accumulate in the extracellular space and form the ECM, which accounts for 10-20% of the brain volume (Nicholson and Sykova 1998) (see 1.4). These molecules, their receptors and remodeling proteases regulate the induction and maintenance of synaptic modifications (Wlodarczyk et al. 2011).

The advances in the understanding of the ECM have led to the progression from atripartite view of synaptic organization (in which perisynaptic astrocytes have been involved in bipartite synaptic mechanisms of pre- and postsynaptic elements) (Araque et al. 1999) to a tetrapartite view in which the ECM has also been involved (Dityatev et al. 2006, 2010; Dityatev and Rusakov 2011; Verkhratsky and Nedergaard, 2014), besides a possible involvement also of microglia (Verkhratsky and Nedergaard 2014) (Fig. 1.11).

As dealt with previously (see 1.4), the ECM in the CNS is organized according to three main patterns: 1) the 'loose' ECM, present throughout the brain and spinal cord, 2) membrane-bound molecules, and 3) lattice-like structures that wrap the soma and dendrites of neuron subtypes in the brain and spinal cord, known as PNNs; these structures interdigitate with synaptic contacts on neuronal soma and proximal dendrites (Celio et al. 1998; Deepa et al. 2006; Soleman et al. 2013).

Of the ECM structures, PNNs are the most widely studied so far (see: 1.4.1). They are highly heterogeneous because of the variety of glycosaminoglycan chains (hyaluronans) attached to the core proteins (chondroitin sulfate proteoglycans), TN-R and linked proteins (see 1.4.1). On one hand, PNNs may play a beneficial role by stabilizing the extracellular milieu and protecting enveloped neurons; on the other hand, PNNs may create a barrier which limits plasticity and counteracts regeneration (Karetko and Skangiel-Kramska 2009). Little attention has been devoted instead the loose interstitial ECM within the CNS.

In particular, information on the ECM organization in the hypothalamus is relatively limited. Two main patterns of organization have been reported in the CSPG-based ECM in different hypothalamic regions (grossly subdivided by the location of the fornix): a lateral zone in which the ECM is mainly organized in PNNs, and a medial zone in which PNNs are relatively loose PNN or the ECM is not organized in PNNs (Horii-Hayashi et al. 2017). These observations have been

based on differences in histochemical reactivity to *Wisteria floribunda* agglutinin (WFA) (Horii-Hayashi et al. 2017). This lectin binds glycoprotein residues (N-acetyl-D-galactosamine) in carbohydrates (e.g. Seeger et al. 1996) and is a widely used marker of ECM in the CNS (Brückner et al. 1996), and in particular of chondroitin sulfates. WFA labeling has become a standard method for identifying CSPGs-containing elements in the CNS (Ajmo et al. 2008).

The finding of a day/night reorganization of synapses onto OX neuron somata (see Chapter 2) opens key questions on the regulation of plasticity in the neural network of the LH. As the ECM is one of the key components involved in neural plasticity, the present study was aimed at testing the hypothesis that the diurnal remodeling of the synaptic wiring of OX cell bodies could involve the ECM. The study was based on double immunofluorescence of WFA and OX neurons in the LH. Furthermore, Western blotting analysis was done to quantify the levels of WFA expression in tissue extracts of the LH.

Since the data on the LH revealed a diurnal fluctuation of ECM organization, other brain areas were also examined, namely the SCN, the master circadian pacemaker located in the anterior hypothalamus (see 1.1.4), the neocortex and the hippocampus.

On the basis of the findings obtained in the LH of healthy mice, the present study was extended at verifying a second hypothesis, i.e. that the day/night features of ECM organization in the LH could be affected in a murine model of African trypanosomiasis.

The extracellular parasite *Trypanosoma brucei* (*T. b.)* is the causative agent of human African trypanosomiasis (HAT), also called sleeping sickness. The parasite subspecies *T. b. gambiense* and *T. b. rhodensiense* cause two different forms of HAT (Büscher et al. 2017). A third subspecies, *T. b. brucei* (*T. b. b.*) is infectious in animals but not in humans, and is widely used in animal models of HAT (Kristensson et al. 2010).

HAT is still endemic in sub-Saharan Africa, though the number of reported cases has considerably declined in recent years (Büscher et al. 2017). The disease evolves from a systemic (hemolymphatic) stage to an encephalitic stage when the

parasites, which are able to cross the blood-brain barrier, invade the CNS parenchyma (Kristensson et al. 2010). The infection leads to a chronic, progressive neuroinflammatory condition, causing a severe neuropsychiatric disease which is fatal if left untreated (Kristensson et al. 2010; Büscher et al. 2017). The clinical picture is dominated by sleep/wake disturbances, with disruption of the sleep/wake cycle leading to somnolence during the day and nocturnal insomnia, as well as alterations of the structure of sleep, with narcoleptic-like changes in humans and in animals (Kristensson et al. 2010; Seke-Etet et al., 2012; Laperchia et al. 2016).

A previous study in rodent models (mice and rats) of *T. b. b.* infection has pointed out a progressive damage of OX neurons as well as of MCH neurons (see 1.1.1), with functional dysregulation of OX neurons as revealed by alterations of the spontaneous day/night oscillation of Fos expression in these cells (Palomba et al. 2015b). These findings prompted further studies on the LH in African trypanosomiasis, and the present investigation is, as mentioned above, focused on the ECM.

4.2 Materials and methods

4.2.1 Animals and infection

Healthy adult (3–5 month-old) male C57BL/6J mice were maintained under a 12/12-h dark/light or light/dark cycle, under veterinarian control and controlled environmental (temperature and humidity) conditions, with free access to food and water. The animals (n = 12) were destined for analyses with confocal microscopy, and Western blotting from tissue sampled from brain sections (see below) at two different time points in antiphase (see Chapters 2 and 3). They were therefore randomly divided in two groups sacrificed during a 2-h period during the day (*Zeitgeber* time, ZT, 3–4, n = 4), or night (ZT 15–16, n = 4) (ZT 0 corresponds to the lights-on time).

Male CX3CR1-GFP mice (3 month-old) were used for the study of the ECM in African trypanosomiasis. In these mice microglial cells are GFP-tagged, via GFP tagging of the chemokine fractalkine receptor CX3CR expressed by microglia (Mizutani et al. 2012). The use of these mice for the infection paradigm was motivated by interest in analyses of microglia, that are being pursued in a separate study. These animals were kept uninfected as controls (n = 6) or infected (n= 6) by ip injection of *T. b. b.* as described by Laperchia et al. (2016). Briefly, *T. b. b.* AnTat 1/1E, a pleiomorphic clone derived from stabilate EATRO (East African Trypanosomiasis Research Organization) 1125, supplied by the Laboratory of Serology, Institute of Tropical Medicine Prince Leopold, Antwerp, Belgium), were injected intraperitoneally (100 parasites/g body weight). Parasitaemia was assessed at 3 and 5 days post-infection (dpi) in a blood sample from the tail vein. The mice were sacrificed at 14 dpi together with the matched control mice, during day or night, at the same time points as above (n =3 control and infected mice per time point).

For sacrifice, the animals were deeply anaesthetized with Avertin (2, 2, 2-tribromoethanol, Sigma-Aldrich, St Louis, MO; 0.2 ml/10 g body weight, ip) and transcardially perfused with cold 0.01M phosphate-buffered saline (PBS), followed by 4% paraformaldehyde in phosphate buffer, pH 7.6. The brains were dissected out, postfixed in the same fixative for 2-3 h at room temperature, and then kept in PBS containing sodium 0.1% azide at 4◦C until processing.

All procedures received approval by the Animal Care and Use Committee of the University of Verona (CIRSAL) and authorization by the Italian Ministry of Health, in strict adherence to the European Communities Council (86/609/EEC) directives and the ARRIVE guidelines, in accordance with the National Institute of Health Guide for the Care and Use of Laboratory Animals (NIH Publications No. 80-23), minimizing the number of animals used and avoiding their suffering.

4.2.2 Brain tissue processing and immunofluorescence

Before sectioning, the brains were soaked in 30% sucrose in PBS for 24 h for cryoprotection. The brains were then cut in the coronal plane in adjacent series at a 30 µm thickness with a freezing microtome.

Sections through different brain structures were sampled for immunofluorescence processing. In each experimental group, 3 adjacent brain sections per level and per animal were sampled at the two anteroposterior levels through the SCN (Bregma -0.34 to – 0.82) and the LH (Bregma -1.70 to - 2.46). Sections of the first series were stained with cresyl violet for cytoarchitectonic reference (http://mouse.brain-map.org). The adjacent series were processed free-floating for multiple immunofluorescence. These sections were preincubated in a blocking solution of 2% normal donkey serum (NDS) with 0.2% Triton X-100 in PBS for 1 h. The sections were subsequently incubated overnight at 4°C in either of the following primary antibodies diluted in PBS containing 1% NGS and 0.2% Triton X-100: goat polyclonal antibodies which recognize OX-A (Santa Cruz Biotech; diluted 1:100); goat polyclonal antibodies which recognize parvalbumin (PV) (PVG-214; Swantz, Marly 1, Switzerland; diluted 1:500) and biotinylated WFA (Sigma Aldrich; 1:200), was used to visualize ECM. Following incubation in primary antibody, the sections were thoroughly rinsed and incubated for 2 h in the following secondary antibodies; biotin-conjugated Alexa Fluor 488 or streptavidin-conjugated Alexa Fluor 633, Alexa Fluor- 405 and 568 donkey anti-goat (all from InVitrogen, Carlsbad, CA, USA), diluted 1:1000 in 1% NDS. The sections were then reacted with fluorescent nuclear marker, 4'-6'-diamino-2-phenylindole (DAPI), and then rinsed in PBS. Sections were mounted on gelatinized slides and coverslipped with 0.1% paraphenylenediamine in a glycerol-based medium (90% glycerol and 10% PBS).

Additional sections were used for control, omitting each of the primary antibodies, and no specific immunostaining was observed in these sections.

4.2.3 Microscopy and quantitative analyses

Sections were viewed with the confocal microscope Leica SP5 (Leica, Mannheim, Germany) using X40 (zoom factor 1.9) or 63X (zoom factor 1.8) oil-immersion objective (numerical aperture 1.25). Serial Z planes (0.70 µm) images were captured with the LAS software, and collapsed into a single maximum projection image to which colours were assigned. Acquired images were minimally and equally modified with the Imaris software 7.4 (Bitplane, Zurich, Switzerland) for contrast and brightness.

4.2.4 Western blot

Sections adjacent to those used for the immunofluorescence study (3 sections per animal) were used for the study of ECM expression by Western blotting. Proteins were extracted from the LH tissue sections using a previously validated technique (Tanca et al. 2014; Azeez et al. 2016). Protein concentration was determined using the PierceTM Detergent Compatible Bradford Assay (Thermo Fisher Scientific). Each protein extract (25 µg) was applied to two 10% nongradient sodium dodecyl sulfate (SDS)-gels and immunoblotted on Trans-Blot Turbo polyvinylidene fluoride (PVDF) transfer (BioRad Labs, Hercules, CA). The protocol of Ajmo et al. (2008) was followed for WFA blotting. Briefly, the blotted membrane was blocked in a solution in 2% bovine serum albumin (BSA) diluted in 0.1% PBS-Tween (PBST) for 2 h and incubated with biotinylated WFA (Sigma Aldrich; 1:500) overnight at 4°C. Biotinylated WFA was detected with specific secondary antibody, avidin conjugated to horseradish peroxidase (Sigma Aldrich, Steinheim, Germany; 1:2000). Chemiluminescent reagent (ECL, WBLUR050, Luminata Crescendo Western HRP substrate, Merck) was used for visualization.

4.3 Statistical analyses

For Western blotting, nonsaturated data were analysed with the ImageJ software using the Gel Analysis method (http://rsbweb.nih.gov/ij/docs/guide/146-30.html#toc-Subsection-30.13; Analyze 30.13 Gels). The WFA optical density (OD) units were expressed as mean ± SEM per group and were statistically evaluated with the Student's *t*-test using the Graph pad Prism 5 System (San Diego, CA). The significance threshold was set at $p<0.05$.

4.4 Results

4.4.1 Diurnal organization of the extracellular matrix in the lateral hypothalamus and other regions in basal conditions

In the field of the LH where OX neurons are distributed, and which were investigated in the present study, the ECM was revealed by WFA immunoreactivity in the neuropil, and very few PNNs were observed (Fig. 4.1A). These PNNs surrounded OX-immunonegative neurons (Fig. 4.1A), and were not observed around OX somata or dendrites.

Dramatic differences in the organization of the ECM were seen in the LH between the sampled time points. WFA immunofluorescence appeared diffusely distributed in the neuropil during daytime, with punctate labelling in close proximity, and frequently apposed, to OX cell bodies and proximal dendrites (Fig. 4.1A). At night, WFA immunofluorescence appeared considerably increased, with a more compact organization and a condensation around cell bodies, both around OX-immunopositive and OX immunonegative neurons (Fig. 4.1B,D).

In the SCN, the ECM was not structurally organized into PNNs, and was seen to be diffusely distributed in the neuropil (Fig. 4.2C,D). A similar organization ws

observed in the major subdivisions of the SCN (i.e. the dorsomedial shell and the ventrolateral core). Interestingly, no overt variations were seen in the ECM phenotype, as revealed by WFA immunofluorescence, in the SCN (Fig. 4.2C,D). However, OX fibers within the SCN appeared denser and more intensely immunolabelled at night compared to daytime (Fig. 4.2E,F).

In the neocortex, the ECM appeared essentially organized in PNNs, which surrounded the somata and proximal dendrites of PV-containing neurons (Fig. 4.3). No overt changes in the intensity and organization of PNN immunofluorescence at day and night were observed (Fig. 4.3). Interestingly, however PV immunofluorescence was more intense at night compared to daytime (Fig. 4.3).

The ECM was organized in PNNs also in the hippocampus (Fig. 4.4). As in the neocortex, PNNs were equally intensely labelled and structurally organized at night and day (Fig. 4.4). OX fibers were seen to reach the cells enwrapped by PNNs (Fig. 4.4).

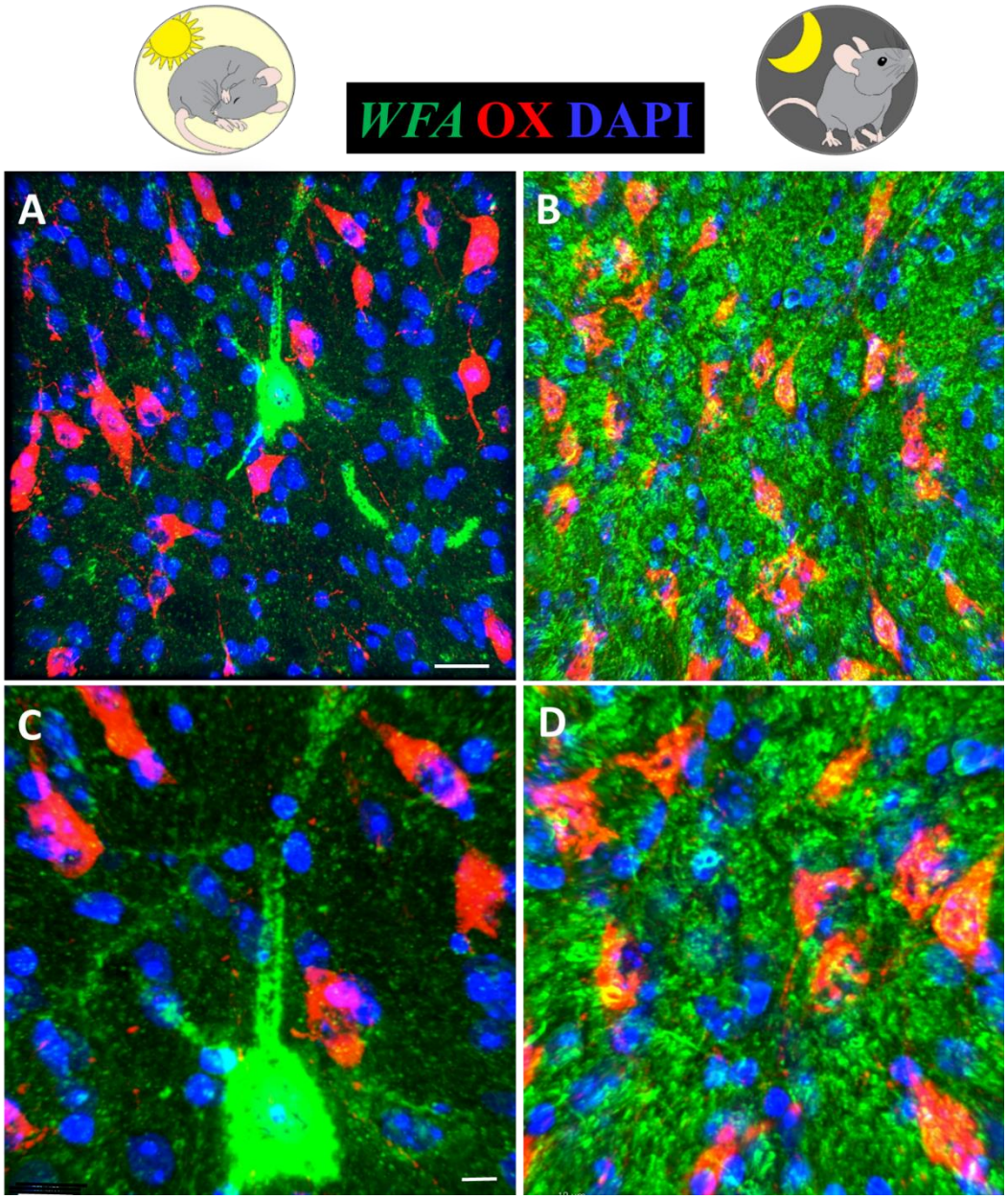

Fig. 4.1: Organization of the ECM, as revealed by WFA immunofluorescence in the LH field containing OX neurons (also visualized by immunofluorescence) in basal conditions. The sections are stained also with DAPI, revealing cell nuclei. Note at daytime (**A,C**) the sparse, diffuse distribution of WFA immunolabelling, with intense PNN labelling around an OX-immunonegative neuron, and the more compact organization and condensation around OX cell bodies at night (**B,D**). Scale bars; A-B = 30 μm, C-D = 10 μm

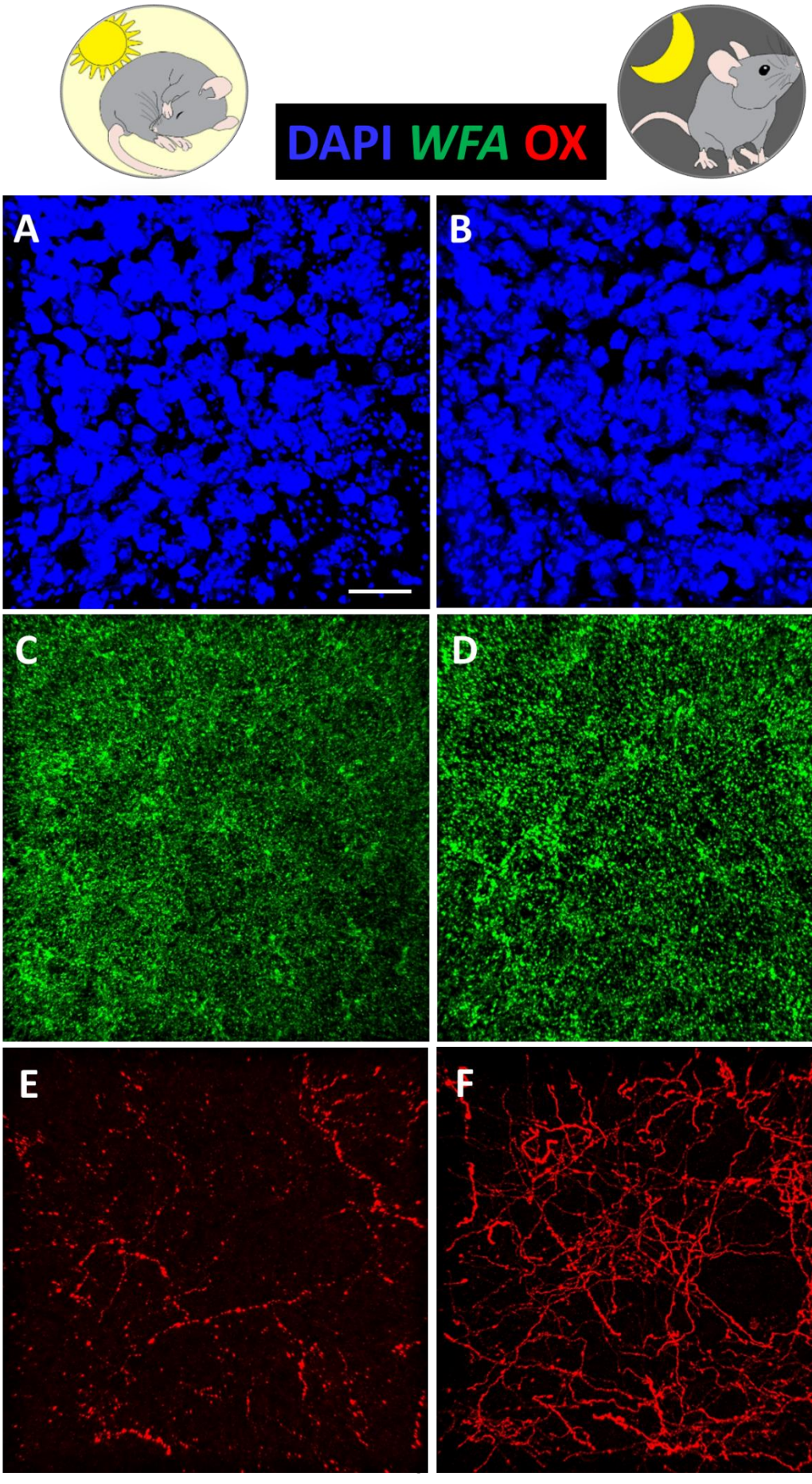
DAPI WFA OX
A
B
C
D
E
F

Fig. 4.2: ECM organization in the SCN in basal conditions revealed by WFA immunofluorescence (**C,D**) together with DAPI staining of cell nuclei (**A,B**), and OX immunofluorescence (**E,F**). The images include both the ventrolateral (so-called "core") and dorsomedial (so-called "shell") of the SCN (see 1.1.4). Note in A and B the high cell density typical of the SCN, in C and D the similar organization of WFA labelling at day and night, and in F the orexinergic network evident in the SCN at night and its dampening at daytime (due to a diurnal fluctuation of OX synthesis and release (see 1.1.3). Note also in C and D the absence of PNNs within the SCN. Scale bar = 30 μm

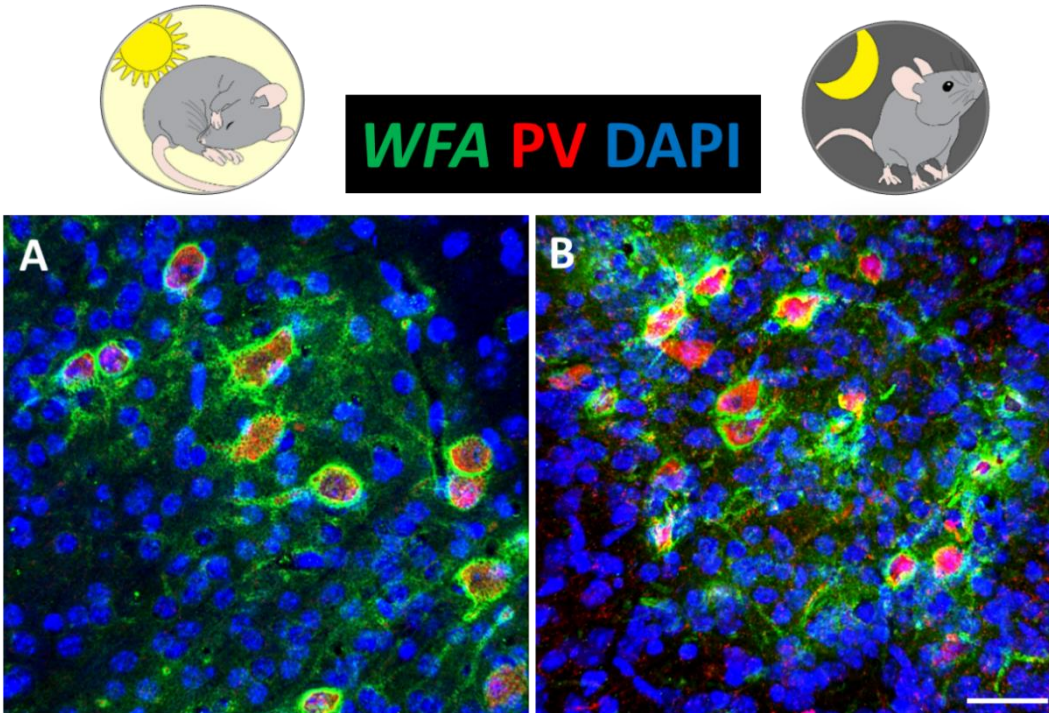

Fig. 4.3 ECM labelling WFA immunofluorescsnce in the somatosensory cortex, combined with parvalbumin (PV) immunofluorescence in basal conditions, and DAPI staining of cell nuclei. Note the abundance of PNNs around PV-immunopositive neurons, and note the absence of overt fluctuation of the PNN labelling between day and night. Note, however, a fluctuation in the PV immunosignal, which is dampened at daytime (A) compared to the night (B). Scale bar = 30 μm

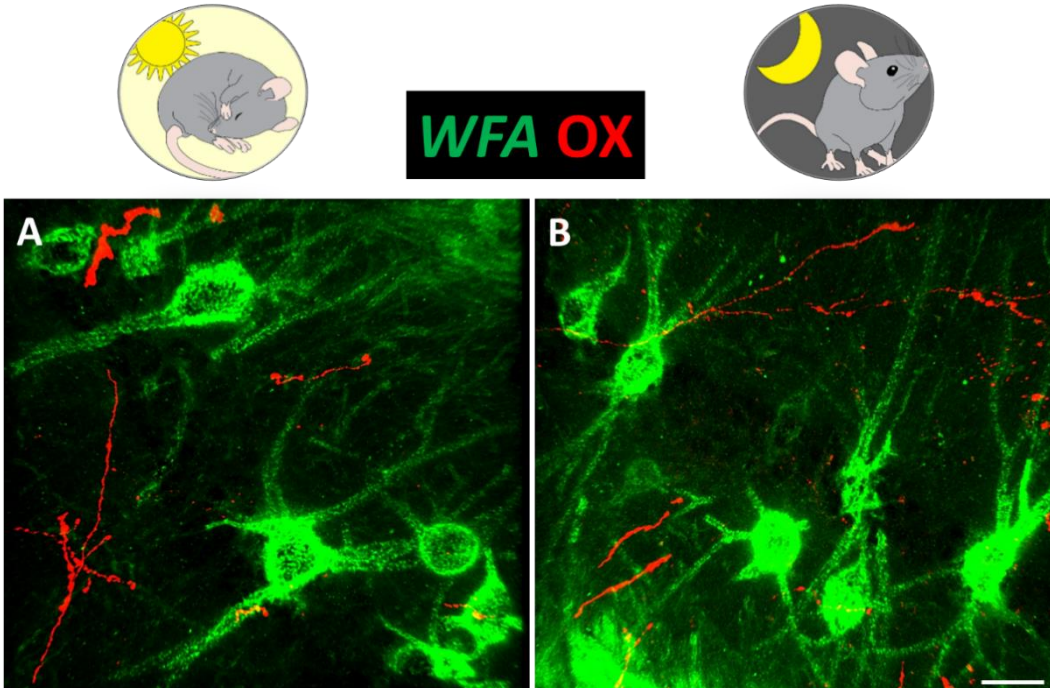

Fig. 4.4: ECM labelling by WFA immunofluorescence in the hippocampal CA1 field in basal conditions. Note the abundance of PNNs, and note that their labellig is similar during day (**A**) and night (**B**). Note also in many instances the close proximity to PNNs of orexinergic fibers. Scale bar = 20 μm

4.4.2 Western blot analysis

As mentioned above, Western blotting was performed on the LH tissue extracts from sections in basal conditions. LH homogenates were subjected to SDS-PAGE and probed with biotin-WFA to identify the molecular species in mouse brain detected by the N-terminal region. The high molecular weight isoform of WFA described in detail by Ajmo et al. (2008) showed a higher expression in the animals sacrificed at night compared to daytime (Fig. 4.5). Quantitative analysis showed a significant difference in the levels of WFA expression at the two time points (Fig. 4.5).

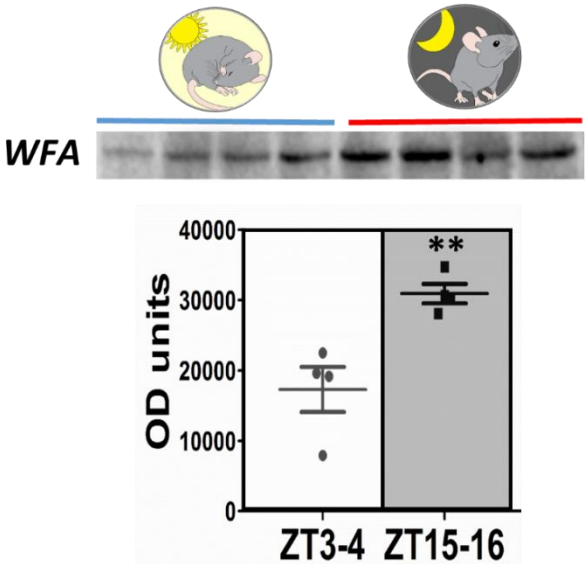

Fig. 4.5: Western blotting of the WFA protein expression in the LH. **Top**: gel blots from mice sacrificed during day (*Zeitgeber* time, ZT, 3-4) and night (ZT15-16) (*n*=4 per time point**). Bottom**: Quantitative analysis of WFA expression (OD, optical density) shows a significant difference with higher levels of expression at the night time point compared to the day. **P<0.01, Student's t-test.

4.4.3 Diurnal organization of the extracellular matrix in the lateral hypothalamus of *Trypanosoma brucei brucei*-infected animals

ECM organization was investigated in the LH of CX3CR1-GFP mice infected with *T. b. b.* sampled during day and night, and compared with uninfected controls. The observations showed that the CX3CR1-GFP mice sacrificed in basal conditions replicated the observations from the C57BL/6J mice, i.e., a diffuse ECM phenotype was observed during daytime while a condensed ECM was observed at night (Fig. 4.6A.B). Interestingly, there were instead no overt differences in the intensity of ECM immunofluorescence between day and night in the *T. b. b.*-infected mice ((Fig. 4.6C.D). Thus, a diffuse, punctate ECM phenotype was observed at both the sampled time points in the infected mice (Fig. 4.6C,D). PNNs around OX-immunonegative neurons were observed in the LH of infected and controld mice (Fig. 4.6A-D), as observed in the C57BL/6J counterparts.

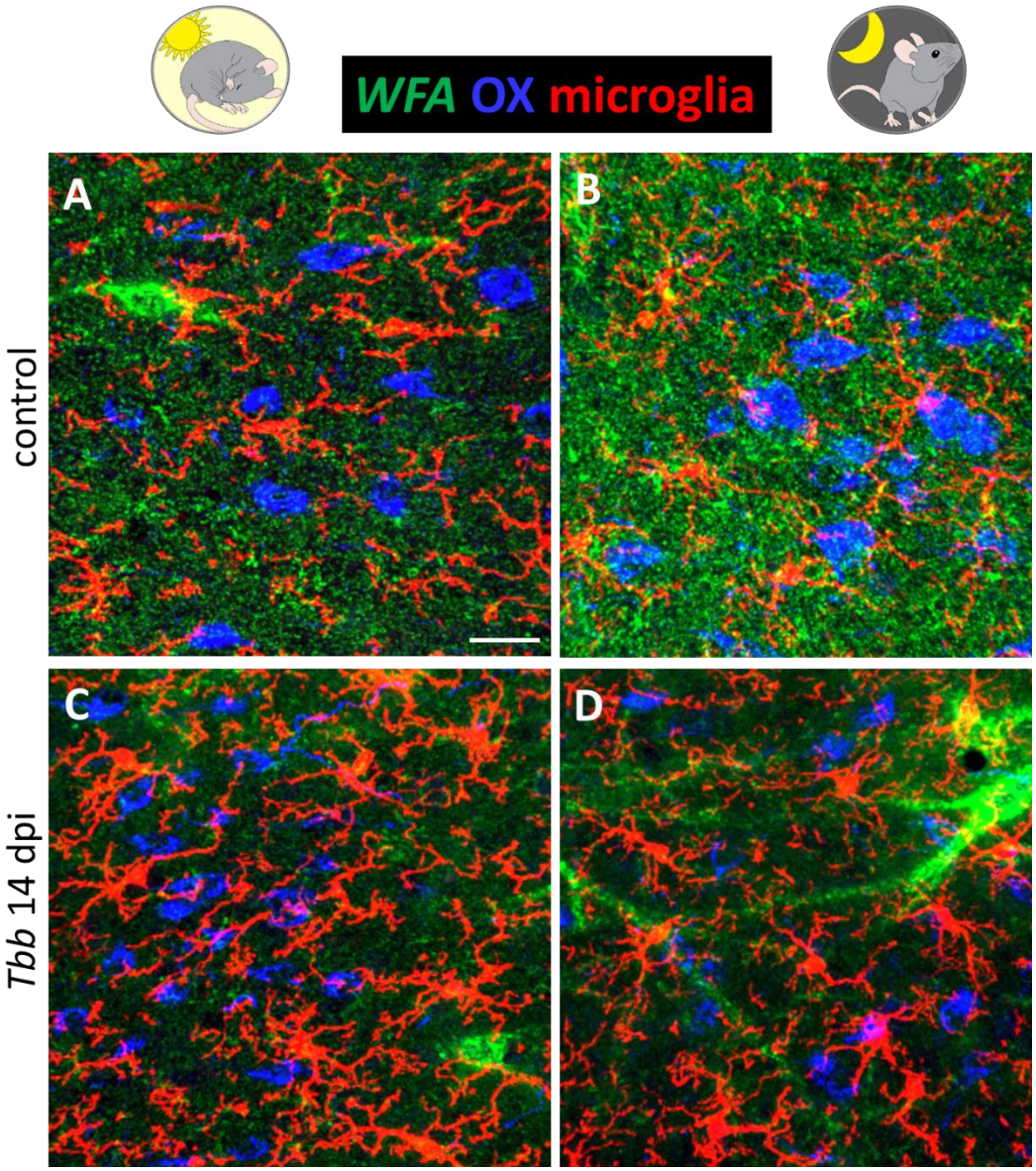

Fig. 4.6: ECM organization in the LH field containing OX neurons at 14 days post-infection (dpi) of CX3CR1-GFP mice infected with *Trypanosoma brucei brucei* (the parasites African trypanosomes) (**C, D**) compared with uninfected CX3CR1-GFP mice (**A, B**). In CX3CR1-GFP mice microglia is fluorescently labelled. Microglial changes are observed in the infected mice, but will be examined in a separate study. Note in **A-D** that, besides the ECM distributed in the neuropil, some PNNs are evident, and they surround OX-immunonegative neurons. Note also that the observed phenomenon of day/night oscillation of ECM organization in the LH, as revealed by WFA immunolabelling (see Fig. 4.1) is also here evident in uninfected mice (**A, B**). However, no day/night variations in ECM organization are evident in the infected mice (**C, D**). Scale bar = 50 μm

4.5 Discussion

To our knowledge, this is the first study of the diurnal organization of the ECM in the brain. It was focused on the LH, and in particular in the LH fields in which OX neurons are distributed, and it was extended to the SCN and to cortical regions (neocortex and hippocampus).

The findings obtained in healthy mice showed a striking diurnal fluctuation in the ECM organization in the LH, which was confirmed by the study of WFA expression in the LH, and which was at variance with the findings observed in the SCN, neocortex and hippocampus, where no day/night overt changes have been here observed.

In the present study, no PNNs were found in the LH around OX cell bodies, and this could potentially represent a factor favoring plasticity in orexinergic networks. It remains to be verified if the ECM in the LH is organized in PNNs enwrapping other groups of neurons, and in particular MCH neurons.

In the neocortex, PNNs were observed around the somata and processes of PV-immunopositive interneurons, in agreement with previous reports (Wegner et al. 2003; Alpár et al. 2006; Deepa et al. 2006). The PV-immunopositive neurons have been proposed as key regulators of plasticity, both during development and in adulthood (Hensch 2005; Donato et al. 2013), and PNNs may support the high activity of PV neurons (Morawski et al. 2015). Thus, PNNs, which have a variable distribution in the neocortex and hippocampus (Lensjø et al. 2017b), may restrict plasticity directly by acting as structural barrier inhibiting synapse remodelling or indirectly through their effects on PV-immunopositive neurons (Lensjø et al. 2017a).

Although no day/night differences were here observed in the PNNs in the neocortex and hippocampus, an overt oscillation of PV immunoreactivity was seen in PV cell bodies investigated in the neocortex. Further studies are needed to confirm the diurnal differences in PV expression here observed.

While there are reports on ECM in the neocortex and hippocampus, to the best of our knowledge, this is the first documentation of the ECM organization in the SCN. The finding of a lack of day/night oscillation of WFA immunofluorescent labelling in the SCN may be somewhat surprising and needs to be confirmed and extended to other ECM components.

In future studies, it will be important to investigate individual ECM proteins such as the brevican, aggrecan and Tenascin-R, and also ECM-modifying proteins such as disintegrin, metallopeptidase and metalloreductase, in the different brain regions here studied. Of note, ECM molecules such as brevican, thrombospondins and Tenascin-C are secreted by astrocytes (Faissner et al. 2010).

In a chronic neuroinflammatory condition represented by African trypanosome infection, which causes circadian disturbances in humans and animals, the diurnal fluctuation observed in basal conditions in the LH in healthy mice was found to be severely perturbed. This is the first observation of the ECM organization in animal models of this parasitic infection. The findings suggest a circadian control of ECM variations with disruption during experimental sleeping sickness. On the other hand, a wealth of clinical and experimental data point to circadian dysfunction in African trypanosome infection (Kristensson et al. 2010), which has also been supported by recent experimental findings (Rijo-Ferreira et al. 2018).

The study of synaptic wiring of OX neurons in this paradigm of neuroinflammation is at present in progress, so that correlations with the daily pattern of ECM organization in the LH and the synaptic wiring of OX neurons cannot be done at present. Previous analyses in rodent models of *T. b. b.* (Palomba et al. 2015) and *T. b. gambiense* (Laperchia et al. 2018) infection have shown partial and progressive loss of OX and MCH neurons during the infection. Functional alterations of the activity OX neurons, based on the daily fluctuation of spontaneous Fos expression in these cells, have also been reported in *T. b. b.* infection (Palomba et al. 2015), indicating that peptidergic sleep-wake-regulatory neurons of the LH are vulnerable to this chronic neuroinflammatory condition.

Insults to the CNS result in alterations of the ECM, and the extent of this depends on the severity or chronicity of the insult (Lau et al. 2013). ECM alterations have been mostly associated with inflammatory lesions and have been described in pathological conditions including AD (Karetko et al. 2009) and in demyelinating diseases such as MS (Van Horssen et al. 2006).

In conclusion, the findings point to day/night oscillation of ECM organization and WFA expression in the LH, but not in PNNs in the neocortex and hippocampus. The results thus indicate a regionally selective and marked day/night variation of ECM organization in the LH, which could be involved in synaptic plasticity phenomena, and the disruption of this organization in a chronic neuroinflammatory pathology which leads to sleep-wake dysregulation and to the alterations of sleep structure.

5. Summary and conclusions

Overall, the main findings of each experimental series can be summarized as follows:

Question	Answer (main findings)
• OX soma wiring in adult (3-5 m) mice	✓ day/night fluctuation of the inhibitory/excitatory synaptic input
• OX soma wiring in aged (20 m) mice	✓ decreased innervation ✓ no day/night fluctuation
• OX soma wiring in young (3 m) TASTPM mice (Tg AD model)	✓ decreased innervation ✓ dampened day/night fluctuation
• OX soma wiring in aged (20 m) TASTPM mice	✓ decreased innervation ✓ no day/night switch
• ECM structural organization in the LH in adult (3-5 m) mice	✓ day/night rearrangement
• ECM structural organisation in adult (3-5 m) after African trypanosome infection	✓ no day/night rearrangement

Altogether the findings show a striking daily oscillation in the axosomatic wiring of orexinergic neurons during day/night in adult mice, with a switch from a prevalence of excitatory innervation during wakefulness to a prevalence of inhibitory innervation during sleep.

Preliminary observations here presented also suggest a possible rearrangement of the spatial orientation of astrocytic ramifications in the LH at day and night.

The prevalence of excitatory terminals found at night in young adult animals was drastically dampened in aged mice at night, and the evaluation of the relative proportion of inhibitory terminals in aged mice showed similar values at night and day. This resulted in the lack of a diurnal fluctuation in excitatory/inhibitory balance of OX soma innervation and in a prevalence of inhibitory innervation in the aged mice. The data thus show striking changes during the physiological aging process, which could be involved in aging-related changes of sleep-wake stability, arousal, energy metabolism.

The same analyses showed interesting findings also in the murine model of AD provided by TASTPM Tg mice. In the young Tg mice, despite a decrease in OX cell body innervation compared to young WT mice, the day/night fluctuation was maintained, though dampened. In the aged Tg mice, loss of synaptic contact on OX cell bodies was especially marked, and the number of excitatory terminals on OX, as well as that of inhibitory terminals, at night and day were very similar.

In addition to marked significant reduction in the presynaptic terminals apposed to OX somata in aged WT mice and in TASTPM mice of both age groups, degenerative cell features of OX neurons were observed, and in particular in the AD mice.

The findings that OX soma wiring is altered in physiological and pathological aging process open a novel perspective in the understanding of the changes in the aging brain.

Furthermore, experimental evidence is here provided of a diurnal rearrangement of the ECM structural organization in the LH, which seems to be regionally selective. Of note, such oscillation is lost in experimental sleeping sickness.

All these sets of findings are here reported for the first time, and open many questions on the underlying mechanisms of molecular and cellular regulation in health and disease, on their vulnerability to physiological aging, on their susceptibility to neuroinflammatory and neurodegenerative conditions, on the influence from and on other brain regions, on the crosstalk between neurons, glia and ECM, on the plasticity of neural networks in state-dependent behavior.

6. References

[i] Abrahamson EE, Leak RK, Moore RY (2001) The suprachiasmatic nucleus projects to posterior hypothalamic arousal systems. Neuroreport 12:435–440 . doi: 10.1097/00001756-200102120-00048

Adidharma W, Leach G, Yan L (2012) Orexinergic signaling mediates light-induced neuronal activation in the dorsal raphe nucleus. Neuroscience 220:201–207 . doi: 10.1016/j.neuroscience.2012.06.020

Ajmo JM, Eakin AK, Hamel MG, Gottschall PE (2008) Discordant localization of WFA reactivity and brevican/ADAMTS-derived fragment in rodent brain. BMC Neurosci 9:14 . doi: 10.1186/1471-2202-9-14

Alam MN, Szymusiak R, Gong H, et al (1999) Adenosinergic modulation of rat basal forebrain neurons during sleep and waking: Neuronal recording with microdialysis. J Physiol 521:679–690 . doi: 10.1111/j.1469-7793.1999.00679.x

Alpár A, Gärtner U, Härtig W, Brückner G (2006) Distribution of pyramidal cells associated with perineuronal nets in the neocortex of rat. Brain Res 1120:13–22 . doi: 10.1016/j.brainres.2006.08.069

Alpár A, Harkany T (2013) Orexin neurons use endocannabinoids to break obesity-induced inhibition. Proc Natl Acad Sci U S A 110:9625–6 . doi: 10.1073/pnas.1307389110

Angelov DN, Walther M, Streppel M, et al (1998) Tenascin-R is antiadhesive for activated microglia that induce downregulation of the protein after peripheral nerve injury: a new role in neuronal protection. J Neurosci 18:6218–29

Anlar B, Gunel-Ozcan A (2012) Tenascin-R: Role in the central nervous system. Int J Biochem Cell Biol 44:1385–1389 . doi: 10.1016/j.biocel.2012.05.009

Antle MC, Silver R (2005) Orchestrating time: Arrangements of the brain circadian clock. Trends Neurosci. 28:145–151

Antony PMA, Diederich NJ, Krüger R, Balling R (2013) The hallmarks of Parkinson's disease. FEBS J. 280:5981–5993

Antunes LC, Levandovski R, Dantas G, et al (2010) Obesity and shift work: Chronobiological aspects. Nutr Res Rev 23:155–168 . doi: 10.1017/S0954422410000016

Apergis-Schoute J, Iordanidou P, Faure C, et al (2015) Optogenetic Evidence for Inhibitory Signaling from Orexin to MCH Neurons via Local Microcircuits. J Neurosci 35:5435–5441 . doi: 10.1523/JNEUROSCI.5269-14.2015

Appelbaum L, Wang G, Yokogawa T, et al (2010) Circadian and homeostatic regulation of structural synaptic plasticity in hypocretin neurons. Neuron 68:87–98 . doi: 10.1016/j.neuron.2010.09.006

Araque A, Parpura V, Sanzgiri RP, Haydon PG (1999) Tripartite synapses: Glia, the unacknowledged partner. Trends Neurosci. 22:208–215

Azeez IA, Olopade F, Laperchia C, et al (2016) Regional myelin and axon damage and neuroinflammation in the adult mouse brain after long-term postnatal vanadium exposure. J Neuropathol Exp Neurol 75: . doi: 10.1093/jnen/nlw058

Aziz A, Fronczek R, Maat-Schieman M, et al (2008) Hypocretin and melanin-concentrating hormone in patients with Huntington disease. Brain Pathol 18:474–483 . doi: 10.1111/j.1750-3639.2008.00135.x

Back SA, Tuohy TMF, Chen H, et al (2005) Hyaluronan accumulates in demyelinated lesions and inhibits oligodendrocyte progenitor maturation. Nat Med 11:966–972 . doi: 10.1038/nm1279

Bäckberg M, Hervieu G, Wilson S, Meister B (2002) Orexin receptor-1 (OX-R1) immunoreactivity in chemically identified neurons of the hypothalamus: Focus on orexin targets involved in control of food and water intake. Eur J Neurosci 15:315–

328 . doi: 10.1046/j.0953-816x.2001.01859.x
Baig S, Wilcock GK, Love S (2005) Loss of perineuronal net N-acetylgalactosamine in Alzheimer's disease. Acta Neuropathol 110:393–401 . doi: 10.1007/s00401-005-1060-2
Balducci C, Forloni G (2011) App transgenic mice: Their use and limitations. NeuroMolecular Med. 13:117–137
Balsalobre A, Brown SA, Marcacci L, et al (2000) Resetting of circadian time in peripheral tissues by glucocorticoid signaling. Science (80-) 289:2344–2347 . doi: 10.1126/science.289.5488.2344
Bandtlow CE, Zimmermann DR (2000) Proteoglycans in the developing brain: new conceptual insights for old proteins. Physiol Rev 80:1267–1290 . doi: 10.1006/dbio.1999.9308
Baracchi F, Opp MR (2008) Sleep-wake behavior and responses to sleep deprivation of mice lacking both interleukin-1 beta receptor 1 and tumor necrosis factor-alpha receptor 1. Brain Behav Immun 22:982–993 . doi: S0889-1591(08)00040-8 [pii]\r10.1016/j.bbi.2008.02.001
Baumann CR, Clark EL, Pedersen NP, et al (2008) Do enteric neurons make hypocretin? Regul Pept 147:1–3 . doi: 10.1016/j.regpep.2007.11.006
Baumann CR, Mignot E, Lammers GJ, et al (2014) Challenges in Diagnosing Narcolepsy without Cataplexy: A Consensus Statement. Sleep. doi: 10.5665/sleep.3756
Becquet D, Girardet C, Guillaumond F, et al (2008) Ultrastructural plasticity in the rat suprachiasmatic nucleus. Possible involvement in clock entrainment. Glia 56:294–305 . doi: 10.1002/glia.20613
Belle MDC, Diekman CO, Forger DB, Piggins HD (2009) Daily electrical silencing in the mammalian circadian clock. Science (80-) 326:281–284 . doi: 10.1126/science.1169657
Belle MDC, Hughes ATL, Bechtold DA, et al (2014) Acute Suppressive and Long-Term Phase Modulation Actions of Orexin on the Mammalian Circadian Clock. J Neurosci 34:3607–3621 . doi: 10.1523/JNEUROSCI.3388-13.2014
Belle MDC, Piggins HD (2017) Circadian regulation of mouse suprachiasmatic nuclei neuronal states shapes responses to orexin. Eur J Neurosci 45:723–732 . doi: 10.1111/ejn.13506
Belmer A, Klenowski PM, Patkar OL, Bartlett SE (2017) Mapping the connectivity of serotonin transporter immunoreactive axons to excitatory and inhibitory neurochemical synapses in the mouse limbic brain. Brain Struct Funct 222:1297–1314 . doi: 10.1007/s00429-016-1278-x
Bentivoglio M, Kristensson K (2007) Neural-immune interactions in disorders of sleep-wakefulness organization. Trends Neurosci. 30:645–652
Bernardinelli Y, Muller D, Nikonenko I (2014) Astrocyte-synapse structural plasticity. Neural Plast. 2014
Berryman M, Franck Z, Bretscher A (1993) Ezrin is concentrated in the apical microvilli of a wide variety of epithelial cells whereas moesin is found primarily in endothelial cells. J Cell Sci 105:1025–1043
Bertile F, Oudart H, Criscuolo F, et al (2003) Hypothalamic gene expression in long-term fasted rats: Relationship with body fat. Biochem Biophys Res Commun 303:1106–1113 . doi: 10.1016/S0006-291X(03)00481-9
Biegańska K, Sokołowska P, Jöhren O, Zawilska JB (2012) Orexin a suppresses the growth of rat C6 glioma cells via a caspase-dependent mechanism. J Mol Neurosci 48:706–712 . doi: 10.1007/s12031-012-9799-0
Bingham S, Davey PT, Babbs AJ, et al (2001) Orexin-A, an hypothalamic peptide with analgesic properties. Pain 92:81–90 . doi: 10.1016/S0304-3959(00)00470-X
Bittencourt JC (2011) Anatomical organization of the melanin-concentrating hormone peptide family in the mammalian brain. Gen. Comp. Endocrinol. 172:185–197

Blasiak A, Gundlach AL, Hess G, Lewandowski MH (2017) Interactions of circadian rhythmicity, stress and orexigenic neuropeptide systems: Implications for food intake control. Front. Neurosci. 11

Blouin AM, Fried I, Wilson CL, et al (2013) Human hypocretin and melanin-concentrating hormone levels are linked to emotion and social interaction. Nat Commun 4: . doi: 10.1038/ncomms2461

Bluet-Pajot M -T, Presse F, Voko Z, et al (1995) Neuropeptide-E-1 Antagonizes the Action of Melanin-Concentrating Hormone on Stress-Induced Release of Adrenocorticotropin in the Rat. J Neuroendocrinol 7:297–303 . doi: 10.1111/j.1365-2826.1995.tb00761.x

Boddum K, Hansen MH, Jennum PJ, Kornum BR (2016) Cerebrospinal fluid hypocretin-1 (orexin-a) level fluctuates with season and correlates with day length. PLoS One 11: . doi: 10.1371/journal.pone.0151288

Bonaconsa M, Colavito V, Pifferi F, et al (2013) Cell clocks and neuronal networks: neuron ticking and synchronization in aging and aging-related neurodegenerative disease. Curr Alzheimer Res 10:597–608 . doi: 10.2174/15672050113109990004

Bonneh-Barkay D, Wiley CA (2009) Brain extracellular matrix in neurodegeneration. Brain Pathol. 19:573–585

Bonneh-Barkay D, Wiley C (2009) Brain extracellular matrix in neurodegeneration. Brain Pathol 19:573–585 . doi: 10.1111/j.1750-3639.2008.00195.x.Brain

Borgland SL, Storm E, Bonci A (2008) Orexin B/hypocretin 2 increases glutamatergic transmission to ventral tegmental area neurons. Eur J Neurosci 28:1545–1556 . doi: 10.1111/j.1460-9568.2008.06397.x

Borgland SL, Taha SA, Sarti F, et al (2006) Orexin a in the VTA is critical for the induction of synaptic plasticity and behavioral sensitization to cocaine. Neuron 49:589–601 . doi: 10.1016/j.neuron.2006.01.016

Borowsky B, Durkin MM, Ogozalek K, et al (2002) Erratum: Antidepressant, anxiolytic and anorectic effects of a melanin-concentrating hormone-1 receptor antagonist. Nat Med 8:825–830 . doi: 10.1038/nm741

Bradbury EJ, Moon LDF, Popat RJ, et al (2002) Chondroitinase ABC promotes functional recovery after spinal cord injury. Nature 416:636–640 . doi: 10.1038/416636a

Broberger C, De Lecea L, Sutcliffe JG, Hokfelt T (1998) Hypocretin/orexin- and melanin-concentrating hormone-expressing cells form distinct populations in the rodent lateral hypothalamus: Relationship to the neuropeptide Y and agouti gene-related protein systems. J Comp Neurol 402:460–474 . doi: 10.1002/(SICI)1096-9861(19981228)402:4<460::AID-CNE3>3.0.CO;2-S

Brown TM, Coogan AN, Cutler DJ, et al (2008) Electrophysiological actions of orexins on rat suprachiasmatic neurons in vitro. Neurosci Lett 448:273–278 . doi: 10.1016/j.neulet.2008.10.058

Brownell SE, Conti B (2010) Age- and gender-specific changes of hypocretin immunopositive neurons in C57Bl/6 mice. Neurosci Lett 472:29–32 . doi: 10.1016/j.neulet.2010.01.048

Brückner G, Härtig W, Kacza J, et al (1996) Extracellular matrix organization in various regions of rat brain grey matter. J Neurocytol 25:333–46 . doi: 10.1007/BF02284806

Brückner G, Hausen D, Härtig W, et al (1999) Cortical areas abundant in extracellular matrix chondroitin sulphate proteoglycans are less affected by cytoskeletal changes in Alzheimer's disease. Neuroscience 92:791–805 . doi: 10.1016/S0306-4522(99)00071-8

Brückner G, Kacza J, Grosche J (2004) Perineuronal nets characterized by vital labelling, confocal and electron microscopy in organotypic slice cultures of rat parietal cortex and hippocampus. J Mol Histol 35:115–122 . doi:

10.1023/B:HIJO.0000023374.22298.50
Brundin L, Björkqvist M, Träskman-Bendz L, Petersén Å (2009) Increased orexin levels in the cerebrospinal fluid the first year after a suicide attempt. J Affect Disord 113:179–182 . doi: 10.1016/j.jad.2008.04.011
Bubser M, Fadel JR, Jackson LL, et al (2005) Dopaminergic regulation of orexin neurons. Eur J Neurosci 21:2993–3001 . doi: 10.1111/j.1460-9568.2005.04121.x
Buijs RM, Kalsbeek A (2001) Hypothalamic integration of central and peripheral clocks. Nat Rev Neurosci 2:521–526 . doi: 10.1038/35081582
Burt J, Alberto CO, Parsons MP, Hirasawa M (2011) Local network regulation of orexin neurons in the lateral hypothalamus. Am J Physiol Regul Integr Comp Physiol 301:R572–R580 . doi: 10.1152/ajpregu.00674.2010
Büscher P, Cecchi G, Jamonneau V, Priotto G (2017) Human African trypanosomiasis. Lancet 390:2397–2409
Butterick TA, Nixon JP, Billington CJ, Kotz CM (2012) Orexin A decreases lipid peroxidation and apoptosis in a novel hypothalamic cell model. Neurosci Lett 524:30–34 . doi: 10.1016/j.neulet.2012.07.002
Cabello CR, Thune JJ, Pakkenberg H, Pakkenberg B (2002) Ageing of substantia nigra in humans: Cell loss may be compensated by hypertrophy. Neuropathol Appl Neurobiol 28:283–291 . doi: 10.1046/j.1365-2990.2002.00393.x
Callander GE, Olorunda M, Monna D, et al (2013) Kinetic properties of “dual” orexin receptor antagonists at OX1R and OX2R orexin receptors. Front Neurosci. doi: 10.3389/fnins.2013.00230
Carnemolla B, Leprini A, Borsi L, et al (1996) Human tenascin-R: Complete primary structure, pre-mRNA alternative splicing and gene localization on chromosome 1q23-q24. J Biol Chem 271:8157–8160
Celio MR, Spreafico R, De Biasi S, Vitellaro-Zuccarello L (1998) Perineuronal nets: past and present. Trends Neurosci. 21:510–5
Chou TC, Lee CE, Lu J, et al (2001) Orexin (hypocretin) neurons contain dynorphin. J Neurosci 21:RC168 . doi: 20015644 [pii]
Chowdhury S, Yamanaka A (2016) Optogenetic activation of serotonergic terminals facilitates GABAergic inhibitory input to orexin/hypocretin neurons. Sci Rep 6: . doi: 10.1038/srep36039
Chung S, Saito Y, Civelli O (2009) MCH receptors/gene structure-in vivo expression. Peptides 30:1985–1989 . doi: 10.1016/j.peptides.2009.07.017
Clasadonte J, McIver SR, Schmitt LI, et al (2014) Chronic Sleep Restriction Disrupts Sleep Homeostasis and Behavioral Sensitivity to Alcohol by Reducing the Extracellular Accumulation of Adenosine. J Neurosci 34:1879–1891 . doi: 10.1523/JNEUROSCI.2870-12.2014
Clasadonte J, Scemes E, Wang Z, et al (2017) Connexin 43-Mediated Astroglial Metabolic Networks Contribute to the Regulation of the Sleep-Wake Cycle. Neuron
Colavito V, Tesoriero C, Wirtu AT, et al (2015) Limbic thalamus and state-dependent behavior: The paraventricular nucleus of the thalamic midline as a node in circadian timing and sleep/wake-regulatory networks. Neurosci. Biobehav. Rev. 54:3–17
Corrada MM, Brookmeyer R, Paganini-Hill A, et al (2010) Dementia incidence continues to increase with age in the oldest old the 90+ study. Ann Neurol 67:114–121 . doi: 10.1002/ana.21915
Corvetti L (2005) Degradation of Chondroitin Sulfate Proteoglycans Induces Sprouting of Intact Purkinje Axons in the Cerebellum of the Adult Rat. J Neurosci 25:7150–7158 . doi: 10.1523/JNEUROSCI.0683-05.2005
Cristino L, Busetto G, Imperatore R, et al (2013) Obesity-driven synaptic remodeling affects endocannabinoid control of orexinergic neurons. Proc Natl Acad Sci 110:E2229–E2238 . doi: 10.1073/pnas.1219485110
Crocker A, España RA, Papadopoulou M, et al (2005) Concomitant loss of dynorphin,

NARP, and orexin in narcolepsy. Neurology 65:1184–1188 . doi: 10.1212/01.WNL.0000168173.71940.ab
Czopka T, Von Holst A, Schmidt G, et al (2009) Tenascin C and tenascin R similarly prevent the formation of myelin membranes in a RhoA-dependent manner, but antagonistically regulate the expression of myelin basic protein via a separate pathway. Glia 57:1790–1801 . doi: 10.1002/glia.20891
DALLMAN MF, AKANA SF, STRACK AM, et al (1995) The Neural Network that Regulates Energy Balance Is Responsive to Glucocorticoids and Insulin and Also Regulates HPA Axis Responsivity at a Site Proximal to CRF Neurons. Ann N Y Acad Sci 771:730–742 . doi: 10.1111/j.1749-6632.1995.tb44724.x
Davies CA, Mann DMA, Sumpter PQ, Yates PO (1987) A quantitative morphometric analysis of the neuronal and synaptic content of the frontal and temporal cortex in patients with Alzheimer's disease. J Neurol Sci 78:151–164 . doi: 10.1016/0022-510X(87)90057-8
de Lecea L, Huerta R (2014) Hypocretin (orexin) regulation of sleep-to-wake transitions. Front. Pharmacol. 5 FEB
de Lecea L, Kilduff TS, Peyron C, et al (1998) The hypocretins: Hypothalamus-specific peptides with neuroexcitatory activity. Proc Natl Acad Sci 95:322–327 . doi: 10.1073/pnas.95.1.322
Deats SP, Adidharma W, Lonstein JS, Yan L (2014) Attenuated orexinergic signaling underlies depression-like responses induced by daytime light deficiency. Neuroscience 272:252–260 . doi: 10.1016/j.neuroscience.2014.04.069
Deboer T, Overeem S, Visser NAH, et al (2004) Convergence of circadian and sleep regulatory mechanisms on hypocretin-1. Neuroscience 129:727–732 . doi: 10.1016/j.neuroscience.2004.07.049
Deepa SS, Carulli D, Galtrey C, et al (2006) Composition of perineuronal net extracellular matrix in rat brain: A different disaccharide composition for the net-associated proteoglycans. J Biol Chem 281:17789–17800 . doi: 10.1074/jbc.M600544200
DeMattos RB, Lu J, Tang Y, et al (2012) A Plaque-Specific Antibody Clears Existing β-amyloid Plaques in Alzheimer's Disease Mice. Neuron 76:908–920 . doi: 10.1016/j.neuron.2012.10.029
Derouiche A, Anlauf E, Aumann G, et al (2002) Anatomical aspects of glia-synapse interaction: The perisynaptic glial sheath consists of a specialized astrocyte compartment. J Physiol Paris 96:177–182 . doi: 10.1016/S0928-4257(02)00004-9
Derouiche A, Frotscher M (2001) Peripheral astrocyte processes: Monitoring by selective immunostaining for the actin-binding ERM proteins. Glia 36:330–341 . doi: 10.1002/glia.1120
Desarnaud F, Murillo-Rodriguez E, Lin L, et al (2004) The diurnal rhythm of hypocretin in young and old F344 rats. Sleep 27:851–856
Diano S, Horvath B, Urbanski HF, et al (2003) Fasting activates the nonhuman primate hypocretin (orexin) system and its postsynaptic targets. Endocrinology 144:3774–3778 . doi: 10.1210/en.2003-0274
Dityatev A, Brückner G, Dityateva G, et al (2007) Activity-dependent formation and functions of chondroitin sulfate-rich extracellular matrix of perineuronal nets. Dev Neurobiol 67:570–588 . doi: 10.1002/dneu.20361
Dityatev A, Frischknecht R, Seidenbecher CI (2006) Extracellular matrix and synaptic functions. Results Probl Cell Differ 43:69–97 . doi: 10.1007/400_025
Dityatev A, Rusakov DA (2011) Molecular signals of plasticity at the tetrapartite synapse. Curr. Opin. Neurobiol. 21:353–359
Dityatev A, Schachner M, Sonderegger P (2010a) The dual role of the extracellular matrix in synaptic plasticity and homeostasis. Nat Rev Neurosci 11:735–746 . doi: 10.1038/nrn2898

Dityatev A, Seidenbecher CI, Schachner M (2010b) Compartmentalization from the outside: The extracellular matrix and functional microdomains in the brain. Trends Neurosci. 33:503–512

Donato F, Rompani SB, Caroni P (2013) Parvalbumin-expressing basket-cell network plasticity induced by experience regulates adult learning. Nature 504:272–276 . doi: 10.1038/nature12866

Dours-Zimmermann MT, Maurer K, Rauch U, et al (2009) Versican V2 Assembles the Extracellular Matrix Surrounding the Nodes of Ranvier in the CNS. J Neurosci 29:7731–7742 . doi: 10.1523/JNEUROSCI.4158-08.2009

Downs JL, Dunn MR, Borok E, et al (2007) Orexin neuronal changes in the locus coeruleus of the aging rhesus macaque. Neurobiol Aging 28:1286–1295 . doi: 10.1016/j.neurobiolaging.2006.05.025

Drouot X, Moutereau S, Nguyen JP, et al (2003) Low levels of ventricular CSF orexin/hypocretin in advanced PD. Neurology 61:540–543 . doi: 10.1212/01.WNL.0000078194.53210.48

Druzin M, Haage D, Malinina E, Johansson S (2002) Dual and opposing roles of presynaptic Ca2+ influx for spontaneous GABA release from rat medial preoptic nerve terminals. J Physiol 542:131–146 . doi: 10.1113/jphysiol.2001.015610

Duffy JF, Cain SW, Chang A-M, et al (2011) Sex difference in the near-24-hour intrinsic period of the human circadian timing system. Proc Natl Acad Sci 108:15602–15608 . doi: 10.1073/pnas.1010666108

Duncan EA, Proulx K, Woods SC (2005) Central administration of melanin-concentrating hormone increases alcohol and sucrose/quinine intake in rats. Alcohol Clin Exp Res 29:958–964 . doi: 10.1097/01.ALC.0000167741.42353.10

Edwards CMB, Abusnana S, Sunter D, et al (1999) The effect of the orexins on food intake: Comparison with neuropeptide Y, melanin-concentrating hormone and galanin. J Endocrinol 160: . doi: 10.1677/joe.0.160R007

Eggermann E, Bayer L, Serafin M, et al (2003) The wake-promoting hypocretin-orexin neurons are in an intrinsic state of membrane depolarization. J Neurosci 23:1557–1562 . doi: 23/5/1557 [pii]

Eggermann E, Serafin M, Bayer L, et al (2001) Orexins/hypocretins excite basal forebrain cholinergic neurones. Neuroscience 108:177–181 . doi: 10.1016/S0306-4522(01)00512-7

El Ayachi I, Fernandez C, Baeza N, et al (2011) Spatiotemporal distribution of tenascin-R in the developing human cerebral cortex parallels neuronal migration. J Comp Neurol 519:2379–2389 . doi: 10.1002/cne.22632

Elbaz I, Foulkes NS, Gothilf Y, Appelbaum L (2013) Circadian clocks, rhythmic synaptic plasticity and the sleep-wake cycle in zebrafish. Front Neural Circuits 7:9 . doi: 10.3389/fncir.2013.00009

Elbaz I, Levitas-Djerbi T, Appelbaum L (2017a) The Hypocretin/Orexin Neuronal networks in zebrafish. In: Current Topics in Behavioral Neurosciences. pp 75–92

Elbaz I, Zada D, Tovin A, et al (2017b) Sleep-Dependent Structural Synaptic Plasticity of Inhibitory Synapses in the Dendrites of Hypocretin/Orexin Neurons. Mol Neurobiol 54:6581–6597 . doi: 10.1007/s12035-016-0175-x

Estabrooke I V, Mccarthy MT, Ko E, et al (2001) Fos Expression in Orexin Neurons Varies with Behavioral State. J Neurosci 21:1656–1662 . doi: 10.1152/jn.00927.2005

Etet PFS, Palomba M, Colavito V, et al (2012) Sleep and rhythm changes at the time of Trypanosoma brucei invasion of the brain parenchyma in the rat. Chronobiol Int 29:469–481 . doi: 10.3109/07420528.2012.660713

Ettorre M, Lorenzetto E, Laperchia C, et al (2012) Glutamatergic neurons induce expression of functional glutamatergic synapses in primary myotubes. PLoS One 7: . doi: 10.1371/journal.pone.0031451

Fadel J, Pasumarthi R, Reznikov LR (2005) Stimulation of cortical acetylcholine release by orexin A. Neuroscience 130:541–547 . doi: 10.1016/j.neuroscience.2004.09.050
Faissner A, Pyka M, Geissler M, et al (2010) Contributions of astrocytes to synapse formation and maturation - Potential functions of the perisynaptic extracellular matrix. Brain Res Rev 63:26–38 . doi: 10.1016/j.brainresrev.2010.01.001
Farach-Carson MC, Warren CR, Harrington DA, Carson DD (2014) Border patrol: Insights into the unique role of perlecan/heparan sulfate proteoglycan 2 at cell and tissue borders. Matrix Biol 34:64–79 . doi: 10.1016/j.matbio.2013.08.004
Farajnia S, Michel S, Deboer T, et al (2012) Evidence for Neuronal Desynchrony in the Aged Suprachiasmatic Nucleus Clock. J Neurosci 32:5891–5899 . doi: 10.1523/JNEUROSCI.0469-12.2012
Ferrari LL, Park D, Zhu L, et al (2018) Regulation of lateral hypothalamic orexin activity by local GABAergic neurons. J Neurosci 1925–17 . doi: 10.1523/JNEUROSCI.1925-17.2017
Florenzano F, Viscomi MT, Mercaldo V, et al (2006) P2X2R purinergic receptor subunit mRNA and protein are expressed by all hypothalamic hypocretin/orexin neurons. J Comp Neurol 498:58–67 . doi: 10.1002/cne.21013
Flores Á, Valls-Comamala V, Costa G, et al (2014) The hypocretin/orexin system mediates the extinction of fear memories. Neuropsychopharmacology 39:2732–2741 . doi: 10.1038/npp.2014.146
Fogarty MJ, Hammond LA, Kanjhan R, et al (2013) A method for the three-dimensional reconstruction of Neurobiotin™-filled neurons and the location of their synaptic inputs. Front Neural Circuits 7: . doi: 10.3389/fncir.2013.00153
Foley D, Ancoli-Israel S, Britz P, Walsh J (2004) Sleep disturbances and chronic disease in older adults: Results of the 2003 National Sleep Foundation Sleep in America Survey. J. Psychosom. Res. 56:497–502
Frantz C, Stewart KM, Weaver VM (2010) The extracellular matrix at a glance. J Cell Sci 123:4195–4200 . doi: 10.1242/jcs.023820
Friedman LF, Zeitzer JM, Lin L, et al (2007) In Alzheimer disease, increased wake fragmentation found in those with lower hypocretin-1. Neurology 68:793–794 . doi: 10.1212/01.wnl.0000256731.57544.f9
Frischknecht R, Happel MFK (2016) Impact of the extracellular matrix on plasticity in juvenile and adult brains. e-Neuroforum 7:1–6 . doi: 10.1007/s13295-015-0021-z
Frischknecht R, Heine M, Perrais D, et al (2009) Brain extracellular matrix affects AMPA receptor lateral mobility and short-term synaptic plasticity. Nat Neurosci 12:897–904 . doi: 10.1038/nn.2338
Fronczek R, Baumann CR, Lammers GJ, et al (2009) Hypocretin/orexin disturbances in neurological disorders. Sleep Med Rev 13:9–22 . doi: 10.1016/j.smrv.2008.05.002
Fronczek R, Overeem S, Lee SYY, et al (2007) Hypocretin (orexin) loss in Parkinson's disease. Brain 130:1577–85 . doi: 10.1093/brain/awm090
Fujiki N, Yoshida Y, Ripley B, et al (2001) Changes in CSF hypocretin-1 (orexin A) levels in rats across 24 hours and in response to food deprivation. Neuroreport 12:993–7 . doi: 10.1097/00001756-200104170-00026
Furutani N, Hondo M, Kageyama H, et al (2013) Neurotensin Co-Expressed in Orexin-Producing Neurons in the Lateral Hypothalamus Plays an Important Role in Regulation of Sleep/Wakefulness States. PLoS One 8: . doi: 10.1371/journal.pone.0062391
Gallone S, Boschi S, Rubino E, et al (2014) Is HCRTR2 a genetic risk factor for Alzheimer's disease? Dement Geriatr Cogn Disord 38:245–253 . doi: 10.1159/000359964
Galtrey CM, Kwok JCF, Carulli D, et al (2008) Distribution and synthesis of extracellular matrix proteoglycans, hyaluronan, link proteins and tenascin-R in the rat spinal cord. Eur J Neurosci 27:1373–1390 . doi: 10.1111/j.1460-9568.2008.06108.x

Games D, Adams D, Alessandrini R, et al (1995) Alzheimer-type neuropathology in transgenic mice overexpressing V717F beta-amyloid precursor protein. Nature 373:523–7 . doi: 10.1038/373523a0
Gao X-B, Hermes G (2015) Neural plasticity in hypocretin neurons: the basis of hypocretinergic regulation of physiological and behavioral functions in animals. Front Syst Neurosci 9: . doi: 10.3389/fnsys.2015.00142
García-Alías G, Fawcett JW (2012) Training and anti-CSPG combination therapy for spinal cord injury. Exp. Neurol. 235:26–32
Gaudet AD, Popovich PG (2014) Extracellular matrix regulation of inflammation in the healthy and injured spinal cord. Exp. Neurol. 258:24–34
Georgescu D (2005) The Hypothalamic Neuropeptide Melanin-Concentrating Hormone Acts in the Nucleus Accumbens to Modulate Feeding Behavior and Forced-Swim Performance. J Neurosci 25:2933–2940 . doi: 10.1523/JNEUROSCI.1714-04.2005
Gerashchenko D, Murillo-Rodriguez E, Lin L, et al (2003) Relationship between CSF hypocretin levels and hypocretin neuronal loss. Exp Neurol 184:1010–1016 . doi: 10.1016/S0014-4886(03)00388-1
Gerashchenko D, Shiromani PJ (2004) Different neuronal phenotypes in the lateral hypothalamus and their role in sleep and wakefulness. Mol. Neurobiol. 29:41–59
Gerstner JR, Perron IJ, Pack AI (2012) The nexus of Aβ, aging, and sleep. Sci Transl Med 4:150fs34 . doi: 10.1126/scitranslmed.3004815
Gerstner JR, Vander Heyden WM, LaVaute TM, Landry CF (2006) Profiles of novel diurnally regulated genes in mouse hypothalamus: Expression analysis of the cysteine and histidine-rich domain-containing, zinc-binding protein 1, the fatty acid-binding protein 7 and the GTPase, ras-like family member 11b. Neuroscience 139:1435–1448 . doi: 10.1016/j.neuroscience.2006.01.020
Giamanco KA, Morawski M, Matthews RT (2010) Perineuronal net formation and structure in aggrecan knockout mice. Neuroscience 170:1314–1327 . doi: 10.1016/j.neuroscience.2010.08.032
Goldbart A, Peppard P, Finn L, et al (2014) Narcolepsy and predictors of positive MSLTs in the Wisconsin Sleep Cohort. Sleep 37:1043–51 . doi: 10.5665/sleep.3758
Grassi-Zucconi G, Giuditta A, Mandile P, et al (1994) c-fos sponteneous expression during wakefulness is reversed during sleep in neuronal subsets of the rat cortex. J Physiol - Paris 88:91–93 . doi: 10.1016/0928-4257(94)90096-5
Grassi???Zucconi G, Menegazzi M, De Prati AC, et al (1993) C???fos mRNA is Spontaneously Induced in the Rat Brain During the Activity Period of the Circadian Cycle. Eur J Neurosci 5:1071–1078 . doi: 10.1111/j.1460-9568.1993.tb00960.x
Graybill NL, Weissig V (2017) A review of orexin's unprecedented potential as a novel, highly-specific treatment for various localized and metastatic cancers. SAGE Open Med 5:205031211773577 . doi: 10.1177/2050312117735774
Guan JL, Uehara K, Lu S, et al (2002) Reciprocal synaptic relationships between orexin- and melanin-concentrating hormone-containing neurons in the rat lateral hypothalamus: A novel circuit implicated in feeding regulation. Int J Obes 26:1523–1532 . doi: 10.1038/sj.ijo.0802155
Guesdon B, Paradis E, Samson P, Richard D (2009) Effects of intracerebroventricular and intra-accumbens melanin-concentrating hormone agonism on food intake and energy expenditure. Am J Physiol Regul Integr Comp Physiol 296:R469–R475 . doi: 10.1152/ajpregu.90556.2008
Gundelfinger ED, Frischknecht R, Choquet D, Heine M (2010) Converting juvenile into adult plasticity: A role for the brain's extracellular matrix. Eur. J. Neurosci. 31:2156–2165
Guthrie PB, Knappenberger J, Segal M, et al (1999) ATP released from astrocytes mediates glial calcium waves. J Neurosci 19:520–528
Gutowski NJ, Newcombe J, Cuzner ML (1999) Tenascin-R and C in multiple sclerosis

lesions: Relevance to extracellular matrix remodelling. Neuropathol Appl Neurobiol 25:207–214 . doi: 10.1046/j.1365-2990.1999.00176.x
Hajek M, Meier-Ewert K, Wirz-Justice A, et al (1989) Bright white light does not improve narcoleptic symptoms. Eur Arch Psychiatry Neurol Sci 238:203–207 . doi: 10.1007/BF00381466
Hamada T, Antle MC, Silver R (2004) The role of Period1 in non-photic resetting of the hamster circadian pacemaker in the suprachiasmatic nucleus. Neurosci Lett 362:87–90 . doi: 10.1016/j.neulet.2004.02.061
Hara J, Beuckmann CT, Nambu T, et al (2001) Genetic ablation of orexin neurons in mice results in narcolepsy, hypophagia, and obesity. Neuron 30:345–354 . doi: 10.1016/S0896-6273(01)00293-8
Hara J, Yanagisawa M, Sakurai T (2005) Difference in obesity phenotype between orexin-knockout mice and orexin neuron-deficient mice with same genetic background and environmental conditions. Neurosci Lett 380:239–242 . doi: 10.1016/j.neulet.2005.01.046
Hargus G, Cui Y, Schmid JS, et al (2008) Tenascin-R promotes neuronal differentiation of embryonic stem cells and recruitment of host-derived neural precursor cells after excitotoxic lesion of the mouse striatum. Stem Cells 26:1973–1984 . doi: 2007-0929 [pii]10.1634/stemcells.2007-0929
Harris GC, Wimmer M, Aston-Jones G (2005) A role for lateral hypothalamic orexin neurons in reward seeking. Nature 437:556–559 . doi: 10.1038/nature04071
Härtig W, Brauer K, Bigl V, Brückner G (1994) Chondroitin sulfate proteoglycan-immunoreactivity of lectin-labeled perineuronal nets around parvalbumin-containing neurons. Brain Res 635:307–311 . doi: 10.1016/0006-8993(94)91452-4
Hassani OK, Lee MG, Jones BE (2009) Melanin-concentrating hormone neurons discharge in a reciprocal manner to orexin neurons across the sleep-wake cycle. Proc Natl Acad Sci 106:2418–2422 . doi: 10.1073/pnas.0811400106
Hayashi Y, Koyanagi S, Kusunose N, et al (2013) The intrinsic microglial molecular clock controls synaptic strength via the circadian expression of cathepsin S. Sci Rep 3: . doi: 10.1038/srep02744
Haynes AC, Jackson B, Chapman H, et al (2000) A selective orexin-1 receptor antagonist reduces food consumption in male and female rats. Regul Pept 96:45–51
Heller JP, Rusakov DA (2015) Morphological plasticity of astroglia: Understanding synaptic microenvironment. Glia 63:2133–2151
Henny P, Jones BE (2008) Projections from basal forebrain to prefrontal cortex comprise cholinergic, GABAergic and glutamatergic inputs to pyramidal cells or interneurons. Eur J Neurosci 27:654–670 . doi: 10.1111/j.1460-9568.2008.06029.x
Henny P, Jones BE (2006) Innervation of orexin/hypocretin neurons by GABAergic, glutamatergic or cholinergic basal forebrain terminals evidenced by immunostaining for presynaptic vesicular transporter and postsynaptic scaffolding proteins. J Comp Neurol 499:645–661 . doi: 10.1002/cne.21131
Hensch TK (2005) Critical period plasticity in local cortical circuits. Nat. Rev. Neurosci. 6:877–888
Herdegen T, Leah JD (1998) Inducible and constitutive transcription factors in the mammalian nervous system: Control of gene expression by Jun, Fos and Krox, and CREB/ATF proteins. Brain Res. Rev. 28:370–490
Hervieu G (2003) Melanin-concentrating hormone functions in the nervous system: food intake and stress. Expert Opin Ther Targets 7:495–511 . doi: 10.1517/14728222.7.4.495
Hobohm C, Günther A, Grosche J, et al (2005) Decomposition and long-lasting downregulation of extracellular matrix in perineuronal nets induced by focal cerebral ischemia in rats. J Neurosci Res 80:539–548 . doi: 10.1002/jnr.20459
Holmqvist T, Åkerman KEO, Kukkonen JP (2001) High specificity of human orexin

receptors for orexins over neuropeptide Y and other neuropeptides. Neurosci Lett 305:177–180 . doi: 10.1016/S0304-3940(01)01839-0
Hondo M, Furutani N, Yamasaki M, et al (2011) Orexin neurons receive glycinergic innervations. PLoS One 6: . doi: 10.1371/journal.pone.0025076
Horii-Hayashi N, Sasagawa T, Matsunaga W, Nishi M (2015) Development and Structural Variety of the Chondroitin Sulfate Proteoglycans-Contained Extracellular Matrix in the Mouse Brain. Neural Plast 2015: . doi: 10.1155/2015/256389
Horii-Hayashi N, Sasagawa T, Nishi M (2017) Insights from extracellular matrix studies in the hypothalamus: structural variations of perineuronal nets and discovering a new perifornical area of the anterior hypothalamus. Anat Sci Int 92:18–24 . doi: 10.1007/s12565-016-0375-5
Horvath TL, Gao XB (2005) Input organization and plasticity of hypocretin neurons. Possible clues to obesity's association with insomnia. Cell Metab 1:279–286 . doi: 10.1016/j.cmet.2005.03.003
Howlett DR, Bowler K, Soden PE, et al (2008) A?? deposition and related pathology in an APP x PS1 transgenic mouse model of Alzheimer's disease. Histol Histopathol 23:67–76
Howlett DR, Richardson JC (2009a) The pathology of APP transgenic mice: a model of Alzheimer's disease or simply overexpression of APP. Histol Histopathol 24:18
Howlett DR, Richardson JC (2009b) The pathology of APP transgenic mice: A model of Alzheimer's disease or simply overexpression of APP? Histol. Histopathol. 24:83–100
Howlett DR, Richardson JC, Austin A, et al (2004) Cognitive correlates of A?? deposition in male and female mice bearing amyloid precursor protein and presenilin-1 mutant transgenes. Brain Res 1017:130–136 . doi: 10.1016/j.brainres.2004.05.029
Hsia AY, Masliah E, McConlogue L, et al (1999) Plaque-independent disruption of neural circuits in Alzheimer's disease mouse models. Proc Natl Acad Sci U S A 96:3228–3233 . doi: 10.1073/pnas.96.6.3228
Hughes ATL, Piggins HD (2012) Feedback actions of locomotor activity to the circadian clock. Prog Brain Res 199:305–336 . doi: 10.1016/B978-0-444-59427-3.00018-6
Hunt NJ, Rodriguez ML, Waters KA, Machaalani R (2015a) Changes in orexin (hypocretin) neuronal expression with normal aging in the human hypothalamus. Neurobiol Aging 36:292–300 . doi: 10.1016/j.neurobiolaging.2014.08.010
Hunt NJ, Rodriguez ML, Waters KA, Machaalani R (2015b) Changes in orexin (hypocretin) neuronal expression with normal aging in the human hypothalamus. Neurobiol Aging 36:292–300 . doi: 10.1016/j.neurobiolaging.2014.08.010
Inan M, Blazquez-Llorca L, Merchan-Perez A, et al (2013) Dense and Overlapping Innervation of Pyramidal Neurons by Chandelier Cells. J Neurosci 33:1907–1914 . doi: 10.1523/JNEUROSCI.4049-12.2013
Inutsuka A, Inui A, Tabuchi S, et al (2014) Concurrent and robust regulation of feeding behaviors and metabolism by orexin neurons. Neuropharmacology 85:451–460 . doi: 10.1016/j.neuropharm.2014.06.015
Inutsuka A, Yamanaka A (2013) The regulation of sleep and wakefulness by the hypothalamic neuropeptide orexin/hypocretin. Nagoya J Med Sci 75:29–36
Inutsuka A, Yamashita A, Chowdhury S, et al (2016) The integrative role of orexin/hypocretin neurons in nociceptive perception and analgesic regulation. Sci Rep 6: . doi: 10.1038/srep29480
Ippolito DM, Eroglu C (2010) Quantifying Synapses: an Immunocytochemistry-based Assay to Quantify Synapse Number. J Vis Exp. doi: 10.3791/2270
Itano N, Kimata K (2002) Mammalian hyaluronan synthases. IUBMB Life 54:195–199
Itano N, Sawai T, Yoshida M, et al (1999) Three isoforms of mammalian hyaluronan synthases have distinct enzymatic properties. J Biol Chem 274:25085–25092 . doi:

10.1074/jbc.274.35.25085
Jászberényi M, Bujdosó E, Pataki I, Telegdy G (2000) Effects of orexins on the hypothalamic-pituitary-adrenal system. J Neuroendocrinol 12:1174–1178 . doi: 10.1046/j.1365-2826.2000.00572.x
Jezová D, Bartanusz V, Westergren I, et al (1992) Rat melanin-concentrating hormone stimulates adrenocorticotropin secretion: Evidence for a site of action in brain regions protected by the blood-brain barrier. Endocrinology 130:1024–1029 . doi: 10.1210/endo.130.2.1310274
Jöhren O, Neidert SJ, Kummer M, et al (2001) Prepro-orexin and orexin receptor mRNAs are differentially expressed in peripheral tissues of male and female rats. Endocrinology 142:3324–3331 . doi: 10.1210/en.142.8.3324
Ju YES, Lucey BP, Holtzman DM (2014) Sleep and Alzheimer disease pathology-a bidirectional relationship. Nat. Rev. Neurol. 10:115–119
Kaminska B, Filipkowski RK, Biedermann IW, et al (1997) Kainate-evoked modulation of gene expression in rat brain. Acta Biochim Pol 44:781–9.
Kang J-E, Lim MM, Bateman RJ, et al (2009) Amyloid- Dynamics Are Regulated by Orexin and the Sleep-Wake Cycle. Science (80-) 326:1005–1007 . doi: 10.1126/science.1180962
Kantor S, Mochizuki T, Janisiewicz AM, et al (2009) Orexin neurons are necessary for the circadian control of REM sleep. Sleep 32:1127–1134
Karetko M, Skangiel-Kramska J (2009) Diverse functions of perineuronal nets. Acta Neurobiol Exp 69:564–577
Karlsson C, Aziz AMA, Rehman F, et al (2016) Melanin-Concentrating Hormone and Its MCH-1 Receptor: Relationship Between Effects on Alcohol and Caloric Intake. Alcohol Clin Exp Res 40:2199–2207 . doi: 10.1111/acer.13181
Karnani MM, Venner A, Jensen LT, et al (2011) Direct and indirect control of orexin/hypocretin neurons by glycine receptors. J Physiol 589:639–651 . doi: 10.1113/jphysiol.2010.198457
Karteris E, Randeva HS, Grammatopoulos DK, et al (2001) Expression and coupling characteristics of the CRH and orexin type 2 receptors in human fetal adrenals. J Clin Endocrinol Metab 86:4512–4519 . doi: 10.1210/jc.86.9.4512
Katsuki H, Michinaga S (2012) Anti-Parkinson Drugs and Orexin Neurons. Vitam Horm 89:279–290 . doi: 10.1016/B978-0-12-394623-2.00015-9
Kessler BA, Stanley EM, Frederick-Duus D, Fadel J (2011) Age-related loss of orexin/hypocretin neurons. Neuroscience 178:82–88 . doi: 10.1016/j.neuroscience.2011.01.031
Kilduff TS, Peyron C (2000) The hypocretin/orexin ligand-receptor system: Implications for sleep and sleep disorders. Trends Neurosci. 23:359–365
Kim T-K, Han P-L (2016) Functional Connectivity of Basolateral Amygdala Neurons Carrying Orexin Receptors and Melanin-concentrating Hormone Receptors in Regulating Sociability and Mood-related Behaviors. Exp Neurobiol 25:307–317 . doi: 10.5607/en.2016.25.6.307
King M a, Scotty N, Klein RL, Meyer EM (2002) Particle detection, number estimation, and feature measurement in gene transfer studies: optical fractionator stereology integrated with digital image processing and analysis. Methods 28:293–9 . doi: 10.1016/S1046-2023(02)00235-9
Kirchgessner AL, Liu MT (1999) Orexin synthesis and response in the gut. Neuron 24:941–951 . doi: 10.1016/S0896-6273(00)81041-7
Klisch C, Inyushkin A, Mordel J, et al (2009) Orexin A modulates neuronal activity of the rodent suprachiasmatic nucleus in vitro. Eur J Neurosci 30:65–75 . doi: 10.1111/j.1460-9568.2009.06794.x
Koch CE, Leinweber B, Drengberg BC, et al (2017) Interaction between circadian rhythms and stress. Neurobiol. Stress 6:57–67

Kohlmeier KA, Tyler CJ, Kalogiannis M, et al (2013) Differential actions of orexin receptors in brainstem cholinergic and monoaminergic neurons revealed by receptor knockouts: Implications for orexinergic signaling in arousal and narcolepsy. Front Neurosci. doi: 10.3389/fnins.2013.00246

Konadhode RR, Pelluru D, Blanco-Centurion C, et al (2013) Optogenetic stimulation of MCH neurons increases sleep. J Neurosci 33:10257–63 . doi: 10.1523/JNEUROSCI.1225-13.2013

Köppe G, Brückner G, Brauer K, et al (1997) Developmental patterns of proteoglycan-containing extracellular matrix in perineuronal nets and neuropil of the postnatal rat brain. Cell Tissue Res 288:33–41 . doi: 10.1007/s004410050790

Kornum BR, Faraco J, Mignot E (2011) Narcolepsy with hypocretin/orexin deficiency, infections and autoimmunity of the brain. Curr. Opin. Neurobiol. 21:897–903

Kristensson K, Nygård M, Bertini G, Bentivoglio M (2010) African trypanosome infections of the nervous system: Parasite entry and effects on sleep and synaptic functions. Prog Neurobiol 91:152–171 . doi: 10.1016/J.PNEUROBIO.2009.12.001

Krueger JM (2008) The role of cytokines in sleep regulation. Curr Pharm Des 14:3408–16 . doi: 10.2174/138161208786549281

Kruse J, Keilhauer G, Faissner A, et al (1985) The J1 glycoprotein - A novel nervous system cell adhesion molecule of the L2/HNK-1 family. Nature 316:146–148 . doi: 10.1038/316146a0

Kuhlman SJ, Quintero JE, McMahon DG (2000) GFP fluorescence reports Period 1 circadian gene regulation in the mammalian biological clock. Neuroreport 11:1479–82 . doi: 10.1097/00001756-200005150-00023

Kukkonen JP (2013) Physiology of the orexinergic/hypocretinergic system: a revisit in 2012. AJP Cell Physiol 304:C2–C32 . doi: 10.1152/ajpcell.00227.2012

Kuru M, Ueta Y, Serino R, et al (2000) Centrally administered orexin/hypocretin activates HPA axis in rats. Neuroreport 11:1977–80 . doi: 10.1097/00001756-200006260-00034

Kwok JCF, Dick G, Wang D, Fawcett JW (2011) Extracellular matrix and perineuronal nets in CNS repair. Dev Neurobiol 71:1073–1089 . doi: 10.1002/dneu.20974

Kyrou I, Chrousos GP, Tsigos C (2006) Stress, visceral obesity, and metabolic complications. In: Annals of the New York Academy of Sciences. pp 77–110

Laperchia C, Imperatore R, Azeez IA, et al (2017) The excitatory/inhibitory input to orexin/hypocretin neuron soma undergoes day/night reorganization. Brain Struct Funct 222: . doi: 10.1007/s00429-017-1466-3

Laperchia C, Palomba M, Seke Etet PF, et al (2016) Trypanosoma brucei Invasion and T-cell Infiltration of the Brain Parenchyma in Experimental Sleeping Sickness: Timing and Correlation with Functional Changes. PLoS Negl Trop Dis 10: . doi: 10.1371/journal.pntd.0005242

Lau LW, Cua R, Keough MB, et al (2013) Pathophysiology of the brain extracellular matrix: A new target for remyelination. Nat. Rev. Neurosci. 14:722–729

Lavialle M, Aumann G, Anlauf E, et al (2011) Structural plasticity of perisynaptic astrocyte processes involves ezrin and metabotropic glutamate receptors. Proc Natl Acad Sci 108:12915–12919 . doi: 10.1073/pnas.1100957108

Lee C, Parks GS, Civelli O (2011) Anxiolytic effects of the MCH1R antagonist TPI 1361-17. J Mol Neurosci 43:132–137 . doi: 10.1007/s12031-010-9425-y

Lee J-HH, Bang E, Chae K-JJ, et al (1999) Solution structure of a new hypothalamic neuropeptide, human hypocretin-2/orexin-B. Eur J Biochem 266:831–9 . doi: 10.1046/j.1432-1327.1999.00911.x

Lee MG (2005) Discharge of Identified Orexin/Hypocretin Neurons across the Sleep-Waking Cycle. J Neurosci 25:6716–6720 . doi: 10.1523/JNEUROSCI.1887-05.2005

Lee SY, Haydon PG (2011) A Cytokine-Dependent Switch for Glial-Neuron Interactions. Neuron 69:835–837

Lemańska-Perek A, Leszek J, Krzyanowska-Gołąb D, et al (2009) Molecular status of plasma fibronectin as an additional biomarker for assessment of alzheimer's dementia risk. Dement Geriatr Cogn Disord 28:338–342 . doi: 10.1159/000252764

Lensjø KK, Christensen AC, Tennøe S, et al (2017) Differential Expression and Cell-Type Specificity of Perineuronal Nets in Hippocampus, Medial Entorhinal Cortex, and Visual Cortex Examined in the Rat and Mouse. eneuro 4:ENEURO.0379-16.2017 . doi: 10.1523/ENEURO.0379-16.2017

Lepelletier F-X, Mann DMA, Robinson AC, et al (2015) Early changes in extracellular matrix in Alzheimer's disease. Neuropathol Appl Neurobiol n/a-n/a . doi: 10.1111/nan.12295

Li Y, Li Z-X, Jin T, et al (2017) Tau Pathology Promotes the Reorganization of the Extracellular Matrix and Inhibits the Formation of Perineuronal Nets by Regulating the Expression and the Distribution of Hyaluronic Acid Synthases. J Alzheimer's Dis 57:395–409 . doi: 10.3233/JAD-160804

Liao H, Bu WY, Wang TH, et al (2005) Tenascin-R plays a role in neuroprotection via its distinct domains that coordinate to modulate the microglia function. J Biol Chem 280:8316–8323 . doi: 10.1074/jbc.M412730200

Liblau RS, Vassalli A, Seifinejad A, Tafti M (2015) Hypocretin (orexin) biology and the pathophysiology of narcolepsy with cataplexy. Lancet Neurol 14:318–328 . doi: 10.1016/S1474-4422(14)70218-2

Liguori C, Nuccetelli M, Izzi F, et al (2016) Rapid eye movement sleep disruption and sleep fragmentation are associated with increased orexin-A cerebrospinal-fluid levels in mild cognitive impairment due to Alzheimer's disease. Neurobiol Aging 40:120–126 . doi: 10.1016/j.neurobiolaging.2016.01.007

Liguz-Lecznar M, Skangiel-Kramska J (2007) Vesicular glutamate transporters VGLUT1 and VGLUT2 in the developing mouse barrel cortex. Int J Dev Neurosci 25:107–114 . doi: 10.1016/j.ijdevneu.2006.12.005

Lim RG, Salazar LL, Wilton DK, et al (2017) Developmental alterations in Huntington's disease neural cells and pharmacological rescue in cells and mice. Nat Neurosci 20:648–660 . doi: 10.1038/nn.4532

Lin R, Rosahl TW, Whiting PJ, et al (2011) 6-Sulphated chondroitins have a positive influence on axonal regeneration. PLoS One 6: . doi: 10.1371/journal.pone.0021499

Linehan V, Fang LZ, Hirasawa M (2018) Short-term high-fat diet primes excitatory synapses for long-term depression in orexin neurons. J Physiol 596:305–316 . doi: 10.1113/JP275177

Liu R-J, van den Pol AN, Aghajanian GK (2002) Hypocretins (orexins) regulate serotonin neurons in the dorsal raphe nucleus by excitatory direct and inhibitory indirect actions. J Neurosci 22:9453–9464 . doi: 22/21/9453 [pii]

Liu RY, Zhou JN, Hoogendijk WJ, et al (2000) Decreased vasopressin gene expression in the biological clock of Alzheimer disease patients with and without depression. J Neuropathol Exp Neurol 59:314–322

Liu RY, Zhou JN, Van Heerikhuize J, et al (1999) Decreased melatonin levels in postmortem cerebrospinal fluid in relation to aging, Alzheimer's disease, and apolipoprotein E-??4/4 genotype. J Clin Endocrinol Metab 84:323–327 . doi: 10.1210/jc.84.1.323

Lundell A, Olin AI, Mörgelin M, et al (2004) Structural basis for interactions between tenascins and lectican C-type lectin domains: Evidence for a crosslinking role for tenascins. Structure 12:1495–1506 . doi: 10.1016/j.str.2004.05.021

Macneil DJ (2013) The role of melanin-concentrating hormone and its receptors in energy homeostasis. Front Endocrinol (Lausanne) 4:49 . doi: 10.3389/fendo.2013.00049

Mahler S V., Moorman DE, Smith RJ, et al (2014) Motivational activation: A unifying hypothesis of orexin/hypocretin function. Nat. Neurosci. 17:1298–1303

Mahlios J, De la Herrán-Arita AK, Mignot E (2013) The autoimmune basis of narcolepsy. Curr. Opin. Neurobiol. 23:767–773
Mandrekar-Colucci S, Landreth GE (2010) Microglia and inflammation in Alzheimer's disease. CNS Neurol Disord Drug Targets 9:156–67 . doi: 10.2174/18715271079101207 1
Marcus JN, Aschkenasi CJ, Lee CE, et al (2001) Differential expression of orexin receptors 1 and 2 in the rat brain. J Comp Neurol 435:6–25 . doi: 10.1002/cne.1190
Marpegan L, Swanstrom AE, Chung K, et al (2011) Circadian Regulation of ATP Release in Astrocytes. J Neurosci 31:8342–8350 . doi: 10.1523/JNEUROSCI.6537-10.2011
Marston OJ, Williams RH, Canal MM, et al (2008) Circadian and dark-pulse activation of orexin/hypocretin neurons. Mol Brain 1:19 . doi: 10.1186/1756-6606-1-19
Matsuoka Y, Picciano M, Malester B, et al (2001) Inflammatory responses to amyloidosis in a transgenic mouse model of Alzheimer's disease. Am J Pathol 158:1345–54 . doi: 10.1016/S0002-9440(10)64085-0
Matthews RT, Kelly GM, Zerillo C a, et al (2002) Aggrecan glycoforms contribute to the molecular heterogeneity of perineuronal nets. J Neurosci 22:7536–7547 . doi: 22/17/7536 [pii]
Mavanji V, Perez-Leighton CE, Kotz CM, et al (2015) Promotion of Wakefulness and Energy Expenditure by Orexin-A in the Ventrolateral Preoptic Area. Sleep 38:1361–1370 . doi: 10.5665/sleep.4970
Maywood ES, Okamura H, Hastings MH (2002) Opposing actions of neuropeptide Y and light on the expression of circadian clock genes in the mouse suprachiasmatic nuclei. Eur J Neurosci 15:216–220 . doi: 10.1046/j.0953-816x.2001.01852.x
McGeer PL, Schwab C, Parent A, Doudet D (2003) Presence of Reactive Microglia in Monkey Substantia Nigra Years after 1-Methyl-4-Phenyl-1,2,3,6-Tetrahydropyridine Administration. Ann Neurol 54:599–604 . doi: 10.1002/ana.10728
McGranaghan PA, Piggins HD (2001) Orexin A-like immunoreactivity in the hypothalamus and thalamus of the Syrian hamster (Mesocricetus auratus) and Siberian hamster (Phodopus sungorus), with special reference to circadian structures. Brain Res 904:234–244 . doi: 10.1016/S0006-8993(01)02463-5
McGregor R, Shan L, Wu MF, Siegel JM (2017) Diurnal fluctuation in the number of hypocretin/orexin and histamine producing: Implication for understanding and treating neuronal loss. PLoS One 12: . doi: 10.1371/journal.pone.0178573
McGregor R, Wu M-F, Barber G, et al (2011) Highly Specific Role of Hypocretin (Orexin) Neurons: Differential Activation as a Function of Diurnal Phase, Operant Reinforcement versus Operant Avoidance and Light Level. J Neurosci 31:15455–15467 . doi: 10.1523/JNEUROSCI.4017-11.2011
Megías M, Emri Z, Freund T., Gulyás A. (2001) Total number and distribution of inhibitory and excitatory synapses on hippocampal CA1 pyramidal cells. Neuroscience 102:527–540 . doi: 10.1016/S0306-4522(00)00496-6
Messina A, Bitetti I, Precenzano F, et al (2018) Non-Rapid Eye Movement Sleep Parasomnias and Migraine: A Role of Orexinergic Projections. Front Neurol 9:95 . doi: 10.3389/fneur.2018.00095
Mieda M (2017) The roles of orexins in sleep/wake regulation. Neurosci. Res. 118:56–65
Mikrouli E, Wörtwein G, Soylu R, et al (2011) Increased numbers of orexin/hypocretin neurons in a genetic rat depression model. Neuropeptides 45:401–406 . doi: 10.1016/j.npep.2011.07.010
Mileykovskiy BY, Kiyashchenko LI, Siegel JM (2005) Behavioral correlates of activity in identified hypocretin/orexin neurons. Neuron 46:787–798 . doi: 10.1016/j.neuron.2005.04.035
Mistlberger RE, Antle MC (2011) Entrainment of circadian clocks in mammals by

arousal and food. Essays Biochem 49:119–136 . doi: 10.1042/bse0490119
Miyamoto A, Wake H, Moorhouse AJ, Nabekura J (2013) Microglia and synapse interactions: fine tuning neural circuits and candidate molecules. Front Cell Neurosci 7: . doi: 10.3389/fncel.2013.00070
Miyata S, Kitagawa H (2016) Chondroitin 6-Sulfation Regulates Perineuronal Net Formation by Controlling the Stability of Aggrecan. Neural Plast 2016: . doi: 10.1155/2016/1305801
Miyata S, Komatsu Y, Yoshimura Y, et al (2012) Persistent cortical plasticity by upregulation of chondroitin 6-sulfation. Nat Neurosci 15:414–422 . doi: 10.1038/nn.3023
Mizutani M, Pino PA, Saederup N, et al (2012) The Fractalkine Receptor but Not CCR2 Is Present on Microglia from Embryonic Development throughout Adulthood. J Immunol 188:29–36 . doi: 10.4049/jimmunol.1100421
Modirrousta M, Mainville L, Jones BE (2005) Orexin and MCH neurons express c-Fos differently after sleep deprivation vs. recovery and bear different adrenergic receptors. Eur J Neurosci 21:2807–2816 . doi: 10.1111/j.1460-9568.2005.04104.x
Moore RY (1992) The fourth C.U. Ariens Kappers lecture. The organization of the human circadian timing system. Prog Brain Res 93:97–99 . doi: 10.1016/S0079-6123(08)64567-7
Moore RY, Speh JC, Leak RK (2002) Suprachiasmatic nucleus organization. Cell Tissue Res. 309:89–98
Morawski M, Filippov M, Tzinia A, et al (2014) ECM in brain aging and dementia. Prog Brain Res 214:207–227 . doi: 10.1016/B978-0-444-63486-3.00010-4
Morawski M, Reinert T, Meyer-Klaucke W, et al (2015) Ion exchanger in the brain: Quantitative analysis of perineuronally fixed anionic binding sites suggests diffusion barriers with ion sorting properties. Sci Rep 5: . doi: 10.1038/srep16471
Morin LP, Allen CN (2006) The circadian visual system, 2005. Brain Res. Rev. 51:1–60
Moriya T, Yoshinobu Y, Kouzu Y, et al (2000) Involvement of glial fibrillary acidic protein (GFAP) expressed in astroglial cells in circadian rhythm under constant lighting conditions in mice. J Neurosci Res 60:212–218 . doi: 10.1002/(SICI)1097-4547(20000415)60:2<212::AID-JNR10>3.0.CO;2-P
Mucke L, Masliah E, Yu GQ, et al (2000) High-level neuronal expression of abeta 1-42 in wild-type human amyloid protein precursor transgenic mice: synaptotoxicity without plaque formation. J Neurosci 20:4050–8 . doi: 20/11/4050 [pii]
Muenchhoff J, Poljak A, Song F, et al (2015) Plasma protein profiling of mild cognitive impairment and Alzheimer's disease across two independent cohorts. J Alzheimers Dis 43:1355–73 . doi: 10.3233/JAD-141266
Muschamp JW, Dominguez JM, Sato SM, et al (2007) A role for hypocretin (orexin) in male sexual behavior. J Neurosci 27:2837–45 . doi: 10.1523/JNEUROSCI.4121-06.2007
Nader N, Chrousos GP, Kino T (2010) Interactions of the circadian CLOCK system and the HPA axis. Trends Endocrinol. Metab. 21:277–286
Nair-Roberts RG, Chatelain-Badie SD, Benson E, et al (2008) Stereological estimates of dopaminergic, GABAergic and glutamatergic neurons in the ventral tegmental area, substantia nigra and retrorubral field in the rat. Neuroscience 152:1024–1031 . doi: 10.1016/j.neuroscience.2008.01.046
Najjar RP, Zeitzer JM (2017) Anatomy and Physiology of the Circadian System. In: Sleep and Neurologic Disease. pp 29–53
Nicholson C, Sykova E (1998) Extracellular space structure revealed by diffusion analysis.[see comment]. Trends Neurosci 21:207–215 . doi: 10.1016/S0166-2236(98)01261-2
Nitz D, Andersen A, Fahringer H, et al (1995) Altered distribution of cholinergic cells in the narcoleptic dog. Neuroreport 6:1521–1524

Nixon JP, Mavanji V, Butterick TA, et al (2015) Sleep disorders, obesity, and aging: The role of orexin. Ageing Res. Rev. 20:63–73
Nixon JP, Smale L (2007) A comparative analysis of the distribution of immunoreactive orexin A and B in the brains of nocturnal and diurnal rodents. Behav Brain Funct 3: . doi: 10.1186/1744-9081-3-28
Nuñez Á, Rodrigo-Angulo ML, De Andrés I, Garzón M (2009) Hypocretin/Orexin neuropeptides: participation in the control of sleep-wakefulness cycle and energy homeostasis. Curr Neuropharmacol 7:50–59 . doi: 10.2174/157015909787602797
Palomba M, Nygård M, Florenzano F, et al (2008) Decline of the presynaptic network, including GABAergic terminals, in the aging suprachiasmatic nucleus of the mouse. J Biol Rhythms 23:220–231 . doi: 10.1177/0748730408316998
Palomba M, Seke-Etet PF, Laperchia C, et al (2015a) Alterations of orexinergic and melanin-concentrating hormone neurons in experimental sleeping sickness. Neuroscience 290:185–195 . doi: 10.1016/j.neuroscience.2014.12.066
Palomba M, Seke-Etet PF, Laperchia C, et al (2015b) Alterations of orexinergic and melanin-concentrating hormone neurons in experimental sleeping sickness. Neuroscience 290:185–195 . doi: 10.1016/J.NEUROSCIENCE.2014.12.066
Palus K, Chrobok L, Lewandowski MH (2015) Orexins/hypocretins modulate the activity of NPY-positive and -negative neurons in the rat intergeniculate leaflet via OX<inf>1</inf> and OX<inf>2</inf> receptors. Neuroscience 300:370–380 . doi: 10.1016/j.neuroscience.2015.05.039
Pankevich DE, Teegarden SL, Hedin AD, et al (2010) Caloric Restriction Experience Reprograms Stress and Orexigenic Pathways and Promotes Binge Eating. J Neurosci 30:16399–16407 . doi: 10.1523/JNEUROSCI.1955-10.2010
Papouin T, Dunphy JM, Tolman M, et al (2017) Septal Cholinergic Neuromodulation Tunes the Astrocyte-Dependent Gating of Hippocampal NMDA Receptors to Wakefulness. Neuron 94:840–854.e7 . doi: 10.1016/j.neuron.2017.04.021
Parsons MP, Hirasawa M (2010) ATP-Sensitive Potassium Channel-Mediated Lactate Effect on Orexin Neurons: Implications for Brain Energetics during Arousal. J Neurosci 30:8061–8070 . doi: 10.1523/JNEUROSCI.5741-09.2010
Parsons MP, Hirasawa M (2011) GIRK channel-mediated inhibition of melanin-concentrating hormone neurons by nociceptin/orphanin FQ. J Neurophysiol 105:1179–84 . doi: 10.1152/jn.00791.2010
Pekala D, Blasiak T, Raastad M, Lewandowski MH (2011) The influence of orexins on the firing rate and pattern of rat intergeniculate leaflet neurons - electrophysiological and immunohistological studies. Eur J Neurosci 34:1406–1418 . doi: 10.1111/j.1460-9568.2011.07868.x
Perriard G, Mathias A, Enz L, et al (2015) Interleukin-22 is increased in multiple sclerosis patients and targets astrocytes. J Neuroinflammation 12: . doi: 10.1186/s12974-015-0335-3
Pesheva P, Gloor S, Schachner M, Probstmeier R (1997) Tenascin-R is an intrinsic autocrine factor for oligodendrocyte differentiation and promotes cell adhesion by a sulfatide-mediated mechanism. J Neurosci 17:4642–4651
Pesheva P, Probstmeier R (2000) The yin and yang of tenascin-R in CNS development and pathology. Prog. Neurobiol. 61:465–493
Peterseén Å, Gil J, Maat-Schieman MLC, et al (2005) Orexin loss in Huntington's disease. Hum Mol Genet 14:39–47 . doi: 10.1093/hmg/ddi004
Petersén Å, Puschban Z, Lotharius J, et al (2002) Evidence for dysfunction of the nigrostriatal pathway in the R6/1 line of transgenic Huntington's disease mice. Neurobiol Dis 11:134–146 . doi: 10.1006/nbdi.2002.0534
Petsakou A, Sapsis TP, Blau J (2015) Circadian Rhythms in Rho1 Activity Regulate Neuronal Plasticity and Network Hierarchy. Cell 162:823–835 . doi: 10.1016/j.cell.2015.07.010

Peyron C, Faraco J, Rogers W, et al (2000) A mutation in a case of early onset narcolepsy and a generalized absence of hypocretin peptides in human narcoleptic brains. Nat Med 6:991–997 . doi: 10.1038/79690
Peyron C, Sapin E, Leger L, et al (2009) Role of the melanin-concentrating hormone neuropeptide in sleep regulation. Peptides 30:2052–2059 . doi: 10.1016/j.peptides.2009.07.022
Peyron C, Tighe DK, van den Pol a N, et al (1998) Neurons containing hypocretin (orexin) project to multiple neuronal systems. J Neurosci 18:9996–10015 . doi: 10.1.1.335.5389
Piccoli L, Di Bonaventura MVM, Cifani C, et al (2012) Role of orexin-1 receptor mechanisms on compulsive food consumption in a model of binge eating in female rats. Neuropsychopharmacology 37:1999–2011
Pillai JA, Leverenz JB (2017) Sleep and Neurodegeneration: A Critical Appraisal. Chest 151:1375–1386
Pissios P, Bradley RL, Maratos-Flier E (2006) Expanding the scales: The multiple roles of MCH in regulating energy balance and other biological functions. Endocr. Rev. 27:606–620
Pizzorusso T (2002) Reactivation of Ocular Dominance Plasticity in the Adult Visual Cortex. Science (80-) 298:1248–1251 . doi: 10.1126/science.1072699
Pollak CP, Perlick D (1991) Sleep Problems and Institutionalization of the Elderly. J Geriatr Psychiatry Neurol 4:204–210 . doi: 10.1177/089198879100400405
Porkka-Heiskanen T, Alanko L, Kalinchuk A, et al (2004) The effect of age on prepro-orexin gene expression and contents of orexin A and B in the rat brain. Neurobiol Aging 25:231–8
Praschak-Rieder N, Willeit M, Wilson AA, et al (2008) Seasonal variation in human brain serotonin transporter binding. Arch Gen Psychiatry 65:1072–1078 . doi: 10.1001/archpsyc.65.9.1072
Prolo LM (2005) Circadian Rhythm Generation and Entrainment in Astrocytes. J Neurosci 25:404–408 . doi: 10.1523/JNEUROSCI.4133-04.2005
Randeva HS, Karteris E, Grammatopoulos D, Hillhouse EW (2001) Expression of orexin-a and functional orexin type 2 receptors in the human adult adrenals: Implications for adrenal function and energy homeostasis. J Clin Endocrinol Metab 86:4808–4813 . doi: 10.1210/jc.86.10.4808
Rao Y, Liu Z-W, Borok E, et al (2007a) Prolonged wakefulness induces experience-dependent synaptic plasticity in mouse hypocretin/orexin neurons. J Clin Invest 117:4022–4033 . doi: 10.1172/JCI32829
Rao Y, Liu ZW, Borok E, et al (2007b) Prolonged wakefulness induces experience-dependent synaptic plasticity in mouse hypocretin/orexin neurons. J Clin Invest 117:4022–4033 . doi: 10.1172/JCI32829
Rao Y, Lu M, Ge F, et al (2008) Regulation of Synaptic Efficacy in Hypocretin/Orexin-Containing Neurons by Melanin Concentrating Hormone in the Lateral Hypothalamus. J Neurosci 28:9101–9110 . doi: 10.1523/JNEUROSCI.1766-08.2008
Rathjen FG, Wolff JM, Chiquet-Ehrismann R (1991) Restrictin: a chick neural extracellular matrix protein involved in cell attachment co-purifies with the cell recognition molecule F11. Development 113:151–64
Rattan SI, Rasmussen LM, Bjerring P, et al (1988) Unchanged concentrations of plasma fibronectin in Alzheimer's disease. J Clin Pathol 41:476
Rauch U (2004) Extracellular matrix components associated with remodeling processes in brain. Cell Mol Life Sci 61: . doi: 10.1007/s00018-004-4043-x
Reti IM, Reddy R, Worley PF, Baraban JM (2002) Selective expression of Narp, a secreted neuronal pentraxin, in orexin neurons. J Neurochem 82:1561–1565 . doi: 10.1046/j.1471-4159.2002.01141.x

Richardson JC, Kendal CE, Anderson R, et al (2003) Ultrastructural and behavioural changes precede amyloid deposition in a transgenic model of Alzheimer's disease. Neuroscience 122:213–228 . doi: 10.1016/S0306-4522(03)00389-0
Rogers AE, Meehan J, Guilleminault C, et al (1997) HLA DR15 (DR2) and DQB1*0602 typing studies in 188 narcoleptic patients with cataplexy. Neurology 48:1550–6 . doi: 10.1212/WNL.48.6.1550
Roh JH, Huang Y, Bero AW, et al (2012) Disruption of the Sleep-Wake Cycle and Diurnal Fluctuation of -Amyloid in Mice with Alzheimer's Disease Pathology. Sci Transl Med 4:150ra122-150ra122 . doi: 10.1126/scitranslmed.3004291
Romijn HJ, Van Uum JFM, Emmering J, et al (1999) Colocalization of VIP with AVP in neurons of the human paraventricular, supraoptic and suprachiasmatic nucleus. Brain Res 832:47–53 . doi: 10.1016/S0006-8993(99)01468-7
Ross CA, Aylward EH, Wild EJ, et al (2014) Huntington disease: Natural history, biomarkers and prospects for therapeutics. Nat. Rev. Neurol. 10:204–216
Roth T, Dauvilliers Y, Mignot E, et al (2013) Disrupted nighttime sleep in narcolepsy. J. Clin. Sleep Med. 9:955–965
Roy M, David N, Cueva M, Giorgetti M (2007) A Study of the Involvement of Melanin-Concentrating Hormone Receptor 1 (MCHR1) in Murine Models of Depression. Biol Psychiatry 61:174–180 . doi: 10.1016/j.biopsych.2006.03.076
Rozario T, DeSimone DW (2010) The extracellular matrix in development and morphogenesis: A dynamic view. Dev. Biol. 341:126–140
Ruoslahti E (1996) Brain extracellular matrix. Glycobiology 6:489–492 . doi: 10.1093/glycob/6.5.489
Rutten BPF, Van Der Kolk NM, Schafer S, et al (2005) Age-related loss of synaptophysin immunoreactive presynaptic boutons within the hippocampus of APP751SL, PS1M146L, and APP751SL/PS1M146Ltransgenic mice. Am J Pathol 167:161–173 . doi: 10.1016/S0002-9440(10)62963-X
Saito YC, Tsujino N, Hasegawa E, et al (2013) GABAergic neurons in the preoptic area send direct inhibitory projections to orexin neurons. Front Neural Circuits 7: . doi: 10.3389/fncir.2013.00192
Sakurai T (2007) The neural circuit of orexin (hypocretin): Maintaining sleep and wakefulness. Nat. Rev. Neurosci. 8:171–181
Sakurai T (2014) The role of orexin in motivated behaviours. Nat. Rev. Neurosci. 15:719–731
Sakurai T, Amemiya A, Ishii M, et al (1998) Orexins and orexin receptors: A family of hypothalamic neuropeptides and G protein-coupled receptors that regulate feeding behavior. Cell 92:573–585 . doi: 10.1016/S0092-8674(00)80949-6
Sakurai T, Mieda M (2011) Connectomics of orexin-producing neurons: Interface of systems of emotion, energy homeostasis and arousal. Trends Pharmacol. Sci. 32:451–462
Sakurai T, Nagata R, Yamanaka A, et al (2005) Input of orexin/hypocretin neurons revealed by a genetically encoded tracer in mice. Neuron 46:297–308 . doi: 10.1016/j.neuron.2005.03.010
Salomon RM, Ripley B, Kennedy JS, et al (2003) Diurnal variation of cerebrospinal fluid hypocretin-1 (Orexin-A) levels in control and depressed subjects. Biol Psychiatry 54:96–104 . doi: 10.1016/S0006-3223(03)01740-7
Santos JWQ, Araújo JF, Cunha MJB, et al (2005) Circadian variation in GFAP immunoreactivity in the mouse suprachiasmatic nucleus. In: Biological Rhythm Research. pp 141–150
Saper CB (2013) The central circadian timing system. Curr. Opin. Neurobiol. 23:747–751
Saper CB, Scammell TE, Lu J (2005) Hypothalamic regulation of sleep and circadian rhythms. Nature 437:1257–1263
Sarrias MJ, Artigas F, Martínez E, Gelpí E (1989) Seasonal changes of plasma serotonin

and related parameters: Correlation with environmental measures. Biol Psychiatry 26:695–706 . doi: 10.1016/0006-3223(89)90104-2
Sato A, Ohtaki H, Tsumuraya T, et al (2012) Interleukin-1 participates in the classical and alternative activation of microglia/macrophages after spinal cord injury. J Neuroinflammation 9: . doi: 10.1186/1742-2094-9-65
Sawai N, Ueta Y, Nakazato M, Ozawa H (2010) Developmental and aging change of orexin-A and -B immunoreactive neurons in the male rat hypothalamus. Neurosci Lett 468:51–55 . doi: 10.1016/j.neulet.2009.10.061
Scammell TE (2015) Narcolepsy. N Engl J Med 373:2654–2662 . doi: 10.1056/NEJMra1500587
Scammell TE, Matheson JK, Honda M, et al (2012) Coexistence of narcolepsy and Alzheimer's disease. Neurobiol Aging 33:1318–1319 . doi: 10.1016/j.neurobiolaging.2010.12.008
Scammell TE, Winrow CJ (2011) Orexin Receptors: Pharmacology and Therapeutic Opportunities. Annu Rev Pharmacol Toxicol 51:243–266 . doi: 10.1146/annurev-pharmtox-010510-100528
Schaefer L, Schaefer RM (2010) Proteoglycans: From structural compounds to signaling molecules. Cell Tissue Res. 339:237–246
Scheff SW, Price DA (2003) Synaptic pathology in Alzheimer's disease: A review of ultrastructural studies. In: Neurobiology of Aging. pp 1029–1046
Schmitt LI, Sims RE, Dale N, Haydon PG (2012) Wakefulness Affects Synaptic and Network Activity by Increasing Extracellular Astrocyte-Derived Adenosine. J Neurosci 32:4417–4425 . doi: 10.1523/JNEUROSCI.5689-11.2012
Schmitt LI, Wimmer RD (2015) Astrocytic Regulation of Sleep Processes. Curr Sleep Med Reports 1:9–19 . doi: 10.1007/s40675-014-0005-5
Seeger G, Lüth HJ, Winkelmann E, Brauer K (1996) Distribution patterns of Wisteria floribunda agglutinin binding sites and parvalbumin-immunoreactive neurons in the human visual cortex: a double-labelling study. J für Hirnforsch 37:351–66
Segall LA, Milet A, Tronche F, Amir S (2009) Brain glucocorticoid receptors are necessary for the rhythmic expression of the clock protein, PERIOD2, in the central extended amygdala in mice. Neurosci Lett 457:58–60 . doi: 10.1016/j.neulet.2009.03.083
Selbach O, Haas HL (2006) Hypocretins: The timing of sleep and waking. In: Chronobiology International. pp 63–70
Serrano-Pozo A, Frosch MP, Masliah E, Hyman BT (2011) Neuropathological alterations in Alzheimer disease. Cold Spring Harb. Perspect. Med. 1
Shan L, Dauvilliers Y, Siegel JM (2015) Interactions of the histamine and hypocretin systems in CNS disorders. Nat. Rev. Neurol. 11:401–413
Sharma S, Fernandes MF, Fulton S (2013) Adaptations in brain reward circuitry underlie palatable food cravings and anxiety induced by high-fat diet withdrawal. Int J Obes 37:1183–1191 . doi: 10.1038/ijo.2012.197
Shimada M, Tritos NA, Lowell BB, et al (1998) Mice lacking melanin-concentrating hormone are hypophagic and lean. Nature 396:670–679 . doi: 10.1038/25341
Shouse MN, Siegel JM (1992) Pontine regulation of REM sleep components in cats: integrity of the pedunculopontine tegmentum (PPT) is important for phasic events but unnecessary for atonia during REM sleep. Brain Res 571:50–63 . doi: 10.1016/0006-8993(92)90508-7
Silva AA, Roffe E, Lannes-Vieira J (1999) Expression of extracellular matrix components and their receptors in the central nervous system during experimental Toxoplasma gondii and Trypanosoma cruzi infection. Braz J Med Biol Res 32:593–600
Slats D, Claassen JAHR, Verbeek MM, Overeem S (2013) Reciprocal interactions between sleep, circadian rhythms and Alzheimer's disease: Focus on the role of

hypocretin and melatonin. Ageing Res. Rev. 12:188–200
Smith DG, Davis RJ, Rorick-Kehn L, et al (2006) Melanin-Concentrating Hormone-1 Receptor Modulates Neuroendocrine, Behavioral and Corticolimbic Neurochemical Stress Responses in Mice. Neuropsychopharmacology 31:1135–1145 . doi: 10.1038/sj.npp.1300913
Smith DG, Hegde LG, Wolinsky TD, et al (2009) The effects of stressful stimuli and hypothalamic-pituitary-adrenal axis activation are reversed by the melanin-concentrating hormone 1 receptor antagonist SNAP 94847 in rodents. Behav Brain Res 197:284–291 . doi: 10.1016/j.bbr.2008.08.026
Sokołowska P, Urbańska A, Namiecińska M, et al (2012) Orexins promote survival of rat cortical neurons. Neurosci Lett 506:303–306 . doi: 10.1016/j.neulet.2011.11.028
Soleman S, Filippov MA, Dityatev A, Fawcett JW (2013) Targeting the neural extracellular matrix in neurological disorders. Neuroscience 253:194–213 . doi: 10.1016/j.neuroscience.2013.08.050
Song I, Dityatev A (2017) Crosstalk between glia, extracellular matrix and neurons. Brain Res. Bull.
Sorg BA, Berretta S, Blacktop JM, et al (2016) Casting a Wide Net: Role of Perineuronal Nets in Neural Plasticity. J Neurosci 36:11459–11468 . doi: 10.1523/JNEUROSCI.2351-16.2016
Spitzer NC (2015) Neurotransmitter Switching? No Surprise. Neuron 86:1131–1144
Spreafico R, De Biasi S, Vitellaro-Zuccarello L (1999) The Perineuronal Net: A Weapon for a Challenge. J Hist Neurosci 8:179–185 . doi: 10.1076/jhin.8.2.179.1834
Spruston N (2008) Pyramidal neurons: Dendritic structure and synaptic integration. Nat. Rev. Neurosci. 9:206–221
Stanley EM, Fadel J (2012) Aging-related deficits in orexin/hypocretin modulation of the septohippocampal cholinergic system. Synapse 66:445–452 . doi: 10.1002/syn.21533
Stevens RG, Zhu Y (2015) Electric light, particularly at night, disrupts human circadian rhythmicity: is that a problem? Philos Trans R Soc B Biol Sci 370:20140120–20140120 . doi: 10.1098/rstb.2014.0120
Stone JR, Singleton RH, Povlishock JT (2000) Antibodies to the C-terminus of the beta-amyloid precursor protein (APP): a site specific marker for the detection of traumatic axonal injury. Brain Res 871:288–302 . doi: S0006-8993(00)02485-9 [pii]
Stopa EG, Volicer L, Kuo-Leblanc V, et al (1999) Pathologic evaluation of the human suprachiasmatic nucleus in severe dementia. J Neuropathol Exp Neurol 58:29–39 . doi: 10.1097/00005072-199901000-00004
Sutcliffe JG, de Lecea L (2002) The hypocretins: Setting the arousal threshold. Nat. Rev. Neurosci. 3:339–349
Tafti M, Hor H, Dauvilliers Y, et al (2014) DQB1 locus alone explains most of the risk and protection in narcolepsy with cataplexy in Europe. Sleep 37:19–25 . doi: 10.5665/sleep.3300
Tafti M, Nishino S, Liao W, et al (1997) Mesopontine organization of cholinergic and catecholaminergic cell groups in the normal and narcoleptic dog. J Comp Neurol 379:185–197 . doi: 10.1002/(SICI)1096-9861(19970310)379:2<185::AID-CNE2>3.0.CO;2-#
Taheri S, Gardiner J, Hafizi S, et al (2001) Orexin A immunoreactivity and preproorexin mRNA in the brain of Zucker and WKY rats. Neuroreport 12:459–64
Taheri S, Mahmoodi M, Opacka-Juffry J, et al (1999) Distribution and quantification of immunoreactive orexin A in rat tissues. FEBS Lett 457:157–161 . doi: 10.1016/S0014-5793(99)01030-3
Taheri S, Sunter D, Dakin C, et al (2000) Diurnal variation in orexin A immunoreactivity and prepro-orexin mRNA in the rat central nervous system. Neurosci Lett 279:109–112 . doi: 10.1016/S0304-3940(99)00955-6

Takahashi Y, Kanbayashi T, Hoshikawa M, et al (2015) Relationship of orexin (hypocretin) system and astrocyte activation in Parkinson's disease with hypersomnolence. Sleep Biol Rhythms 13:252–260 . doi: 10.1111/sbr.12112
Tanca A, Uzzau S, Addis MF (2014) Full-length protein extraction protocols and gel-based downstream applications in formalin-fixed tissue proteomics. Methods Mol Biol 1295:117–134 . doi: 10.1007/978-1-4939-2550-6_11
Tani E, Ametani T (1971) Extracellular distribution of ruthenium red-positive substance in the cerebral cortex. J Ultrasructure Res 34:1–14 . doi: 10.1016/S0022-5320(71)90002-5
Tarsa L, Goda Y (2002) Synaptophysin regulates activity-dependent synapse formation in cultured hippocampal neurons. Proc Natl Acad Sci U S A 99:1012–6 . doi: 10.1073/pnas.022575999
Terao A, Apte-Deshpande A, Morairty S, et al (2002) Age-related decline in hypocretin (orexin) receptor 2 messenger RNA levels in the mouse brain. Neurosci Lett 332:190–194 . doi: 10.1016/S0304-3940(02)00953-9
Tesoriero C, Codita A, Zhang M-D, et al (2016) H1N1 influenza virus induces narcolepsy-like sleep disruption and targets sleep–wake regulatory neurons in mice. Proc Natl Acad Sci 113:E368–E377 . doi: 10.1073/pnas.1521463112
Thannickal TC, Lai YY, Siegel JM (2007) Hypocretin (orexin) cell loss in Parkinson's disease. Brain 130:1586–1595 . doi: 10.1093/brain/awm097
Thannickal TC, Moore RY, Nienhuis R, et al (2000) Reduced number of hypocretin neurons in human narcolepsy. Neuron 27:469–474 . doi: 10.1016/S0896-6273(00)00058-1
Thannickal TC, Nienhuis R, Siegel JM (2009) Localized loss of hypocretin (orexin) cells in narcolepsy without cataplexy. Sleep 32:993–998
Thannickal TC, Siegel JM, Nienhuis R, Moore RY (2003) Pattern of hypocretin (orexin) soma and axon loss, and gliosis, in human narcolepsy. Brain Pathol 13:340–351
Theodosis DT, Poulain DA, Oliet SHR (2008) Activity-Dependent Structural and Functional Plasticity of Astrocyte-Neuron Interactions. Physiol Rev 88:983–1008 . doi: 10.1152/physrev.00036.2007
Thorpy MJ, Krieger AC (2014) Delayed diagnosis of narcolepsy: Characterization and impact. Sleep Med. 15:502–507
Tobler I, Deboer T, Fischer M (1997) Sleep and sleep regulation in normal and prion protein-deficient mice. J Neurosci 17:1869–1879
Toossi H, del Cid-Pellitero E, Jones BE (2016) GABA Receptors on Orexin and MCH Neurons are Differentially Homeostatically Regulated following Sleep Deprivation. eNeuro 3:1–11 . doi: 10.1523/ENEURO.0077-16.2016
Toossi H, Del Cid-Pellitero E, Stroh T, Jones BE (2012) Somatostatin varicosities contain the vesicular GABA transporter and contact orexin neurons in the hypothalamus. Eur J Neurosci 36:3388–3395 . doi: 10.1111/j.1460-9568.2012.08253.x
Torrealba F, Yanagisawa M, Saper CB (2003) Colocalization of orexin a and glutamate immunoreactivity in axon terminals in the tuberomammillary nucleus in rats. Neuroscience 119:1033–1044 . doi: 10.1016/S0306-4522(03)00238-0
Trotti LM, Staab BA, Rye DB (2013) Test-retest reliability of the multiple sleep latency test in narcolepsy without cataplexy and idiopathic hypersomnia. J Clin Sleep Med 9:789–795 . doi: 10.5664/jcsm.2922
Tsujino N, Sakurai T (2009) Orexin/Hypocretin: A Neuropeptide at the Interface of Sleep, Energy Homeostasis, and Reward System. Pharmacol Rev 61:162–176 . doi: 10.1124/pr.109.001321
Tsunematsu T, Yamanaka A (2012) The Role of Orexin/Hypocretin in the Central Nervous System and Peripheral Tissues. Vitam Horm 89:19–33 . doi: 10.1016/B978-0-12-394623-2.00002-0
Turrigiano GG (1999) Homeostatic plasticity in neuronal networks: The more things

change, the more they stay the same. Trends Neurosci. 22:221–227
Van Den Pol AN, Acuna-Goycolea C, Clark KR, Ghosh PK (2004) Physiological properties of hypothalamic MCH neurons identified with selective expression of reporter gene after recombinant virus infection. Neuron 42:635–652 . doi: 10.1016/S0896-6273(04)00251-X
van den Pol AN, Gao XB, Obrietan K, et al (1998) Presynaptic and postsynaptic actions and modulation of neuroendocrine neurons by a new hypothalamic peptide, hypocretin/orexin. J Neurosci 18:7962–7971
van Esseveldt KE, Lehman MN, Boer GJ (2000) The suprachiasmatic nucleus and the circadian time-keeping system revisited. Brain Res Brain Res Rev 33:34–77
Van Horssen J, Dijkstra CD, De Vries HE (2007) The extracellular matrix in multiple sclerosis pathology. J. Neurochem. 103:1293–1301
Van Horssen J, Vos CMP, Admiraal L, et al (2006) Matrix metalloproteinase-19 is highly expressed in active multiple sclerosis lesions. Neuropathol Appl Neurobiol 32:585–593 . doi: 10.1111/j.1365-2990.2006.00766.x
van Oosterhout F, Lucassen EA, Houben T, et al (2012) Amplitude of the SCN clock enhanced by the behavioral activity rhythm. PLoS One 7: . doi: 10.1371/journal.pone.0039693
Verbich D, Prenosil GA, Chang PKY, et al (2012) Glial glutamate transport modulates dendritic spine head protrusions in the hippocampus. Glia 60:1067–1077 . doi: 10.1002/glia.22335
Verkhratsky A, Butt A (2007) Glial Neurobiology: A Textbook
Verkhratsky A, Nedergaard M (2014) Astroglial cradle in the life of the synapse. Philos Trans R Soc B Biol Sci 369:20130595–20130595 . doi: 10.1098/rstb.2013.0595
Verret L, Goutagny R, Fort P, et al (2003) A role of melanin-concentrating hormone producing neurons in the central regulation of paradoxical sleep. BMC Neurosci 4: . doi: 10.1186/1471-2202-4-19
Videnovic A, Zee PC (2015) Consequences of circadian disruption on neurologic health. Sleep Med Clin 10:469–480 . doi: 10.1016/j.jsmc.2015.08.004
Vitellaro-Zuccarello L, Bosisio P, Mazzetti S, et al (2007) Differential expression of several molecules of the extracellular matrix in functionally and developmentally distinct regions of rat spinal cord. Cell Tissue Res 327:433–447 . doi: 10.1007/s00441-006-0289-y
Weber P, Bartsch U, Rasband MN, et al (1999) Mice deficient for tenascin-R display alterations of the extracellular matrix and decreased axonal conduction velocities in the CNS. J Neurosci 19:4245–4262
Wegner F, Härtig W, Bringmann A, et al (2003) Diffuse perineuronal nets and modified pyramidal cells immunoreactive for glutamate and the GABAAreceptor α1 subunit form a unique entity in rat cerebral cortex. Exp Neurol 184:705–714 . doi: 10.1016/S0014-4886(03)00313-3
Willie JT, Chemelli RM, Sinton CM, et al (2003) Distinct narcolepsy syndromes in orexin receptor-2 and orexin null mice: Molecular genetic dissection of non-REM and REM sleep regulatory processes. Neuron 38:715–730 . doi: 10.1016/S0896-6273(03)00330-1
Winsky-Sommerer R (2004) Interaction between the Corticotropin-Releasing Factor System and Hypocretins (Orexins): A Novel Circuit Mediating Stress Response. J Neurosci 24:11439–11448 . doi: 10.1523/JNEUROSCI.3459-04.2004
Wintergerst ES, Rathjen FG, Schwaller B, et al (2001) Tenascin-R associates extracellularly with parvalbumin immunoreactive neurones but is synthesised by another neuronal population in the adult rat cerebral cortex. J Neurocytol 30:293–301 . doi: 10.1023/A:1014452212067
Wlodarczyk J, Mukhina I, Kaczmarek L, Dityatev A (2011) Extracellular matrix molecules, their receptors, and secreted proteases in synaptic plasticity. Dev

Neurobiol 71:1040–1053 . doi: 10.1002/dneu.20958
Wojcik SM, Katsurabayashi S, Guillemin I, et al (2006) A Shared Vesicular Carrier Allows Synaptic Corelease of GABA and Glycine. Neuron 50:575–587 . doi: 10.1016/j.neuron.2006.04.016
Wollmann G (2005) Direct Excitation of Hypocretin/Orexin Cells by Extracellular ATP at P2X Receptors. J Neurophysiol 94:2195–2206 . doi: 10.1152/jn.00035.2005
Womac AD, Burkeen JF, Neuendorff N, et al (2009) Circadian rhythms of extracellular ATP accumulation in suprachiasmatic nucleus cells and cultured astrocytes. Eur J Neurosci 30:869–76 . doi: 10.1111/j.1460-9568.2009.06874.x
Wu F, Song Y, Li F, et al (2014) Wen-dan decoction improves negative emotions in sleep-deprived rats by regulating orexin-a and leptin expression. Evidence-based Complement Altern Med 2014: . doi: 10.1155/2014/872547
Wu MF, Nienhuis R, Maidment N, et al (2011) Cerebrospinal fluid hypocretin (orexin) levels are elevated by play but are not raised by exercise and its associated heart rate, blood pressure, respiration or body temperature changes. Arch Ital Biol 149:492–498 . doi: 10.4449/aib.v149i4.1315
Wu Y-H, Feenstra MGP, Zhou J-N, et al (2003) Molecular changes underlying reduced pineal melatonin levels in Alzheimer disease: alterations in preclinical and clinical stages. J Clin Endocrinol Metab 88:5898–906 . doi: 10.1210/jc.2003-030833
Xavier AL, Menezes JRL, Goldman SA, Nedergaard M (2014) Fine-tuning the central nervous system: microglial modelling of cells and synapses. Philos Trans R Soc Lond B Biol Sci 369:20130593 . doi: 10.1098/rstb.2013.0593
Xie X, Crowder TL, Yamanaka A, et al (2006) GABABreceptor-mediated modulation of hypocretin/orexin neurones in mouse hypothalamus. J Physiol 574:399–414 . doi: 10.1113/jphysiol.2006.108266
Yamaguchi Y (2000) Lecticans: organizers of the brain extracellular matrix. Cell Mol Life Sci 57:276–289 . doi: 10.1007/PL00000690
Yamamoto T, Nozaki-Taguchi N, Chiba T (2002) Analgesic effect of intrathecally administered orexin-A in the rat formalin test and in the rat hot plate test. Br J Pharmacol 137:170–176 . doi: 10.1038/sj.bjp.0704851
Yamanaka A, Beuckmann CT, Willie JT, et al (2003a) Hypothalamic orexin neurons regulate arousal according to energy balance in mice. Neuron 38:701–713 . doi: 10.1016/S0896-6273(03)00331-3
Yamanaka A, Muraki Y, Tsujino N, et al (2003b) Regulation of orexin neurons by the monoaminergic and cholinergic systems. Biochem Biophys Res Commun 303:120–129 . doi: 10.1016/S0006-291X(03)00299-7
Yamanaka A, Tabuchi S, Tsunematsu T, et al (2010) Orexin Directly Excites Orexin Neurons through Orexin 2 Receptor. J Neurosci 30:12642–12652 . doi: 10.1523/JNEUROSCI.2120-10.2010
Yamanaka A, Tsujino N, Goto K, et al (2002) Orexins activate histaminergic neurons via the orexin 2 receptor. Biochem Biophys Res Commun 290:1237–1245 . doi: 10.1006/bbrc.2001.6318
Yoshida K, McCormack S, España RA, et al (2006) Afferents to the orexin neurons of the rat brain. J Comp Neurol 494:845–861 . doi: 10.1002/cne.20859
Yoshida Y, Fujiki N, Nakajima T, et al (2001) Fluctuation of extracellular hypocretin-1 (orexin A) levels in the rat in relation to the light-dark cycle and sleep-wake activities. Eur J Neurosci 14:1075–1081 . doi: 10.1046/j.0953-816X.2001.01725.x
Yuan L-B, Dong H-L, Zhang H-P, et al (2011) Neuroprotective effect of orexin-A is mediated by an increase of hypoxia-inducible factor-1 activity in rat. Anesthesiology 114:340–54 . doi: 10.1097/ALN.0b013e318206ff6f
Zeitzer JM, Buckmaster CL, Parker KJ, et al (2003) Circadian and homeostatic regulation of hypocretin in a primate model: implications for the consolidation of wakefulness. J Neurosci 23:3555–60 . doi: 23/8/3555 [pii]

Zhang JH, Sampogna S, Morales FR, Chase MH (2005) Age-related ultrastructural changes in hypocretinergic terminals in the brainstem and spinal cord of cats. Neurosci Lett 373:171–174 . doi: 10.1016/j.neulet.2003.08.085

Zhang S, Zeitzer JM, Yoshida Y, et al (2004) Lesions of the suprachiasmatic nucleus eliminate the daily rhythm of hypocretin-1 release. Sleep 27:619–627

Zhou JN, Hofman MA, Swaab DF (1995) VIP neurons in the human SCN in relation to sex, age, and Alzheimer's disease. Neurobiol Aging 16:571–576 . doi: 10.1016/0197-4580(95)00043-E

Zhou JN, Liu RY, Kamphorst W, et al (2003) Early neuropathological Alzheimer's changes in aged individuals are accompanied by decreased cerebrospinal fluid melatonin levels. J Pineal Res 35:125–130 . doi: 10.1034/j.1600-079X.2003.00065.x

Zink AN, Perez-Leighton CE, Kotz CM (2014) The orexin neuropeptide system: physical activity and hypothalamic function throughout the aging process. Front Syst Neurosci 8:211 . doi: 10.3389/fnsys.2014.00211